THE UNIVERSITY OF ASTON IN BIRMINGHAM

THE ELECTRICAL AND MECHANICAL PROPERTIES OF ELECTROGRAPHITE-METAL INTERFACES

THESIS
620.1781
FIS

A Thesis Submitted for the Degree of

DOCTOR OF PHILOSOPHY

by

JOHN FISHER B.Sc.

3dec73 167633

Physics Department
September 1973.

ABSTRACT

Experiments are described on the sliding of an electrographitic brush material against a number of counterface materials, using a pin and disk machine. The electrical and mechanical characteristics of the interface; frictional force, wear rate and contact resistance, were measured, and have been explained by physical changes occurring at the interface.

Three wear regimes were encountered, mild wear, severe wear and catastrophic wear. The wear mechanisms involved in these regimes were attributed to fatigue, adhesion and abrasion; which of these mechanisms predominated was dependent upon brush load and current. The transition from mild wear to severe wear was caused by mechanical disruption of any protective oxide layer, when a critical load was exceeded. A general wear theory is proposed, but this is limited by the necessity of considering each metal individually to determine whether or not oxide breakdown will occur.

The use of aluminium as an alternative to copper for slip-rings and commutators was investigated. Pure aluminium was found unsuitable because of a low, mild wear-severe wear transition load, due to the onset of plastic deformation. The use of aluminium is also severely limited by catastrophic failure of the brushes when carrying relatively small electric currents, caused by the production of abrasive particles.

The contact resistance of the brushes sliding on all the metals investigated was controlled by the formation of oxide films upon the metal surface. The variations in contact resistance with electric current were attributed to electrical breakdown of the oxides.

Finally, the frictional force behaviour was investigated and was explained in terms of the formation of lubricating, thin graphite films upon the brush surface.

Index

Chapter 1. Review of Brush Sliding Behaviour.

1.1. Introduction to Carbon Brushes

The discovery, during the latter part of the Nineteenth Century, that blocks of graphite could be used to carry current to and from electrical machines instead of bundles, or brushes, of copper wire has enabled the development of electrical machines; or any system relying on current collection between members in relative motion, to keep up with other technical developments.

Since this discovery much investigation has taken place into the behaviour of carbon and graphite for use as brush materials. Most of this work has, however, been carried out on the sliding of these brush materials on copper collector surfaces, either as slip rings or commutators. This is to be expected since the vast majority of electrical machines in use employ copper as the rotating member.

Investigations carried out into carbons sliding on other materials have generally been to study the use of carbon as a bearing material or rotating seal. Recently a number of investigations into the wear of "nuclear" graphites, under conditions similar to those found in nuclear reactors have been carried out. When used as a moderator, graphite has to withstand high temperatures and irradiation, two conditions not usually present when it is used as a brush material.

The work carried out on carbon as a seal or moderator material does not in general bear any relation to the problem of carbon as a brush material, either because of the conditions under which the experiments were carried out or because the type of carbon or graphite used was far removed from that used as a brush material.

Both the brush manufacturing and the electrical machine industries

have carried out a vast amount of work on carbon brushes, but most of this has been to find out the most suitable brush material to use on a particular machine or under certain conditions; for example in corrosive atmospheres or aerospace applications, or for the evaluation and comparison of brush materials. By comparison very little fundamental research into the mechanisms involved at the interface has been carried out.

Most of the fundamental work published on the sliding of carbon brushes on copper tends to be contradictory or, because of the nature of the experiments, the conditions under which the work was carried out, or the brush material used it cannot be satisfactorily compared with other work.

A very large number of brush materials, or grades, is made by each brush manufacturer. The brush materials can differ in composition, in the manufacturing method and in the amount of graphitisation which takes place during heat treatment. Since each of these factors has been found to influence the running characteristics of the brushes the results of workers who have used brushes made by different manufacturers, or different grades from the same manufacturer cannot be reliably compared.

The most important characteristics of the brush, from both the machine manufacturers and machine users viewpoint are: the rate of the wear of the brush and any damage which the brush causes to the sliding machine member, the frictional force between the brush and the metal, and the contact resistance across the brush - metal interface.

The brush wear rate and damage must both be kept to a minimum to reduce both the cost of brush replacement and the loss in manufacturing time when the machine is out of use for maintenance.

The frictional force should naturally be kept to a minimum to reduce

the power usage of the machine. The contact resistance should also be kept to a minimum when the brushes are used on a slip ring or for current collection from overhead cables or rails to reduce power loss at the interface. However, when the brushes are used on a commutator the contact resistance needs to be an optimum value, giving good commutation and minimising power wastage.

1.2 Frictional Force of Carbon Brushes.

The first theory to explain the lubricating properties and low friction of graphite was put forward by W.L.Bragg (1). After an investigation into the crystallographic structure of graphite, shown in Figure 1.1, he postulated that the low friction of graphite was due to low shear strength between the basal planes of the graphite, and that the mechanisms of graphite lubrication was that of slip between adjacent crystallites in contact. This view was further supported by the work of Jenkins (2) who showed that after polishing, graphite was found to have the basal planes of the crystallites nearly parallel to the sliding surface. Until the onset of the 1939-45 war, Bragg's theory was considered to fully explain the friction and wear behaviour of graphite. However, the operation of aircraft at high altitudes during the war resulted in very high wear of the brushes in their alternators. This high wear could not be explained by Bragg's theory.

Van Brunt(3) and Savage(4) carried out investigations into the failure of brushes at high altitudes. They performed a series of experiments in which carbon brushes were run under controlled conditions in a variety of atmospheres.

They came to the conclusion that the lubrication and low friction of graphite were not intrinsic properties of the graphite, but were due to

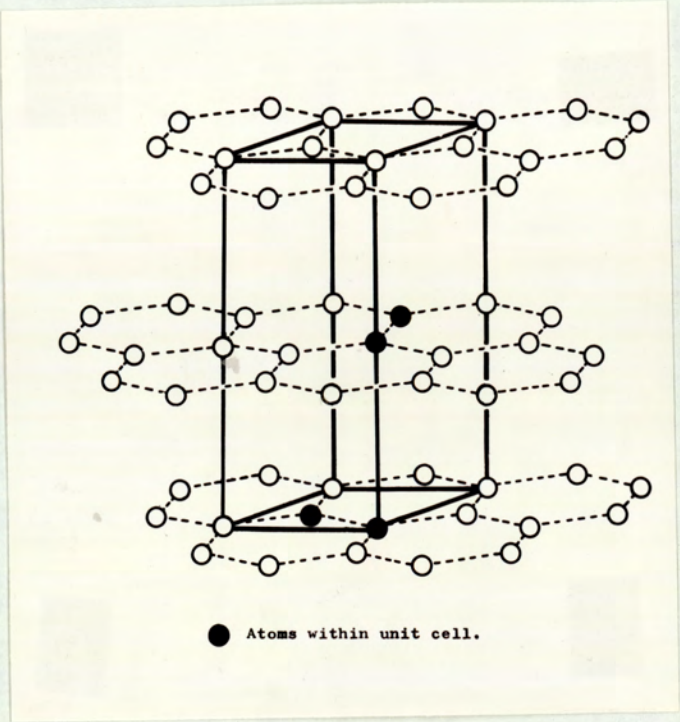

Figure 1.1 Hexagonal Structure of Graphite showing unit cell and atoms belonging to unit cell.

an adsorbed layer of molecules on the contact surface. Water vapour was found to decrease both friction and wear in proportion to its pressure up to a value of about 4 m.m. Hg. after which saturation occurred and no further reduction took place. Oxygen was found to have a similar effect but at much higher pressure, about 100 times higher.

In both dry air and vacuum they found that friction was high and catastrophic wear or "dusting", of the brushes took place. They suggested that the partial pressure of oxygen in dry air was not high enough to enable a complete adsorbed layer to be formed. High friction and dusting also occurred in dry nitrogen and was not affected by the pressure of the gas.

Savage suggested that the low friction of graphite was due to reduction in the surface forces of the graphite crystallites by the adsorbed film. He also demonstrated that wear debris produced during catastrophic failure had a very high absorptive power.

The nature and importance of the black film laid down by brushes sliding on copper on the running properties of the brushes was investigated by Van Brunt and Savage (5). They found that the film was composed of graphite and cuprous oxide and suggested that it consisted of a layer of cuprous oxide covered by a layer of graphite upon which the brush slid.

Later work carried out by Fullam and Savage(6) also investigated the surfaces formed by the sliding carbon brushes on copper. They found that graphite platelets present in the surfaces were not parallel to the sliding surfaces, but that the brush face consisted of a large number of tilted

"fingers" which were projections on the larger irregularities of the brush face. These projections showed a directional overlap which depended upon the direction of motion of the brush. This orientation of the crystallites of the graphite in the brush and laid down film has been reported by various authors and a great deal of discussion has centred around the question of which factor is most important in controlling the friction of graphite, the orientation of the graphite crystalites on the sliding surfaces or an adsorbed layer of molecules on the surfaces.

Campbell and Kozac(7) have attempted to rationalize the theories of Bragg and Van Brunt and Savage.

They investigated the effect of water vapour, oxygen and carbon dioxide on the dusting of carbon brushes. They found that a brush which had been run in the presence of water vapour of sufficient pressure exhibited low friction and wear in agreement with Savage and Van Brunt, but that these remained low for relatively long periods after dry nitrogen had been introduced into the system. When the running of the brushes was started in dry nitrogen; with no previous running in the presence of water vapour, dusting took place but stopped immediately if water vapour was introduced at sufficient pressure into the atmosphere.

Electron diffraction studies of the sliding surfaces revealed that in the conditions where the wear rate was small the graphite crystallites on both brush and track showed a high degree of orientation, in the cases where heavy wear had taken place no orientation was found.

They studied the effect of orientation of the crystallites by cutting brushes from a block of highly oriented natural graphite. The brushes were then run in one of three positions: with the cleavage planes parallel to the sliding surfaces, or in one of the two possible positions with the

cleavage planes perpendicular to the sliding planes.

When the brushes were run in a dry nitrogen atmosphere dusting took place if the cleavage planes were perpendicular to the sliding surfaces When the cleavage planes were parallel to the sliding surfaces the wear rate was very low. Similar results were obtained when an electric current of 114 amps/in^2 was passed through the brush. The authors also showed that the amount of dusting tended to decrease as the hardness of the metal upon when they were running was increased.

The authors suggested that the very high wear rate of the brushes was due, in part, to a breaking of welded carbon-carbon bonds. In a randomly orientated brush the material was soft and for a given load the real area of contact would be high, thus needing a high force to shear the bonds, resulting in high friction. The ploughing effect of those crystallites oriented such that they made contact at their edges also contributed to this high friction.

The introduction of water vapour to the interface was supposed to have a two fold effect. It tended to separate the two surfaces, hence reducing the number of welded contacts and also enabled the crystallites to orient until they were parallel to the sliding surface. This produced the condition of hard cleavage plane sliding upon hard cleavage plane, thus the area of contact was small and the friction low.

Savage's theory of low friction being associated with adsorbed surface layers was elaborated by Deacon and Goodman (8). They investigated the friction during sliding of various lamellar solids: graphite, molybdenum disulphide, boron nitride and talc. They proposed that the surface energies of the plate-like crystallites (low at the faces of the crystallites and high at the edges) were responsible for the cohesive friction of the material .

The authors suggested that in the presence of certain gases the edges of the crystallites reacted with the gases and a reduction of the surface energy at the edges occurred. This reduced the adhesion between the crystallites and accounted for the low friction. The orientation of the graphite crystallites did not cause the low friction but resulted from the low adhesion between crystallites enabling them to orient into their most favourable positions.

Although the experiments which they carried out had very little in common with the running of carbon brushes the results obtained by Porgess and Wilman(9) were very interesting. They investigated the effect of orientation on the friction of reactor graphite. The reactor graphite was rubbed on emery paper of various grades, and it was found that both the coefficient of friction, and the degree or orientation of the crystallites varied with the emery particle size.

The authors found the relationship $\mu = \tan^{-1}\delta$ to apply, where μ was the coefficient of friction and δ the angle between the normal to the basal plane of the crystallite and the normal to the running surface.

A more detailed study of the orientation effects of carbon brushes was carried out by Quinn. In 1963 he published a paper (10) describing the effect of load and surface finish of the copper on the topography and crystallography of the brush surface.

In the investigation into the effect of surface finish the brushes were run with a high load, about 500 p.s.i.(11N) on two disks, one of surface finish 2 μin C.L.A. and the other of surface finish 30μ in C.L.A. Reflection electron microscopy and reflection electron diffraction studies of the resulting surfaces showed that the surface finish had little effect on the crystallography of the surfaces but a marked effect on the~~ir~~ rubbed topographies.

The work showed that although less graphite had been laid down upon the smooth disk than on the rough disk, the brush which had been running on the smooth disk was much more heavily scarred than the one which had been running on the rougher disk. Quinn found that the surfaces of the brushes consisted of large smooth areas standing proud from the surrounding rougher brush material. He suggested that these large areas could have been areas which had been back transferred to the brush from the film on the copper although he found no evidence that any copper had been transferred to the brush.

In the investigation into the effect of load on the frictional force, the crystallography and topography of the surfaces the load was varied from 0.1N to 60N. The frictional force at each load was measured and the two running surfaces examined by reflection electron microscopy and reflection electron diffraction.

Reflection electron microscopy showed that for loads less than 1N and laods greater than 10N the track on the copper was rough with little laid down graphite. For loads between these two the track was much smoother and a lot of graphite had been laid down.

The reflection electron diffraction studies showed that the load also had a very marked effect on the orientation of the graphite crystallites on the brush surface as shown in Figure 1.2. For loads less than 3N, the angle between the surface of the specimen and the 0002 arcs on the diffraction photograph remained constant at an angle of about 20°. For loads between 3N and 60N the angle decreased with load to a value slightly above zero. For loads above 60N the crystallites reverted to random orientation.

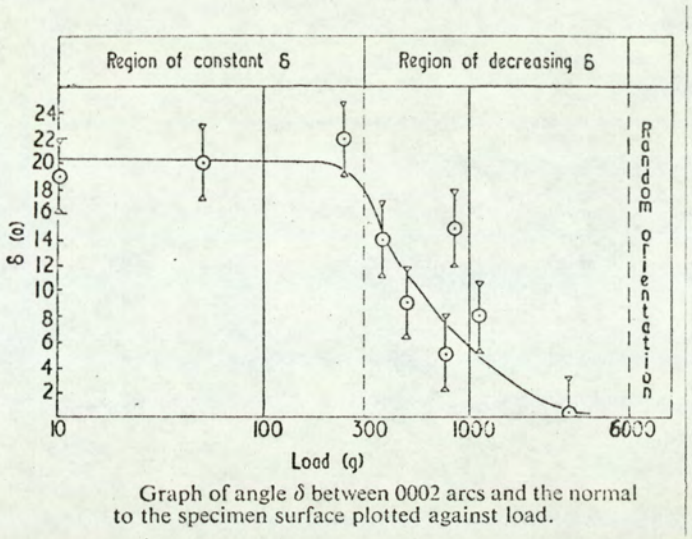

Graph of angle δ between 0002 arcs and the normal to the specimen surface plotted against load.

Figure 1.2 Variation in Angle of Tilt of Graphite Crystallites with Applied Load According to Quinn (10).

Quinn suggested that at loads less than 3N the orientation was due to twinning of the mosaic block in the electrographite as the brush wore. The effect of increasing the load was to increase the angle between the twins until a load was reached at about 60N when, in order to relieve the stresses set up, the crystallites had to take up a random orientation.

The relationship he obtained between the coefficient of friction at each load and the angle δ was more complex than that found by Porgesss and Wilman and was of the form $\mu = m \tan \theta +$ constant, shown in Figure 1.3.

In these experiments Quinn did not measure the wear rates of the brushes. The orientation could be a result of the wearing away of those crystallites which were not in a favourable position. At the high loads one would expect a very high wear rate which could lead to a condition where the brush was being worn away at such a high rate that very little oriented material was left behind.

The loads used by Quinn resulted in very high brush pressures; in the range from about 50 p.s.i. to about 3,000 p.s.i., compared with pressures

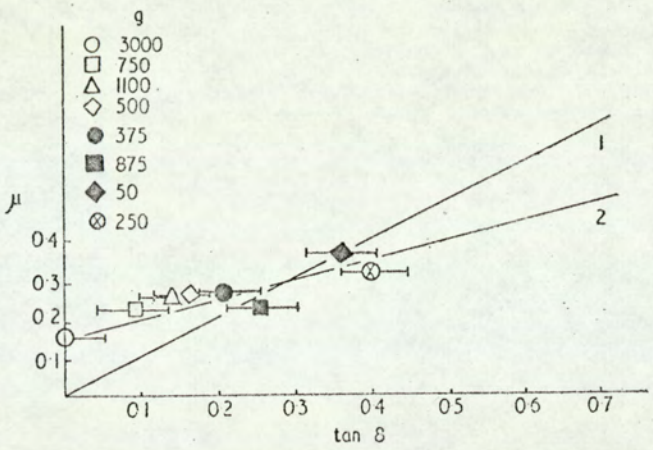

Comparison of observed coefficient of friction μ with tan δ, where δ is the tilt of the (0002) planes of the surface crystallites.

Figure 1.3 Relationship Between Coefficient of Friction and Angle of Tilt of Graphite Crystallites According to Quinn (10).

recommended for the running of brushes of $2\frac{1}{2}$ - 10 p.s.i. However, it has not yet been established whether the pressure at the interface, or the absolute load on the brush is the factor which decides the wear rate.

In a later paper Quinn (11) was able to remove the film which had been laid down on copper by an electrographite brush under a load of 1.1 kg. He used transmission electron diffraction to study the orientation of the film at varying depths. This showed that the film laid down under these particular conditions of sliding had an orientation with $\delta = 10^{\circ}$ at the surface, just below the surface increased to about 22° and at a greater depth below the surface the orientation of the crystallites became random. This sliding texture was explained by twinning of the transferred graphite crystallites. The work by Quinn suggested that variations in frictional forces may have been due to changes in orientation but he did not try to explain why high frictional forces occur when brushes are run without water vapour or oxygen and no attempt was made to control the atmosphere.

In contrast to the theory of Bragg (1)and the results obtained by Quinn (11) it has been shown by Midgley & Teer (12) that orientation of the crystallites is not a pre-requisite for low frictions. They investigated the friction of three types of carbon materials: a non-graphitic carbon,a graphitic carbon and graphite. They found that both the graphite and graphitic carbon became highly oriented after sliding. The non-graphitic carbon also became oriented but only after sliding for a long time. The coefficient of friction of this non-graphitic carbon was however as low as that of either graphitic carbon or graphite. The authors believe that the orientation of the non-graphitic carbon was due to a preferential wearing away of unfavourably oriented crystallites, leaving behind only the oriented ones. The low friction of the non-graphitic carbon was achieved even though initially a high proportion of the crystallites had their basal planes at large angles to the sliding surface.

The authors concluded that since it was evident that preferred orientation was not necessary for the low friction of non-graphitic carbon there was no reason to believe that it was necessary for the low friction of graphitic carbons or graphite. The temporary increase in friction which took place on reversal of the direction of sliding was explained by the authors as being due to interlocking of unfavourably oriented crystallites. This increase in friction was therefore due to a ploughing effect and due to adhesive friction between platelets.

In a similar series of experiments reported by Arnell, Midgley and Teer (13) the authors carried out an investigation into the friction of highly-oriented pyrolytic graphite sliding against steel. In these experiments, specimens of graphite were run with each of the three crystallographic directions in turn being normal to the sliding plane.

No significant differences in the friction between the steel and the graphite sliding in the three separate orientations was found. Similar results were also reported in a paper by Longley, Midgley and Teer (14).

The results of these three papers were thought by the authors to support the theory by Savage that the lubricating properties and low friction of graphite are not due to the graphitic structure but to an adsorbed layer on the surface, though the structure may be necessary for the formation of the absorbed film, it is not sufficient by itself.

The problem of the possible mechanism of graphite lubrication was further complicated by results reported by Bolmann and Speaborough(15) They found that reactor graphite which had been deposited on a microscope grid by rubbing had a tendency to roll up. They suggested that the low friction of graphite may be due to rolling up of flakes of graphite which then act as roller bearings between the surfaces, however, no further evidence in support of this hypothesis has been reported.

1.3. The Effect of Electric Current on the Friction of Carbon Brush Materials

Carbon brush manufacturers and users have known for a long time that when an electric current is passed through some grades of carbon brushes sliding on copper a decrease in the frictional force occurred - Hayes(16). The frictional coefficient in copper decreases from a value of 0.20 - 0.35 at zero current to a value of about 0.15 at high currents. Lancaster & Stanley (17) found that similar decreases in friction took place for electrographite sliding upon mild steel and other carbons. Figure 1.4 shows the variation in friction obtained by Lancaster & Stanley using a pin and disk assembly. They also found that the contact resistance of the brushes decreased with current even when running upon other carbon

materials. These contact resistance and frictional force changes were found to be irreversible over short periods of time, although recovery to the original values did eventually occur. Crossed carbon cylinder experiments were also carried out, in which the two surfaces rubbed on new material all the time. No decrease in friction between the cylinders occurred until an electric current of the order of 27 amps was passed through the contact. The initial low current and final high current values of frictional force when sliding on crossed cylinders were much lower than the values measured on the pin and disk machine (Figure 1.4) and were also independent of the applied load. From these crossed crylinder, carbon on carbon, experiments Lancaster & Stanley calculated a minimum contact temperature, caused by the heating effect of the current, below which no reduction in friction occurred. The critical temperature was strongly dependent on the type of carbon material used; baked carbon 560°C; natural graphite, 770°C, and electrographite, 900-1350°C. Lancaster and Stanley therefore suggested that both the decrease in friction and decrease in contact resistance arose from a single source, oxidation of the contacts. The mechanism proposed was that preferential oxidation of the brush binder resulted in large contact asperities breaking up into a number of smaller ones. The breakup resulted in a decrease in total real area of contact giving rise to the fall in friction, but an increase in the number of contact asperities hence the fall in contact resistance. The non-reversability of the behaviour was thus attributed to having to remove the oxidised surface layer by wear before the original values would be regained.

Although the oxidation may play an important role in determining the nature of the contact between crossed cylinders at high currents it is very unlikely that these high temperatures, above 600°C, would be reached

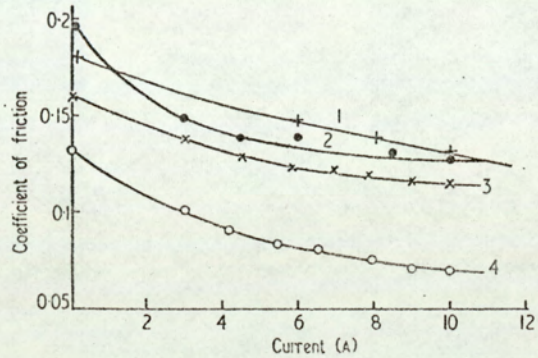

Variation of friction with current for electrographite C on (1) itself, (2) copper, (3) mild steel, (4) baked carbon A. Load 0·1 kg, speed 500 cm sec^{-1}.

Figure 1.4 The Effect of Electric Current on the Frictional Coefficient of an Electrographitic Brush Sliding upon a Variety of Disk Materials. Reproduced from Lancaster and Stanley (17)

during the sliding of graphite on metals passing the relatively low currents at which the decrease in friction first occurred.

E.Holm(18) has made an estimate of the contact temperatures between an electrographite brush sliding on electrographite, copper and gold disks, using a method designed by Holm(19). Running under a load of 240g.f. carrying an electric current of 10amps the maximum contact temperature was of the order of 200°C for isolated cases running on a copper disk, most of the time the temperature would be considerably less than this value.

Holm showed that even at temperatures below 200°C a decrease in the coefficient in friction was possible and this effect was attributed to a decrease in the adhesive or binding forces between graphite platelets. She began by assuming that the frictional force F, was given by $F = \psi A$ where A was the real area of contact and ψ was the specific friction force, or force per unit of area. For a load P the average pressure $\bar{p}$ was given by $\bar{p} = P/A$ and this led to the equation :

$$\mu = \frac{F}{P} = \frac{\psi}{\bar{p}}$$

Thus Holm began with the somewhat simplified assumption that friction coefficient was dependent only upon specific friction force, determined by adhesive forces, and the mean contact pressure. By measuring μ, and assuming $\bar{p}$ remained constant, she was able to show that ψ was dependent upon temperature and obeyed a relationship of the type $\psi(T) = \psi(To)e^{-\phi/kT}$ where ϕ was the binding energy of the graphite. In this paper Holm had assumed that frictional force was wholly dependent upon the adhesion between graphite platelets and ignored any other influences. She did, however, point out that it was unlikely that the absorbed layers of molecules on the surface of the graphite would be much affected by temperature up to 200°C and these effects could be ignored. This theory assumes a high degree of

orientation which as Midley and Teer have shown (12) is not necessary for low friction.

During the initial stages of running Holm found an increase in the frictional force with time of running. This effect was attributed to an increase in the real area of contact as the two running surfaces wore to make more intimate contact.

1.4. The Contact Resistance Behaviour of Carbon Brushes

The contact resistance of a carbon brush is the resistance across the interface between the brush and the moving slip ring or commutator. Under conditions of stable contact and low wear the contact resistance of a carbon brush sliding on copper is probably the most readily explained brush characteristic. The positive or anodic, brush is taken by most workers to be the brush from which conventional current flows to the moving contact, whilst the negative, or cathodic brush is the brush to which conventional current flows, from the moving contact. Under conditions of stable contact, with no arcing across the interface, it has been generally accepted that conduction will take place between contact asperities on the brush, and similar asperities on the copper, and that oxide film on the copper greatly influences the contact resistance behaviour. The contact resistance for carbon brushes has been shown by a number of authors including Davies(20) and Bickerstaff(21), to be non-ohmic over most of the current range used. The contact resistance falls from a value of about 10^{3} ohms at very low currents below 1mA to a value of about 10^{-1} ohms when the current is increased to above 10amps.

Van Brunt(4) has shown that the presence of oxygen increases the contact resistance of carbon brushes and suggested that this was due

to an increase in the thickness of the insulating copper oxide film.

Davies however showed that the effect of oxygen on contact resistance was more complex than reported by Van Brunt. An increase in oxygen pressure increased the contact resistance between the positive brush and the copper, this being in agreement with Van Brunt. The dependance of the contact resistance of the negative brush upon oxygen pressure was found to be influenced by the presence of water vapour. In general, however, a decrease in contact resistance occurred.

Ragnor Holm, in his book (19), has covered the whole field of electric contacts, both static and sliding. Much of this work has formed the basis of the present ideas on the contact between a carbon brush and copper.

The very small areas of two contacting surfaces through which electrical conduction takes place are termed "a" spots. The contact resistance between the two contacting surfaces is due partly to the constriction resistance of the "a" spots arising from the size of the spot and partly to the resistance of any insulating film between the surfaces (19).

The surface of copper in air is normally covered with a relatively thick, insulating, copper oxide film. For conduction to take place between the brush and the copper, the copper oxide on the contact asperities must be broken up, by either electrical or mechanical means. Thus, the contact resistance of the carbon brush must depend upon the equilibrium which is set up between the breakdown of the oxide film and the reoxidation of the copper. Any factors which reduce the oxidation rate, or assist in the breakdown of the oxide should decrease the contact

resistance. Any conditions which accelerate the oxidation of the copper, or lays down other insulating films should increase the contact resistance.

When two stationary contacts are brought together with a thin, insulating film between them, then conduction may take place by tunnelling or by thermionic emission through the film separating the contact asperities. If the voltage across the interface is increased until a field of about 10^8 volts/m is produced across the separating film then electrical breakdown of the film can take place. This electrical breakdown produces "a" spots on the contact asperities through which conduction takes place. The formation of "a" spots by electrical breakdown is known as "A-Fritting" (19).

Holm (22) has shown that at room temperature a copper oxide film of thickness 40Å should conduct mainly by thermionic emission due to movement of electrons over the potential barrier formed by the film. A film thickness 10Å will however conduct mainly by tunnelling through the barrier.

E.Holm(23) carried out work on very smooth films formed by running carbon brushes for long periods without current. She found that films as thin as 60Å required breaking down by A-fritting before electric conduction took place. After breakdown a very thin oxide film, about 10Å, remained on the contact surface through which conduction by tunnelling took place.

Stebbens (24) has used a laminated brush to investigate the contact of electrographitic brushes running on copper. The wave form of the voltage drop across the interface was displayed on an oscilloscope which was triggered by the rotation of the disk. Using this method the waveform between a small area of the brush and a small area of the disk could be

studied. He found that the waveform between the positive brush and any small area on the disk remained the same for a considerable length of time. Since, during this time the brush had worn down appreciably, he suggested that the waveform was due to contact spots on the copper and that the same spots remained conducting for long periods. Stebbens also suggested that the number and area of the contact spots was strongly dependent upon current, an idea which has been expanded by Bickerstaff (25) and this resulted in the non-ohmic behaviour.

The waveform between the negative brush and the copper was not constant or reproducible, and transferred copper was found on the negative brush, a phenomenon known as copper picking. Stebbens suggested that this copper embedded in the brush took over the role of conduction from the normal contact spots on the copper, which remained however as load bearing areas. To support this view he found that conducting spots on the positive brush ceased to conduct almost immediately when the current direction was reversed, but became conducting when the current direction was charged again. Rapid oxidation of the contact spots under the negative brush was thought to happen.

Bickerstaff (21) has carried out an ivestigation into the effect of mechanical load and electric current on the contact resistance of electrographite brushes sliding on copper and gold. He confined the work mainly to a study of the characteristics of the positive brush because of the complications caused by copper picking onto the surface of the negative brush. Shown in Figure 1.5 are the contact resistance versus applied voltage characteristics obtained by Bickerstaff.

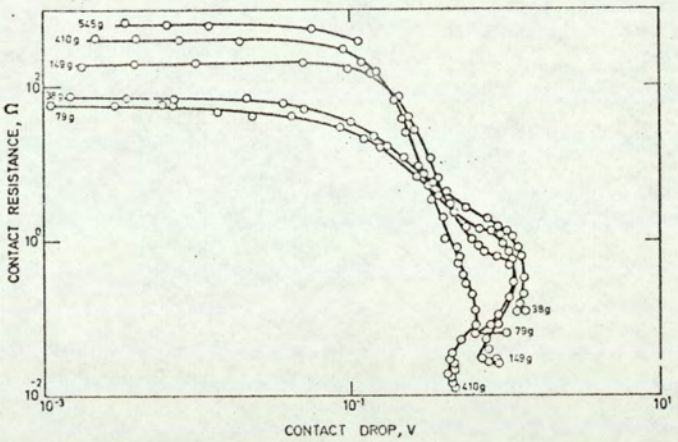

Resistance–voltage characteristic at various loads from 38 g to 545 g

Figure 1.5 Variation in Contact Resistance of an Electrographite Brush, Sliding on Copper with, Contact Potential at Various Loads. Reproduced from Bickerstaff (21).

Figure 1.4

These results showed that the contact resistance of brushes running on copper, in air, was ohmic for a range of loads, between 0.37N and 5.4N provided the voltage drop across the interface did not exceed about 0.1 volts. In this ohmic region the contact resistance for a load of 0.37N was about 10^2 ohms but increased with load to about 10^3 ohms for a load of 5.4N. When the potential across the interface was increased above 0.1volts the contact resistance fell sharply to a value of about 1 ohm at a potential of 1.0 volts. Above this voltage the resistance was again ohmic until arcing across the interface occurred. The fall in contact resistance which took place between the two ohmic regions was assumed to be due to electrical disruption of the oxide film at the edges of the conducting spots causing an increase in the area available for conduction. At high voltage complete disruption of the oxide film resulted in the

contact resistance being due almost entirely to the constriction resistance of the contacts, and the interface behaved in an ohmic manner. An increase in load caused an increase in the load bearing area of the contact with a resultant decrease in contact resistance.

The opposite effect was observed for the low voltage ohmic region, an increase in load causing an increase in contact resistance. Bickerstaff suggested that as the brush load was increased the two contact surfaces became smoother, due to increased polishing thus making more intimate contact. The reduction in real pressure at the contacts which therefore occurred enabled thicker oxide films to build up at the contacts, resulting in higher resistances.

At high currents the contact resistance was unaffected by changes in atmosphere indicating that large scale disruption of the oxide film had taken place.

The resistance characteristics of electrographite sliding on gold were the same in both air and nitrogen. The resistance was low and ohmic up to large currents when a slight decrease occurred. At high currents the resistance of brushes running at the same load were the same on both copper and gold. This showed the importance of the oxide layer on copper at low currents. The contact resistance of the brush running on gold, which had no oxide layer, was virtually independent of current and dependent only upon the applied load. This state was not reached on copper until the oxide film had been completely disrupted.

Bickerstaff suggested that the contact resistance of electrographite sliding on copper was controlled by oxidation of the copper contact asperities during contact with the brush. The most important factor being the thickness of the oxide layer, which in turn was determined by the depth at which the

oxide recrystallised from the pseudomorphic structure in contact with the copper to the cuprous oxide structure. This proposal by Bickerstaff is in disagreement with many authors, notably Lancaster(26) who maintains that oxidation of the copper is controlled by the time available between contacts, and Spry and Scherer(27) who suggest that the bulk temperature of the copper has a greater influence upon oxidation than does the flash temperature of the contacts.

An investigation has also been carried out by Bickerstaff(25) into the number of contact spots between an electrographitic brush and a copper surface. Using a method devised by Holm(28) he measured the number of contacts beneath the brush at currents from 2mA to 10A. He found that the number of contacts remained more or less constant for currents between 10mA and 1.0A. The fall in contact resistance with increasing current which occurred in this range must have been caused by an increase in conducting area of existing contact spots rather than the formation of new areas.

The author suggested that since the number of electrical conducting spots remained constant, the number of electrical contacts would equal the number of load bearing asperities. If this were not the case some load-bearing spots would have to remain insulating due to oxide. This requires the existence of a second type of contact with a greater affinity for oxygen.

At currents below 10mA, the number of contacts apparently decreased. Bickerstaf thought that this may have been due to packed carbon debris building up around the copper contact asperities and relieving them of their conducting role. A second explanation could possibly be re-oxidation of small, lightly stressed contact asperities causing these asperities to become insulating.

At high currents, above 1.0A, the number of contacts appeared to increase. However, using this method he could not determine whether this was a real increase in number or a lengthening in the spot in the direction of sliding, as reported by Shobert(29).

Bickerstaff(30) suggested that at high current densities Joule heating could result in softening of the copper. If this happened the contact spots could enlarge or merge to form large contact areas.

1.5. The Wear of Carbon Brushes

The wear rate of brush materials is the characteristic which is most liable to be affected by running conditions. Atmosphere, brush pressure, brush or commutator vibration and high current density are just a few of the many factors which change the wear rate, usually adversely.

There is little evidence to support the view that wear by an electrical process takes place when brushes are carrying moderate electric currents. When arcing takes place across the interface, a high wear rate normally occurs, but this is most likely due to oxidation and erosion of the carbon. The effect of current on the wear rate is probably due to changes in the physical properties of the brush or copper, or both.

The wear rate of brushes is normally measured by the volume of material removed per unit distance of sliding (e.g. mm per mm sliding). An acceptable value for an electrographitic brush material sliding on copper would be of the order of $10^{-9} mm^3/(mm)$. A change in the running conditions can increase this by two or three orders of magnitude but it is very unlikely that the wear mechanism remains the same under the different conditions.

When a newly prepared brush is run on a freshly-machined copper surface, the initial wear rate of the brush is high. This is because the relatively rough surfaces of the brush and copper cause brush wear by an abrasive mechanism. Under normal conditions, the surface of the brush will wear to suit the topography of the copper. The higher surface asperities of the copper will become worn away and a layer of carbon will become deposited upon the copper, resulting in a smooth surface and a reduction in wear rate.

When both the brush and copper have developed a smooth film-like surface, the wear rate usually reaches an equilibrium value.

Lancaster (26) has studied the effect of load, sliding speed current and apparent area of contact on the wear of an electrographite brush sliding on copper. He suggested that the wear rate of the brush was controlled mainly by the nature of any film formed on the copper, and the way in which any parameter affected this film formation determined the influence that parameter would have on the wear rate. In this paper Lancaster also demonstrated that the initial decrease in wear rate which occurs when a new brush is run on a freshly prepared copper surface is due almost entirely to changes taking place on the copper surface .

Lancaster carried out investigations into the effect of load, sliding speed, electric current and apparent area on the topography, crystallography and composition of the surface film. The results obtained were thought by Lancaster to show that the oxide layer on the copper not only controlled the contact resistance but also played an important part in controlling the wear rate of the electrographite. At a high load, 500 gf and a high sliding speed the wear rate of the brush was relatively high and the copper surface was covered by a black, continuous layer of graphite.

The contact resistance was low, in the region of 0.05ohms, suggesting that only a very thin layer of oxide was present on the copper contacts. Lancaster measured the contact resistance using a milliohmeter which applied a potential across the interface not exceeding 0.1 volts. Using the same load Bickerstaff(21) has shown the contact resistance to be high and ohmic at these potentials. This example illustrates how different authors operating under approximately the same conditions, using similar materials, can obtain conflicting results from different wear test machines. Electron diffraction studies of the film formed on the copper at 500gf load revealed that the major constituent was graphite, with little Cu_2O or CuO, although it is doubtful whether this analysis gives information about oxidation of the contact asperities. The wear rate of the brushes remained constant up to large values of electric current when a slight decrease began to occur. Lancaster suggested that this decrease was due to the oxide film beginning to reform because of the heating effect of the current.

At a low load, 50gf, the copper surface was covered by a light brown film, which was shown by electron diffraction to consist mainly of Cu_2O with very little graphite. When running at this load the wear rate was low and the contact resistance high, about 200 ohms. When an electric current was passed through a brush operating under these condition the wear rate increased, together with the amount of graphite laid down on the copper. An upper limit to the wear rate was reached only when the track was completely covered with graphite.

In general, the surfaces formed upon the copper could be divided into the two categories described above, characterised by a little laid down graphite or, a thick layer of graphite. Which type of surface formed depended upon the running conditions, in particular, the wear rate of the brush. However, no such division could be made for the

brush surface which had the same appearance irrespective of the running conditions. Reflection electron microscopy and optical microscopy showed that the brush surface consisted of very large smooth areas with regions where graphite had apparently been back-transferred to the brush surface from the track on the copper. Electron diffraction showed that Cu_2O was transferred to the brush face.

When using conical brushes, and brushes with a small cross-sectional area, Lancaster found a critical load of 100 gf below which the wear rate was low with little laid-down graphite and a high contact resistance 10^2-10^3 ohms. Above the critical load the contact resistance fell to 10^{-2} ohms, the wear rate increased and a thick layer of graphite was deposited on the copper. A similar sudden increase in wear rate has been reported by White (31) at about the same load, although the pressure was much lower.

Lancaster suggested that the action of the copper oxide was to inhibit the deposition of a layer of graphite on the copper and that the high wear rate of the electrographite when no oxide was present was a consequence of the laid-down film, not vice versa. The laid-down film in the severe wear region was in dynamic equilibrium. Below the critical load the layer of copper oxide prevented the formation of a graphite film and low wear took place. The effect of load was to mechanically disrupt the oxide and enable graphite deposition to occur, although Holm (23) has shown that without electrical breakdown a very thin oxide film may still cover the copper.

The effect of current was also to disrupt the oxide, enabling graphite to be laid down upon the copper, thus increasing the wear rate of the brush. At high currents the oxidation of the copper increased

and the wear rate decreased slightly. This suggestion by Lancaster implied that at high currents the rate of oxidation induced by the current was greater than the rate of breakdown of the oxide by mechanical and electrical means. This seems unlikely, since the work of Bickerstaff shows that complete disruption of the oxide takes place at relatively low currents.

One would expect, if Lancaster's suggestion is right, that the limiting value of wear rate would be attained at much lower currents than the values he measured.

The thickness of the oxide film, and hence the wear rate was also thought by Lancaster to be dependent upon the time between contacts and the mean temperature of the copper. Any factor which increased the time between contacts, e.g. a decrease in speed, should decrease the wear rate and Lancaster showed this to be true in certain cases.

The mechanism of wear taking place at the interface was proposed by Lancaster to be one of fatigue for both mild and severe wear. The stresses set up in the material in the mild wear case of graphite sliding on copper oxide and in the severe case of graphite sliding on graphite were elastic, due to the very smooth sliding surfaces. In the mild wear case, the elastic stresses were very low and a large number of cycles were needed before failure of the graphitic material took place, producing a low wear rate.

In the case of severe wear, the surfaces were still very smooth and the stresses elastic. But, due to the friction of graphite on graphite being greater than that of graphite on copper oxide, the stresses were much higher. Hence a lower number of stress cycles were needed before failure occurred and the wear rate was higher.

No other evidence has been reported that the friction of graphite on graphite is greater than graphite on copper oxide. In fact, if this were the case, as the current passing through the brush increased the amount of graphite laid down should increase, according to Lancaster, and an increase in friction should occur. In practice the opposite effect is found, a decrease in friction takes place with increasing current.

More evidence to support his view that wear was by a fatigue mechanism was presented in another paper by Lancaster(32). He demonstrated that if the slopes of the surface irregularities were below a value needed to produce plastic deformations then wear by fatigue could be a probable mechanism. The maximum slope of a surface irregularity which can be deformed elastically is inversely proportional to its modulus of elasticity. In the case of metals this slope is about 1° but for carbon it is within the range 7°-15°. Reflection electron micrographs of the carbon surfaces showed that in most cases the slopes of the irregularities were below or within this range. The value of surface slope quoted by Lancaster was calculated with the assumption that the modulus of elasticity of the surface film of carbon was the same as that of the bulk material. This is very unlikely since the modulus of elasticity of bulk carbon must be affected by the porous nature of the material.

In the experiment Lancaster used crossed-cylinders of carbon with a load applied between them and one of the cylinders sliding against the other. He measured the number of cycles required at various loads before pitting of the carbon surfaces occurred. The relationship between mean Hertzian stress at the contact surface and the critical number of cycles before failure was found to be of a fatigue type.

These results were elaborated upon in work reported by Clark &

Lancaster(33). Cylinders of graphite or baked carbon were run against cylinders of the same material or copper. Cylinders running against ones of a similar material exhibited a short period when polishing of the surfaces occurred and negligible wear took place, the duration of this period decreased with load. After this initial period the wear rate increased but remained low, about 10^{-11} cm^3/cm/kg., for another period which also decreased with increasing load. After this period the wear rate was high, about 10^{8} cm^3/cm/kg. The change to high wear rate was found to be associated with the formation of blisters on the surface, which then broke up leaving behind a rough surface. The whole cycle was then repeated.

The duration of the period during which wear occurred decreased with load in a similar fashion to the way in which the number of cycles to failure varied with Hertzian stress, as reported previously.

The thickness of the surface film was about 60μ and was of the same order as the size of the wear debris, about 50μ . The surface damage however, seemed to extend much deeper into the carbon about 450μ . The authors suggested that the eventual failure at the surface may have been caused by relative movement of the subsurface region.

When running on copper some of the materials exhibited much the same characteristics as when sliding upon themselves and after failure the wear particle was transferred to the surface of the copper. No transfer of material to the copper took place until a degraded layer had formed on the surface of the carbon. It appeared that transfer to the copper took place only if the carbon material was of a comparable hardness to that of the copper or softer. Following this transfer to the copper the amount of degradation of the surface increased and the authors

suggested that this was responsible for the observed increased wear rate.

White (31) has used the scanning electron microscope to investigate the failure of electrographitic brush material sliding upon copper. His micrographs suggest that wear takes place by a fatigue process which initiates blistering of the graphite film. This blistering leads to cracking and break up of the film causing wear to take place as flakes of graphite became detached from the film.

Both load and current were found to increase the wear rate, and a discontinuity was found in the graph of wear rate against load similar to that reported by Lancaster (26). Micrographs of the surfaces formed at a light load with current and a higher load without current showed that the topographies were very different, even though the wear rates under the two conditions were similar. This suggests that the wear mechanisms under the two conditions were not the same.

The micrographs also indicate that failure of the films took place at different depths within the film at different loads. This it appears that increasing the load increased the stress at existing load bearing areas, thus causing failure deeper within the film, instead of increasing the number of load bearing areas and keeping the stress constant. Bickerstaff (34) has shown,however,that increasing the load increases the number of electrically conducting spots in an almost linear manner. He has also shown that the number of electrically conducting areas give a good measure of the number of load bearing areas. Thus it would appear that these two results are conflicting even though the work was carried out on almost identical material and under very similar conditions. White (31) suggests that the wear rate of the brush may be dependent upon the depth at which failure occurs within the surface layer.

1.6 Summary of the present "state of the art" and outline of research carried out in this investigation

From the results of published work described in the preceding sections, it is clear that the mechanisms of operation and failure of carbon when being used as a sliding electric contact, are not fully understood. Many of the results are in some instances contradictory. One of the major problems in interpreting and comparing results arises from the extremely large number of possible combinations of carbon-brush material and slipring, or commutator, metal. To investigate even a fraction of these combinations would present an impossible task and most researchers have chosen only to look at one or a very small number of possible combinations.

Many of the problems encountered in using carbon as a sliding contact have been investigated by brush manufacturers or machine-users in an empirical manner. A variety of brush materials, or grades, have been run on the machine under the required conditions until a satisfactory,or compromise, solution has been reached. Most of these solutions have come about with little fundamental scientific research. It would also appear true that few of the investigations described have yielded results which have been used by brush manufacturers to improve brush performance, one possible exception being the development of brushes for high altitude use.

Debate still continues on the importance of orientation of the graphite crystallites in the sliding behaviour of carbon. In spite of the relatively large amount of material published on this topic, two schools of thought still continue. On the one hand is a group which considers the crystallography of the carbon material to be of prime importance in

determining the sliding characteristics. On the other hand, there is another group which considers the lubricating properties of carbon to arise entirely from an absorbed molecular layer on the graphite surface, and any orientation of the graphite crystallites is a result of the sliding mechanisms. It is not intended that this project should become directly involved in this question, although any relevant information obtained will obviously be discussed.

The contact resistance between a carbon brush and a copper surface has been investigated by a number of workers and this aspect of carbon-brush behaviour is probably the most fully understood. It has been generally accepted that the contact resistance at the interface of most metals is dependent more upon the nature of any oxide films at the interface, than the constriction resistance of the contacts. The decrease in contact resistance with increasing electric current has been universally attributed to an initial breakdown of the copper oxide film when the electric field across the oxide exceeds a value of about 10^8 volts/m. This electrical breakdown is followed by further disruption of the oxide as the electric current is increased. The effect that changing the running conditions has upon this oxide breakdown has not however been fully investigated. Work now being carried out by Bickerstaff(35) suggests that this explanation may be only part of the full picture and that variations in the contact resistance may arise from physical changes in the oxide film other than electrical or mechanical breakdown.

One of the most important characteristics of carbon brushes from a machine-users viewpoint is the decrease in frictional force between some types of carbon brushes and the slip ring or commutator with increasing electric current. Neither the oxidation theory of Lancaster nor the temperature dependence theory of Holm (both of which have been proposed

to explain this phenomenon) has been accepted by brush manufacturers since each one can only apply under specific conditions.

At the beginning of the literature survey it was pointed out that most of the investigations have been carried out into the sliding carbon brushes on copper surfaces since this is the most common metal used for slip rings or commutators. This restriction of the investigations by many authors to one metal has also restricted the scope of the solution since they were looking for answers to only a very precise problem. Another method of investigation is to consider the carbon-copper situation as only one small aspect of a much wider problem, that of carbon sliding upon any material. If broad patterns of behaviour can be established, then it should be possible to apply these broad solutions to explain the brush behaviour under more specific conditions. This thesis will describe a programme of research which has been carried out in which particular carbon brush material has been slid upon a range of materials in order to establish how the brush sliding characteristics vary with load and current. The three properties which have been fully investigated are the wear rates(of both brush and slip ring material) the contact resistances and the frictional forces.

Aluminium was chosen as one of the slip ring materials for two reasons, namely (i) because of its physical properties and (ii) because of interest in aluminium as a sliding contact from economic considerations. Pure aluminium is one of the softest materials which would be considered as a slip-ring material and hence could be used in any investigation into the effects of hardness. The oxide formed upon the surface is a hard, semi-passive protective film and is thought to act as an abrasive in a sliding situation. Thus a wide range of possible variables are present using one material. The other reason for choosing aluminium as one of the slip ring

materials was because of interest shown by some electric-motor manufacturers in the use of aluminium as a commutator material for fractional H.P.electric motors. In recent years, because of political uncertainty in some copper-producing areas and a world-wide shortage of copper, the price of copper has been steadily increasing. The high price of copper has forced many of its users to turn to aluminium as a substitute for copper electrical conductors.

In cases where the physical strength of the material is not of prime importance and the same volume of either copper or aluminium can be used to produce the component, as in the case of small commutators, an 80% reduction in the cost of materials can be achieved. This reduction in cost amounts to a considerable saving by manufacturers who produce a large number of electric motors, for example the manufacturers of vacuum cleaners and electric drills. The change to aluminium alloy commutators would also reduce the possibility of any disruption in production due to a shortage of copper.

At the time of writing two major problems prevent manufacturers changing to aluminium alloy commutators in fractional H.P. electric motors. The first difficulty lies in joining the armature windings to the commutator. At present, copper windings are spot-welded onto the copper armature. If the saving in material cost is to be realized then aluminium alloy must also be used as the armature winding. Unfortunately, difficulties in welding the aluminium alloy windings to the aluminium alloy commutators have resulted in increased production costs swallowing up any saving on material cost.

The other problem is of a tribological nature. Brush manufacturers and users have dismissed aluminium and its alloys as unsuitable commutator

materials because of high wear of both the brush and the metal. These high wear rates have been attributed mainly to the softness of the metal, although no results have been published which either confirm or refute this belief. Development work is however being carried out by at least one electric motor manufacturer to find a suitable graphite brush - aluminium alloy combination for use as the commutator in fractional H.P. electric motors.

The research about to be described has had two main, fairly broad, aims. The first aim was to investigate the sliding of a carbon brush upon a number of slip ring materials and not concentrate upon carbon-copper contacts. The investigation involved measurements of those parameters of most concern to electrical machine users, namely wear rate, frictional force and contact resistance. An attempt was made to correlate these characteristics with any physical changes occurring at the contact interface and the physical properties of the contact materials. From the results of this survey it was hoped to build up a broad picture from which it would be possible to predict how other brush-slip ring combinations will behave under given conditions of load, speed and current. An analysis of the surfaces generated during sliding at various currents was also carried out to try to explain the decrease in frictional force between some types of carbon brushes and copper surfaces with increasing electric current. Any explanations arising from this broad investigation must of course fit in with the knowledge already obtained about carbon brushes sliding upon copper.

The second main aim of the project was to investigate in some detail the sliding of a carbon brush upon slip rings of pure aluminium under controlled conditions. From the investigation it was hoped to obtain

information about the failure modes of such a system, in particular the wear rates of the brush and aluminium. It was hoped that any information gained would be of use to manufacturers of brushes and electric motors wishing to develop a brush-aluminium alloy combination suitable for use in fractional H.P. electric motors. The aims of the project do not, however, embrace any attempt to develop, or even suggest, suitable combinations.

To carry out this research programme it was necessary to build a reliable wear test machine, which could withstand almost continual running throughout the project, together with any required ancilliary measuring equipment. The wear test machine and associated equipment will be described in detail in Chapter 2. Measurements were made of the three main parameters used to describe a carbon brush - slip ring assembly, namely, wear rate, frictional force and contact resistance on a variety of slip ring materials. Wear specimens generated during these experiments have been studied by a number of analytical techniques to gain information about any possible changes occurring at the interface or in the underlying material.

The brush manufacturers produce a very wide range of brush materials which have been developed for use under various conditions of operation. Some of these brush materials have a very limited application whilst others are of a more universal type. A brush material from the latter category was chosen for these experiments, namely, an electrographite grade (EG14) manufactured by Morganite Carbon Co.,Ltd. This brush material is used in a wide range of electrical machines operating under fairly diverse conditions. Another reason for choosing this material is that there have been a number of reported investigations using this or very similar electrographites under conditions similar to those proposed here. This brush material is also known to exhibit

a decrease in frictional force with increasing electric current.

The literature survey has shown that the sliding characteristics of carbon brushes are influenced to some degree by both sliding speed and atmospheric humidity. To reduce the number of variables these two parameters were kept fixed during most of the experiments. Very little variation in sliding characteristics takes place over a wide range of sliding speed or humidity either side of the chosen values.

Chapter 2 The Wear Test Machine and Ancillary Equipment

2.1 Wear Test Machine

The experiments were carried out on the pin and disk machine shown in Figure 2.1. The machine consisted of a bearing housing and main shaft assembly mounted upon a thick steel plate which formed the "bed" of the machine. Supported on this steel plate by three pillars was a duralumin plate above which the disk under investigation rotated, on the end of the main shaft. The carbon brushes under investigation were carried in brush holders mounted upon the duralumin plate. The area above this plate was covered by a large bell jar.

The duralumin plate and bell jar isolated the part of the machine where the experiments were carried out from the "mechanical" components and this prevented contamination of the surfaces.

The main shaft was driven by a variable speed electric motor. The wear machine was mounted upon a rigid steel frame.

2.2 Bearing Housing Assembly

The design and construction of the bearing housing, Figure 2.2, was a major factor in deciding the performance and reliability of the wear test machine. The disk under investigation must be free from lateral and axial vibrations and this can only be achieved if the main shaft runs true in its bearings. The experiments performed necessitated running the machine continuously for periods as long as three months and the bearing assembly must be capable of carrying out this requirement without failure or appreciable wear of the bearings.

A cross sectional view of the bearing assembly is shown in Figure 2.3. The two inner surfaces of the outer housing which

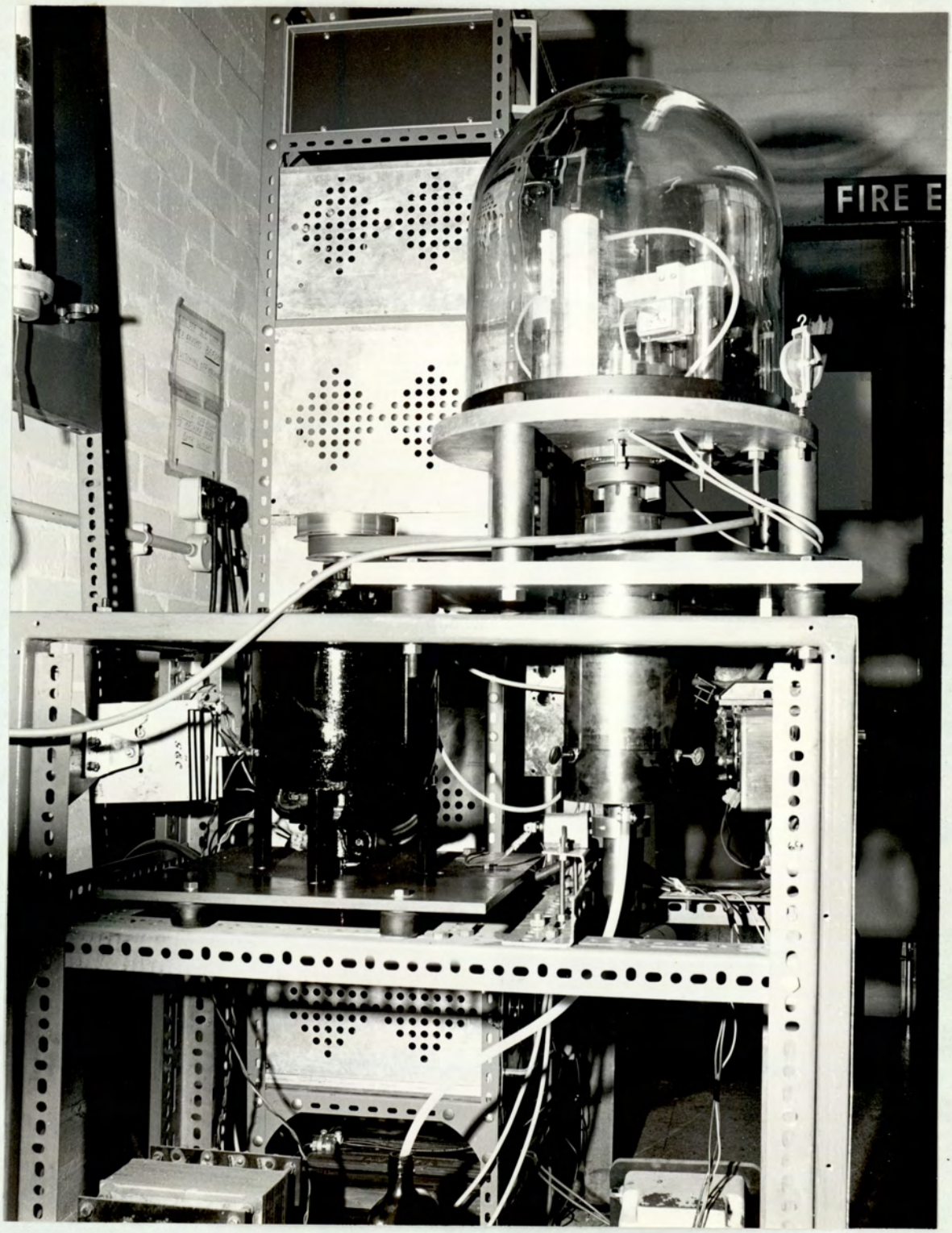

Figure 2.1 General View of Wear Test Machine.

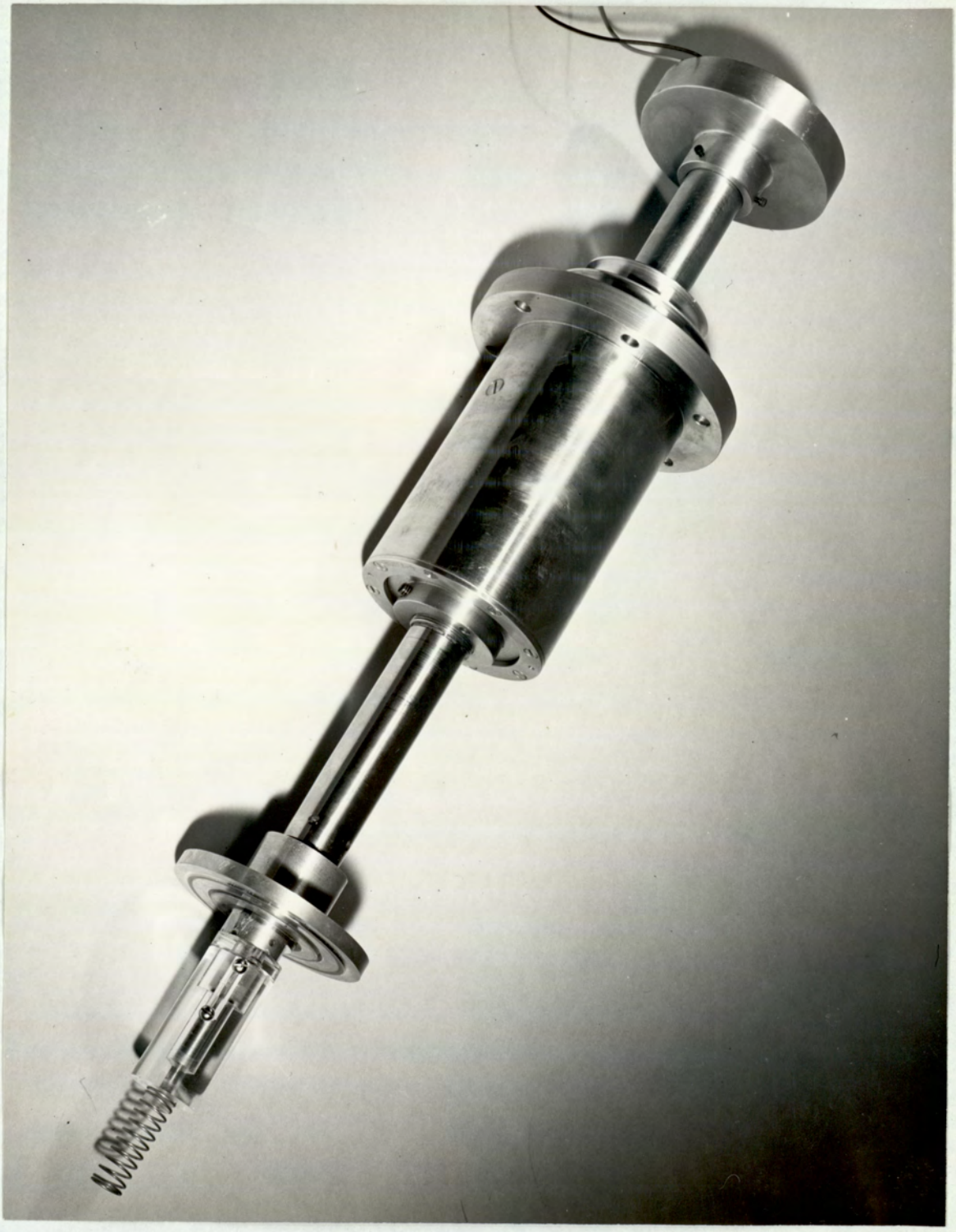

Figure 2.2 Bearing Housing, Main Shaft and Mercury Contact Assembly.

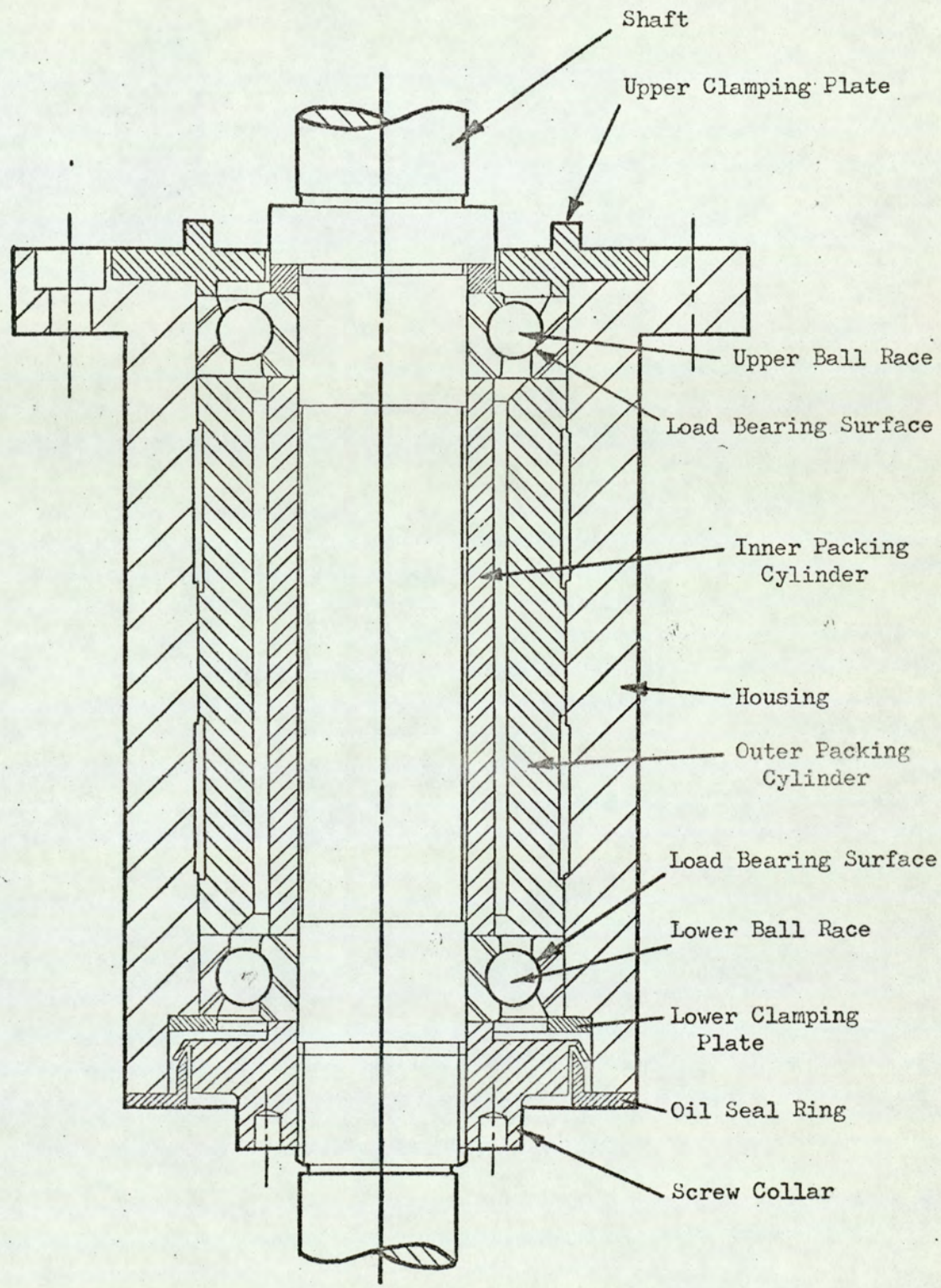

BEARING HOUSING ASSEMBLY

FIGURE 2.3

mate with the ball races were coaxially ground so that the races were an interference fit inside the casing. The two bearings were pressed into the housing and the outer two races held a fixed distance apart by a packing cylinder. Two clamping plates at the top and bottom of the casing held the outer races firmly in position. The two inner races were held a fixed distance apart by the inner packing cylinder and two collars on the main shaft. The upper collar formed an integral part of the shaft whilst the lower collar screwed onto the shaft and held the two inner races firmly in position.

The amount of end float in the bearings was measured and the length of the inner packing cylinder adjusted with shims until the load was taken on the surface of the outer races shown. After this adjustment the bearing assembly acted as a thrust bearing and no wobble of the shaft occurred. Unfortunately any wear of the ball races will alter the end float of the bearings and readjustment will be required.

The bearing assembly was originally designed to preload the bearings with a spring loaded cylinder as shown in Figure 2.4. The outer race of the upper bearing was held in position by a fixed cylinder. Thedistance between the two inner races was determined by the length of the inner cylinder and these were held in place by the two collars. The outer race of the lower bearing was free to slide in the housing and was held in position by the spring loaded cylinder. This system compensated for any change in the end float as the bearings wore.

The advantage with this system is the correction for changes in end float, unlike the other design where reshimming is necessary. There is however the possibility that the lower race could become

slack in the housing, causing vibrations of the shaft.

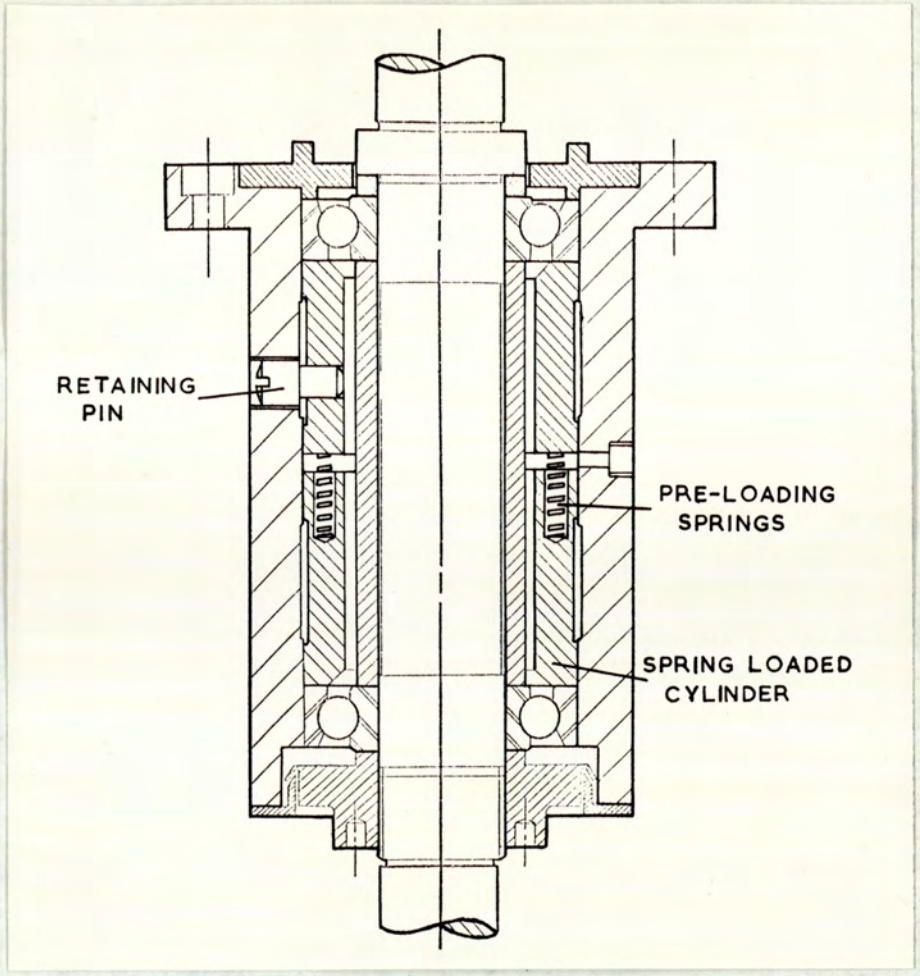

Figure 2.4. Original bearing housing design.

For this reason the method of preloading using shims was chosen since wear of the housing should be very small if the system is correctly lubricated.

2.3 Main Shaft

The main shaft, which can be seen in Figure 2.2 was constructed from HE805 heat treated steel. The total length of the shaft was 21", and great care had to be taken in machining the surfaces since any misalignment would possibly have resulted in flexing of the shaft at high speeds and vibration of the disk surface.

The centre of the shaft was bored out to a diameter of $\frac{1}{2}$" so that wires could be taken from the disk at the top of the shaft to a rotating contact assembly at the lower end of the shaft.

The top of the shaft was ground to a taper to accommodate the top plate upon which the disks under investigation were mounted. This brass top plate was made on the same machine tool as the taper on the shaft so that the same taper was machined on both parts, ensuring a perfect fit. The top plate was held onto the shaft by three screws locking onto an undercut portion of the shaft. Locking on to the undercut portions prevented damage to the tapered part and misalignment of the plate.

2.4 Bearing Lubrication.

The bearing assembly was packed with grease on assembly. Further lubrication was provided by a grease nipple and an oil way to each ball race.

2.5 Electric Motor

The shaft was belt driven by a $\frac{1}{2}$ H.P., 110 volt, D.C. electric motor. The amount of torque needed to drive the shaft and overcome the friction of the brushes was relatively small. The small torque required meant that the simplest way to control the motor speed was to vary the d.c. supply to the field and armature connected in parallel. The variable d.c.supply was obtained by rectifying the output from a full wave bridge network, no smoothing was required, this being carried out by the motor. At low voltages the torque produced by the motor was very low and not sufficient to drive the shaft. To obtain low speeds of rotation a variable resistance was included in series with the armature winding, thus

the armature current could be reduced, but the field voltage maintained at a suitable value to obtain sufficient torque to drive the shaft.

A variable resistance motor starter was used to protect the motor. This incorporated an overload cut out and a mains failure cut out.

2.6 Belt Drive System

The drive between the motor and the shaft was by a flat belt and a pair of crowned pulleys. The use of this drive meant that the drive and driven pulleys had to be correctly aligned (otherwise the belt would pull off) and this reduced the possibility of vibrations of the shaft due to misalignments. The use of a flat belt also helped to isolate vibrations of the motor from the bearings and shaft. To isolate the motor still further from the shaft and measuring instruments both the electric motor and the steel plate forming the base of the test rig were attached to the frame by rubber mounting pads.

2.7 Measurement of Rotational Speed

The speed of rotation of the shaft was measured using a magnetic impulse tachometer. A short electrical pulse was produced by passing a piece of ferrous metal between the pole pieces of the magnetic pickup. Four pulses were required for each revolution of the shaft, these were provided by four mild steel inserts in a brass ring fixed on the lower portion of the shaft.

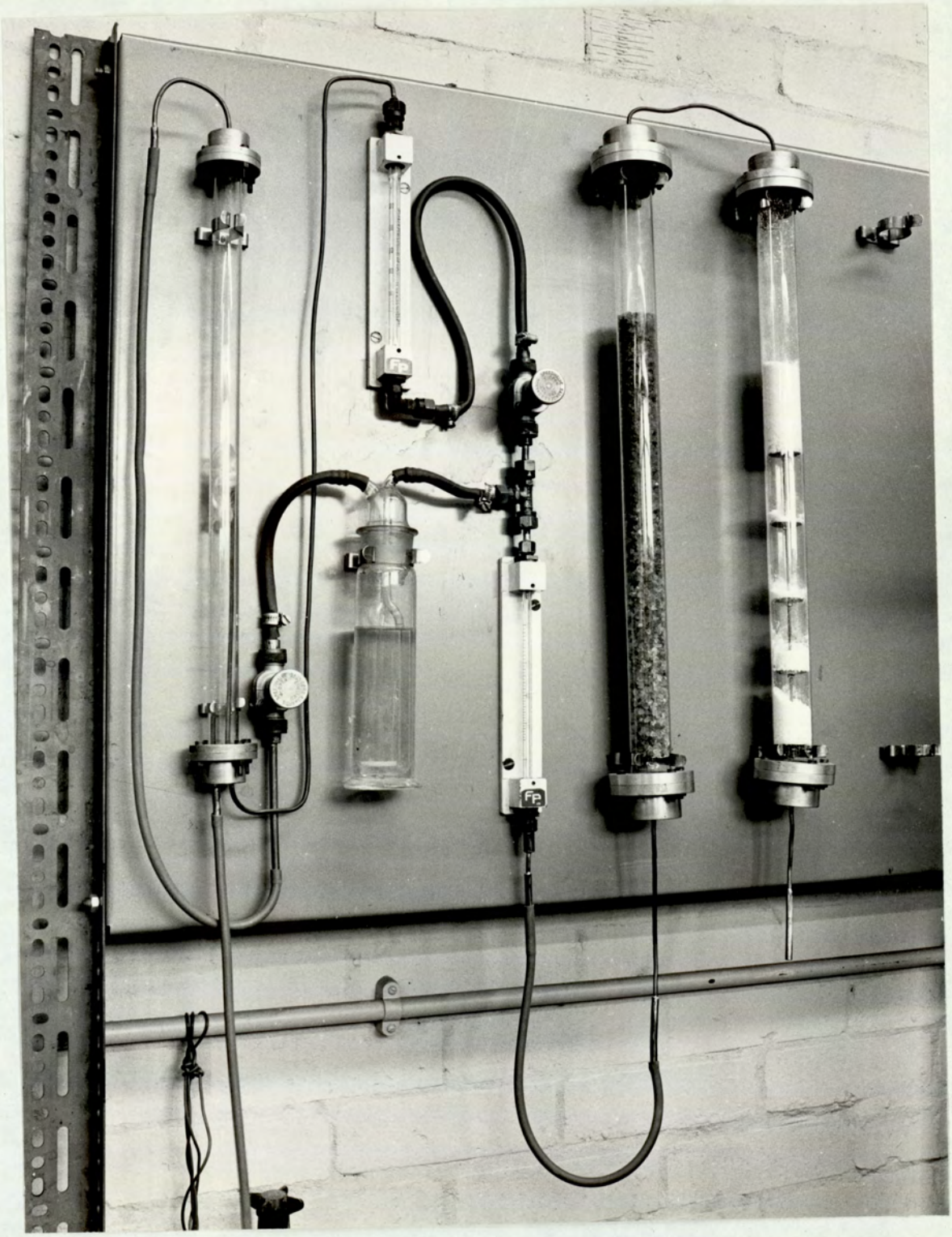

Figure 2.5 Controlled Atmosphere Supply.

2.8 Controlled Atmosphere

As explained in the introduction the atmosphere in which the brushes ran could influence the running characteristics. It was therefore necessary to be able to control the composition of the atmosphere in which the brushes were running. This control was provided by covering the running area of the wear test rig by a large bell jar into which the required atmosphere was fed. The majority of experiments were carried out in an atmosphere of air with a relative humidity of 50%.

The apparatus for controlling the relative humidity of the air is shown in Figure 2.5. Air, obtained from bottles was passed into the two drying tubes shown on the right hand side of the apparatus. These tubes contain silica gel and calcium chloride. The amount of air entering the drying tubes was measured by the lower of the two flow meters. After passing through this flow meter some of the dry air was fed through a control valve into a saturation column containing distilled water. The remaining dry air was passed through another flow meter into a mixing tube where it was mixed with the wet air from the saturation column. The proportions of dry and saturated air entering the mixing tube, and then into the bell jar, was varied to give the required humidity. The relative humidity within the bell jar was measured with a hair hygrometer.

Where the rotating shaft passed through the duralumin plate a seal was necessary to reduce the flow of air required to maintain the correct atmosphere. This was provided by a graphite ring which was a close fit on the shaft, running on a brass ring attached to the underside of the duralumin plate. The graphite was held firmly against the brass ring by a spring on the shaft.

2.9 Wear Machine Working Surface

The portion of the wear machine normally housed beneath the bell jar can be seen in Figure 2.6. This consisted of what was in effect the "Working surface" of the machine, mounted on or above the large circular plate. The disk under investigation, fitted at the top of the main shaft, can be seen in the centre. Suspended above the disk was the brush holder assembly. The frictional force measurement transducers and pillars carrying the probes for measuring wear rate can also be seen (details of these are given in subsequent sections).

2.10 Brush Holder Assembly

The prime purpose of the brush holders was to support the brushes vertically against the disk and enable a known force to be applied to the brushes perpendicular to the disk surface. The holders also had to allow the frictional force between the brush and the disk to be measured and an electric current to be passed to or from the brush.

The brush holder assembly can be seen in Figure 2.7 (for clarity all fixing screws and fixing holes have been omitted from this figure as has the brush retaining plate on the front of the brush holder). The brushes slid in vertical slots cut in blocks of brass. The brushes were made to fit closely in the slots so that only free vertical movement was allowed. The brushes were held in the slots by perspex plates covering the front of the brush holders. A narrow slot was cut down the centre of this plate so that electrical connections could be made directly to the brush.

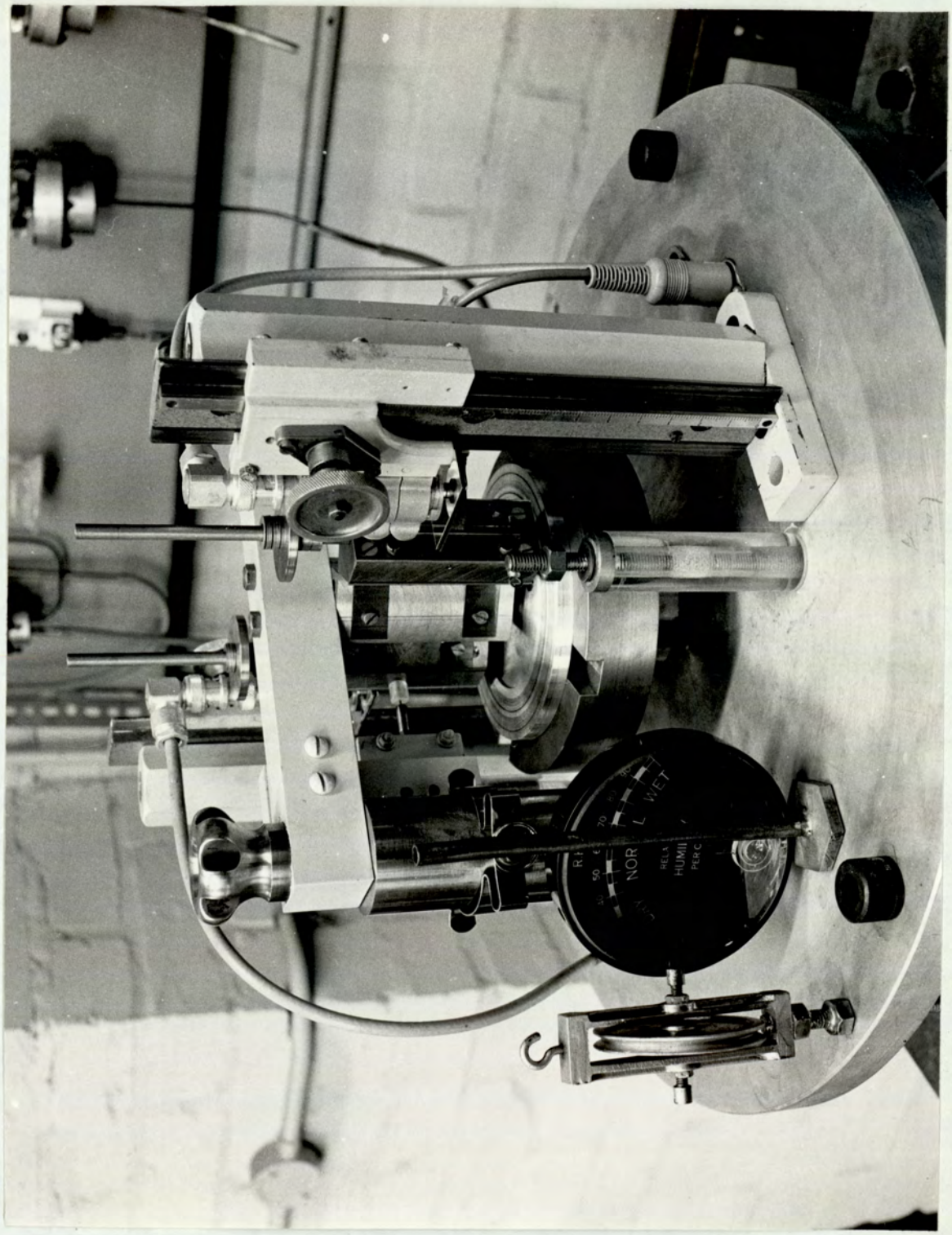

Figure 2.6 View of Wear Machine Showing Disk, Brush Holders and Transducers for Wear Rate and Frictional Force Measurement.

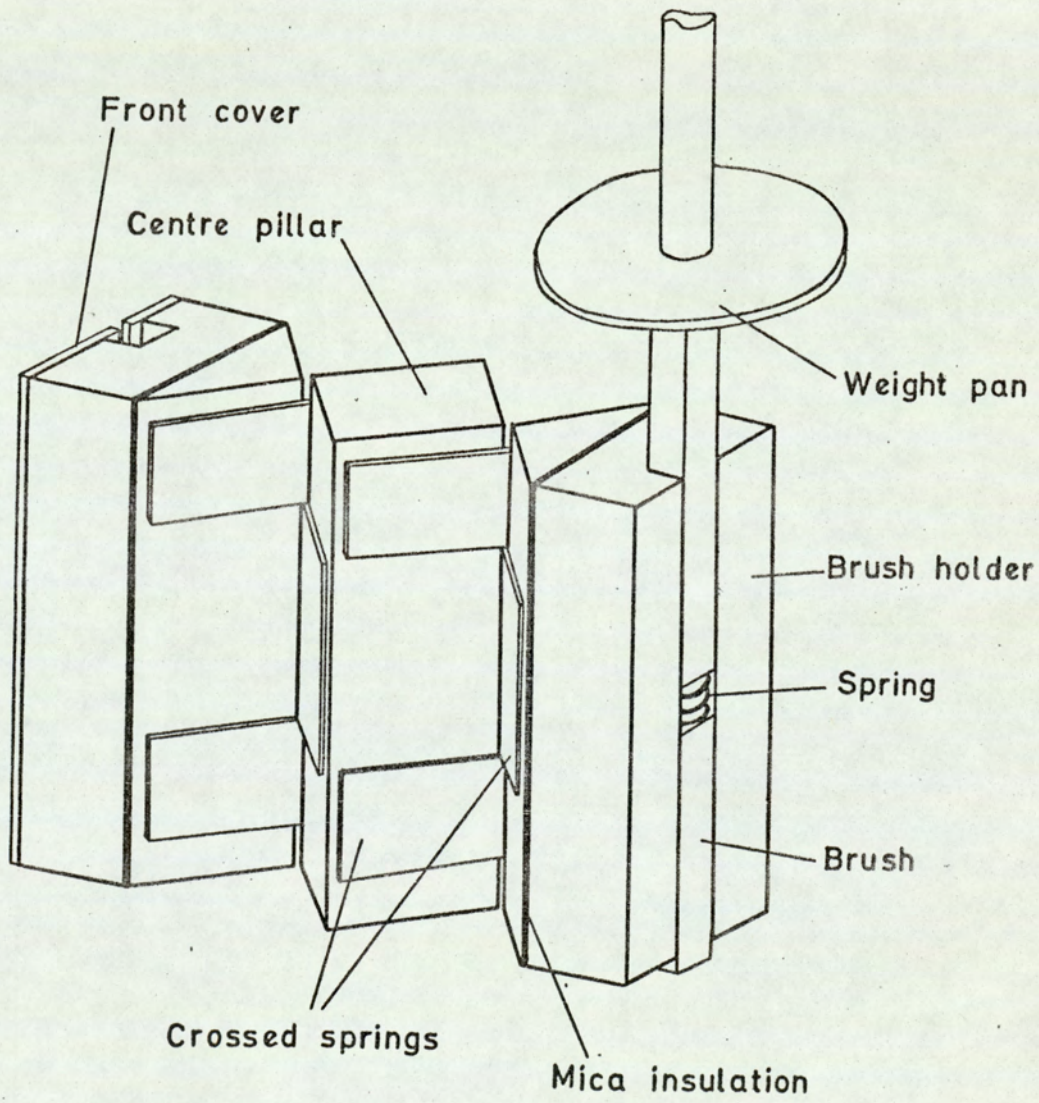

BRUSH HOLDER ASSEMBLY

FIGURE 2.7

The brush holders were attached to a central pillar by a crossed-spring arrangement. The springs consisted of three strips of phospher-bronze 0.030" thick. This arrangement allowed the brush holders to move only in a horizontal arc, centred at the intersection of the springs, no vertical movement or twisting of the brush holders was possible. The assembly was checked to see if twisting occurred by mounting dial gauges against the brush holders, one at the bottom and one at the top. Forces were applied at various positions on the brush holders and the resultant displacement measured. Twisting of the brush holders would have caused different movements at the top and bottom of the holders, no difference could be detected.

The centre support pillar was attached to a horizontal beam held above the disk by two vertical pillars. The centre pillar was displaced $\frac{1}{8}$" from the centre of the disk so that the brushes ran on different radii tracks, the difference in radii being $\frac{1}{4}$".

The brush holders were electrically insulated from the spring assembly by mica strips and held in position by nylon screws.

2.11 Brush Loading

The brushes were loaded by a dead weight system. The weights were supported on a weight pan attached to a rod of square cross-section. This rod fitted into the slot in the brush holder and applied the load to the brush. A small spring was placed between the top of the brush and the weight pan rod. The spring enabled the brush to follow any slight irregularity in the disk surface without vibrations of the brush and weights occurring.

2.12 Measurement of Frictional Force

The frictional force between the brush and the rotating disk resulted in a displacement of the brush holders in an arc, centred about a line running through the intersection of the crossed springs. If this axis could have been made at the centre of the disk the radius of the track would have remained constant, no matter what the displacement of the brush holders. Unfortunately the use of two brush holders meant that the intersection of the crossed springs could not be placed at the disk centre. Any displacement of the brush holders from their central position therefore resulted in a decrease in the radius of the brush track.

Variations in the frictional force would cause changes in the displacements of the brush holders and the position of the brush track would be altering continuously. For the system to be as stable as possible the amount of movement of the brush holders had to be kept to a minimum.

For this reason a strain gauge transducer was used to measure frictional force. The transducers used were manufactured by Pye-Ether Limited and had a displacement of only 0.0015" at their maximum measuring capacity. The strain gauge transducer effectively held the brush holder rigidly in one position . The electrical output from the transducer was easily monitored and a continuous measurement and recording of frictional force was possible.

The transducer consisted of a light armature supported in frame by two flexible cantilever springs. Four strain gauge elements were wound between insulated posts mounted upon the frame and armature to form a fully active bridge network. These elements were wound in opposition to maintain the armature in equilibrium. When a force was applied to the transducer the deflection of the

armature resulted in an increase in resistance of one pair of windings and a decrease in the resistance of the other pair. The application of a voltage across the bridge resulted in an output voltage which was proportional to the force.

In the transducer the strain gauge windings were the stiffness elements and no intermediate stress member was required. This produced a relatively robust transducer which was very responsive to changes in the applied force.

The power supply for the transducers was provided by Ether conditioning units. These units provided a stable, variable d.c. supply. (Stability was better than 400:1 against 10% variations in mains voltage and better than 0.05%/deg C temperature stability). The unit contained a zero control which eliminated zero unbalance in the transducers. The zero control enabled the output from the transducers to be set at zero even though a small force was applied to the transducers to eliminate any possible backlash in the crossed spring assembly. The unit also provided a range calibration control which altered the electrical output from the transducers with respect to the mechanical input. This enabled the transducer to be easily calibrated by either applying a known force to the transducer or using the calibration facility provided. Built in calibration was provided by placing an accurately known resistance across one arm of the bridge, thus causing a predetermined unbalance of the bridge and a resultant output signal.

The transducers were mounted upon the horizontal beam suspended above the disk. The frictional force between the brush and the disk produced a tendency for the brush holder to move away from the transducer, thus applying a tensile force

to the transducer. The transducers were accurately positioned on the beam so that the transducer operating arm could be linked to the brush holders at a point corresponding to the centre line of the brush. Once the transducers had been attached to the beam the whole assembly, including transducers and brush holders, could be removed from the machine for brush or disk replacement without disturbing the relative positions of the components. The length of the link between the transducer and the brush holder could be easily adjusted to apply the required small preloading force to the transducer. The link was made so that the brush holder was electrically insulated from the transducer arm.

Two different pairs of transducers were used. One pair could be used to measure a maximum force of 450 gms.f . The transducers gave an output at the maximum force of 4.7mV per Volt applied. Using the highest operating voltage of 15 volts gave an output of 70mV for a load of 450 gms.f . At low brush loads, resulting in a low frictional force, the electrical output would have been of the order of only 1mV. For frictional force measurements at low brush loads another pair of transducers was used. These transducers could measure a maximum force of 50 gms. f. At that force the output being about 50 mV. When using low brush loads the electrical output was about 6mV and the frictional force could be measured more accurately.

The output from the transducers was measured by potentiometric chart recorders. The chart recorders had a maximum sensitivity corresponding to a full scale deflection of 10" for an input of 3.5mV. The undamped response time of the chart recorders was 1.5 seconds for full scale deflection. This response was too slow for following fast changes in friction, but was adequate for

monitoring changes in the average value of frictional force. A potentiometric indicator was also used to monitor the output from the transducers. This was used mainly for the calibration of the transducers and to ensure that no zero drift or change in calibration of the chart recorders had taken place.

2.13 Calibration of Frictional Transducers

The transducers were calibrated to measure frictional force by applying a known force to the brush holder and adjusting the range control of the conditioning unit to give a suitable reading of the indicator or chart recorder.

The force was applied to the brush holder by weights hung over a light pulley. The weights were attached by a light cord to a point on the brush holder corresponding to the centre-line of the brush. Care was taken to ensure that the cord remained horizontal and tangential to the brush track. A slight error was introduced into the calibration by the friction in the pulley, the force required to rotate the pulley was about 0.25gms.f. A correction was made by increasing the weights by the same amount.

The linearity of the system was checked by increasing the applied force from zero up to the maximum required then reducing it in stages to zero, and noting the deflection of the indicator and chart recorder. No non-linearity could be detected.

Once the transducer had been calibrated using this dead weight method the calibration could be easily checked using the facility provided on the conditioning unit.

2.14 Measurement of Wear Rate

Wear rate of the brushes was the most difficult parameter to measure

due to the small amounts of wear taking place and the operating conditions. The method used had to be capable of measuring the small amounts of wear taking place and giving an output which could be turned into a continuous recording of wear rate whilst causing minimum interference to the brush contact system.

Several methods were available for measuring wear rate, the main ones in use being the following (i) Measurement in the length of the pin, (ii) weighing the pin before and after running, the resultant loss in weight giving a measure of wear rate (iii) Measuring the weight of all the debris produced in running (iv) Using wedge or conical shaped pins, the increase in pin width or diameter during running enabling the wear to be calculated.

Weighing either the brush or the wear debris was not a suitable method to use for graphite brushed. Due to absorption by the carbon it was possible for the weight of the brush material to vary. This variation would have produced very large errors when trying to detect small changes in the weight of the brush due to wear. Measurement of the wear rate by weighing the wear debris was also unsuitable. The design of the pin and disk machine made collection of all the wear debris very difficult, and since the debris would be collected from both brushes only the average weight loss of both brushes could be found. Any debris produced by wear of the disk would also be weighed.

Both these methods could give only the average amount of wear taking place between weighings, no continuous recording of wear rate would be possible. Weighing the brush would also have disturbed the system since the brush would have been removed from the brush holder.

One of the most common methods of measuring small amounts of

of wear is to use a tapered pin;the size of the wear scar can be accurately measured using a travelling microscope and in most cases reliable results obtained. However, the pins have to be removed formeasurements to be made and only average wear rates over long periods are obtainable. Another disadvantage with this method is that the apparent area of contact of the pin increases as the pin wears.

The final method considered was to measure the change in length of the brush as it wore. The easiest way of doing this would be to remove the pin and measure the length with a micrometer. This however gives only average values of wear and would disturb the brush contact.

The most suitable way of measuring wear without removing the brush from the brush holders was to measure the change in height of the brush above the disk surface. For accuracy the change in height of the brush above the track on the disk should be measured since any wear of the disk surface would alter the height of the brush. In practice using the rotating disk as the reference surface is very difficult. One possible method would be to mount a travelling microscope above the disk and brush. Focussing first on the wear track then on the top of the brush would give a measure of the pin height. With this method an error is introduced by the operator having to decide when the surfaces are in focus, this error would be increased by the rotation of the disk. Once again the results obtained would give only average values of wear rate over long periods.

The majority of methods giving rise to a continuous measurement of wear involve the conversion of vertical movements of the brush into an electrical output. Such an output can be obtained by

attaching a strain gauge transducer to the brush so that as wear takes place the transducer is loaded and an electrical signal obtained. Unfortunately this method will, unless great care is taken in setting up the transducer, disturb the brush contact system. The mechanical resistance of the transducer must be small otherwise the brush will not be free to move under the effect of the brush load. There is also a possibility that this transducer would disturb the measurement of frictional force. This method has the advantage however that the small amounts of wear could be accurately measured and the electrical output easily monitored.

An electrical output could also be easily obtained by attaching the brush to the sliding contact of an accurate linear potentiometer. If a voltage is applied across the potentiometer a change in height of the pin will produce a change in the voltage from the centre contact. As in the case of the strain gauge transducer there will be a mechanical restraint upon the brush. The accuracy of measurement using this method is also limited by the size of the wire used for the potentiometer windings.

The method eventually chosen to measure the wear involved the measurement of electrical capacitance. In its simplest form the equipment consisted of a flat, horizontal plate attached to the top of the brush with another similar plate held in a fixed position above it, Fig.2.8. As the brush wore the lower plate moved away from the fixed upper one. The increase in thickness of the air gap between the plates resulted in a change in capacitance of the plates.

In its simplest form the capacitance between the plates can be expressed as

$$C = \frac{A}{d}$$

neglecting edge effects.

For two plates having a fixed area the capacitance is inversely proportional to the plate separation.

The system was calibrated by measuring the distance between the plates using feeler gauges and measuring the capacitance between the plates using a Wayne-Kerr capacitance bridge with source and detector. The Calibration curve obtained is shown in Fig.2.9.

The disadvantage with this system lay in the measurement of capacitance. With the source supplying a constant frequency and amplitude signal, the bridge was adjusted to give a null point on the detector. With the disk rotating it was very difficult to judge the balance point, large errors in measuring the wear rate being produced. The disk could be stopped for the balance point to be found without disturbing the brush contact too much. The main disadvantage of using the method in the way described was that no output was available for continuously recording the wear.

The wear of the brushes was measured using a Wayne-Kerr distance measurement bridge, described below.

2.15 Wayne-Kerr Distance Meter

The principle of operation of this meter is the continuous measurement of the capacitance between two surfaces in close proximity. One of these surfaces was a capacitance probe consisting of a central electrode surrounded by a guard ring and the other surface was the metallic plate under investigation.

The capacitance transducer and test surface completed the

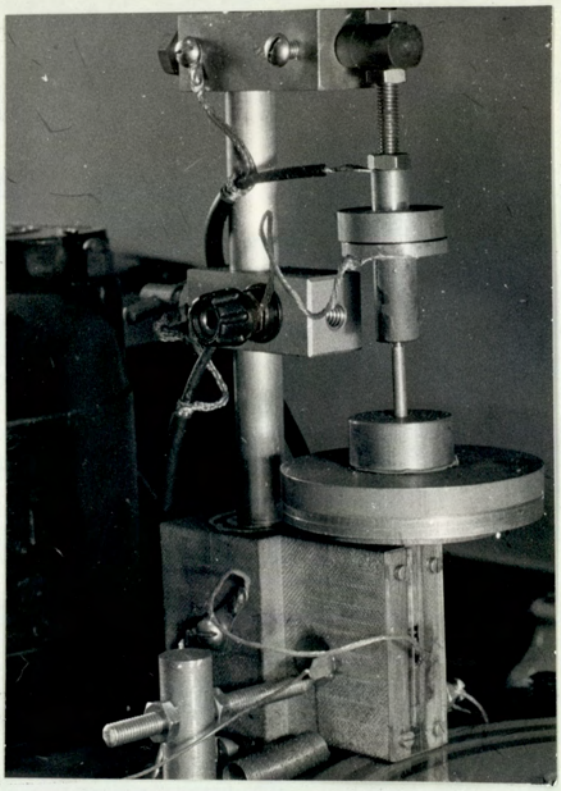

Fig. 2.8 Wear Measurement Capacitance Plates.

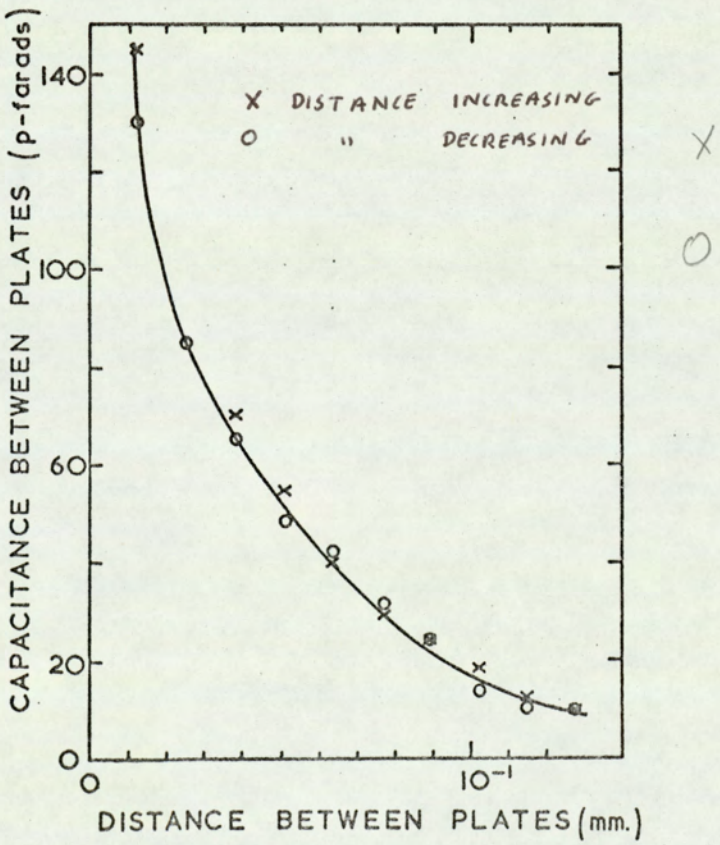

Fig. 2.9. Wear Measurement Calibration curve

negative feedback loop across a high gain amplifier. The amplifier was supplied with a reference input and the output was linearly related to the capacitance probe-surface distance. This output was fed to a meter from which the separation could be read directly. The output was determined by the capacitance between the probe and test surface. Thus by altering the area of the test probe the range of distance represented by the output could be changed.

The output was also available for monitoring by chart recorder, enabling a continuous recording of distance to be made.

A two channel instrument was used which enabled the wear of both brushes to be measured and recorded.

Two different capacitance probes were used. One had an inner sensor diameter of 3.5mm which resulted in a full scale deflection of the meter at a separation of 250μm, the output at full scale deflection being 1.0 volts. The other probe had an inner sensor diameter of 11.5mm and produced full scale deflection (output 1.0V) at a separation of 2.5 m.m.

The wear of the brush was measured by attaching a flat horizontal plate to the rectangular rod of the brush holder, as shown in Fig. 2.10. The plate was made by evaporating a film of aluminium onto a thin glass slide, the metallic surface was connected to the distance meter by a thin coil of very flexible wire. The capacitance probe was held above this plate with its face parallel to the plate surface. As the brush wore, the lower plate moved down and the separation between the probe and plate increased. The output from the meter was monitored by a potentiometer chart recorder and a continuous trace of the wear behaviour obtained.

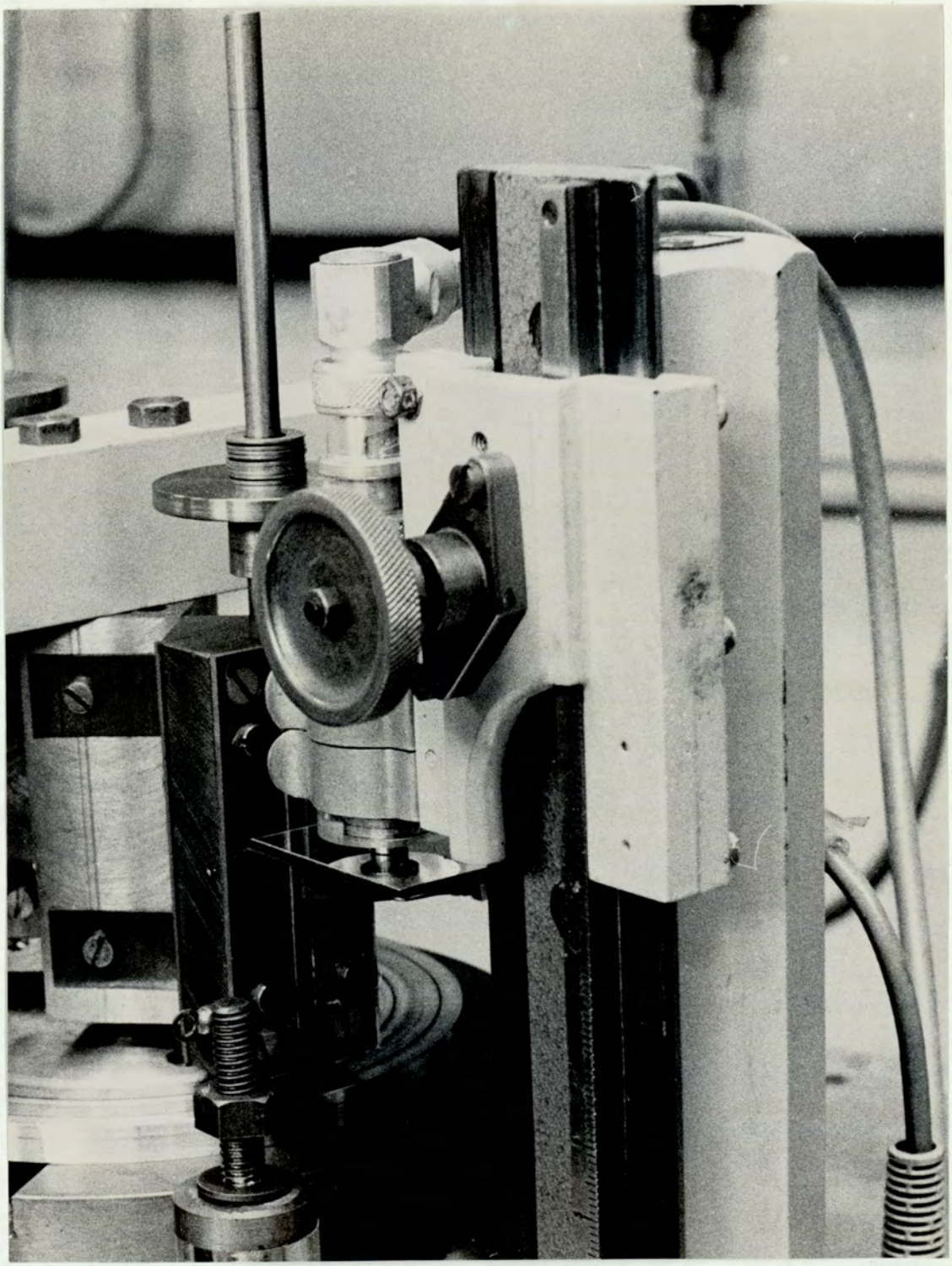

Figure 2.10 Wear Measurement System Showing Capacitance Transducers and Flat Aluminium Coated Plate Attached to Weight Carrying Rod.

When the separation between the plate and probe increased to a value greater than that which gave full scale reading of the meter, the relationship between separation and output voltage became non-linear. When using the smaller diameter probe the maximum amount of wear before full scale deflection was reached was 0.2mm. When this situation was reached the probe had to be moved nearer to the plate. To facilitate this readjustment the probes were mounted upon moveable carriages which were free to slide upon vertical slideways. Movement of the carriage was controlled by a rack and pinion mechanism. Mounting the probes in this way also enabled them to be removed from the machine for brush or disk removal without disturbing their alignment.

The advantages in using the system described was the simplicity with which wear measurements could be made. Once the initial setting up had been carried out, the only further adjustment necessary was moving the probe by the rack and pinion mechanism to give a suitable separation.

Since the probes did not touch the horizontal plates they did not interfere at all with the movement of the brush or the measurement of frictional force.

2.16 The Current Supply to the Brushes

The circuit used for supplying the d.c.current to the brushes is shown in Fig.2.11 overleaf.

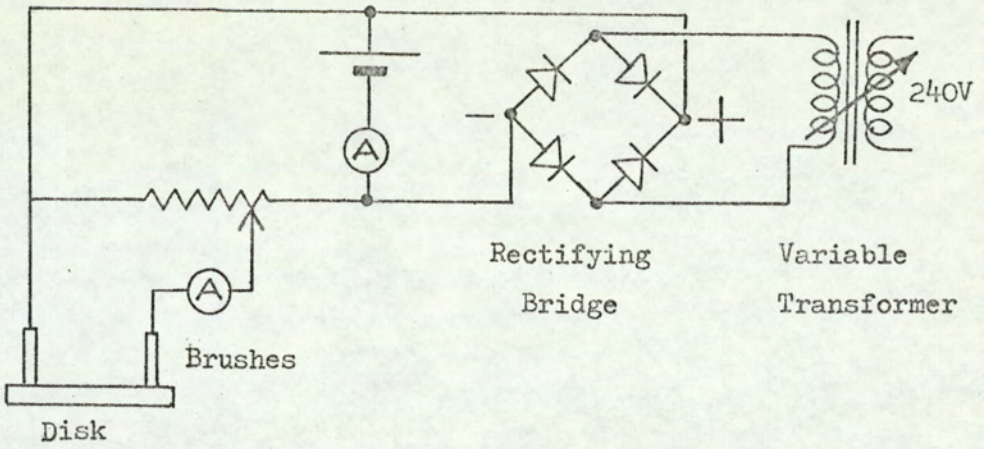

Figure 2.11 D.C. Supply to Brushes.

A variable A.C. supply, obtained from a Variac was rectified, smoothed and connected across a centre reading ammeter and 12 volt accumulator. This provided a very stable d.c.supply which was connected across a potentiometer, from which a variable supply, from 0 to 12 volts was obtained.

The centre reading ammeter indicated whether the battery was charging or discharging, this depended upon the current being drawn for the brushes and the output from the variac.

The current to the brushes passed through an ammeter and surge resistance to one of the brushes, called the positive brush. Conventional current ran from the positive brush to the disk surface, (electron flow was in the opposite direction). From the disk the current passed to the negative brush and through a relay switch. The relay served two purposes, if the brush current accidentally exceeded a preset value the circuit was interrupted causing minimum damage to the contact. Failure of the mains supply also caused an interruption of the brush current circuit,

thus preventing current being passed when the disk was stationary.

2.17 Measurement of Contact Resistance

The contact resistance between the brush and disk surface was determined by measuring the potential difference between the brush and disk. The potential difference was measured using a four contact system. The current "leads" to the resistance were provided by a flexible copper braid fitted to the brush and the other brush contact. The voltage measuring contacts were made by a gold wire connected to the brush as close to the running face as possible and a contact to the rotating disk. The potential difference was measured using a high impedance instrument, either a valve voltmeter, oscilloscope or potentiometric chart recorder. The current drawn by these instruments was very small, a maximum of 10μA for the chart recorder if used to measure 5 volts. This meant that the voltage drop across the rotating contact, which had a resistance less than one ohm, was of the order of 10^{-6} volts, and caused a negligible error in the potential difference measurements.

2.18 Mercury Contact Assembly

The contact to the rotating disk was made using the mercury contact and slip ring assembly which can be seen attached to the lower end of the main shaft (Fig.2.2). The assembly consisted of three copper slip rings, insulated from each other upon which silver graphite brushes were run. The brushes had a very low contact resistance, less than 1 ohm, even for the very small currents required to measure the potential difference. The noise produced in the contacts was also very low, it was negligible even when currents in excess of 10 m A were passed, these currents being much

greater than those required.

A mercury contact was also included in the assembly. This consisted of a copper pin attached to a small hardened steel shaft which rotated with the main shaft. The steel shaft rotated in hardened steel bearings which were oil lubricated. The copper pin dipped into a stationary copper cup containing mercury, from which the contact was obtained. The mercury was first amalgamated with the copper to form a better contact by removing the copper oxide with Nitric acid. This mercury contact assembly was contained within a perspex tube to prevent the escape of mercury vapour.

2.19 Contact Potential Difference Monitoring

Measurement of the potential difference between brush and disk using a chart recorder or valve voltmeter gave only the mean d.c. value. A more detailed study of the nature of the potential difference was carried out using an oscilloscope. When connected between the brush and disk the oscilloscope displayed the voltage between the brush and that portion of the disk track beneath the brush at that instant. A multiple trace was normally obtained due to the time base of the oscilloscope beginning its sweep when different portions of the track were beneath the brush. It was possible to synchronise the time base with the speed of rotation of the disk so that the sweep began as the same portion of the track passed beneath the brush. However this synchronisation was very difficult to achieve in practice and slight differences between the two speeds resulted in the point in the track at which the trace started changing and the trace slowly altering.

A more satisfactory method was to trigger the time base of the oscilloscope by the rotation of the disk using the external trigger facility provided. The oscilloscope was triggered at the same point each revolution and the time base began its sweep each time as the same portion of the track passed beneath the brush. This resulted in a very stable trace.

The time base was triggered by a pulse obtained from a magnetic pickup mounted adjacent to the rotation shaft. The impulse was caused by a small piece of steel fixed to the shaft passing in front of the pickup. The pulse obtained is shown in Fig. 2.12. The width of this pulse enabled the oscilloscope to be triggered at different voltages and the point on the disk at which the trace started to be varied slightly.

The trace obtained on the oscilloscope was recorded using a Polaroid camera attachment.

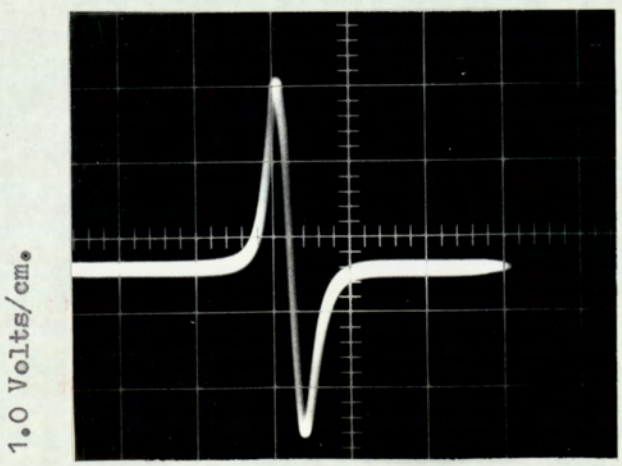

Figure 2.12. Oscilloscope triggering pulse.

Chapter 3. Experimental Details

3.1. Preparation of disks

The surfaces upon which the brushes ran were flat disks fixed by two screws to the brass boss at the top of the main shaft. Some of the earlier experiments were carried out on solid aluminium disks. Unfortunately these disks warped slightly after machining and this caused vibrations of the brush when running. To prevent this warping the centre of the disk was removed, prior to the final machining of the running face, and the annulus thus formed held onto the wear machine by a central clamping plate.

To provide specimens of the surfaces of the disk after running closely fitting removable plugs were inserted into the disk face. The plugs were held firmly into the disk by screws locating against the back of the disk. After fitting the plugs the final running surface was machined.

Final machining of the running face was carried out using a tungsten carbide tool, giving a surface finish of 5 microns.

The hardened EN26 steel disks were produced by heating the disk to a temperature of 850°C and maintaining this for 2 hours. This resulted in a hardness of 570 VPN . After hardening the disk was surface ground to ensure that the two faces were flat and parallel the running face was then radially ground to give a surface finish similar to that of the turned disks.

The electrographite and gold disks were fixed by cementing with conducting adhesives, onto a recessed copper disk which in turn was clamped onto the machine.

Before running the disks were cleaned in acetone and petroleum

ether then placed in a desiccater for the surfaces to reoxidise.

3.2. Preparation of brushes

The brushes used in the experiments were cut from a single block of electrographitic brush material(EG14) supplied by Morganite Carbon Company. The size of the slot in the brush holders was 5m.m. x 5m.m square and the brushes were cut slightly oversize then individually fitted to the brush holders. The brushes were carefully abraded on very fine emery cloth lubricated with petroleum ether until the brush just slid down the brush holder under its own weight, with minimum sideways movement. The abrasive particles were removed from the brush by cleaning in petroleum ether.

Two leads were connected to each brush using an electrically conducting adhesive. One lead, that carrying current, was flexible copper braid cemented near the top of the brush. The voltage measurement lead was a thin gold wire cemented as close to the running face as practicable. This kept to a minimum errors in the contact voltage due to voltage drop in the brush material.

3.3 Running in the brushes

Before it was possible to carry out any experiments the brushes had to be run in. This running in involved changes in the topographies of the two running faces until the surface features were stable and characteristic of the running conditions. The brush was considered to be run in when the whole of its surface was in contact with the track and its wear rate, frictional force and contact resistance had attained steady values. At light loads this running in period was very long, about one month. This running in time would have been decreased by abrading the brush surface or running in under

an increased load or in a dry gas. However, since the purpose of the research was to study the running surfaces this accelerated running in was rejected because of possible changes beneath the surfaces.

3.4. Experiments to determine variations in characteristics with changing loads

For these experiments the brushes were run in at the lowest load to be used. The weight of the weight pans and capacitance plate meant that the lowest load easily obtainable was 60gms wt., this load was, however, within the normally recommended brush load. At this light load the running in period was about 4 weeks.

3.4(i) Measurement of Wear Rate

At light loads the wear rates were very low and the small changes in brush height were difficult to measure. Changes in temperature resulted in short term changes in the length of the brush which affected the wear measurement and the run at light loads lasted several weeks to enable accurate wear rate measurements to be made.

3.4(ii) Measurement of Contact Resistance

During these experiments the brushes were run for most of the time without current passing through the brushes. At each load , however, a short experiment was carried out to measure the contact resistance of the brushes. The voltage across the interface was measured as the current through the brushes was increased from 10μ A. From this the contact resistance at each current was determined (from $R = \frac{V}{I}$). The current through the brushes was increased in small increments until the interface began to behave in a non-ohmic manner (i.e. the contact resistance began to fall). At this stage

the current was switched off to minimise the possibility of permanent damage to the interface occurring. The brushes were then run at the same load until the interface had returned to its original state as indicated by contact resistance measurements using a current of 10μA.

3.4(iii) Measurement of frictional force

During the experiments the frictional force between the brush and disk were constantly recorded. At light loads the frictional force was small, giving a small output from the transducer. Zero drift of the measuring system at these small outputs had an appreciable effect on the measurements and frequent re-zeroing was necessary, but no change in the calibration of the system occurred. At high loads, which gave high frictional forces and transducer outputs this zero drift was negligible.

After each increase in load the brushes were allowed to run in at the new load before any readings were taken.

3.5. Experiments to determine variations in characteristics at constant load

The experiments described in the previous section determined the effect of load on the running of the brushes. Experiments were also carried out at constant load to determine the effect of electric current on the running characteristics.

The number of loads which could be used was severely limited by the length of time taken to perform each experiment. The values of the loads at which to carry out these experiments were determined by how the characteristics varied with load.

3.5(i) Changes in contact resistance with current

This experiment was carried out by passing a known current through the brushes and measuring the potential difference across the brush-disk interface.

The potential across the interface was first measured with no current passing through the brushes to determine whether any thermal e.m.f's were generated at the interface. None could be detected.

Previous workers have shown that the changes which take place when passing current are non-reversible and care therefore had to be taken that the required value of current was not exceeded.

The voltage was measured as soon as steady conditions had been reached after a change in current. Steady conditions were usually attained within two minutes of a change in current. Very slight variations in voltage sometimes took place over a longer period but these were negligible compared with the voltage being measured.

The current was increased until visible sparking occurred beneath the brush, when the experiment was stopped.

3.5(ii) Variation in frictional force with electric current

The frictional force was measured continuously whilst brushes were being run to determine whether any variations in frictional force occurred due to the passage of electric current. When changes did take place equilibrium was established within 15 minutes of an increase in current. Changes in friction due to electric current could be distinguished from apparent changes due to zero drift since the latter were long term slow changes.

3.5(iii) Variation of Wear rate with electric current

In order that a reliable measure of wear rate could be obtained each experiment to measure the wear lasted a relatively long time, from a few days at high loads to several weeks at low loads. These lengthy experiments severely limited the number of measurements of wear rate which could be made. To determine whether any change in wear occurred with electric current the wear rate was measured first with no current flowing through the brushes, then with the maximum current which could pass without arcing across the interface. Measuring the wear rate with no current flowing also provided a check in the repeatability of the experiments since these wear rates should have been the same as those obtained from the previous experiments, where the variation in characteristics with load were determined. With no current flowing through the brushes the wear rates of both brushes running on the disk should have been the same provided they were both running under the same load.

If any difference in the wear rate of the brushes with current flowing from that with no current flowing had been found more experiments would have been performed to measure the wear of intermediate currents.

3.6. Collection of wear debris for examination

The wear debris produced during each experiment was analysed by and X-ray powder technique. The wear debris was collected upon a small artist's paint brush dipped in petroleum ether. The ether was washed from the brush into a test tube containing petroleum ether which was later evaporated leaving behind the dry wear debris. Obviously, this method did not collect all the debris produced, however, by carefully brushing all the exposed surfaces it was probable that the amount of debris uncollected was small and the sample was a fair representation of the wear debris.

After drying, the powder was thoroughly mixed and a sample placed in a low absorption glass capillary tube. The tube was filled by vibrating the powder, either by hand or using an ultrasonic cleaning bath. There was a possibility that the debris components may have segregated during this vibration, and this possibility was checked by analysing the wear debris contained in different portions of the tube. No difference in composition of the debris within the tube could be detected.

At low loads the amount of debris produced was very small, making both collection and examination difficult. After running for two months at a load of 60gms. f. only enough debris would be collected to fill the lower 3m.m. of a capillary tube of diameter 0.5m.m. To analyse the debris this tube was mounted in the camera with the sealed end, containing the powder, irradiated by the X-ray beam.

After each experiment had ended and the wear debris had been collected the surfaces beneath the bell jar were cleaned of any remaining debris, using compressed air and washing with petroleum ether, before the next experiment was begun.

3.7. Specimen preparation for surface examination

The surfaces formed during the experiments were examined by four techniques : - Optical Microscopy; Scanning Electron Microscopy(S.E.M.), using a Cambridge Instrument Stereoscan Mk2A; general area reflection electron diffraction, carried out on an A.E.I.EM66 electron microscope; and Electron Probe Microanalysis (EPMA) carried out on a Cambridge Instrument Microscan MkII.

Where necessary experiments were run specifically to generate surfaces for examination.

No special preparation of the surfaces was required for any of the techniques used. However, the size of the specimen chambers in the instruments limited the size of specimen which could be examined, and the ease with which suitably sized specimens could be obtained had influences the brush and disk design and dimensions. Specimens of the wear tracks on the disks were obtained either from the removeable plugs inserted into the surface or from 5m.m. x 5m.m sections cut from the disk. These specimens were cemented directly onto mounting stubs for examination by scanning electron microscopy or electron diffraction. When specimens were cut from the disk, using a hacksaw, the running surface was positioned so that no cutting debris fell onto the wear track, the disk was also cooled during cutting by a stream of cooling air.

The specimen chamber of the Stereoscan could possibly be modified to accommodate a reasonably sized disk or cylinder, so that the wear tracks could be examined at any stage during an experiment after which the run could be continued using the same specimens.

The 5m.m x 5m.m brushes fitted into all the specimen chambers, the only limit being the height of the specimen, the maximum permissible specimen height for examination by E.P.M.A. being

approximately 4m.m. Small specimens of this length were cut from the brushes after running and mounted upon microscope stubs or into the specimen holder of the microprobe.

The specimens generated were examined by each of the techniques in turn, beginning with the least destructive, optical microscopy, followed by S.E.M. and finally using the technique which was likely to produce most damage to the surface. The accelerating voltage for the electron beam used in the Stereoscan was relatively low, 20KV, and since the beam was being scanned or rastered across the specimen very little surface damage was likely. The next technique used was reflection electron diffraction. Although the accelerating voltage used, 80KV, was much higher than that used in the microprobe the method of specimen of specimen mounting and removal used in the latter instrument made the possibility of surface damage more likely.

3.8 Running Conditions

The relative humidity beneath the bell jar was maintained at a value of 50%, since short preliminary experiments had shown that no variation in running characteristics occurred over a wide range either side of this value.

The speedof rotation of the disk was controlled at 1000 rpm.

Chapter 4. The Sliding of Electrographite upon Aluminium

4.1 The wear rate of electrographite at 60gf. load

The method of measuring the amount of wear has been described in a previous chapter. The wear rate was defined as the wear volume removed per unit sliding distance. A continuous recording of brush height was obtained from which the volume of brush removed and the distance of sliding found, hence the wear rate was determined.

All the experiments were carried out at a constant rotational speed of 1000 r.p.m. and a controlled relative humidity of 50%.

When running under very light loads the wear rate was low and in order for reliable, "trustworthy" results to be obtained the running in period had to last several weeks.

Even after running in for a long period the wear rate was still erratic varying within the range 3.6×10^{-10} $mm^3/m.m.$ of sliding, to $5.0 \times 10^{-10} mm^3/mm$ sliding, although short periods occurred when no wear could be detected. Over a running period of 400 hours, the average wear rate was $4.2 \times 10^{-10} mm^3/mm$

The effect of electric current upon the wear rate was small provided that sparking did not take place. Up to and including a current of 2.0 amps no change in wear rate of the positive brush could be detected. When the current was increased above 2.0 amps sparking occurred beneath the brush and the wear rate increased to $4 \times 10^{-8} mm^3/mm$ sliding. The wear rate of the negative brush increased slightly with current. At a current of 500mA the wear rate was $6.8 \times 10^{-10} mm^3/m.m.$ and at a current of 1.0A had increased to $9.4 \times 10^{-10} mm^3/m.m.$ When a current of 2.0A was passed catstrophic wear took place and the wear rate increased to $4 \times 10^{-8} mm^3/mm.$

During this running period experiments were also carried out to investigate contact resistance and frictional force.

4.2 Wear of Electrographite at 460 gms f.load

This experiment was carried out to determine the wear rate of the brushes at various currents at a load of 460 gms f. The wear of both the positive and negative brushes was continuously recorded and the wear rate determined, these are shown in Table 4.1.

Table 4.1

Wear rates of electrographite at 460 gms.f load

Current	Wear rate of brushes mm^3/mm of sliding	
	Positive	Negative
0	6.2×10^{-8}	6.8×10^{-8}
100 μA	6.2	6.8
10 mA	8.1	7.1
500 mA	7.6	6.7
1 A	6.8	6.5
2 A	8.1	7.0
5 A	7.7	7.8

Above 5A catastrophic wear took place, the wear rate jumping to $10^{-6} mm^3/m.m.$

The higher wear rates at this load were much easier to measure than those at 60 gms.f.load. Again, however, there was quite a large spread of results as indicated by Table 4.1. No significant change in wear

rate outside this normal spread of results could be detected unless sparking took place.

4.3 Wear of Electrographite at 1060gf load

The high wear rate of the brushes at this load made the wear easily measurable. However, the time for which the wear could be measured at any one current was limited by the necessity to perform all the measurements upon one brush, before its length became too short for stability. It was preferable to complete all these measurements upon one brush to eliminate any possible effects due to slight variations in brush composition.

Table 4.2

Wear rate of electrographite at a load of 1060 gms.f.

Current	Wear rate of brushes $mm^3/mm.$ of sliding	
	Positive	Negative
0	2.25×10^{-7}	2.4×10^{-7}
10mA	2.10	2.6
100	2.4	1.9
500	2.5	2.0
1 A	2.8	2.7
2 A	2.6	2.5
5 A	2.7.	2.4

The results obtained are shown in Table 4.2. At the wear rates involved the distance between the wear measurement probe and the capacitance plate increased beyond the full scale reading of the bridge after about 5 hours running and the distance between the two had to be reset. Thus the wear rate was determined from several continuous recordings of wear over these short periods. The values given in Table 4.2 are the mean values from several such wear rate measurements, all of which fell within the range $2 - 3 \times 10^{-7} mm^3/mm$ sliding.

No significant variation in wear rate with electric current occurred until arcing took place at a current of 10A, when the wear rate increased to $10^{-4} mm^3/mm$ of sliding.

4.4. The Variation in Wear Rate with Load

This experiment was carried out to determine how the wear rate of the electrographite depended upon the applied load. The brush was run in for several weeks at a load of 60 gms.f. until a consistent value of wear rate was obtained. The frictional force and contact resistance at low currents were also measured. The load was increased in stages up to 310 gms.f., then reduced to 60 gms.f., the wear rate, frictional force and contact resistance being measured at each load once equilibrium had been restablished.

Fig.4.1 shows how the wear rate of the electrographite varied with load. At low loads the wear rate was low and increased in proportion to the load. However, when the load was increased above 260 gms.f. the wear rate suddenly increased as shown. When the load was reduced to 260 gms.f., the wear rate remained high but dropped back to the lower branch of the graph when the load was reduced below 260 gms.f. The load was not increased above 310 gms.f. since previous experiments had shown that at a load of 460 gms.f. permanent damage to the aluminium surface occurred.

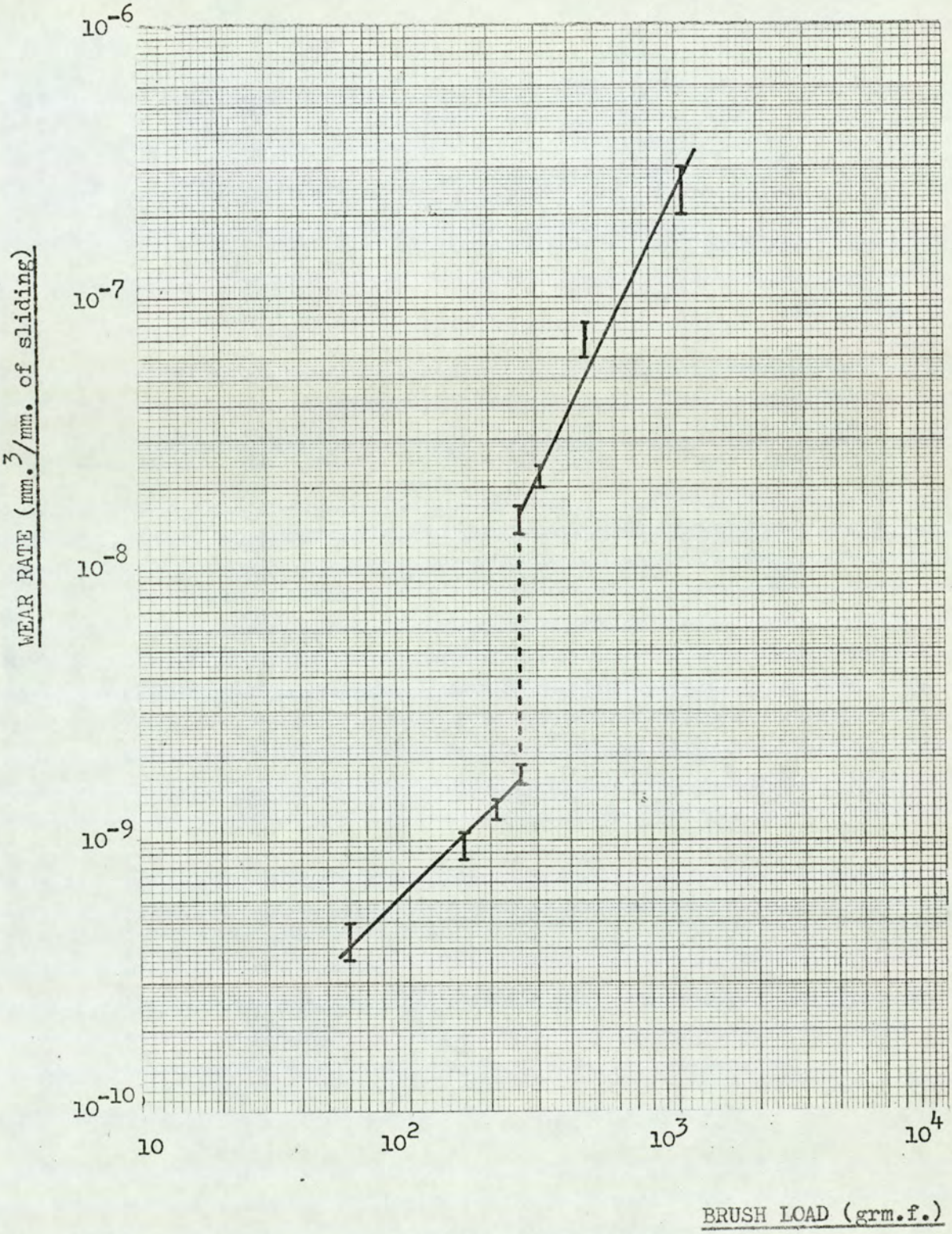

Figure 4.1 Variation in Wear Rate of Electrographite with Applied Load When Sliding on an Aluminium Disk.

Table 4.3

Variation in wear rate of electrographite with load.

	Load gms	Wear Rate mm^3/mm sliding
LOAD INCREASING	60	4.1×10^{-10}
	160	9.5×10^{-10}
	210	1.3×10^{-9}
	260	1.75×10^{-9}
	310	2.2×10^{-8}
LOAD DECREASING	260	1.5×10^{-8}
	210	1.3×10^{-9}
	260	9.5×10^{-10}
	60	4.2×10^{-10}

The close agreement between the results at the lower loads before and after running at 310 gms.f suggested that the transition from "mild wear" to "severe wear" is reversible upon reducing the load, provided that no serious damage to the surface was caused by running at the higher loads.

4.5 The Contact Resistance of Electrographite Sliding on Aluminium at 60 gms.f.load

Continuous measurement of the potential between the brush and the disk at a brush current of 10μA revealed that the contact resistance very

quickly reached an equilibrium value, even though both the wear rate and friction force were varying and the brush was not making apparent contact over its whole face.

The current through the brushes was increased in steps up to a maximum of 2.0 amps, the potential across the interface was measured at each current and the contact resistance determined. When the current through the brushes was increased the new value of potential difference was reached almost immediately and did not significantly vary from this new value. The value of contact resistance was calculated from the potential difference established after equilibrium had been reached. At various stages throughout the experiment the current through the brushes was reduced and the contact resistance determined. In most cases, upon reduction of the current no equilibrium value of contact potential was established; the value kept increasing steadily. At the end of the experiment, when the electric current was turned off, several days running was required before the contact resistance regained its original high value (measured at 10μ A current). The contact resistance was therefore measured immediately the current was reduced. The values of contact resistance are given in Table 4.4.

The variation in contact resistance with electric current is shown in Figure 4.2 for the positive brush and Fig.4.3 for the negative brush. The direction of the arrows indicate whether the current was increasing or decreasing. Up to a current of about 1mA the interface behaved in an ohmic manner, the contact resistance remained constant and the current passing through the interface was proportional to the voltage across the interface. When the current was increased above 1mA the contact resistance decreased with increasing current. Upon reducing the current the characteristics did not follow the same curve, the contact resistance initially remained low but recovered its original high value after several

Table 4.4

Variation in contact resistance with current

Current	Negative Brush		Positive Brush	
	Contact Potential	Contact Resistance (OHMS)	Contact Potential	Contact Resistance (OHMS)
10μ A	16mV	1.6×10^3	56mV	5.6×10^3
20μ A	34	1.7	110	5.5
30μ A	54	1.8	171	5.7
50 μA	94	1.9	275	5.5
100 μA	190	1.9	500	5.0
200 μA	380	1.9	820	4.1
300 μA	560	1.86	1.07V	3.6
500 μA	850 mV	1.7	1.33	2.6
At this stage the current was reduced back to 10μA the contact resistance followed the same curve back.				
1mA	.05V	1.05×10^3	1.25	1.25×10^3
2	1.10	5.5×10^2	1.18	5.9×10^2
3	1.55	5.2	1.55	5.1
4	1.90	4.8	1.55	3.9
5mA	2.20 V	4.4	1.60	3.2
The current was reduced from 5mA to 10 μA but the contact resistance remained low				
1mA	540mV	540	550mV	550
500 A	295	590	340	680
100 A	65	650	89	890
50 A	32	640	50	1000
20 A	13	650	21	1050
10 A	6.5	650	10	1000
10mA	2.25V	225	1.65V	165
30 A	2.4	80	1.65	55
100mA	2.35	23	1.80	18
Current now reduced from 100mA to 100 μA.				
10mA	370mV	37	560mV	56
1mA	38	38	64	64
100 A	5	50	6	60
500mA	2.5	5.0	2.8V	5.6
1.0amps	2.5	2.5	2.8	2.8
2.0	3.0	1.5	3.0	1.5
2.0 amps was the maximum current used due to arcing beneath the brushes .				
The current was reduced from 2.0 amps to 2.0mA				
1.0amps	1.5V	1.5	2.0V	2.0
500mA	1.1	2.2	1.4	2.8
100mA	305mV	3.05	265mV	2.65
30mA	95	3.2	69	2.3
10mA	30	3.0	22	2.2
1mA	2	2.0	4	4.0

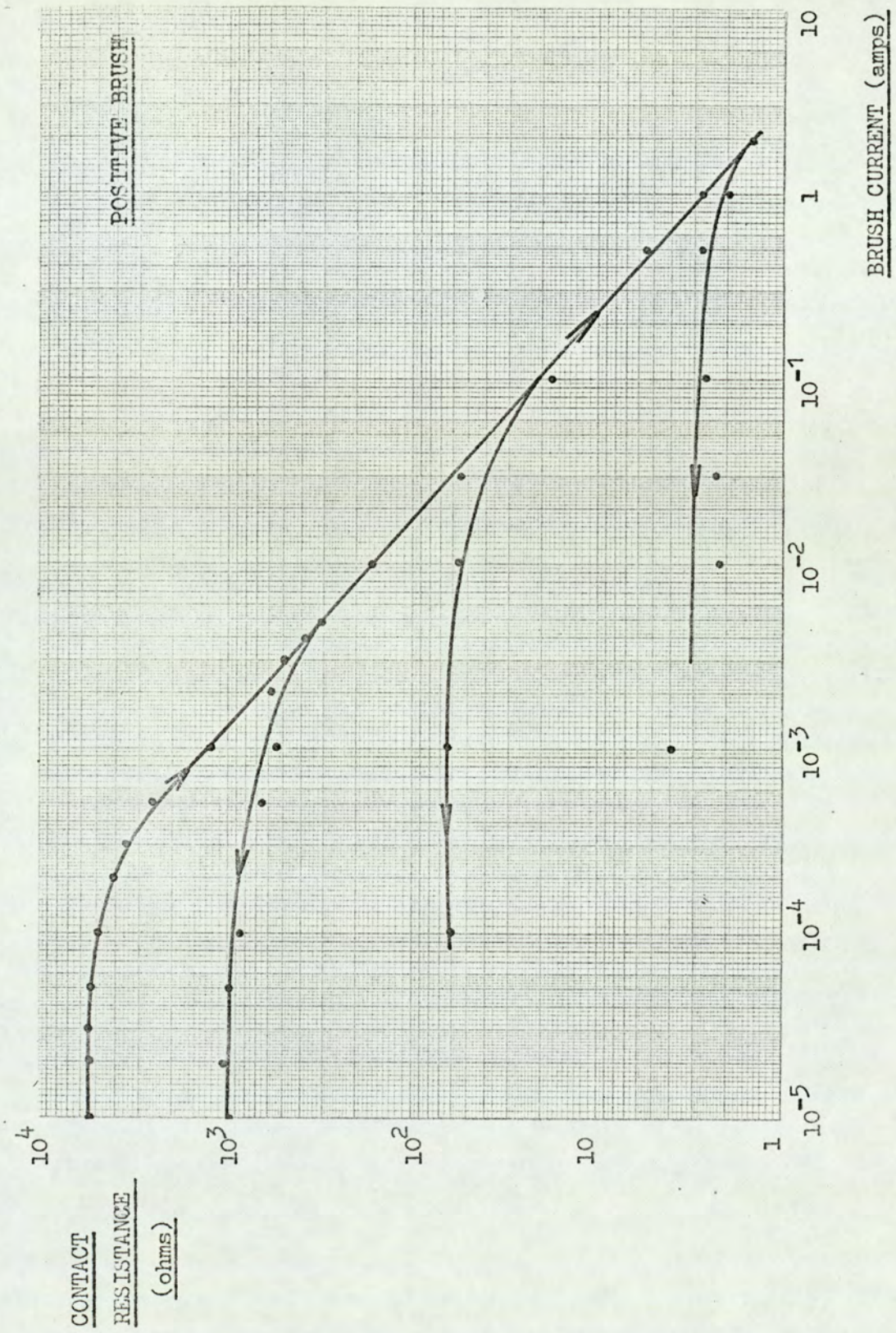

Figure 4.2 Variation of Contact Resistance of Positive Brush with Electric Current at a Load of 60gf. when Sliding upon Aluminium.

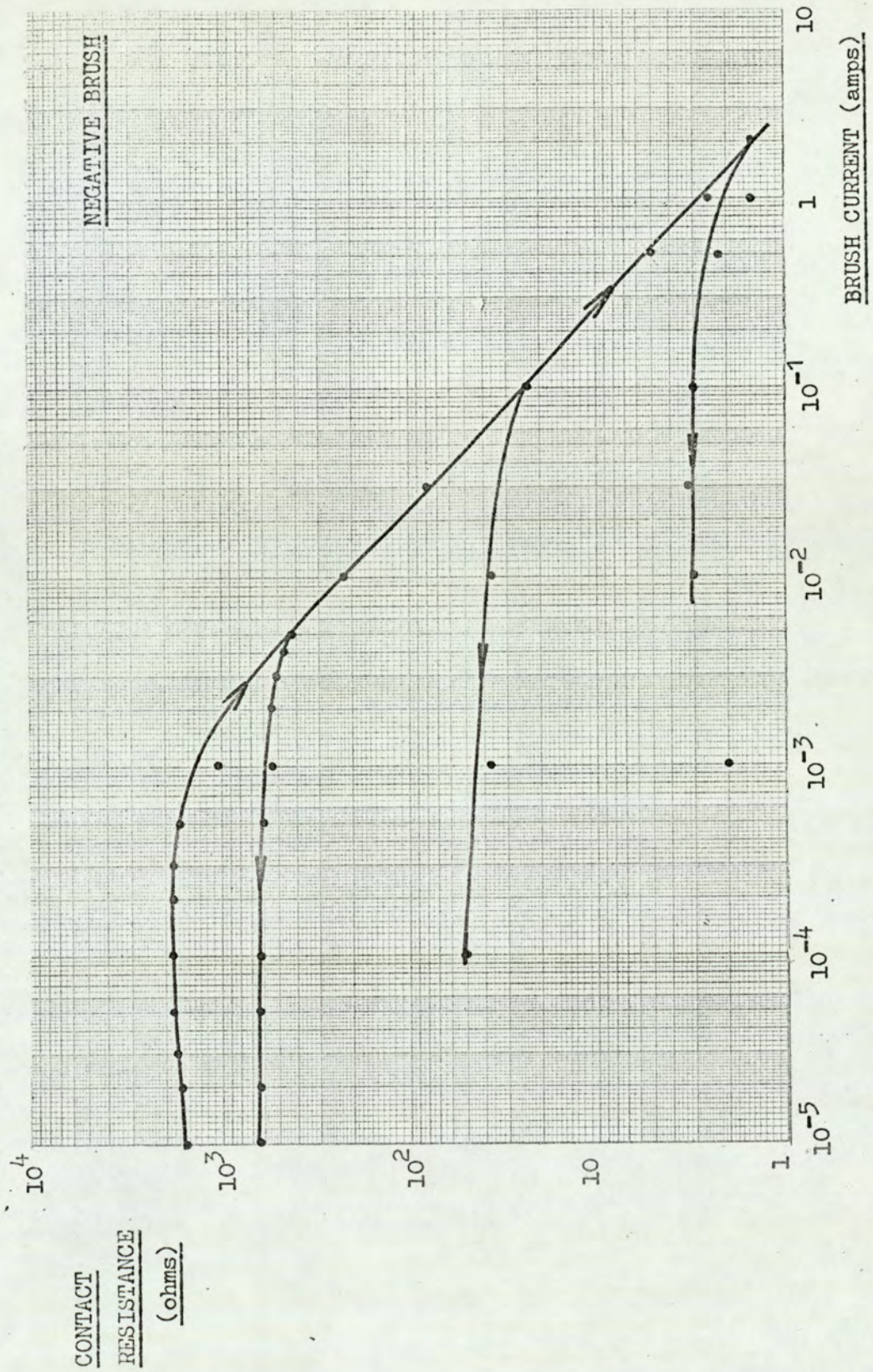

Figure 4.3 Variation in Contact Resistance of Negative Brush with Electric Current at a Load of 60gf. when Sliding upon Aluminium.

days. Very little difference existed between the characteristics of the positive and negative brushes. In the case of the brushes and disk used to obtain the results of Figs.4.2 and 4.3 the initial ohmic resistance of the positive brush was higher than that of the negative brush, that,however, was not always the case. The experiment was repeated several times during the course of the research using different brushes and aluminium disks. In each case the shape of the current-contact resistance curves was the same but the initial high resistance value varied and was independent of polarity.

When the contact resistance was plotted against the potential across the interface the curves in Figs.4.4 and 4.5 were obtained. These curves show that the interface behaved in an ohmic manner until a critical potential was applied, when a rapid decrease in resistance occurred. The potential at the onset of the fall in resistance was the same for both the positive and negative brushes, about 1.1 volts.

4.6. The Variation in Contact Resistance Characteristics with Applied Load

During the experiment carried out to determine the variation in wear rate with load the contact resistance was measured at each load. The measurements were however limited to small electric currents to minimise surface damage. When the contact resistance began to fall the electric current was turned off and the brush run under the same load until the resistance had recovered to its original value measured at 10μ A.

When running under loads of 60 gms.f., 110 gms f., 160 gms.f., and 210 gms.f., the initial ohmic resistance was high and independent of current, as shown in Fig.4.6. At a load of 260 gms.f., a relatively small reduction in resistance occurred but the shape of the characteristic curve remained the same. However, when the load was increased to 310 gms.f.

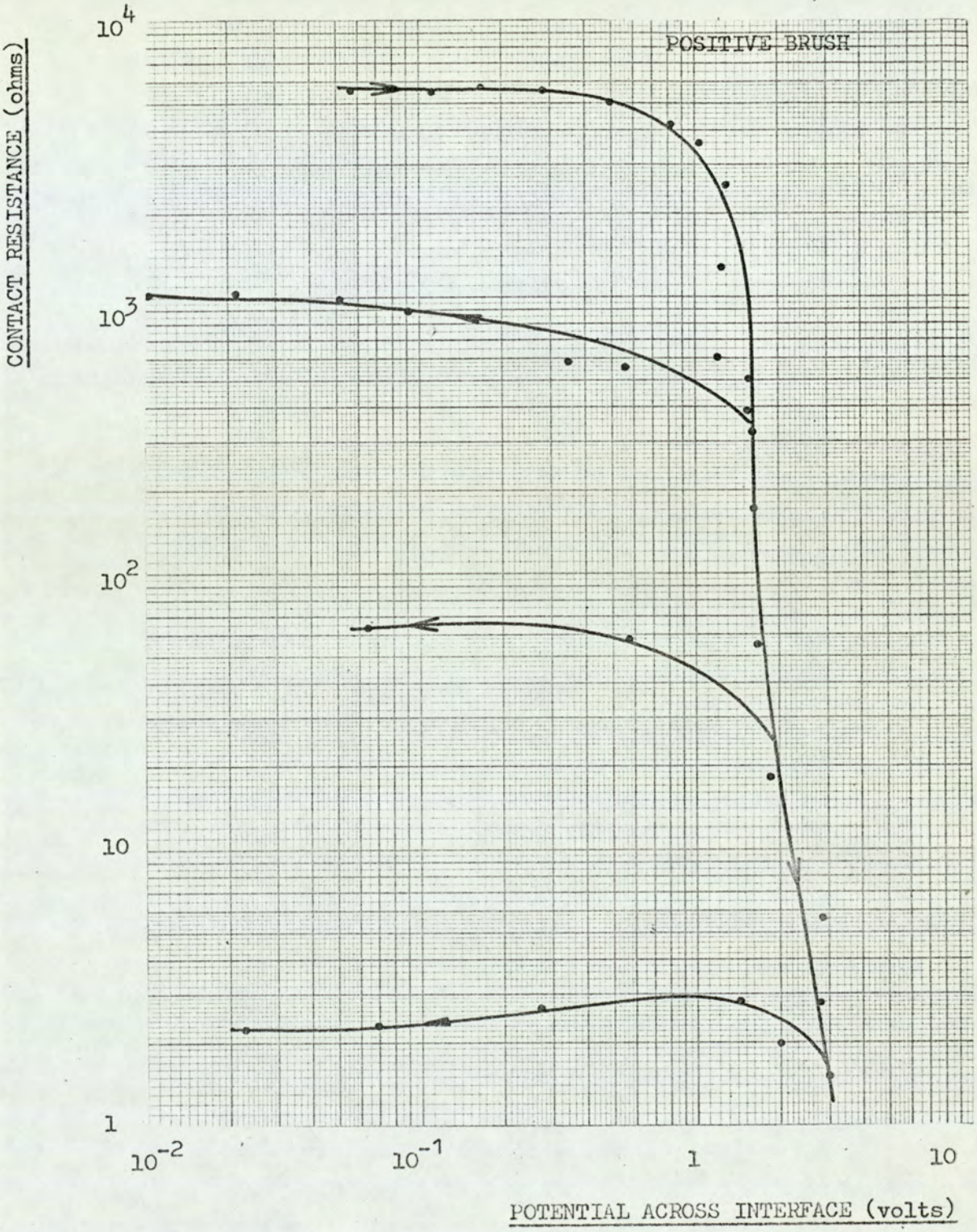

Figure 4.4 Variation in Contact Resistance of Positive Brush with Potential Difference at a Load of 60gf. on Aluminium.

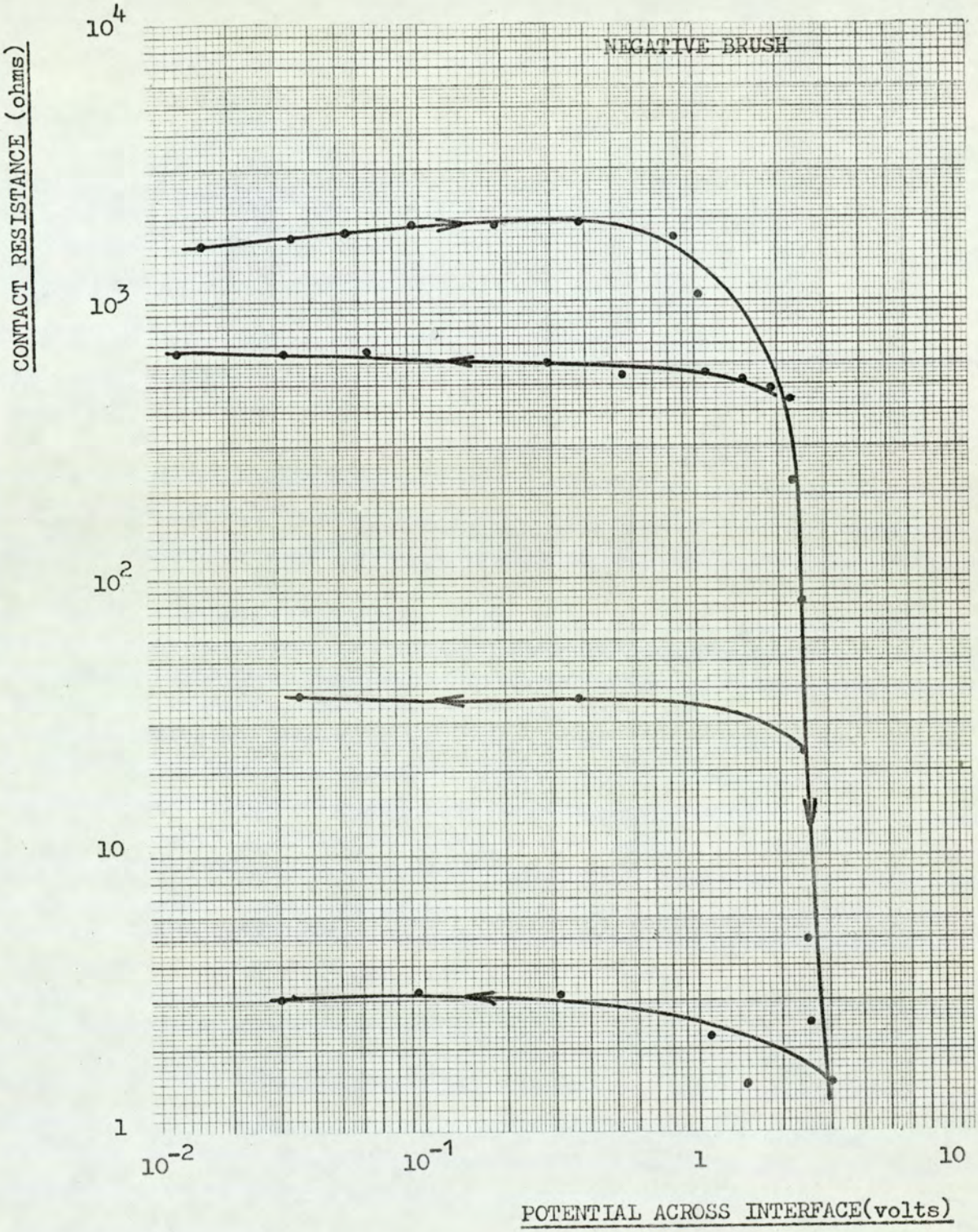

Figure 4.5 Variation in Contact Resistance of Negative Brush with Potential Difference at a Load of 60gf. on Aluminium.

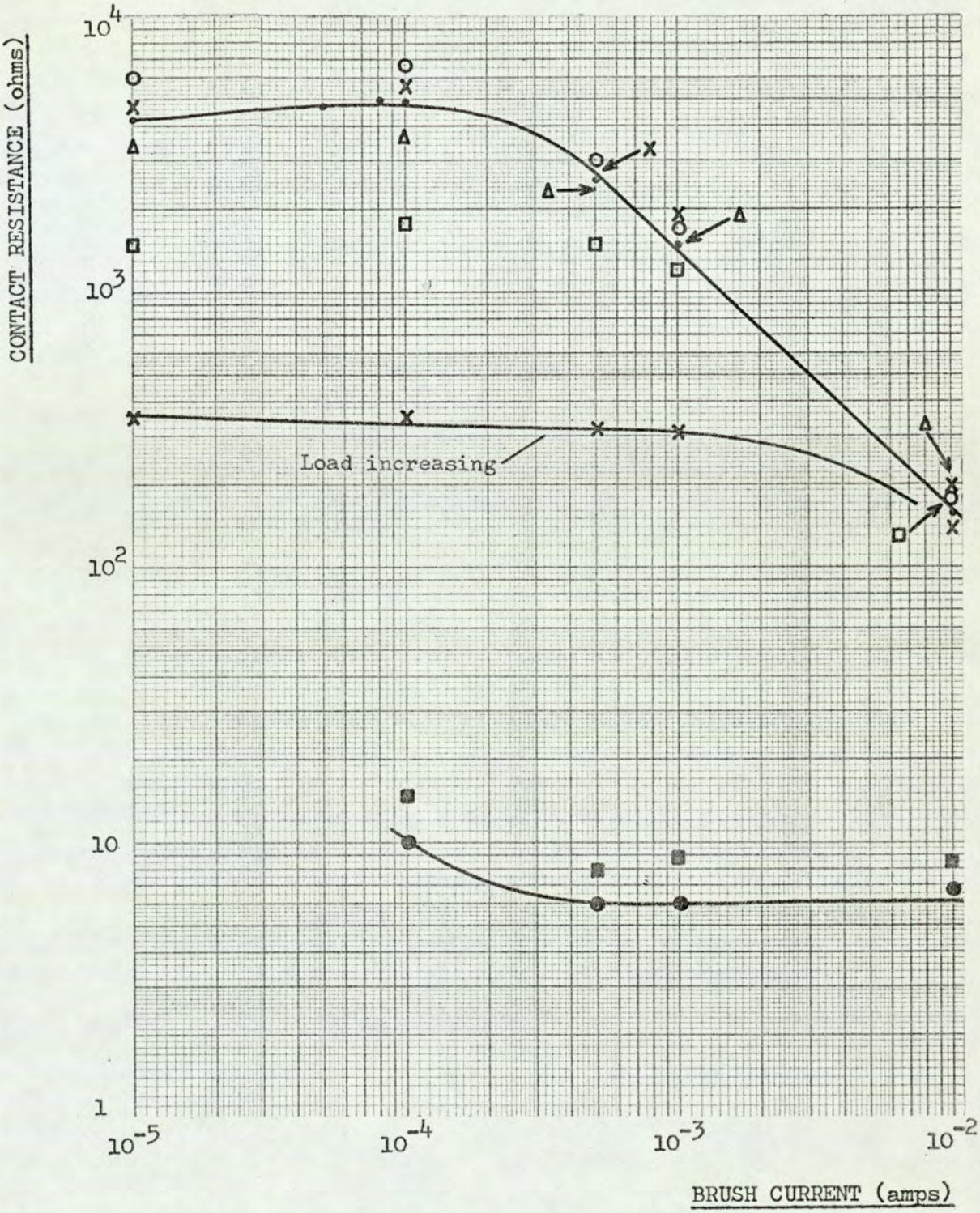

Load increasing. • 60gf. ○ 110gf. X 160gf. Δ 210gf.
□ 260gf. ● 310gf.

Load decreasing ■ 260gf. X 160gf.

Figure 4.6 Variation in Contact Resistance with Current at Various Loads.

Table 4.5

Contact Resistance of Electrographite sliding on Aluminium under a load of 460gms.f measured at various currents

Current	Negative Brush		Positive Brush	
	Contact Potential	Contact Resistance (OHMS)	Contact Potential	Contact Resistance (OHMS)
100 A	1mV	10	1mV	10
500 A	0.5mV	1.0	0.5	1.0
1 A	1.0mV	1.0	2.0	2.0
10 A	9	0.90	17	1.7
10mA	6	0.60	13	1.3
100m A	70	0.70	110	1.1
500m A	360	0.72	560	1.12
500 mA	360	0.72	600	1.2
1 A	670	0.67	1.06V	1.06
1 A	560	0.56	800mV	0.8
1 A	580	0.58	880	0.88
1 A	560	0.56	560	0.56
2 A	1.1V	0.55	1.2V	0.6
2 A	1.0V	0.50	1.04	0.52
5 A	1.6 V	0.32	1.9	0.38

Table 4.6

Contact Resistance of Electrographite sliding upon aluminium under a load of 1060 grms f.

Current	Negative Brush		Positive Brush	
	Contact Potential	Contact Resistance (OHMS)	Contact Potential	Contact Resistance (OHMS)
1mA	1mV	1	2mV	2
10	3	0.3	3	0. 3
50	11	0.22	10	0.2
100	22	0.22	21	0.21
100	22	0.22	28	0.28
500	98	0.96	150	0.30
500	103	0.21	144	0.29
500	116	0.23	144	0.29
1A	250	0.25	280	0.28
2A	500	0.25	520	0.26
2A	440	0.22	440	0.22
2A	420	0.21	440	0.22
2A	400	0.20	440	0.22
5A	920	0.18	1.08	0.22
5A	1.10V	0.22	1.20	0.24
10A	1.60V	0.16	1.80	0.18

there was a marked change in the characteristics. The contact resistance dropped to a low value which was almost independent of current. The load was then reduced to 260 gms.f.,but the interface retained the high load resistance characteristics, with a slightly increased value of the constant resistance. Upon reducing the load further to 160 gms.f., the contact resistance - current characteristic regained its original low load form, although the value of the resistance in the ohmic region was much lower than originally.

4.7. Contact Resistance Characteristics at Loads of 460 gm.f. and 1060 gms.f.

At these high loads the contact resistance was low and depended very little upon the current passing through the brush, the only effect measurable being a slight decrease in resistance at high currents. The results obtained at these high loads are shown in Table 4.5 and 4.6.

4.8. Contact Potential Waveform

The series of experiments described was carried out to determine whether any information about the nature of the contact surfaces could be obtained from a trace of the contact potential. As the disk passed beneath the brush different load bearing areas upon the disk made contact with areas on the brush. Any variation in the total resistance of the contacting asperities beneath the brush would be reflected by variation in the contact potential. When the contact potential was displayed on an oscilloscope the resulting trace showed how the potential between the brush and the disk varied as different regions of the track passed beneath the brush. For any information to be obtained the oscilloscope had to be triggered so that the trace started when the same portion of the track was beneath the brush. This triggering was carried out using the magnetic pick up arrangement described in Chapter 2. The pulse from the pick up head, produced at the

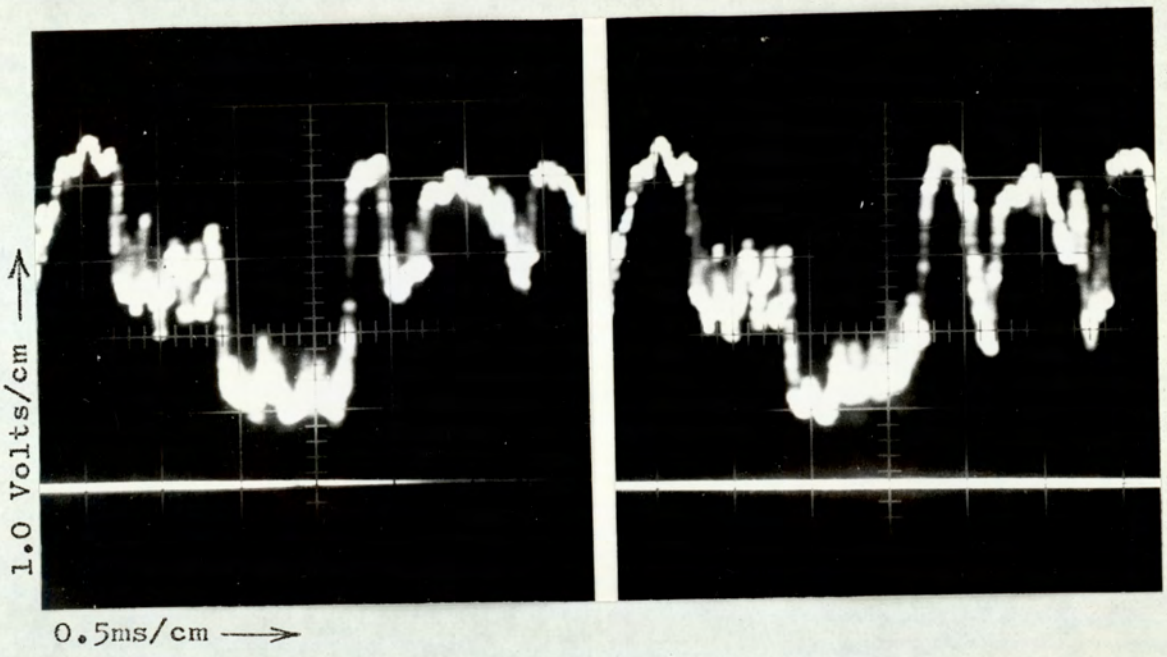

Time 0

(a)

Time 5 mins

(b)

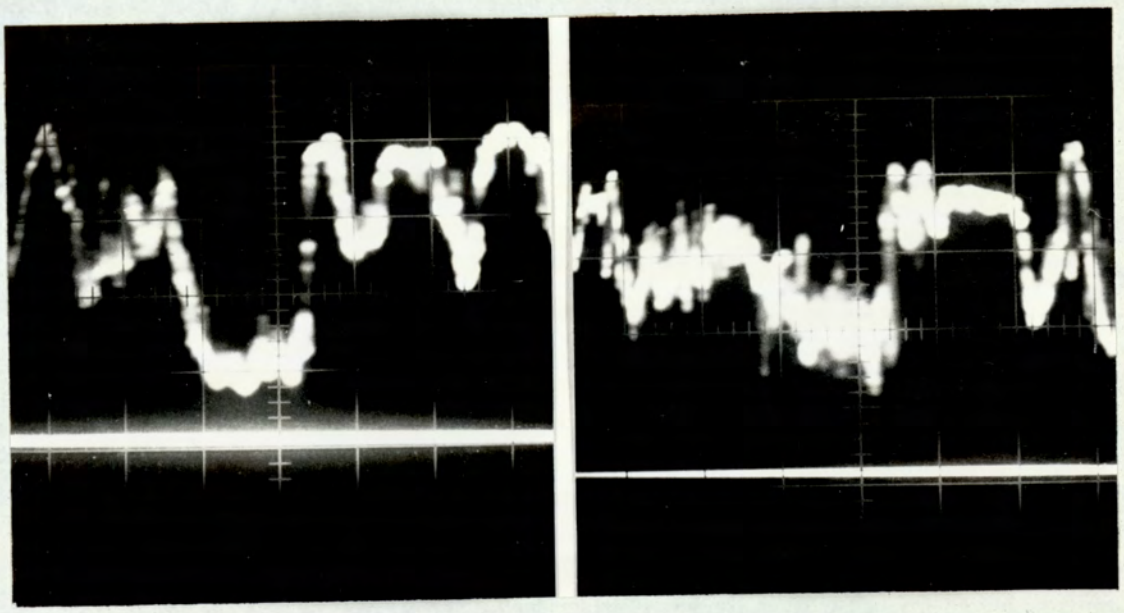

Time 3 hours

(c)

Time 24 hours

(d)

Figure 4.7 Contact potential trace of positive brush running under a load of 60g.f, current 1mA

same point of each rotation was used to externally trigger the oscilloscope. Thus, the oscilloscope showed the potential across the interface each time the same portion of disk traversed the brush.

A current of 1mA was passed through the two brushes which had been running for several days at a load of 60gms.f. A very steady, repeatable trace of the contact voltage was obtained, showing that the same contact asperity configuration was making repeated contact. Figure 4.7(a) shows the trace obtained from the positive brush. Designating the time at which this photograph was taken as zero a series of photographs of the trace at various times up to 24 hours later was taken, some of these photographs are shown in Figure 4.7. No significant change in the waveform was apparent over this period. The photographs show that the region of low potential, indicating an area of low contact resistance was passing beneath the brush, persisted for larger than 24 hours. To ensure that the drop in potential across the positive brush was not caused by a reduction in the brush current the potentials across the negative brush and across a resistance in the current lead were recorded. Had a drop in current occurred a drop in these two voltages would also have been caused, this was not the case.

To discover whether the brush or disk surface played the major role in determining the shape of the contact wave form the following brief experiments were carried out. The two brushes in the holders were interchanged and the resultant potential traces studied. After a very short bedding in period the traces became stable again. Had the potential across the interface been determined by the brush topography the shape of the traces may have been transferred with the brushes. However, after interchanging the brushes the shapes of the traces associated with the brush tracks remained unchanged. Figure 4.8 shows the trace obtained for the brush now running on the positive track, previously this had been

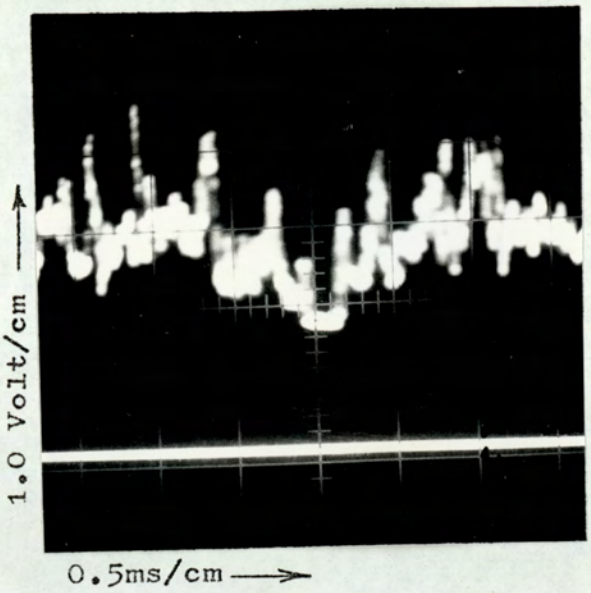

(a) Trace immediately after changing brushes

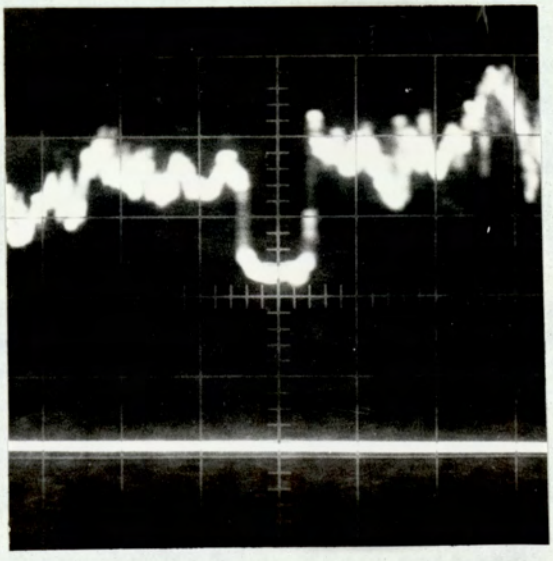

(b) Trace 24 hours after changing brushes

Figure 4.8 Contact potential trace obtained after brushes had been swopped in holders. Load 60g.f., current 1mA positive track.

the negative brush, comparison of the trace in Figure 4.8 with those in Figure 4.7 shows how little the contact had been changed. This result showed that the behaviour of the contact between the brush and the disk was affected by changes in the surface of the disk not by changes in the brush, in agreement with results obtained by Stebbens (24). A further investigation was carried out using wedge shaped brushes running on the positive track. The brushes were mounted such that the whole width of the wedge covered the track but the length of the brushes in the direction of sliding was small. A current of 1mA was passed through the brush and the potential true obtained. After a short running in period the trace became uniform, as in Figure 4.9(a). When the brush was replaced by a new wedge shaped one the trace was almost identical, Figure 4.9(b), confirming that the track played the major role in determining the electrical contact characteristics.

A feature of the potential traces shown in Figures 4.7, 4.8 and 4.9 was a region where a distinct low voltage occurs. In each case the distance travelled by the disk during the time for which the low resistance persisted was the same as the length of the brush in the direction of sliding. For the square section brush running on the positive track these distances are 4 m.m. and 2 m.m. for the brushes before and after interchanging them. This apparent anomaly (the length of the brush was 5 m.m.)was due to the brushes not being completely bedded in over their whole length. Upon examing the faces of the brushes immediately before interchanging them only about 4 m.m. of the positive brush had made contact with the disk. After taking the photographs of Figure 4.9 a further examination revealed that only about 2mm of the brush face was making contact. The distance moved by the disk during

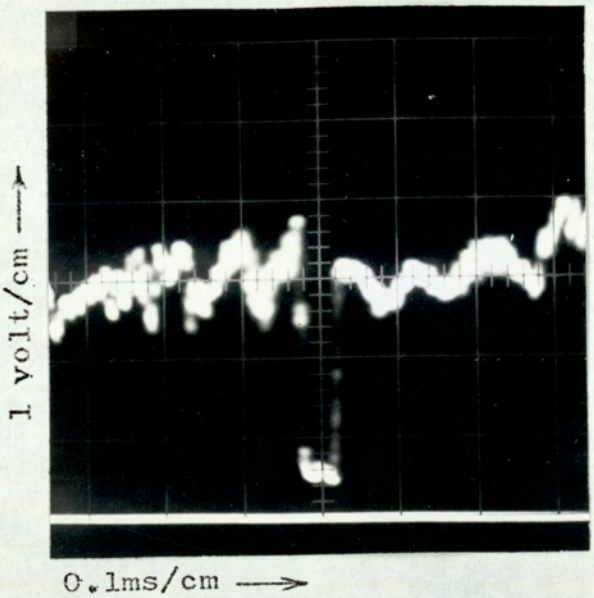

(a) Trace from bedded in wedge shaped brush

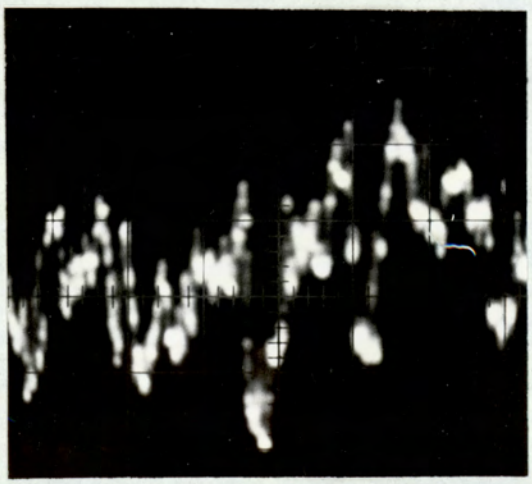

(b) Trace from new wedge shaped brush

Figure 4.9 Contact potential traces from wedge-shaped-brushes, load 60g.f., current 1mA

the time when a low voltage existed between the wedge shaped brushes and the disk was 0.2 - 0.25 m.m. The width of the contacting area of the wedge was measured with a travelling microscope and found to be 0.22 m.m. It would appear that in many cases an area of the disk having a relatively low contact resistance makes contact with the brush over the whole width of the brush as it passes beneath the brush, and not at discreet contact asperities.

At low currents the spread of the potential about its mean position was very large, indicating that some contact regions had a resistance much lower than others. As the current was increased the mean voltage also increased but at currents above the ohmic region the spread of voltage became less, indicating a general evening out of values. At high currents the waveform was still repeatable.

The effect of load upon the behaviour of the trace was investigated during the experiment described previously when the load was progressively increased. The voltage trace was studied at each load during the periods when current was being passed through the brushes to measure the contact resistance. At loads up to 260gms.f. the waveform was still stable and repeatable, changing very little over long periods. At loads above 260gms.f the waveform was constantly changing and at a load of 1060gms.f no waveform could be obtained, only a wide band.

Stebbens suggested that the reason for the non-stable waveform he experienced was due to copper picking by the negative brush. He therefore confined himself to studying the positive brush. No difference in behaviour between the positive and negative brushes could be detected in the experiments described here. Upon reversal of the current through the brushes no effect upon the voltage trace could be detected, apart from

inversion. A simple experiment was carried out to determine whether the instability of the waveform was due to aluminium particles embedded in the brush. The load was quickly reduced from 1060gms.f at which no steady trace was obtainable, to a load of 60gms.f the waveform instantly became stable and reproducible, although the contact resistance remained low (1ohm) for some time afterwards. If the instability at high loads had been caused by metallic debris embedded in the brush one would have expected the instability to persist at lower loads until the metallic debris had been removed from the surface. It seems unlikely that the removal of the embedded particles would occur almost instantaneously. This was verified by Electron probe microanalysis studies of the worn brush surfaces.

4.9 The Frictional force between Electrographite and Aluminium at a load of 60gms.f.

When running the brushes under a load of 60gms.f the frictional force was low, the maximum value being about 25gms.f. The measurement of these relatively small forces necessitated the use of the sensitive strain gauge transducers, which were subject to slight zero drift. Thus the zero had to be periodically checked during thr course of the experiments.

Both brushes were run at the same load, 60gms.f and continuous monitoring of the frictional forces was begun shortly after the run was started. Upon first measuring the frictional force its value was around 5gms.f but increased rather erratically as the run continued to a value which varied between 22-25gms.f for both brushes after running for 5 weeks. Holm(18) found a similar increase in friction during the initial stages of running and suggested that the increase was due to the real area of contact between the brush and metal increasing as the two surfaces wore to make

more intimate contact. However, for the two brushes reported here, running on Aluminium, the frictional force continued to increase after the whole surface of the brush had taken on a smooth, polished appearance and the brush had worn by an appreciable amount.

After the brushes had completely run in and the frictional force had attained a reasonably stable value an electric current was passed through the brushes to study its effect upon the frictional force. The current was increased in stages from 10μA up to 2A, when sparking occurred beneath the brush and the experiment was stopped. No effect upon friction was detected until a current of 30mA was reached when a significant decrease in frictional force occurred. When the electric current was increased the frictional force fell even lower, as indicated in Table 4.7. Upon increasing the current the frictional force fell rapidly to a new equilibrium value, but when the current was reduced the frictional force increased very slowly and took several hours or even days to return to its original high value. Figure 4.10 is a portion of the trace of thecontinuous recording of frictional force between the positive brush and the disk showing the rapid fall in friction which occurred when the current was increased 500mA to 1A. The variation in frictional force of the positive brush with current is shown in Figure 4.11 and the variation in frictional force of the negative brush is shown in Figure 4.12. The frictional behaviour of the two brushes was almost identical, both showed an initial increase in friction from a low value to a much higher steady value which remained unaffected by the passage of current until a current of about 30mA was reached when a decrease in friction occurred. As higher and higher currents were passed through the brushes the friction fell more and approached the original low value.

Current	Positive Brush		Negative Brush	
	Frictional Force Grms.f.	Friction Coefficient	Frictional Force Grms.f.	Friction Coefficient
0	22 - 22	0.37-0.42	22 - 25	0.37 -0.42
10μ	22 - 25	0.37-0.42	22 - 25	0.37 -0.42
100μA	22 - 25	0.37-0.42	22 - 25	0.37 -0.42
1mA	22 - 25	0.37-0.42	22 - 25	0.37 -0.42
10mA	22 - 25	0.37-0.42	22 - 25	0.37 -0.42
30mA	17 -18	0.28-0.30	17 - 18	0.28 -0.30
100mA	17 - 18	0.28-0.30	14 - 16	0.23 -0.27
200mA	17 - 18	0.28-0.30	14 - 16	0.23 -0.27
500mA	13 - 16	0.22-0.27	10 - 12	0.17 -0.20
1 A	10 - 12	0.17-0.20	8 - 10	0.13 -0.17
2 A	6 - 8	0.10-0.13	4 - 6	0.07 -0.10

Table 4.7 Variation in Frictional Force with Current at 60gms.f. Load.

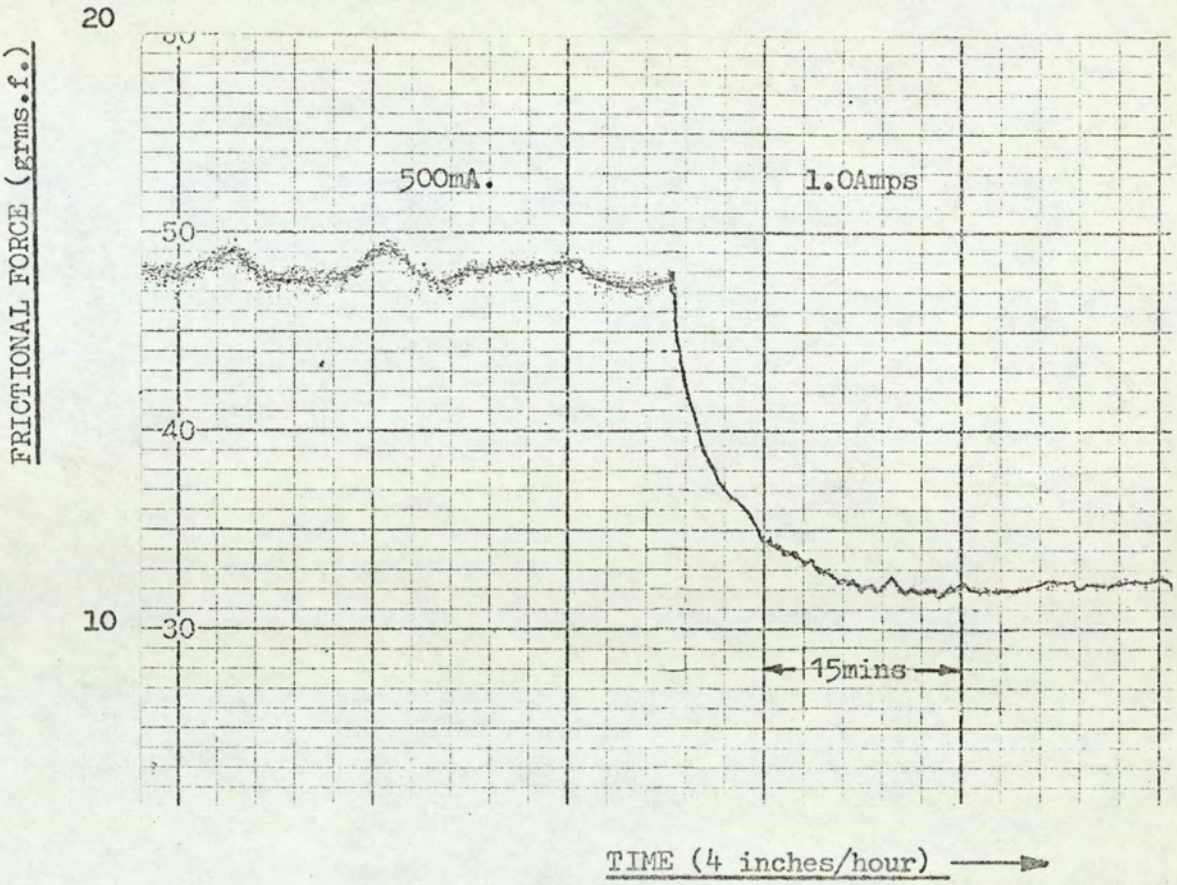

Figure 4.10 . Portion of the continuous record of frictional force between brush and Aluminium disk at a load of 60gms.f.

As previously stated, when the electric current was reduced or switched off the frictional force slowly increased to a higher value consistent with the new running conditions. A short experiment was prepared to determine whether this recovery was dependent upon the time which had elapsed since the reduction in current or dependent upon the distance of sliding during that time. The brushes were run in with no current passing until a high value of frictional force had been established. A current of 1A passed through the brushes for a short time until the frictional force had dropped to 10gmf. The current was turned off and the brushes immediately lifted clear of the disk for several hours. When the brushes

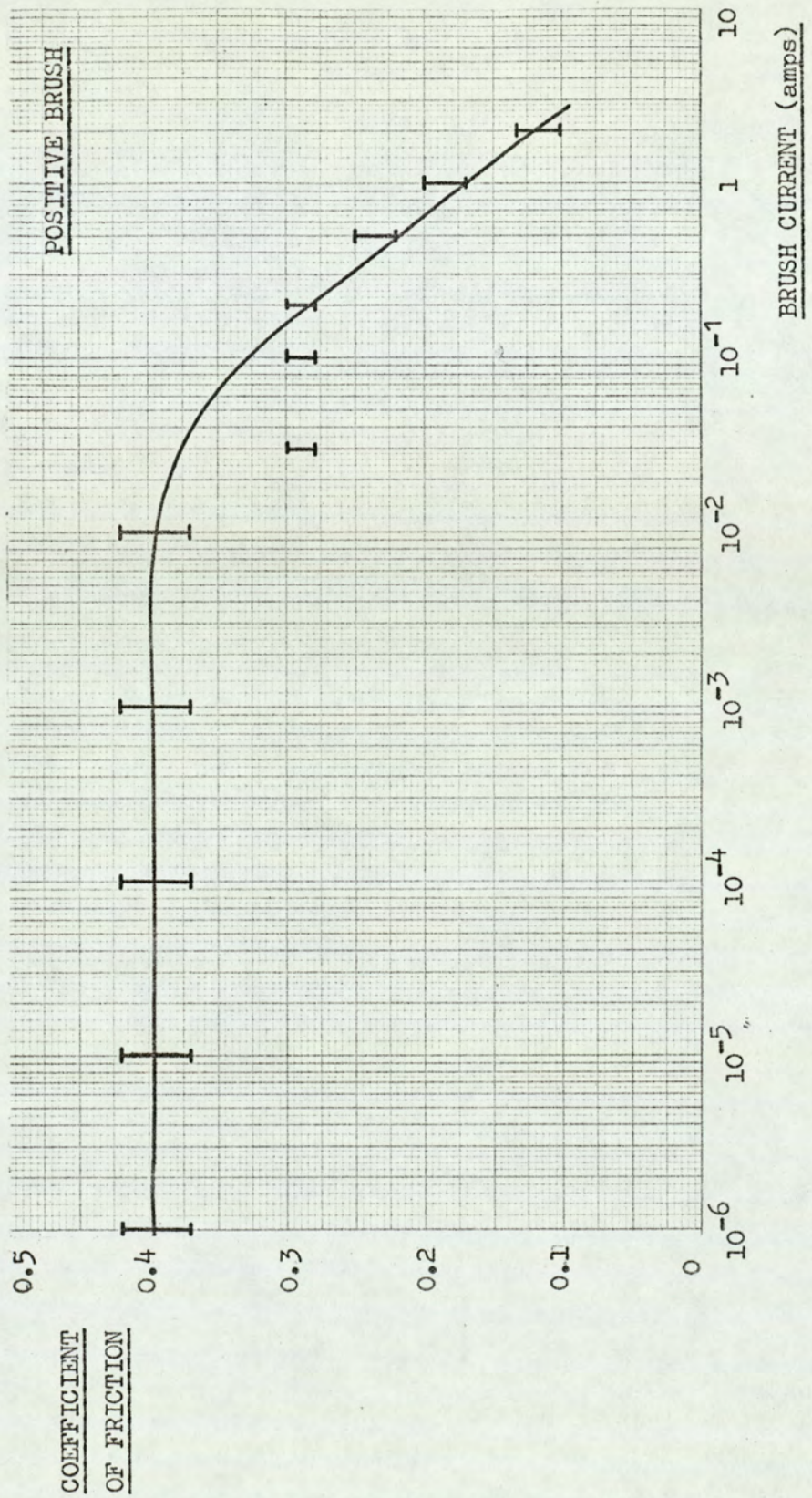

Figure 4.11 Variation in Coefficient of Friction of Positive Brush with Current at a Load of 60gf. on Aluminium.

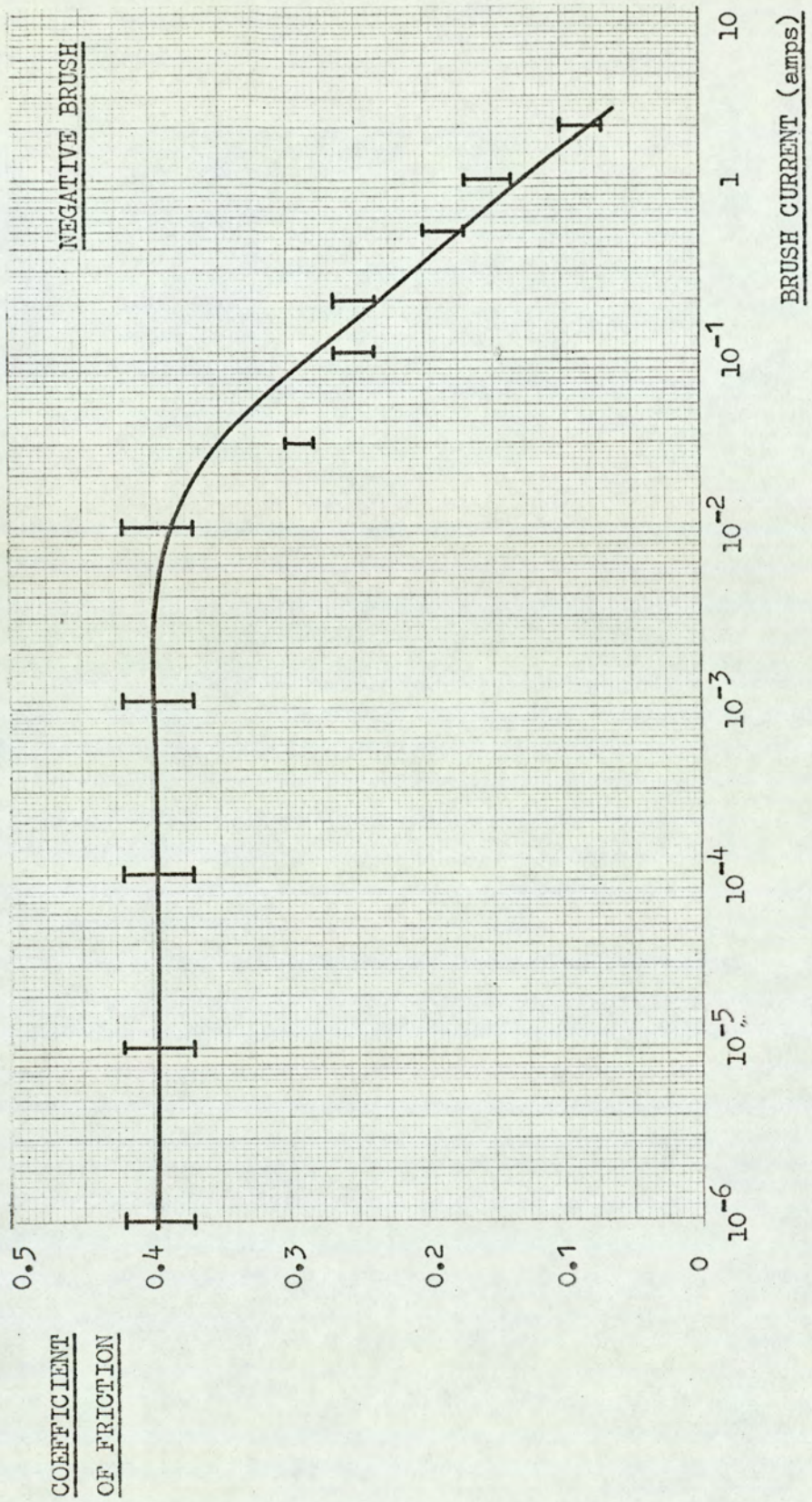

Figure 4.12 Variation in Coefficient of Friction of Negative Brush with Current at a Load of 60gf. on Aluminium.

were lowered back onto the disk again it was noted that the frictional force had remained at the low value and began to rise only when sliding was resumed. During the time that the brushes had been clear of the disk the contact resistance, measured at a current of 10 A had increased from 1 ohm to about 100 ohms. The brushes were run for a further 24 hours before the frictional force reached its original high value.

4.10 The Friction between an electrographite brush and Aluminium at a load of 160gms.f.

The frictional force at a load of 160gms.f was measured for an electrographitic brush being run as the positive brush. Table 4.8 shows the variation in mean frictional force as the current was increased. The behaviour of the friction was much the same as the behaviour at a load of 60gms.f. although the friction did not begin to decrease until a much higher current was passed. The initial value of frictional coefficient with no current flowing was lower than at 60gms.f but the value attained at high currents was about the same for both loads. The variation in friction with electric current is shown in Figure 4.13 which shows for comparison the frictional variation at other loads.

4.11 The Frictional Force between an Electrographite Brush and Aluminium at loads of 460gms.f and 1060gms.f.

At these higher loads the frictional force between the brush and the disk was relatively high and the more robust strain gauge transducers were used to measure the force. Unlike the more fragile transducers these higher load transducers were not subject to zero drift and less frequent calibration checks were needed, thus reducing disturbances to the system under investigation.

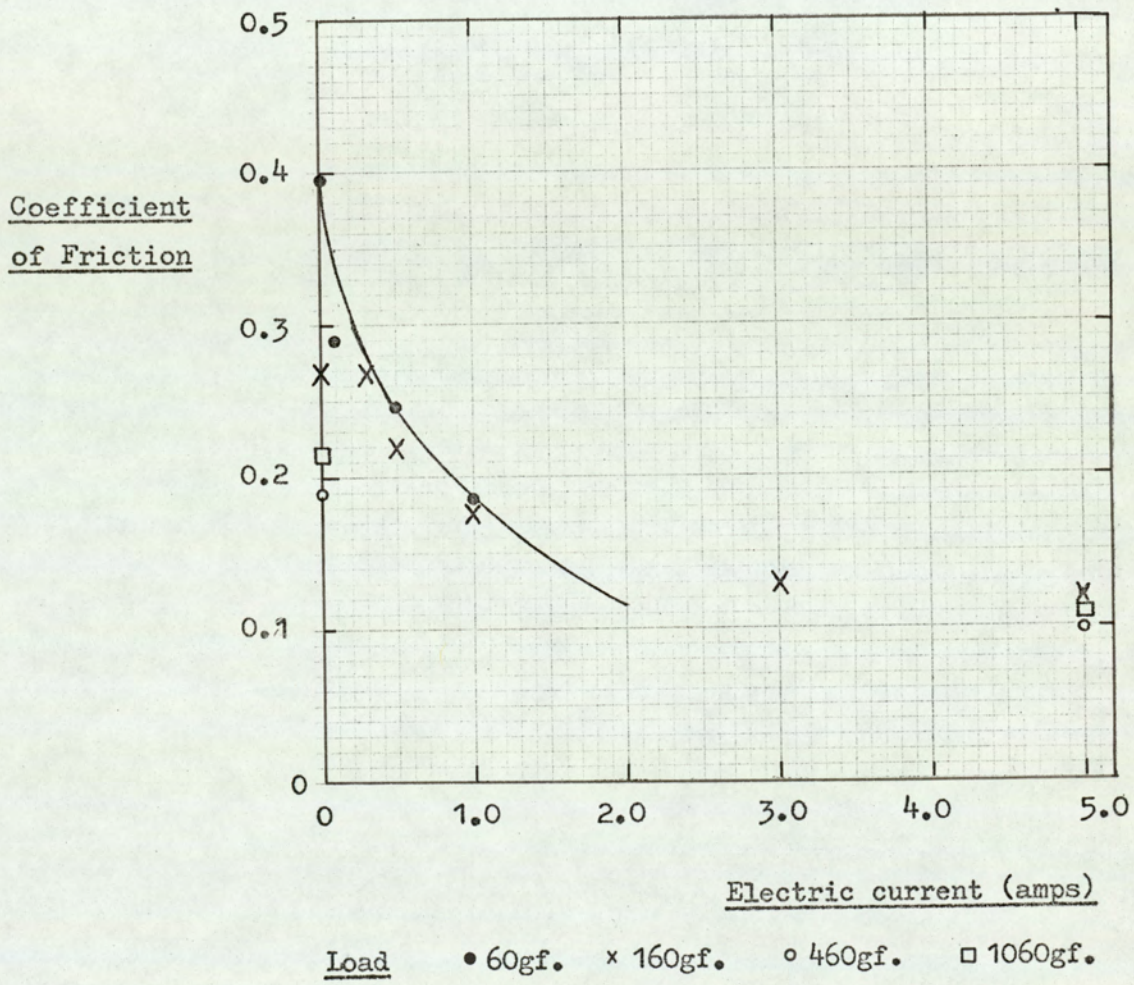

Figure 4.13 Variation in Coefficient of Friction with Electric Current at Various Loads.

Table 4.8

Current	Frictional Force gms.f.	Frictional Coefficient	Contact Resistance ohms
0	43	0.27	3.0K
10μ A	43	0.27	3.0K
100μ A	43	0.27	2.6K
1mA	43	0.27	1.4K
10 mA	43	0.27	200
300 mA	43	0.27	7.0
500 mA	35	0.22	4.0
1 A	29	0.18	2.0
3 A	21	0.13	0.8
5 A	19	0.12	0.5

Variation in Friction of Electrographite Sliding on Aluminium at a Load of 160gms.f.

(i) 460gms.f Load

When a freshly prepared brush was run on a newly turned disk the frictional force was around 50gms.f but increased within a few hours to a higher value which fluctuated between 80gms.f and 95gms.f (Coefficient of friction of 0.175 to 0.21). No variation in frictional force outside this range could be detected when electric current was passed through brush until a current was passed through the brush until a current of 5A was reached. At this current the frictional force dropped to between 40gf. and 50gms.f but was very erratic,the force momentarily increasing to values greater than 100gms.f. When the load upon a brush which had been running for some time at a constant frictional force of 50gms.f was increased from 360gms.f. to 460gms.f the frictional force increased immediately to 80gms.f. The surface of this brush was then lightly abraded with fine emery paper, leaving the surface of the disk undisturbed, and rerun at a load of 460gms.f the frictional froce dropped to 45gms.f then rose after a few hours back to 95gms.f. During this period of running in when the frictional force was increasing no decrease in contact resistance was detected.

(ii) 1060gms.f.Load

The behaviour of the frictional force at this load was almost identical to that at 460gms.f. the frictional force rapidly reached a value which fluctuated between 200gms.f and 250gms.f (Coefficient of friction 0.19 to 0.236). Low currents had no detectable effect upon friction but when currents of 5A and above were passed through the brush the frictional force dropped to around 120gms.f. but again was very erratic with frictional forces in excess of 250gms.f being recorded for very short periods.

4.12 Variation in the Temperature of an Electrographitic Brush with the conditions of sliding

Experiments were carried out with an electrographic brush sliding upon aluminium to determine how the bulk temperature of the brush varied with the sliding conditions. A thin wire Copper-Constantan thermocouple was cemented into an 0.2mm diameter hole drilled into the brush 0.5 mm from the running face. A silver containing adhesive was used to secure the thermocouple and provide thermal contact with the carbon. The cold junction of the thermo couple was maintained at $0^{o}c$ in a mixture of ice and water, and the e.m.f. developed between the junctions was measured by a potentiometer chart recorder capable of accurately measuring voltages as low as a 10^{-5} volts. The chart recorder was zeroed by placing both junctions of the thermocouple in the ice bath. The chart recorder had to be carefully balanced to ensure that the zero did not alter when switching ranges, since the zeroing procedure could not easily be carried out when running. The calibration was checked by immersing the hot junctions in water and heating, the e.m.f. produced was compared with published values as the temperature rose. The recorded e.m.f's were in close agreement with the expected values.

Temperature measurements were first carried out with the brush running under a load of 60 gms.f. As stated in a previous section (4.9) the frictional force at low loads rose slowly until, after several weeks running, an equilibrium value was established. Due to time limitations it was not possible to wait until the frictional force had reached its equilibrium value before commencing temperature measurements. The experiments to determine the effect of electric current upon the temperature of the brush were begun when the following conditions were

satisfied; the brush was in contact with the disk surface over the whole of the running face, the contact resistance (measured with a current of 50 A) was not changing, and neither the frictional force nor temperature were normally expected to vary by more than 2% during the time estimated to complete the experiments. An electric current was passed through the brush and the frictional force and temperature recorded, the contact resistance was also measured. A reversing switch was provided so that the measurements could be made with the current passing through the brush in both directions. The results obtained at loads of 60gms.f. and 160gms.f. are shown in Table 4.9. Since the frictional force had not reached equilibrium the values in this table cannot be compared with previously quoted values. Throughout the experiment the temperature of the enclosure beneath the bell jar was continuously measured using another thermocouple which was also used to periodically measure the bulk temperature of the disk.

When the brush was run at a load of 260gms.f. the frictional force and temperature increased slowly as the run continued. However after running for 3 hours the frictional force had attained a value of 18gms.f. and the temperature had a value of 34°c, the rate of increase in frictional force and temperature at that point being 0.7gms.f/hr and 0.47deg c/hr respectively. When the load was increased to 310gms.f. the frictional force rose immediately to 30gms.f. and the temperature to 35°c. After running for 20 hours the friction had increased to 38gms.f. and the temperature to 37°c, in the last 10 hours the friction having risen from 37 gf. whilst the temperature had not risen by any measurable amount. At a load of 360gms.f. the behaviour was very similar, and after 6 hours running the friction and temperature were 52gms.f. and 38°c respectively but both rising slowly.

Table 4.9 The Temperature of an Electrographite Brush Sliding on Aluminium Under Loads of 60gms.f. and 160 gms.f.

Load gms.f.	Current	Brush Positive				Brush Negative			
		Frictional Force gms.f.	Contact Potential	Contact Resistance Ω	Temperature °C	Frictional Force gms.f.	Contact Potential	Contact Resistance Ω	Temperature °C
60	0	6.5	-	-	26	6.5		-	26
	100μA	6.5	150mV	1.5K	26	6.5	140mV	1.4K	26
	1mA	6.5	1.1 V	1.1K	25	6.5	1.02K	1.02K	26
	10mA	6.5	1.9 V	190	23	6.5	1.9	190	26
	50mA	5.5	2.45V	49	25	5.5	2.8	56	26
	100mA	"	2.4 V	24	26				26
	500mA	5.0	2.68V	5.4	28				29
	1 A	5.0	2.5 V	2.5	32	5.0	2.65V	2.65	32
	2 A*	4.5	3.1	1.5	36	4.4	3.1 V	1.5	39
	5 A* (See note)	3.5			60				
160	0	21	-	-	31.5	21	-	-	31.5
	1mA	21	20mV	20	31	21	19mV	19	31.5
	10mA	21	170mV	17	25	21	150mV	15	31.0
	20mA	21	290mV	15	30	21	300mV	15	31.0
	50mA	20	700mV	14	31	20	680mV	14	31.0
	100mA	erratic	1.16V	12	31	erratic	1.14V	11	31.0
	200mA		1.8 V	9.0	32		1.8 V	9	32.0
	500mA		2.5 V	5.0	33.5				
	1 A	17	2.9 V	2.9	35.5	17			

Throughout these experiments the temperature beneath the bell jar remained within the range 22 - 24°C.

* Load 60gms.f. At a current of 2A the frictional force and contact resistance of the brush (when negative) was erratic. When the current was increased to 5A the temperature rose sharply and the friction became erratic with sudden momentary increases in frictional force in excess of 30gms.f.

When the current was switched off the temperature dropped within 15 minutes to 26°C but the friction remained low.

When the brush was run at loads of 460gms.f. and 1060gms.f. the frictional force and temperature reached equilibrium values within the time available for the experiment. The equilibrium values of the frictional force were in agreement with the values obtained in previous experiments. Immediately after increasing the load from 360gms.f. to 460gms.f. the frictional force was 80gms.f and the temperature was 43°c. After running for 10 hours the frictional force had increased to 89gms.f and the temperature to 44°c and after 34 hours and 50 hours running the frictional force was 92gms.f. and 94gms.f. respectively, but the temperature had not increased from 44°c. The surface of the brush was then lightly abraded with emery paper and the frictional force and temperature subsequently dropped to 40gms.f. and 35°c. Electric current was passed through the brush in the positive direction and the temperature of the brush varied as indicated below.

Current	0	1mA	10mA	20mA	100mA	500mA	1A
Temperature °C	35	34.5	32.5	32.5	34.5	35	37

At a current of 5amps sparking occurred beneath the brush and the temperature increased to 60°c. No variation in friction took place until a current of 5 amps was passed through the brush when the frictional force fell to 35gms.f. with momentary increases to values greater than 60gms.f. When electric current was passed through the interface with the brush negative no change in temperature occurred until a current of 1A was passed, the temperature increasing to 37°c. At a current of 5amps the temperature was 60°c. The frictional behaviour was the same as with the current passing in the positive direction.

At a brush load of 1060gms.f. the frictional force and temperature very quickly reached equilibrium values of 200gms.f and 58°c. No determination of the variation in brush temperature with electric current was carried out at this load.

4.13 Electron Diffraction Studies of the Worn Surfaces

Information about the interfaces produced during sliding was obtained using general area electron diffraction. The studies were carried out on an A.E.I. EM6G electron microscope using the general area diffraction attachment shown in Figure 4.14. This stage held the specimen in the electron beam below the final projector lens and enabled either transmission or reflection electron diffraction to be carried out. The microscope was provided with a vacuum lock to accommodate the stage so that specimens could be easily and rapidly changed. The stage was supplied with interchangeable mounts to enable transmission specimens in the form of microscope grids,or, reflection specimens mounted upon stubs, to be studied.

The diffraction stage had facilities for moving the specimen mount in two directions in a plane perpendicular to the electron beam and for rotating the specimen, so that the electron beam could be made to strike the face of the specimen in any direction. The specimen would also be tilted with respect to the electron beam, an essential feature for carrying out reflection diffraction. A gauge was provided to ensure that reflection specimens were mounted with the surface to be investigated on the tilt axis, so that the specimen did not move across the beam when tilted.

Two of the magnetic microscope lenses were used, the first condenser lens and the first projector lens, the latter lens being used to focus the beam. The broad diffraction rings obtained with carbon prevented the beam being focussed onto each specimen individually. However, since focussing was not critical for this application it was found satisfactory to focus on an aluminium transmission specimen prior to using the microscope for reflection diffraction.

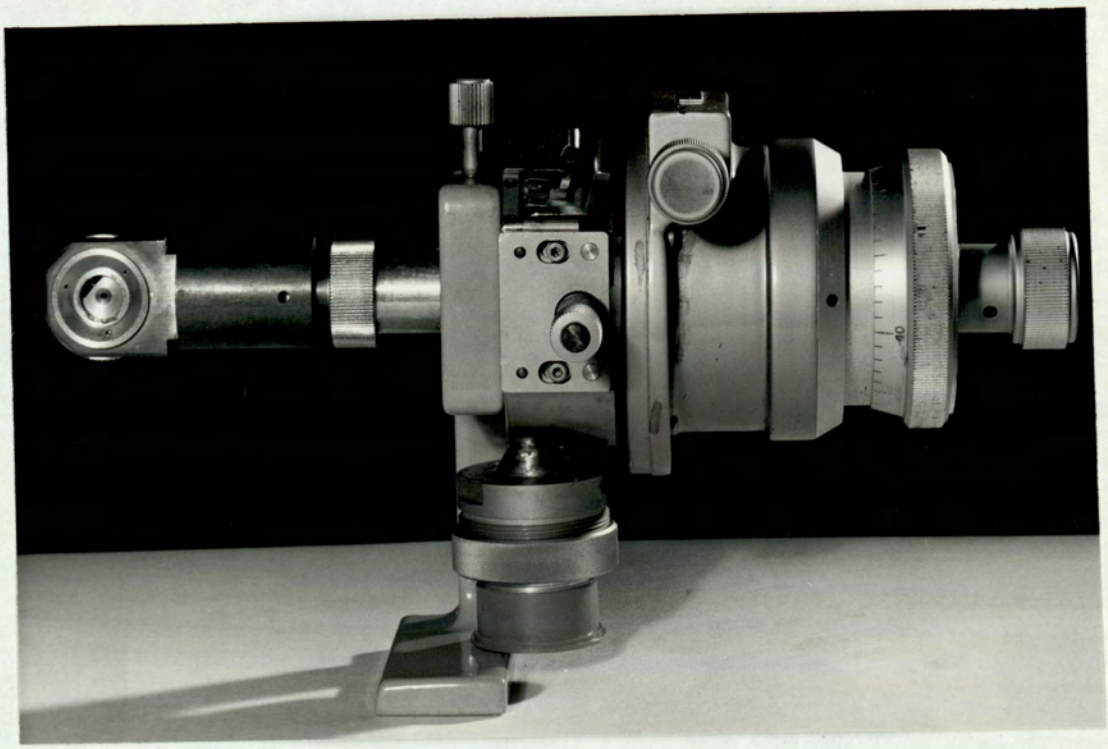

Figure 4.14 General Area Electron Diffraction Stage for A.E.I. EM6G Electron Microscope. The specimen holder is on the extreme left of the attachment and the controls for changing the the position of the specimen are on the right.

4.13(i) Calibration of the Microscope

Before using the microscope for studying the worn surfaces it was necessary to calibrate the microscope and camera to enable subsequent diffraction patterns to be analysed.

A beam of electrons will, like X-rays, be diffracted, by a set of crystal planes and obey Bragg's law.

$$2d_{hkl} \sin\theta = \lambda \qquad \ldots\ldots (1)$$

When d_{hkl} is the interplanar spacing, θ the angle of diffraction and λ the wavelength of the electron beam.

The wavelength of beam of electrons in an electron microscope is small compared with the wavelength of X-rays. A beam of electrons accelerated through 100kV will have an associated wavelength of about 0.04Å compared with the K_α line from copper of 1.54Å. Since the interplaner spacing is of the order of a few angstroms the values of sinθ for diffracted electron beams will be small and as a close approximation Braggs law may be rewritten

$$2\theta d = \lambda \qquad \ldots\ldots (2)$$

After passing through the specimen the electron beams impinge upon a photographic plate, a distance L below the specimen, forming the diffraction pattern. This is shown schematically in Figure 4.15. It is immaterial whether the crystallites considered are contained within a transmission specimen or on the surface of a reflection specimen. If a crystallite gives rise to a diffracted beam at an angle 2θ to the incident beam this will strike the plate a distance r from the centre spot, caused by the undiffracted beam, where : -

$$\tan 2\theta = \frac{r}{L}$$

For a polycrystalline specimen a ring of radius r will be formed. Since the angle θ is small, this may be rewritten $2\theta = r/L$, and substituting in equation (2) gives the relationship

$$rd = \lambda L$$

If the ring pattern is obtained from a polycrystalline material whose d - values are known, the rings can be indexed and the value of the product rd can be calculated for each line. Thus the value λL, called the camera constant can be determined. Having λL the d values of crystalline planes giving rise to subsequent patterns can be found.

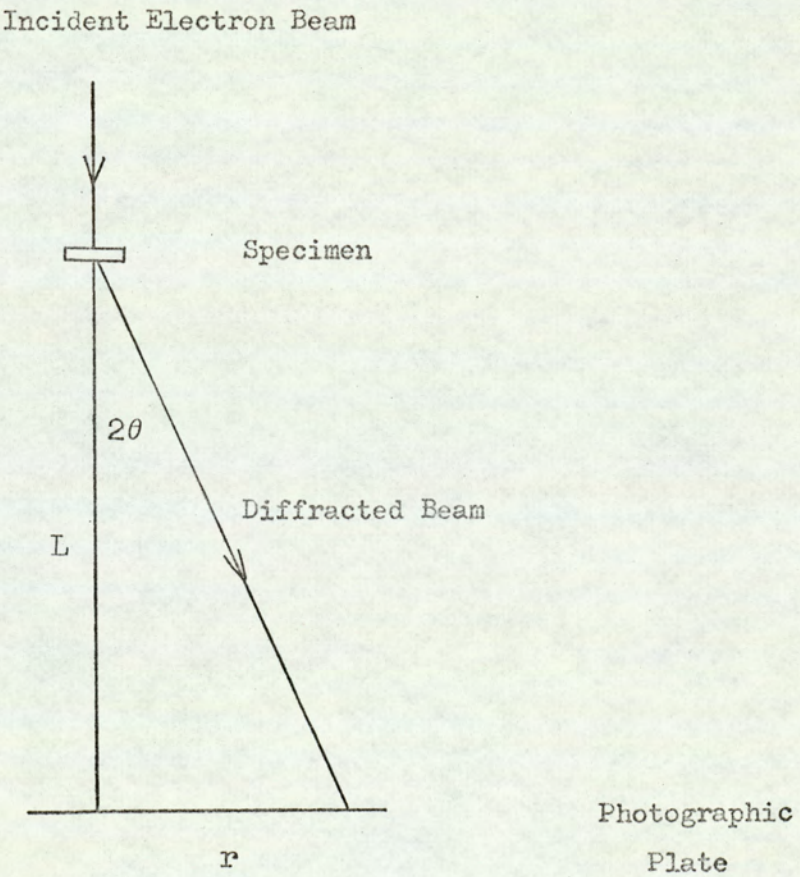

Figure 4.15 Schematic Representation of Electron Diffraction Camera

The EM6G electron microscope and camera were calibrated using a transmission specimen of evaporated aluminium. Figure 4.16 shows the diffraction pattern obtained at an accelerating potential of 80kV. The radius of each ring was measured using a travelling microscope and the appropriate values of d found from X-ray Powder Data File. Table 4.10 shows the values of r,d and the product rd for each line, thus giving the value of the camera constant. The camera constant must be determined for each value of accelerating potential used.

4.13(ii) Examination of Worn Brush Surfaces

The end 3mm of the brushes were cut from the remainder and mounted on the stubs provided. Electrical contact between the specimen and mount was made with a conducting paste. The edges of the running face of the brushes were chamfered to prevent interference with the beams. The specimen was tilted until the running face of the brush was parallel to the direction of the electron beam and the direction of sliding was perpendicular to the electron beam, as shown in Figure 4.17(a).The specimen could be rotated in the electron microscope to examine the surface with the electron beam parallel to the direction of sliding, as in Figure 4.17(b). The direction of the smaller arrows on Figure 4.17 indicate the direction of motion of the other sliding member across the specimen surface.

The position of the specimen within the microscope, and the angle of tilt were adjusted until a diffraction pattern was obtained. The optimum position for diffraction was with the shadow edge produced by the specimen coinciding with, or just masking, the centre spot caused by the uninterrupted electron beam.

Diffraction patterns were obtained with the electron beam both

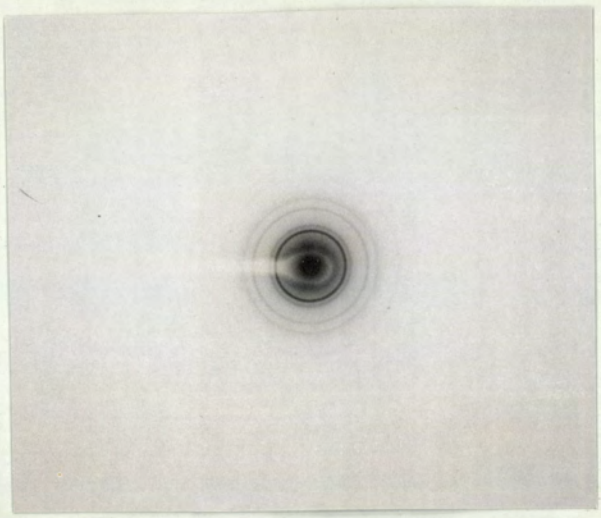

Figure 4.16 Electron Diffraction Pattern From Evaporated Aluminium Standard – 80kV.

Radius of ring (mm)	4.48	5.09	7.35	8.43	9.06	11.00
hkl	111	200	220	311	222	331
Interplaner spacing d(Å)	2.34	2.02	1.43	1.22	1.17	.929
Rd	10.5	10.4	10.5	10.3	10.6	10.3

TABLE 4.10

Calculation of Camera Constant (λL) for EM 6G Electron Microscope at a Potential of 80kV.

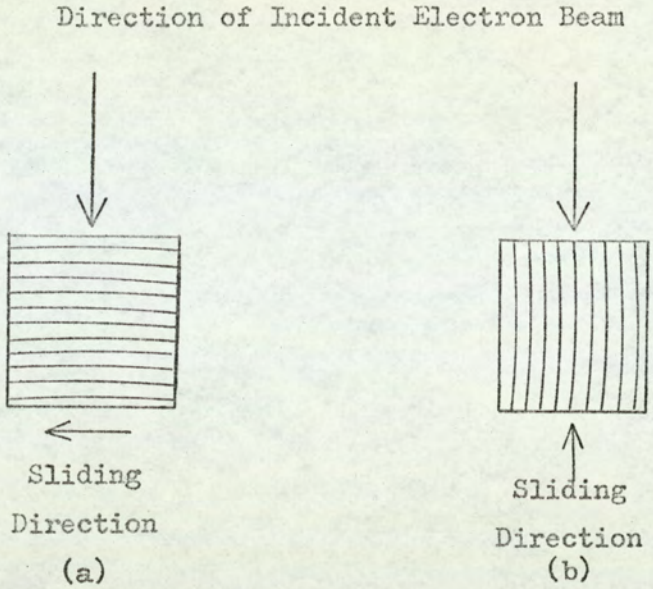

Figure 4.17 Relative Direction of Electron Beam

parallel to and perpendicular to the sliding directions.

The results obtained from running the brushes, quoted in previous sections suggest that the characteristics may be broadly spearated into two categories, the variation in running characteristics with varying load and the variation in characteristics with electric current at low loads. A range of specimens were generated for examination from running conditions which covered both these categories. One set of specimens was obtained running at a light load, 60gms.f. and a variety of electric currents, from zero to 2A. the other set of specimens was obtained running without current at loads between 60gms.f and 1060gms.f. Great care was taken to ensure that the specimen surfaces examined related to the running characteristics quoted in previous sections, and it was necessary at light loads to run the brushes for several weeks before the brushes were run in and the values of frictional force, wear rate and contact resistance, were in close agreement with the equilibrium values obtained previously.

Figure 4.18 shows the diffraction patterns produced by the surfaces of the brushes run at 60gms.f. with various electric currents passing

Direction of Electron Beam

Perpendicular to Sliding Direction

Parallel to Sliding Direction

(a)

(b)

Zero Brush Current

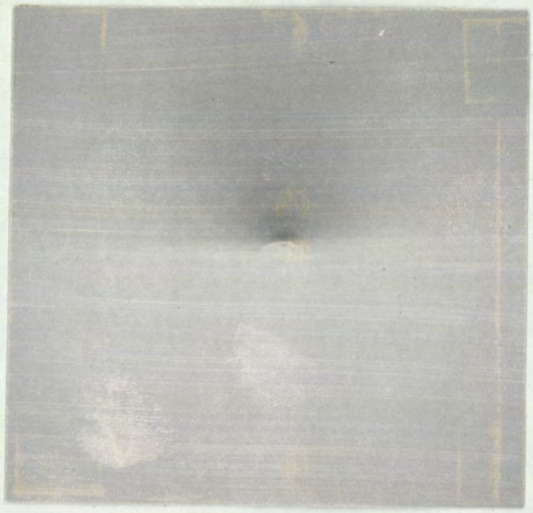

(c)

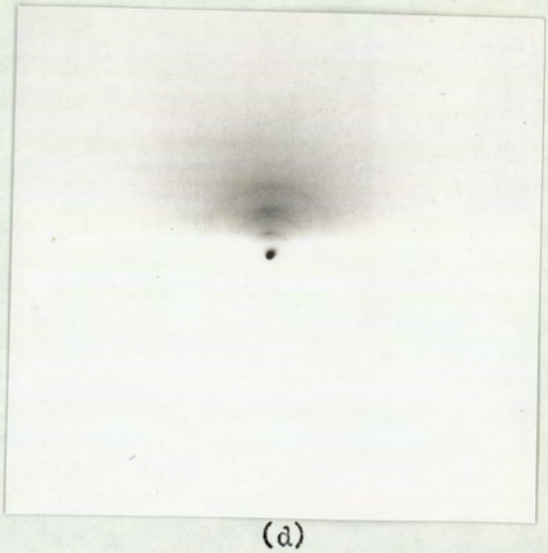

(d)

Brush Current 1mA.

Figure 4.18 Reflection Electron Diffraction Patterns From The Surfaces of Brushes Run At 60 grm.f. Load

Direction of Electron Beam

Perpendicular to Sliding Direction

Parallel to Sliding Direction

(e)

(f)

Brush Current 500 mA.

(g)

(h)

Brush Current 2 Amps

Figure 4.18 Reflection Electron Diffraction Patterns From The Surfaces of Brushes Run At 60 grm.f. Load

through the interface. Patterns obtained with the electron beam parallel to and perpendicular to the sliding direction are shown. The original diffraction patterns, from which measurements were made, were produced on photographic plates and the patterns and shadow edge formed were much more clearly visible than in the reproductions shown in the text.

The diffraction patterns produced by most of the brush surfaces consisted of a series of semicircular rings together with a number of arcs. The semicircular rings were produced by the (111) (200) (220)and (311) planes of aluminium and the (104) (113) and (030) planes of aluminium oxide (α - Al_2O_3). The presence of aluminium and its oxide indicates that aluminium from the disk surface was being transferred to the surface of the brush. Transferred aluminium or its oxide could not be detected on the surface of the brush run at a current of 2 amps. The arcs were identified as being from the (002) (004) and (006) planes of graphite. When the electron beam was directed along the sliding direction the arcs were perpendicular to the shadow edge and when the beam was directed perpendicular to the sliding direction the arcs were inclined at an angle δ° to the shadow edge. Previous workers (2) (10) (12) have obtained similar results for worn graphite surfaces and have concluded that the arcs are caused by an (001) fibre axis, directed along the resultant of the frictional force and normal reaction at the surface. Several diffraction pstterns were obtained from each specimen by moving the brush face across the electron beam, the values of δ measured from each photographic plate are shown in Table 4.11.

These results showed that the value of δ decreased as the value of the electric current passing through the brush increased.The values of δ

Load	Current	Direction of electron beam	δ°	Tan δ
	0	Perpendicular	19	0.344
	0	"	19	0.344
	0	"	20	0.364
	0	Parallel	0	0
	0	"	0	0
	1mA	Perpendicular	18	0.32
	"	"	18	0.32
	"	Parallel	0	0
	"	"	0	0
60gm.f.	500mA	Perpendicular	8	0.14
	"	"	11-12	0.21
	"	"	14	0.25
	"	"	12-13	0.23
	"	"	13	0.23
	"	Parallel	0	0
	"	"	0	0
	"	"	0	0
	2A	Perpendicular	3-4	0.07
	"	"	5-6	0.11
	"	"	4-5	0.09
	"	Parallel	0	0
	"	"	0	0
	"	"	0	0

Table 4.11 Values of δ for Brush Surface measured at various Electric currents under a load of 60gms.f.

are shown in Figure 4.19 plotted against electric current, together with the corresponding values of coefficient of friction. No difference in the diffraction patterns from the positive and negative brushes could be detected. Although the number of results obtained was small they support the view that frictional force and δ are related (9) (10) although the nature of this relationship may be different from that suggested by these authors.

The brush surfaces generated running without current at loads up to 1060 gms.f. were examined by electron diffraction in the same way as the surfaces produced at 60gms.f.load. Again the diffraction patterns consisted of semicircular rings produced by transferred aluminium and aluminium oxide and arcs produced by the graphite crystallites. Table 4.12 shows the values of δ at various loads together with the coefficient of friction.

These results show a strong similarity to the results obtained by Quinn (10) when sliding electrographite upon copper slip rings. For loads between 160gms.f. and 1060gms.f. inclusive little variation in δ was observed. At a lower load, 60gms.f. the value of δ was slightly higher. Quinn found that at a load of 3kg.f. the crystallites were orientated with their (001) fibre axis almost perpendicular to the brush running face whilst at loads above 6kg.f. the crystallites were randomly orientated. Figure 4.19 shows the diffraction patterns obtained from the brush surfaces at loads of 460gms.f. and 1060gms.f. At 460gms.f. the arcs from the oriented material were very strong but at 1060gms.f. the arcs were much weaker compared with the strength of the lines from the randomly oriented material, indicating a decrease in the number of oriented crystallites at this higher load. A decrease in the number of oriented crystallites could be due to either a lessening of the areas of orientation or a reduction in

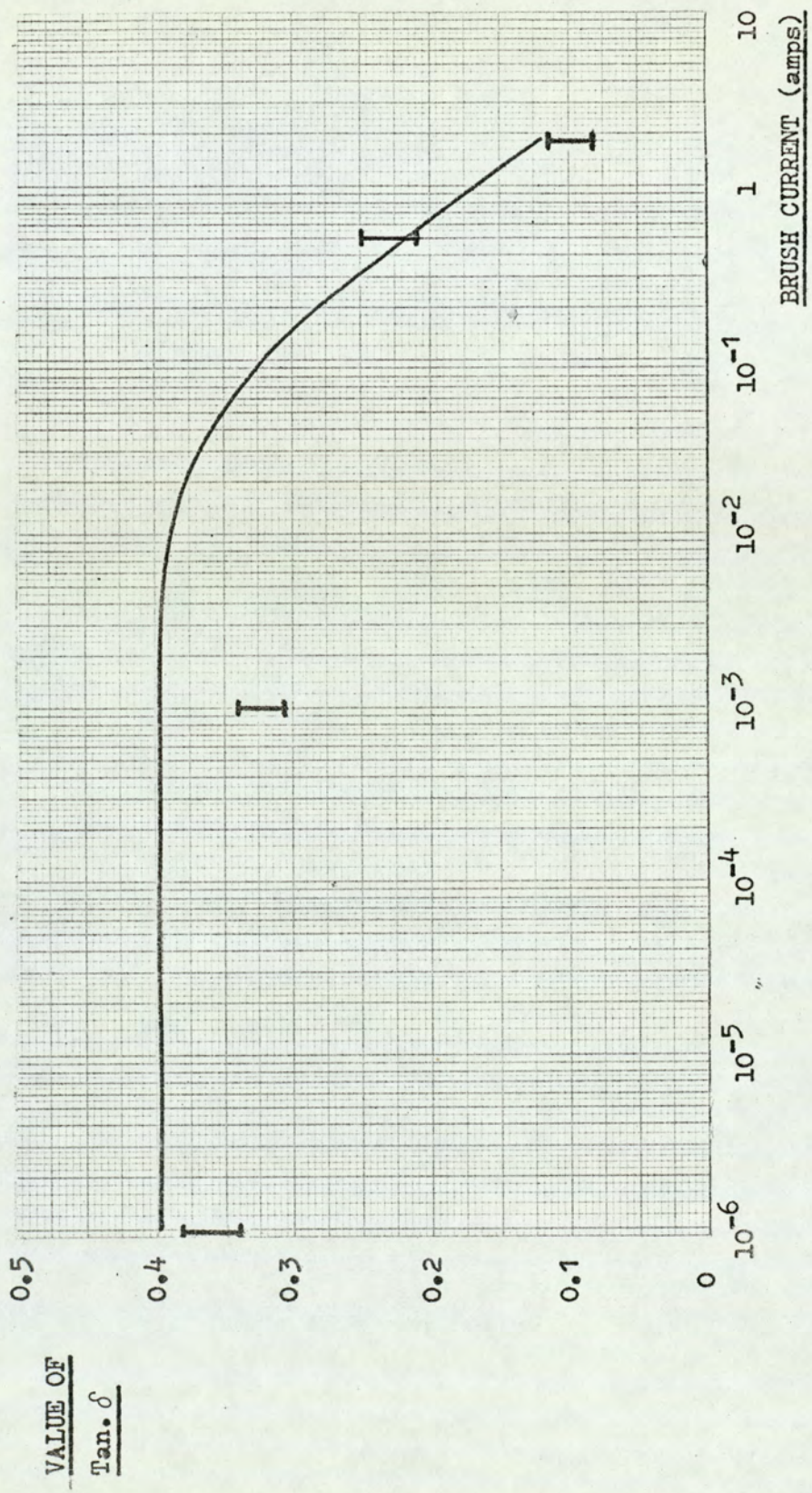

Figure 4.19 Variation in Angle of Tilt of Graphite Crystallites with Electric Current for an Electrographite Brush Siding on Aluminium at a Load of 60gf.

Load gms.f.	Direction of electron beam	δ^{o}	tan δ	μ_{Mean}
60gms.f.	Perpendicular	19	0.344	
60gms.f.	Perpendicular	19	0.344	
60gms.f.	Perpendicular	20	0.364	0.4
60gms.f.	Parallel	0	0	
60gms.f.	Parallel	0	0	
60gms.f.	Parallel	0	0	
160	Perpendicular	10	0.176	
160	Parallel	0	0	0.27
260	Perpendicular	6	0.105	
260	Perpendicular	7	0.123	
260	Perpendicular	9	0.158	0.23
260	Parallel	0	0	
360	Parallel	10	.176	
360	Parallel	0	0	0.23
460	Perpendicular	8	0.141	
460	Perpendicular	8	0.141	0.2
460	Parallel	0	0	
460	Parallel	0	0	
1060	Perpendicular	7	0.123	
1060	Parallel	0	0	0.22

Table 4.12 Values of δ^{o} for brush surface measured at various loads, no current

the depth of the oriented layer.

4.13(iii) Examination of Worn Aluminium Surfaces

The crystallography of the worn aluminium surfaces was investigated by studying either the removable plugs inserted into the disks, or specimens of the wear track cut from the disk. The running tracks generated at various currents under a brush load of 60gms.f. and without current at loads up to 1060gms.f. were examined with the electron beam both parallel to and perpendicular to the direction of sliding.

Diffraction rings from the polycrystalline bulk aluminium surface were naturally present in the diffraction patterns from these specimens. Faint rings from aluminium oxide were also visible in some of the diffraction patterns. The presence of these aluminium lines could not be connected with the value of either load or electric current. This random appearance of oxide rings was not unexpected since diffraction takes place from both the contact and non-contact areas and oxidation of the aluminium surface after running could not be prevented.

The diffraction patterns obtained from the graphite deposited upon the surface were, without exception, faint compared with the rings from the aluminium. Apart from when running at a load of 60gm.f the graphite deposited into the aluminium was randomly oriented. The orientation of the crystallites at various currents deposited under a brush load of 60gm.f. is shown in Table 4.13 . At low currents the crystallites were oriented with their (001) fibre axes at small angles to the normal to the running

surface, but at higher currents the crystallites were randomly orientated. These results were consistentwith those obtained by Quinn(10), when sliding electrographite upon copper, who found that the transferred graphite was either randomly oriented or oriented with a very small value of δ .

Load	Current	Direction of electron beam	δ
60gms.f.	0	Perpendicular	7
	"	"	7
	"	"	5
	"	"	4
	"	"	5
	"	"	7
	"	"	6
	"	Parallel	0
	"	"	0
	"	"	0
	"	"	0
	"	"	0
	"	"	0
	1mA	Perpendicular	2
	"	Parallel	0
	500mA	Perpendicular	7
	"	"	5
	"	Parallel	0
	"	"	0
	2A	Perpendicular	)Randomly
	"	Parallel	)oriented

Table 4.13 Variation in for Aluminium Surfaces at a Brush Load of 60gms.f.

4.14 Electron Probe Microanalysis of Worn Brush Surfaces.

Copper picking is a term used by carbon brush manufacturers and users to describe the presence of copper particles upon the faces of brushes run against copper slip rings or commutators (19) (24). The transfer of a thin, but visible film of copper to the brush, or the adhesion of relatively large particles of copper is normally associated with poor electrical contact due to adverse mechanical conditions. Copper picking is detrimental to machine commutation since copper particles upon the running face of one brush results in that brush carrying a larger proportion of the total machine current than the unaffected brushes, Stebbens (24) suggested that copper is transferred to the surface of the negative brush only and takes over the role of the contact spots from the brush asperities.

The electron diffraction studies of worn brush surfaces described in section 4.13 have shown that aluminium and aluminium oxide were present upon the running faces of brushes sliding against aluminium rings at all loads between 60gms.f. and 1060gm.f. without current flowing. When an electric current was passed through the brushes running at 60gms.f. load aluminium and aluminium oxide were still present upon the worn surfaces, until a current of 2 Amps was passed through the brushes; at this current no transferred material was detected.

Electron probe microanalysis of the brush running faces was carried out with several objectives. These were (i) to confirm the presence of aluminium upon the worn brush surfaces (ii) to determine how the aluminium, if present, was distributed on the surface and (iii) to confirm the reduction in the amount, or the complete absence, of aluminium upon the brush surface at high currents, as suggested by electron diffraction.

Electron probe microanalysis gave information about the distribution of elements upon the specimen surface but, unlike x-ray or electron diffraction did not reveal the crystallographic structure of the surface or what compounds were present. In the electron probe microanalyser, or microprobe, a beam of electrons is focussed onto the specimen and scanned or rastered, across a small area of the surface. Two modes of operation are possible; the electrons scattered or emitted by the surface can be detected by a scintillation counter and used to obtain an electron image of the surface topography or the characteristic x-rays emitted by the surface elements can be studied. The beam of electrons incident upon the specimen penetrated to a depth of the order of a few microns, dependent upon accelerating voltage and specimen material, and the elements contained within this depth emit x-rays in all directions. Each element present gives rise to a characteristic set of frequencies, called the x-ray emission spectra. The emitted x-rays are analysed by an x-ray crystal spectrometer to determine what elements are present. The x-ray crystal spectrometer consists of a crystal of known interplaner spacing, either Lithium Fluoride or Gypsum, which can be rotated so that some x-rays from the specimen undergo Bragg diffraction at the crystal and are incident upon a radiation detector. Knowing the interplaner spacing of the crystal and the angle of diffraction, the wavelength of the diffracted x-rays and hence the element giving rise to that characteristic x-ray can be determined. The output from the detector can be amplified and displayed either on a scaler in counts per second or as a deflection on a meter. Alternatively the output can be displayed as a spot on a cathode ray tube which is synchronised with the rastered beam, so that the distribution of an element on the specimen surface is displayed on the cathode ray tube

screen.

Before using the microprobe to investigate any particular element the crystal spectrometer has to be set to detect only characteristic x-rays from that element. This calibration procedure was carried out using a pure specimen of the element under investigation, which was placed in the instrument specimen chamber beneath the electron. The crystal was rotated to give the required Bragg angle and fine adjustment of the angle carried out to give a maximum count rate on the scalar or meter, thus tuning the spectrometer to receive x-rays from the element if present upon the surface of any subsequent specimens.

The worn electrographite brush surfaces were examined by scanning a small area of the brush 0.6mm x 0.6mm, and displaying the resultant x-rays from aluminium on the cathode ray tube, thus giving a record of the distribution of aluminium on the brush surface. No special preparation of the brushes was required since they fitted conveniently into the specimen holders provided. All the investigations described were carried out using an electron accelerating potential of 20KV.

Shown in Figure 4.20 are a selection of x-ray images showing the distribution of aluminium upon the surfaces of brushes which had been run under a load of 60 gmd.f. at various brush currents. Electron image micrographs of the topographies of some worn areas and also shown in some cases. All the X-ray images shown in Figure 4.20 were obtained at an exposure time of 15 minutes.

Figure 4.20(a) shows that when the brush was run without current aluminium was distributed over the whole of the area under investigation. A comparison of the X-ray distribution and the electron

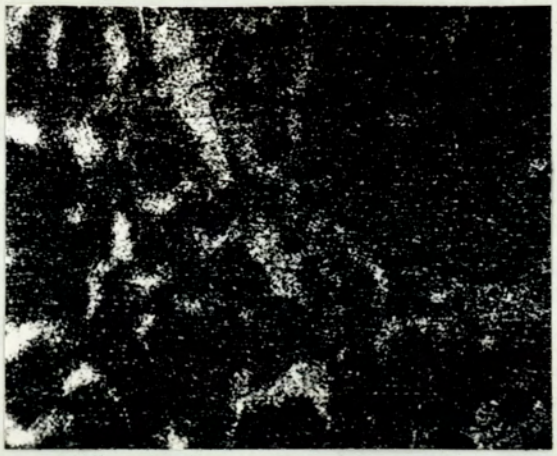

Figure 4.20(a) Aluminium X-Ray Image From Surface of Electrographite Brush Run Without Current. Magnification x175.

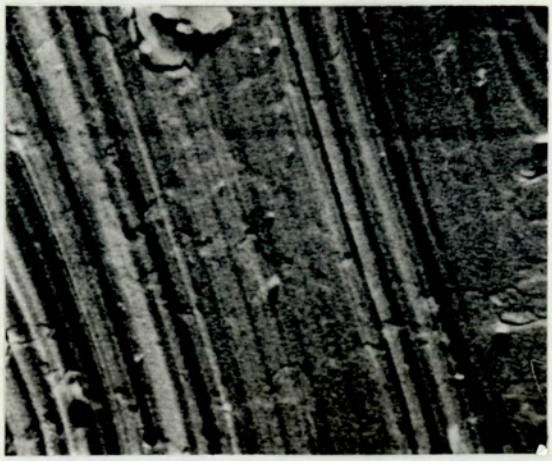

Figure 4.20(b) Electron Image Showing Topography of the Area Shown in Fig.4.20(a).

image of the topography, Figure 4.20(b), revealed that the aluminium was concentrated mostly in small hollows in the smooth brush or in regions where there were cracks running across the direction of sliding.

The same type of distribution occurred when small electric currents, 1mA, were passed through the interface. The X-ray and electron images formed for a brush passing 1mA (Figures 4.20(c) and 4.20(d) respectively), show that the aluminium was again concentrated in cracks or hollows in the smooth, raised areas of the brush face. These micrographs obtained from brushes run with no current or low currents reveal that any aluminium present upon the surface must in in the form of particles of a diameter of 10^{-3}mm or less.

Aluminium X-ray images of brush surfaces produced when passing currents of 500mA and 2.0 amps are shown in Figures 4.20(e), and (f) and (g). These show a marked decrease in the amount of aluminium detected on the brush surface and in the case of the areas shown in Figures 4.20(e) and (f) there is some doubt whether any aluminium was present in these areas, since much of the X-ray image must be attributed to background radiation. The electron diffraction studies carried out in Section 4.13 have, however, shown the presence of aluminium upon the surface of the brush run with a current of 500mA and Figures 4.20(g) and (h) show small amounts of aluminium concentrated in depressions on the brush face which had been run at 2 amps.

The distribution of aluminium on the surface of brushes run at 2.0 amps was further investigated using longer exposure times, 2 hours, to form the X-ray image, thus increasing the amount of radiation detected from any aluminium present. The amount of background radiation shown on the X-ray images was estimated by obtaining an x-ray image from an unworn portion

Figure 4.20(c) Aluminium X-Ray Image From Surface of Positive Electrographite Brush Run With a Current of 1mA. Magnification x175.

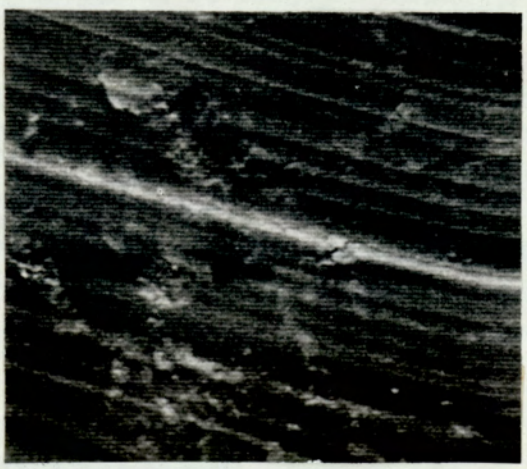

Figure 4.20(d) Electron Image Showing Topography of the Area in Fig.4.20(e). Magnification x175.

Figure 4.20(e) Aluminium X-Ray Image From Surface of Positive Electrographite Brush Run With a Current of 500mA. Magnification x175.

Figure 4.20(f) Aluminium X-Ray Image From Surface of Negative Brush Run With a Current of 2.0 amps. Magnification x175.

Figure 4.20(g) Aluminium X-Ray Image From Surface of Positive Electrographite Brush Run With a Current of 2.0amps. Magnification x175.

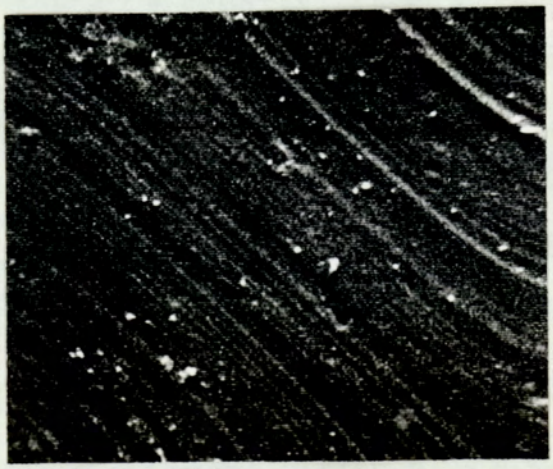

Figure 4.20(h) Electron Image Showing Topography of the Area in Fig.4.20(i). Magnification x175.

of the brush. A portion of the brush face was cut away to reveal unworn material which could not have contained aluminium from contact with the disk, this cut away portion is shown in the upper right hand portion of the electron image, Figure 4.21(b). A comparison of the electron image with the X-ray image of the same area, Figure 4.21(a) reveals that much of the evenly distributed radiation was due to random background, not to aluminium present upon the surface. Any concentrations of X-rays were confined to small areas of the brush surface and comparison of the X-ray and electron images showed that the X-rays originated from discreet fragments on the brush surface.

Further X-ray and electron images, Figures 4.21(c) and 4.21(d) confirmed that the aluminium on the surfaces of brushes run at a current of 2.0 amps was contained within wear fragments up to 2×10^{-2}mm in diameter adhering to the brush face. It was unlikely that these fragments consisted of pure aluminium since such large particles would have shown clearly on the original 15 minute exposure X-ray images. The aluminium was most likely to be in the form of aluminium oxide produced during sliding at elevated temperatures. These large particles of aluminium oxide would not have been detected by electron diffraction.

The variation in the distribution of aluminium upon the brush surface as the load was increased was also investigated to determine whether any significant change occurred at a load of 260gm.f., the load at which the sudden increase in wear rate took place. The surfaces of brushes which had been run at loads of 60gms.f, 160gms.f, 260gms.f, 360gms.f, 460gms.f, and 1060gms.f., without current passing were examined. Electron and X-ray images were obtained from the brush surfaces, the exposure time for the latter being 1 hour. Typical X-ray images from the surfaces of brushes

Figure 4.21(a) Aluminium X-Ray Image From Surface of Negative Brush Run With a Current of 2.0amps. Also Showing an Unworn Portion of Brush.
Magnification x175.

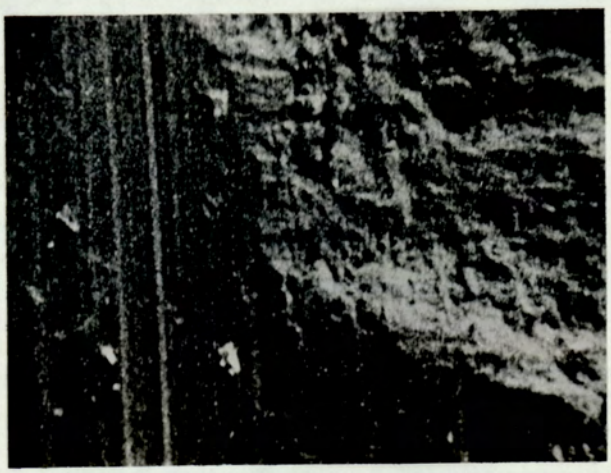

Figure 4.21(b) Electron Image Showing Topography of the Area in Fig.4.21(a)
Magnification x175.

Figure 4.21(c) Aluminium X-Ray Image From Surface of Negative Brush Run With a Current of 2.0 amps. Magnification x175.

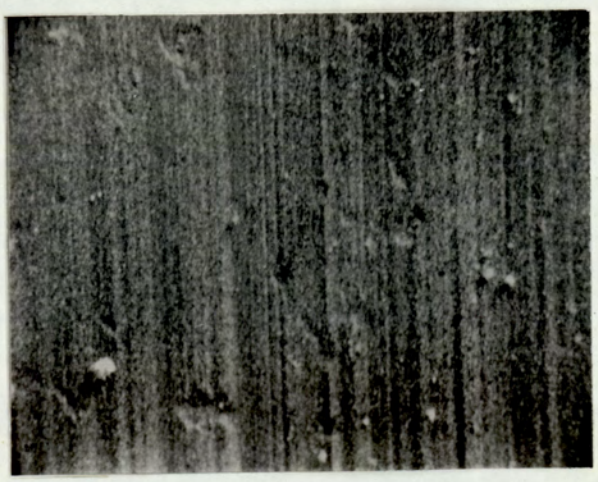

Figure 4.21(d) Electron Image Showing Topography of the Area in Fig.4.21(c). Magnification x175.

run at loads of 160gms.f and 260gms.f are shown in Figures 4.22(a) and 4.22(b). An examination of the X-ray and corresponding electron images reveals that at loads below the transition the distribution of aluminium on the brush surfaces follows the same pattern as that already described for a load of 60gms.f, the aluminium being mainly confined to cracks and hollows in the surface.

At loads above the transition the amount of aluminium detected on the brush surfaces was greatly reduced, as shown by Figure 4.23 which shows images obtained from brush surfaces run at loads of 360gms.f and 1060gms.f. No concentrations of aluminium were present at these loads. The aluminium was very sparsely distributed over the brush face, although it was mainly confined to grooves or low lying regions.

The lack of aluminium upon the brush surfaces at loads above the transition implied that the unstable voltage waveform at these loads, reported in section 4.8, cannot be attributed to the mechanism suggested by Stebbens, on copper.

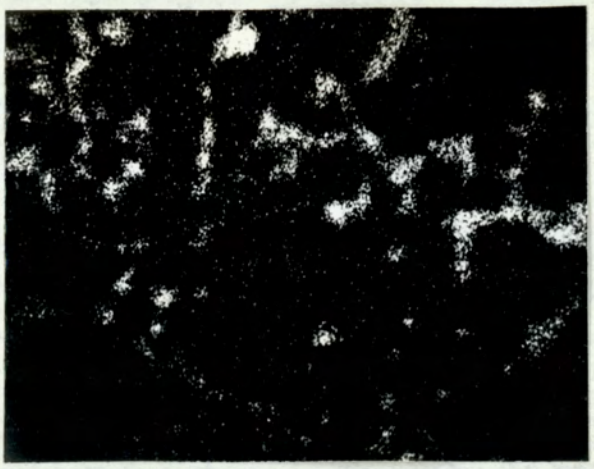

Figure 4.22(a) Aluminium X-ray Image for Surface of Brush Run at a Load of 160 grs.f. Magnification x 175

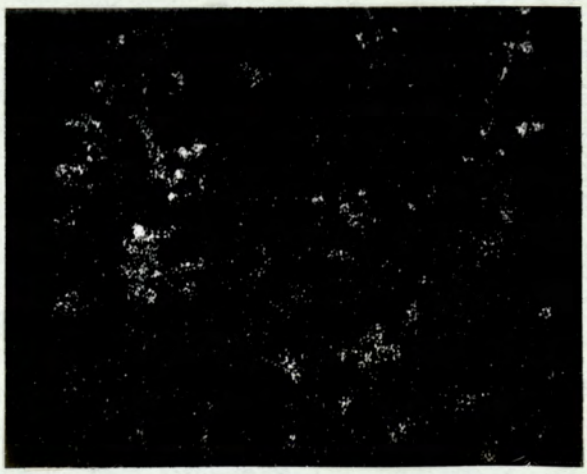

Figure 4.22(b) Aluminium X-ray Image for Surface of Brush Run at a Load of 260 grs.f. Magnification x 175

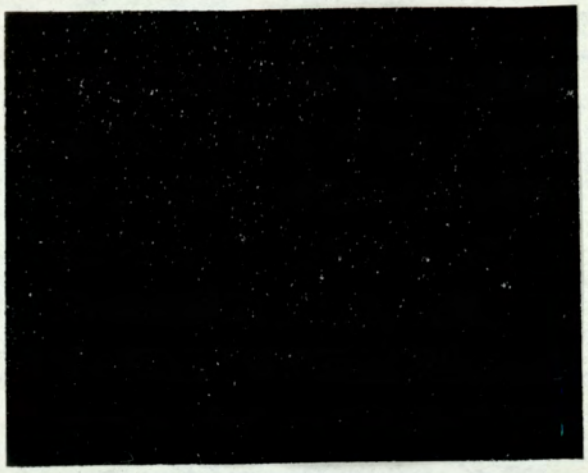

Figure 4.23 (a) Aluminium X-ray Image from Surface of Brush run at a Load of 360 grs.f. Magnification x 175

Figure 4.23(b) Aluminium X-ray Image from Surface of Brush run at a Load of 1060 grs.f. Magnification x 175

4.15 Topographical Study of the Worn Surfaces

Previous topographical studies of worn surfaces have been carried out using optical microscopy (33), reflection electron microscopy (6) (10), and electron microscopy of replicas (36). These techniques however suffer serious drawbacks when investigating surfaces formed by the sliding of graphite. Optical microscopes have small depths of field at high magnifications rendering them unsuitable for topographical studies. Reflection electron microscopy, although having a large depth of field, suffers from difficulties in setting up the instrument and from difficulties in the interpretation of the resulting micrographs. Replica techniques also suffer from this interpretation drawback as well as the added difficulty of producing artifact free replicas. The replication of transferred films, as is necessary for an investigation into the sliding of graphite, is very difficult, since pieces of the graphite film adhere to the replicating plastic producing replicas which are not representative of the original surface.

The scanning electron microscope (S.E.M.) on which the topographical studies described here were carried out has none of the above drawbacks. The scanning electron microscope has a large depth of field even at large magnifications making it especially suitable for studying worn surfaces; the worn surfaces can be studied directly alleviating the need to produce replicas, and, after a little practice at studying surfaces with known topographical features, the micrographs can be easily interpreted. Unfortunately the resolution of the scanning electron microscope is only about 200 Å compared with 4-5 Å for an electron microscope operated in the transmission mode. Metallic, or carbon, specimens require no special preparation apart from cementing them onto specimen holders provided, ensuring an electrical contact between the specimen and specimen holder.

After studying the worn surfaces two general catagories of features became apparent, features which generally characterised the worn surfaces; and special, or interesting features which may, or may not, have played a role in determining the nature of the sliding behaviour. Different areas of the specimen surfaces could easily be studied, enabling a picture of what the general surface topography was like to be built up. Special features could also be located and recorded photographically. Although these special features may only occur on any one specimen surface they could not be discounted until all specimen surfaces had been examined, to see whether these features re-occurred under different conditions. However, the ease with which special features could be located and photographs resulted in the danger that in the subsequent analysis of the micrographs these special features may have been afforded greater importance in determining mechanisms of wear than they deserved.

Two methods were available for building up a picture of the general surface topographies. The first method was to photograph a large number of areas of the worn surfaces and, after subsequent examinations of the micrographs, build up a comprehensive picture of the topography. This method had the advantage that provided the micrographs were chosen from a wide area in a random manner the subsequent pictures should have been free from the influence of the microscope operator. Unfortunately a very large number of photographs had to be taken which was very time consuming both in obtaining the micrographs and examining them afterwards. The other method was for the operator to study the surface using the scanning microscope and build up a mental picture of the general surface topography. This method had the advantage of being quicker and more flexible, there was however always the possibility that the operator would influence the choice of representative micrographs and a false picture of the general topography would be built up. The latter method of studying the surfaces was however

adopted but during the initial investigations several "random" micrographs were taken, after those chosen as representative, to check on the validity of the resulting surfaces.

During the course of these investigations several hundred micrographs of the worn surfaces were obtained, but obviously only a small number can be shown here. These have been selected to illustrate how the surface changed with load and current and the possible effects that these changes would have upon the friction and wear behaviour.

4.15(i) The Effect of Load upon the Worn Surface Topographies

The wear tracks formed upon the aluminium disks and the worn brushes were examined by optical and scanning electron microscopy to determine whether any changes in topography occurred at the transition load which could account for the increase in wear rate.

One very obvious topographical change taking place at the transition load was a marked increase in the amount of transferred graphite upon the wear tracks. When running in the mild wear regime the aluminium track had a sparse covering of graphite (about 10% coverage). Upon increasing the load above the transition load the amount of graphite on the surface increased to almost 100% coverage.

A microscopic examination of the wear track produced in the mild wear regime showed that the graphite transferred to the disk formed smooth islands and narrow bands. A micrograph of one such island can be seen in Figure 4.24(a) which shows raised plateaux of transferred graphite containing areas where graphite fragments have apparently been removed by a wear process. Another feature of the surfaces formed by mild wear sliding was cracking and blistering of some of these smooth graphite plateaux. Areas such as this, although not typical of every smooth region, appeared much too often upon the mild wear surfaces to be regarded as isolated

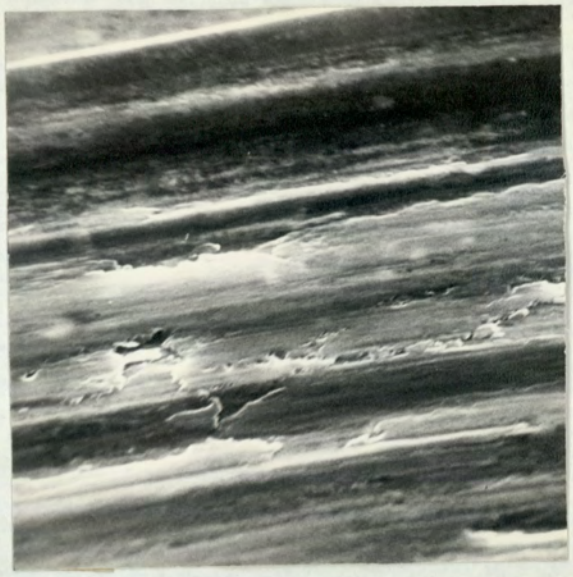

10 μ

(a)

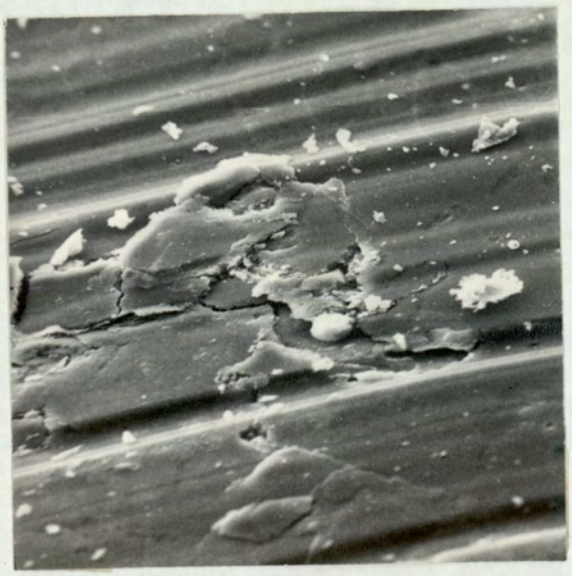

20 μ

(b)

10 μ

(c)

Figure 4.24. Typical Mild Wear Topography of Disk Surface, Formed on Aluminium under a Load of 60gf.

occurrences with no significance. Two such cracked area are shown in Figures 4.24(b) and 4.24(c). The presence of such features upon the surface implied that after the formation of the transferred graphite film the surface was remaining stable long enough for such features to develop by cyclic stressing of the graphite islands. Thus it would appear that, after detachment from the brush, the transferred graphite upon the aluminium underwent a period of consolidation and stabilisation, followed by eventual failure of small areas by a fatigue type process.

In contrast to these mild wear surfaces the micrographs obtained from severe wear specimens showed no characteristic features. Although the wear track was completely covered by transferred graphite it was extremely difficult to select a"typical" surface topography. The nature of the laid down graphite varied from point to point on the same wear track, and also varied with load in an apparently "random" manner. Figures 4.25(a), (b), (c), (d), (e) and (f) show surfaces formed at various loads in the sever wear regime. These surfaces are not typical of any particular load but are merely a selection to illustrate some of the surfaces encountered in the severe wear regime. Although no one surface could be selected as typical, one feature was very apparent, this was the absence of the cracking and blistering that had occurred in the mild wear regime. The wide variety of severe wear surfaces and the absence of fatigue features suggests that in the severe wear regime the disk surface was in a state of rapid change and did not establish a dynamic equilibrium, except perhaps for very short periods.

The surfaces formed upon the brush running faces could, however, quite definitely be categorised into either mild wear or severe wear

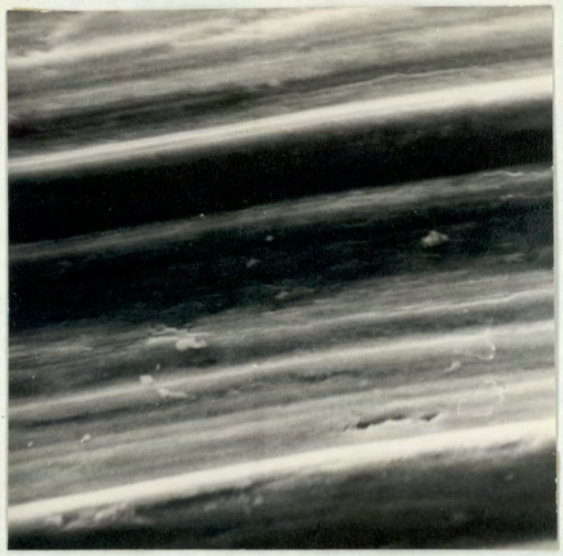

10 μ

(a) Load 260gf.

10μ

(b) Load 260gf.

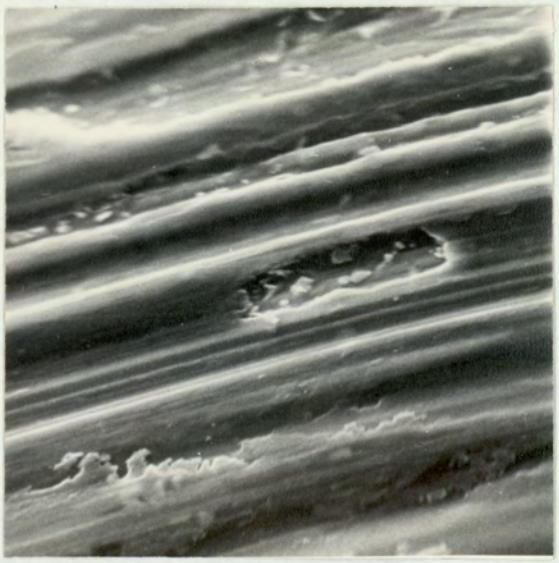

10 μ

(c) Load 360gf.

10 μ

(d) Load 460gf.

Figure 4.25. Typical Severe Wear Topographies of Disk Surface, Formed on Aluminium under Various Loads.

10 μ

(e) Load 1060gf.

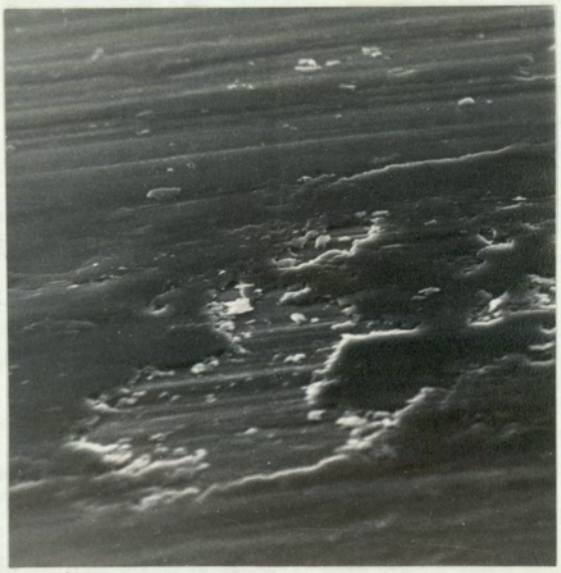

20 μ

(f) Load 1060gf.

Figure 4.25. (Continued)

topographies. One feature which became instantly apparent when studying the worn brush surfaces, either optically or using scanning electron microscopy, was that the normally porous brush surface had been replaced by a smooth, continuous surface. This is shown clearly in a comparison of Figure 4.26(a), an optical micrograph of a metallurgically polished brush surface, with Figure 4.26(b) which shows an optical micrograph of a brush surface which had been run at 60gf. load without current. In the past it has been assumed that the smooth, polished brush surface had been produced by wear debris packed into the exposed pores. The scanning electron micrographs clearly show, however, that in the mild regime this was not the case and the formation of the brush running face was a much more complex process.

Figure 4.27(a) shows an area of a brush which had been running in the mild wear regime under a load of 60 g f without current. This surface is typical of that formed at all loads in the mild wear regime and shows once again how the porous brush material had been replaced by an apparently homogeneous surface. A more detailed examination of the brush surface revealed widespread instances where heavy cracking had occurred, and examples of such areas are shown in Figures 4.27(b), (c) and (d). Closer investigation of these cracked areas showed that the brush surface was not formed by loose wear debris packed into the pores but that it consisted of a compacted graphite film completely covering the bulk brush material. The nature of this film is shown in Figure 4.28 where a section of the overlaid graphite film can be seen lifting from the bulk brush material .

The vast majority of the scanning electron micrographs of the worn surfaces were obtained with the specimen surface inclined at an angle of 45° to the electron beam since this provided good contrast between surface features and was especially suitable for topographical studies.

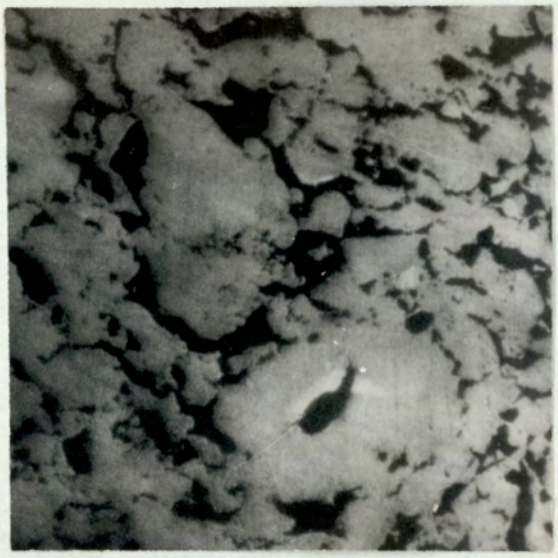

100 μ

(a) Surface of Polished Electrographite Before Sliding.

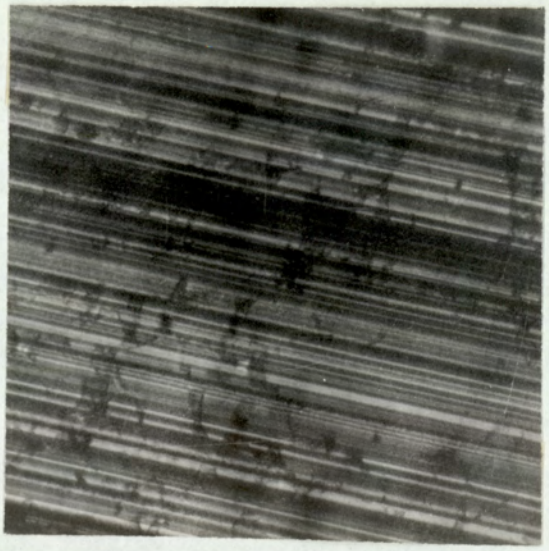

100 μ

(b) Surface of Electrographite after Sliding at a Load of 60gf.

Figure 4.26. Optical Micrographs of Brush Surface.

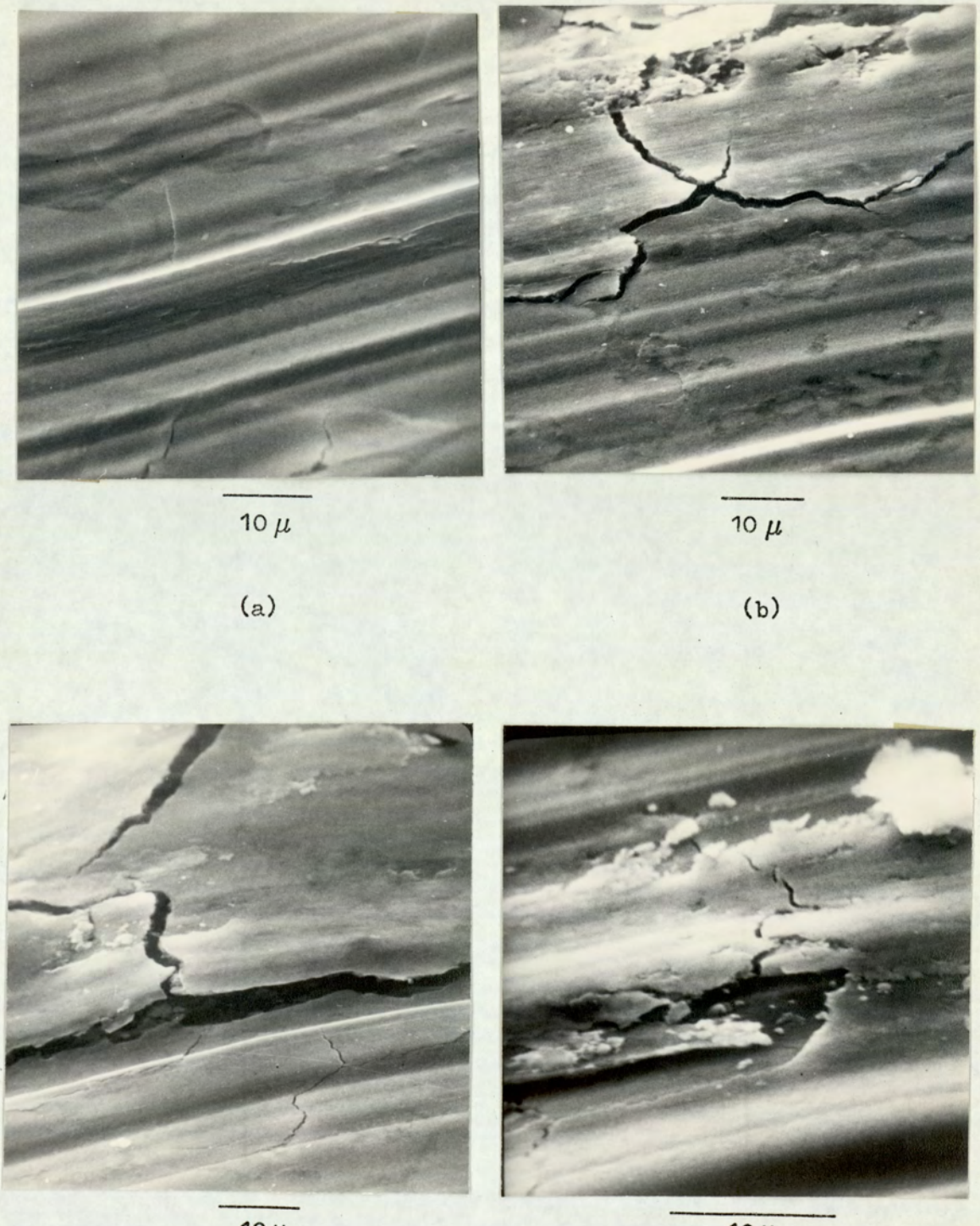

Figure 4.27. Surface Topography of Brush, Formed During Mild Wear Sliding at a Load of 60gf., Showing Failure of Surface Film.

However, to study the nature of the surface film in more detail it was necessary to view some areas with the specimen surface almost parallel to the beam axis. The micrographs shown in Figure 4.28 were taken with the normal to the surface at an angle of 85° to the electron beam. At these large angles of tilt it was extremely difficult to keep the required area within the field of vision. As the specimen was tilted in the microscope the height of the area under observation changed, unless it was exactly on the axis of rotation, and, in spite of the large depth of field constant refocussing was necessary, especially at the high magnification required to detect the surface cracks. The specimen holder also moved sideways and rotated as the angle of tilt was varied, making frequent re-positioning of the specimen necessary. By using this technique, however, it was possible to make a detailed examination of the surface film and in some instances see beneath it, to view the supporting material.

Although it is probable that the porous regions must have contained packed wear debris to support the film this could not be verified due to poor contrast in the areas beneath the film. The micrographs in Figure 4.28 indicates that in this instance the area beneath the film contained some material with a particle size of about 2μ. This particle size was about ten times greater than the carbon blacks used to manufacture the brush material. In Figure 4.36(b) and (c) can be seen regions where removal of the surface film had left a depression which contained loose debris, once again approximately 2μ in size. It is probable however that these particles were pieces of surface film which had been redistributed into the hollow after removal of the film.

The thickness of the graphite film formed upon the brush surface at a load of 60 g.f. with no current flowing was about 1μ. No separate

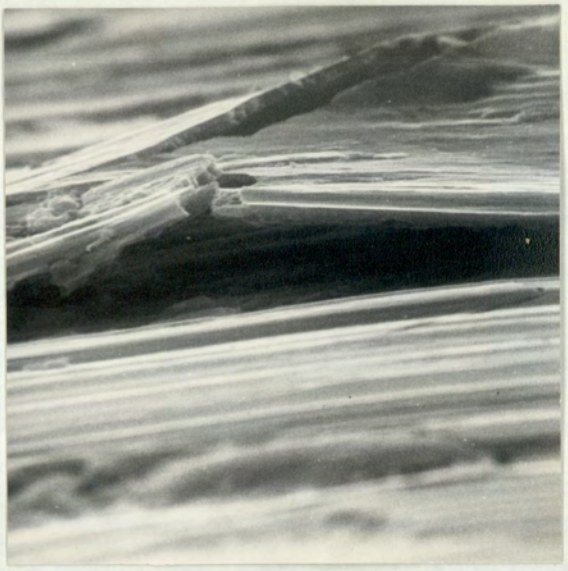

10 μ

(a) Tilt Angle 85°

2 μ

(b) Tilt Angle 85°

Figure 4.28. Graphite Film Formed on a Brush Surface During Mild Wear Running on Aluminium, Load 60gf.

grains could be distinguished in this surface film, indicating that its component particles were considerably smaller than the carbon black material. The surface film must therefore have been formed by degradation and consolidation of larger particles from the bulk brush material. An idea of the size of the undergraded bulk brush material can be obtained from Figure 4.39(c) which shows an area where a piece of the brush surface has been removed to reveal the bulk brush material. The constituent carbon particles can be clearly seen, their diameters being approximately 0.2μ.

Thus the type of brush surface formed under mild wear conditions, consisted of a smooth degraded graphite film with areas of extensive cracking and flaking. In contrast to this, scanning electron microscopy of brush surfaces produced during severe wear sliding revealed no evidence of the formation of a surface film and very little surface cracking. The brush surfaces formed in the severe wear regime were extremely smooth with very few notable features. A typical "severe wear surface" formed at a load of 460g.f. is shown in Figure 4.29 and, unlike "mild wear surfaces" there was an absence of any systematic cracking. Cracking of the surfaces was confined to the apparent opening up of the surface to reveal theporosity of the material. Figure 4.30 shows the formation of such cracks upon the surface of a brush run at 360g.f. load. Although the examination of the surfaces revealed that the overlaid graphite film was no longer formed areas existed where layering of the surface occurred (Figure 4.31), but these layers appeared to follow the contour of the underlying material, rather than form a surface film .

Failure of the brush surface in the severe wear regime appeared to take place without the preliminary cracking or flaking which occurred in the mild wear regime. Figures 4.32(a) and (b) show areas of the brush surface formed by severe wear at a load of 260g.f. Failure of this

10μ

Figure 4.29. Typical Severe Wear Topography of Brush Surface; Formed at a Load of 460gf.

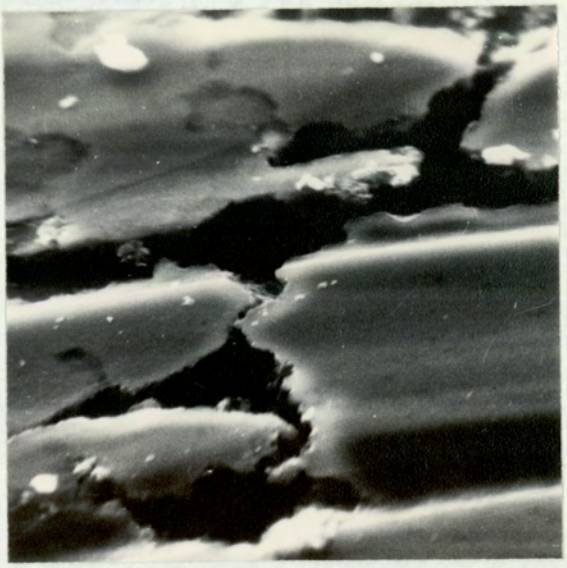

10μ

Figure 4.30. Surface Cracking of a Brush Surface Formed During Sliding in Severe Wear Regime at a Load of 360gf.

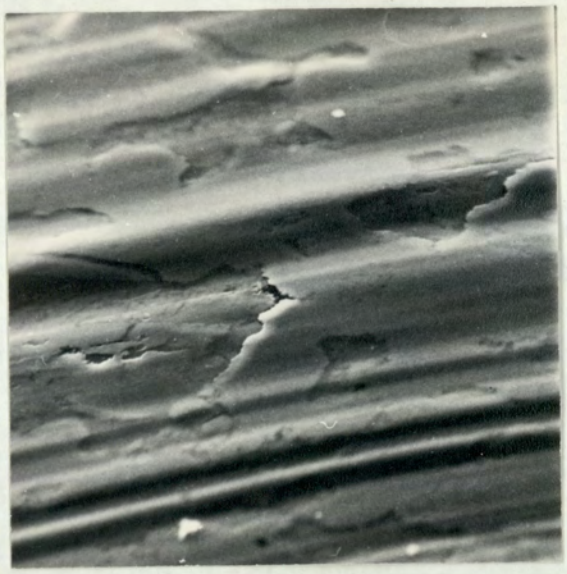

20 μ

Figure 4.31. Layered Area of Brush Surface Formed at a Load of 360gf.

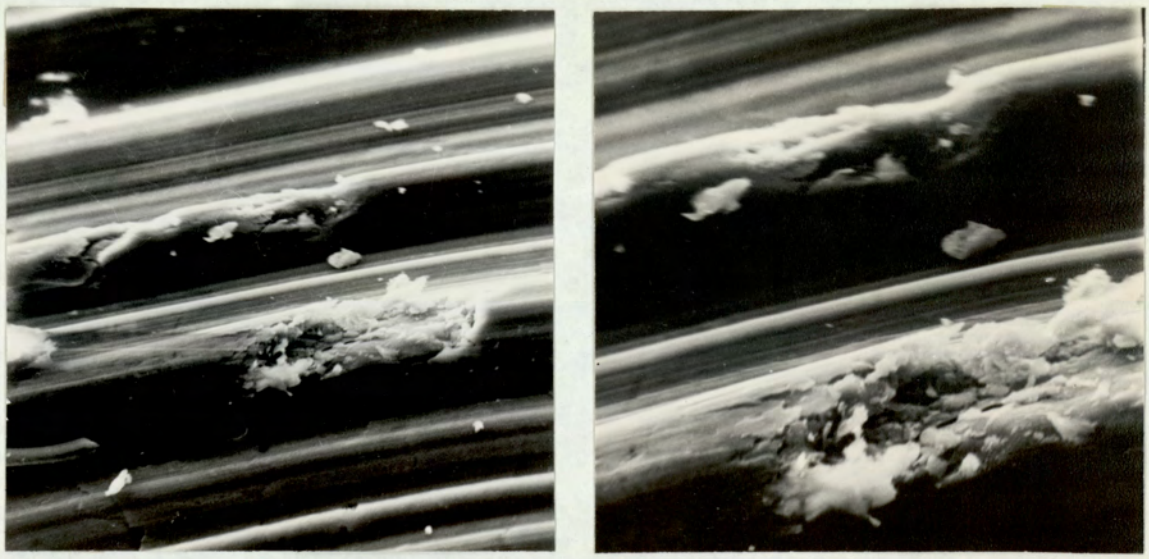

20μ 10μ

(a) (b)

Figure 4.32. Failure of Brush Surface Sliding under Severe Wear Conditions, Load 260gf.

surface had occurred by the removal of a fragment of the brush material leaving behind a cavity which was beginning to fill with small particles of loose wear debris.

4.15 (ii) The Effect of Electric Current upon the Worn Surface Topography

An intensive study of the effects of electric current upon the worn surface topography was restricted to examining surfaces formed in the mild wear regime at a load of 60gf. The worn aluminium surfaces produced during sliding in the severe wear regime were so varied that it was impossible to detect any change in topography caused by current until arcing and catastrophic wear occurred. Nor was there any noticable effect upon the brush topography until catastrophic wear took place. Figures 4.33(a) and (b) show areas of the aluminium wear tracks after running at loads of 460gf. and 1060gf., and electric currents of 5amps and 10 amps. Under these conditions catastrophic wear of the electrographite occurred and the wear rate of the aluminium was extremely high. In Figure 4.33 (a) regions are shown were the underlying aluminium was penetrating the transferred graphite apparently, caused by melting of the aluminium, due to arcing across the interface. Another feature showing the deformation of the aluminium surface is shown in figure 4.33 (b). These micrographs show that very heavy deformation of the aluminium was occurring, due probably to softening, or even melting, of the aluminium junctions caused by the passage of electric current. The surface of the brush produced when running under catastrophic wear conditions exhibited heavy scoring and pitting, (Figure 4,33(c)), and took on an etched appearance in some areas.

Even when running under mild wear conditions at a load of 60 gf. there was very little change in the topography of the wear track on the aluminium until arcing occurred beneath the brushes. As with the higher

5 μ

(a) Load 460gf. Current 5.0amps.

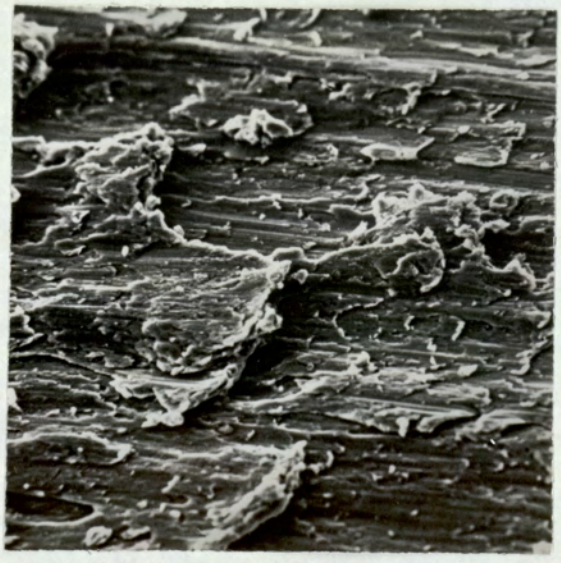

40μ

(b) Load 1060gf. Current 5.0amps.

Figure 4.33 Catasrophically Failed Disk Surface.

100 μ

(c) Load 1060gf. Current 5.0amps.

Figure 4.33. Catastophically Failed Brush Surface

loads when sparking occurred the wear rate of both the brush and aluminium increased considerably. At the onset of arcing there was a slight increase in the amount of graphite transferred to the disk, but thiswas a very small increase compared with that taking place at the transition load. The worn surfaces produced by a load of 60 gf , and a current of 2 amps under catastrpohic wear conditions are shown in Figures 4.34 and 4.35. The transparent film on the aluminium, shown in Figures 4.34(a), (b), (c) and (d), has changed from smooth islands with fatigue type cracking to a rough pitted topography littered with loose wear debris. The wear debris consisted o a large number of flakes of material about 0.2 - 0.5μ thick and 2 - 5μlong.

In contrast however the effect of electric current upon the mild wear brush topography was noticeable even at quite small currents. The surfaces of brushes which had been run under a load of 60g.f. without current, and with currents of 1mA, 500mA and 2 amps were examined by scanning electron microscopy. The surface formed at a current of 2 amps had not, in this instance, been produced by arcing or catastrophic wear.

As previously described, the surface of the brush formed without current consisted of a smooth film overlaying the porous brush material. This graphite film is shown clearly in the micrographs of Figures 4.28 and 4.36. This film, about 1μ thick, had been formed by the consolidation of degraded brush material. The load bearing compacted film was supported by the bulk brush material underneath and possibly by larger pieces of debris packed more lossely into the pores of the brush.

The surface produced when a current of 1mA was passed through the brush was very similar to the no current surface except that cracking was less frequent, which made examination of the surface film more difficult. It appeared from the micrographs obtained from this specimen, Figure 4.37,

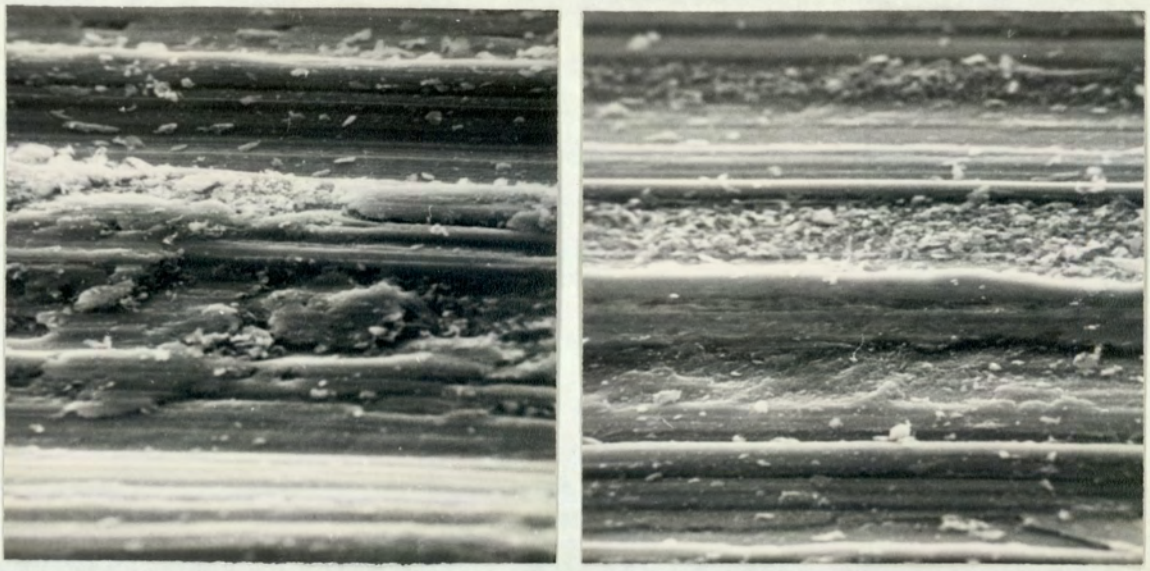

10 μ

(a)

10 μ

(b)

2 μ

(c)

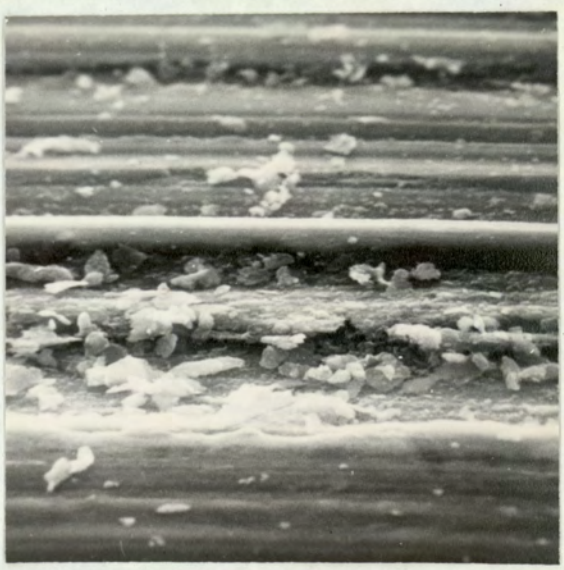

5μ

(d)

Figure 4.34. Surface of Wear Track Upon Aluminium Produced During Catastrophic Failure at a Load of 60gf. and an Electric Current of 2amps.

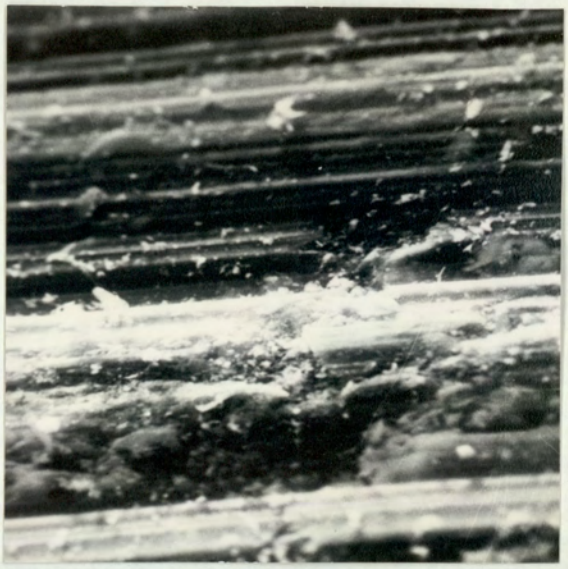

20 μ

(a)

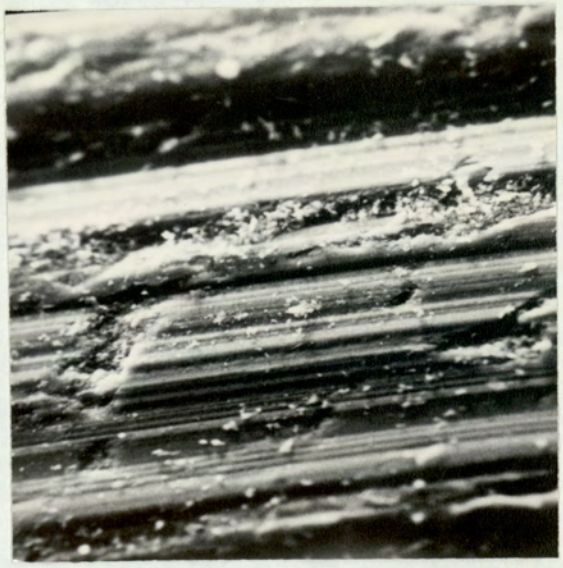

20 μ

(b)

Figure 4.35. Surface of Brush Produced By Catastrophic Wear upon Aluminium under a Load of 60gf. and a Current of 2amps.

2μ

(a) Tilt Angle 80°

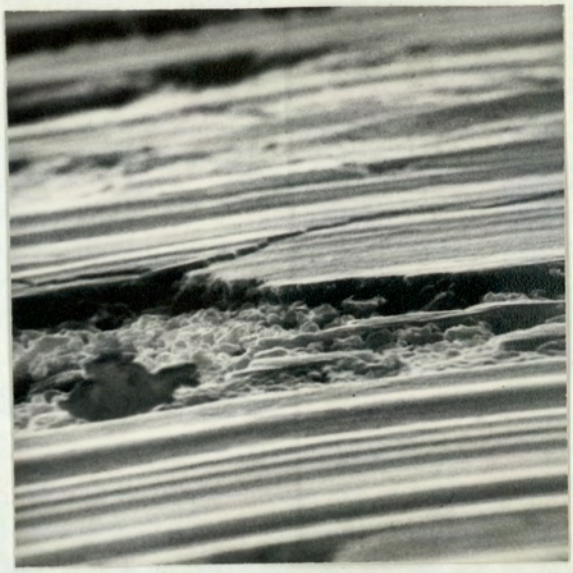

5μ

(b) Tilt Angle 81°

2μ

(c) Tilt Angle 81°

Figure 4.36. Surface Film on Brush Formed at a Load of 60gf. with No Current Flowing.

5 μ

(a) Tilt Angle 46°

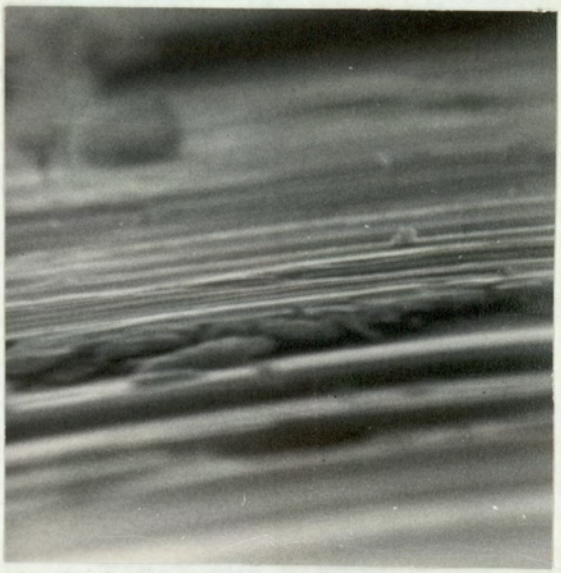

5 μ

(b) Tilt Angle 80°

Figure 4.37. Surface Film on Positive Brush Formed at a Load of 60gf. with a Current of 1mA Flowing.

that the degraded graphite film of thickness 1μ was still formed.

When the current through the brush was increased to 500mA a moticeable change in the surface topography occurred. Instances of fatigue cracking of the surface were few and the brush surface was very similar to that formed in the severe wear regime, shown in Figure 4.29 and 4.31. Figure 4.38 shows an area where the film is lifting away from the surface, and a closer examination of this region showed that the thickness of the compacted film had been considerably reduced, to 0.3-0.5μ .

The surface produced at a current of 2 amps showed none of the features typical of mild wear. No surface film could be detected and there was an absence of any fatigue cracking. The mode of failure of the brush material appeared to be very similar to that observed for severe wear failure, that is the removal of particles from the surface without prior cracking, as shown in Figure 4.39(c). A more detailed examination of these failed areas, Figures 4.39(a), (b) and (c) confirmed that no surface film was formed. The bulk brush material, 0.2μ diameter, continued right up to the sliding interface, although it is probable that an extremely thin degraded surface layer formed upon some areas of the brush. Such a layer could not, however, support any stress and would be confined to the non-porous regions.

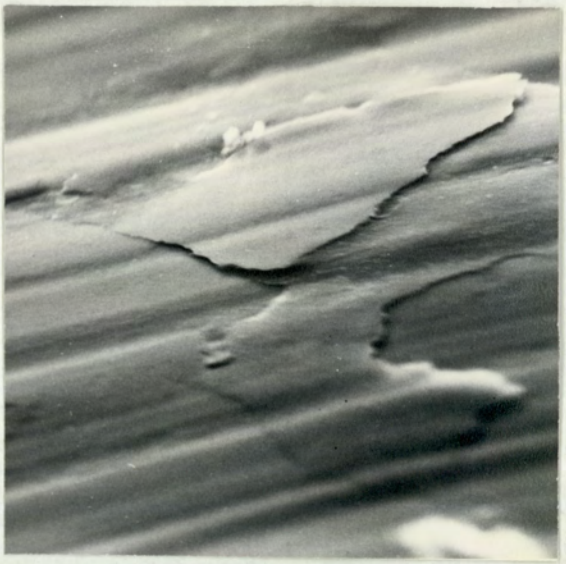

(a) Tilt Angle 45°

(b) Tilt Angle 86°

Figure 4.38. Surface Film on Positive Brush Formed at a Load of 60gf. with a Current of 500mA. Flowing.

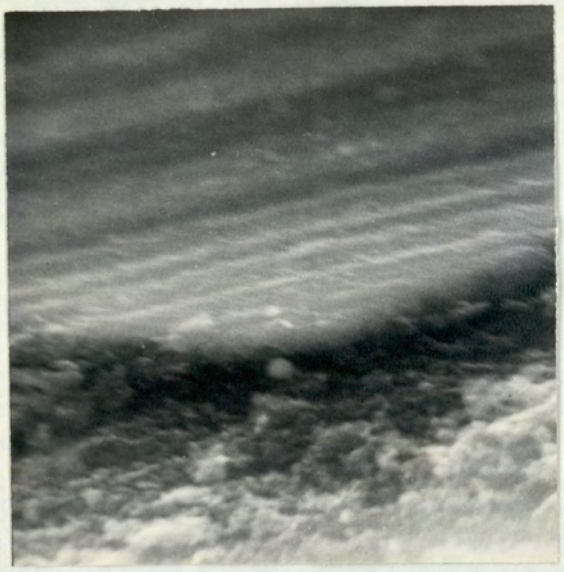

5 μ

(a) Tilt Angle 65°

2 μ

(b) Tilt Angle 80°

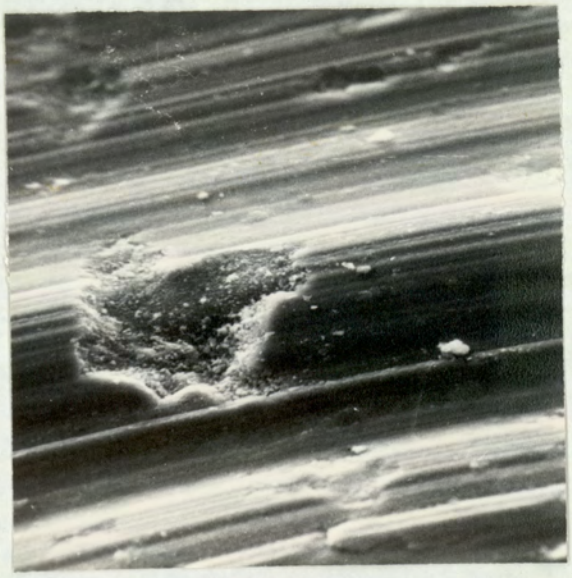

2 μ

(c) Tilt Angle 45°

Figure 4.39. Surface of Positive Brush Formed at a Load of 60gf. with a Current of 2amps Flowing.

4.16 X-Ray Analysis of Wear Debris

4.16(i) X-Ray source, camera and procedure

After the wear debris had been collected and contained within a capillary tube the sample was mounted in a standard Debye-Scherer powder diffraction camera of diameter 114.6m.m.

The powder was irradiated with X-rays obtained from a fine focus copper tube operated at a potential and filament current of 40 kV and 20mA respectively. The radiation used was from the Kα line, obtained using a nickel filter, the wavelength being 1.542 Å .

Exposure times of the samples varied from 30 minutes to 8 hours, depending upon the proportions of the constituents in the wear debris.

From the powder pattern the Bragg Angle of the diffracted X-ray beams were measured and the d- spacings of the crystal planes giving rise to these beams calculated. The components of the wear debris were identified from these d-spacings using the X-ray Powder Data File.

The intensity of the diffracted beam was dependent upon, amongst other factors, the volume of material giving rise to that diffracted beam which was irradiated by the incident X-ray beam.

Quantitative analysis could not be performed simply by comparison of the intensities of the diffraction maxima from the powder components with the intensities of the maxima from pure materials. This was due to differences in the absorption of the powder and pure material.

Averbach and Cohen (37) have made use of an internal standard for quantitative analysis. Using a glancing angle technique they estimated

the amount of retained austenite in tool steel by comparison of the intensities of the diffraction maxima from the austenite with the diffraction maxima from the martensitic phase, which was taken as the standard. They also showed the necessity of using the integrated intensity of the diffracted beam, not the peak height, since the integrated intensity was independent of particle size or lattice distortions.

The method of Averbach and Cohen has been adapted by Quinn (38) to investigate the wear debris produced by the sliding of carbon steels.

4.16(ii) The intensity of the Diffracted Beam.

The intensity of the diffracted beam of X-rays from a set of crystal planes (hkl), at an angle of diffraction 2θ to the incident beam is given by (39) : -

$$I_{hkl} \alpha \left| F_{hkl} \right|^2 \left(\frac{1 + \cos^2 2\theta}{\sin^2 \theta \cos \theta} \right) \frac{m e^{-B \sin^2 \theta / \lambda^2}}{v^2} VA_{(\theta)} \quad \cdots \quad \text{Eqn. (B)}$$

where :

F_{hkl} - is the structure factor of the component giving rise to the diffracted beam.

$\frac{1 + \cos^2 2\theta}{\sin^2 \theta \cos \theta}$ - is the Lorentz polarisation factor (Lp)

m - is the multiplicity factor, the number of families of planes having the same values of d_{hkl}

v - is the volume of the unit cell

$e^{-B \sin^2 \theta / \lambda^2}$ - is the Debye-Waller temperature coefficient

V - is the volume of the constituent irradiated.

$A(\theta)$ - is the sample absorption coefficient, dependent upon the angle of diffraction.

However, since for any sample only the relative intensities are required Equation (A) may be written

$$I_x = R_x V_x A_\theta \qquad \ldots\ldots\ldots \text{Eqn. (B)}$$

and the factor $R = |F_{hkl}|^2 \frac{Lpme^{-2Bsin^2\theta/\lambda^2}}{v^2}$

can be calculated for each diffraction maxima.

4.16((iii) Determination of relative proportions

For a powder consisting of two components A and B the intensities of the beams from these two constituents will be given by

$$I_A = R_A V_A A_\theta \text{ and } I_B = R_B V_B A_\theta$$

thus, the relative intensities of the diffracted beams will depend upon the proportions of A and B present in the mixture.

However, since the absorption coefficient A_θ varies with the angle of diffraction the intensities of the diffracted beams cannot be directly compared if the maxima occur at different values of 2θ. If the values of I_A/R_B for each maxima are plotted against the corresponding value of θ the resultant graph will show how A_θ varies with the angle of diffraction.

Assuming that absorption of the X-rays depends upon the mixture as a whole, not on the individual components giving rise to the maxima, then the ratio of the value of the curve through I_{a/R_a} to that through I_B/R_B

taken at the same angle of diffraction will be in the same ratio as the volumes.

$$\left\{ \frac{I_A/R_A}{I_B/R_B} \right\}_\theta = \frac{V_A}{V_B}$$

4.16(iv) Calculation of Structure Factors

The structure factor F_{hkl} can be calculated if the positions of the atoms within the unit cell are known. For a set of planes (hkl) the structure is given by:-

$$F_{hkl} = \left\{ \sum_{i=1}^{n} f_i \cos 2\pi (hx_i+ky_i+lz_i) \right\}^2 + \left\{ \sum_{i=1}^{n} f_i \sin 2\pi (hx_i+ky_i+lz_i) \right\} \quad \text{Eqn.(C)}$$

Where the summation is taken for each atom, i varies from 1 to n, the number of atoms within the unit cell. x_i, y_i and z_i are the coordinates of the i_{th} atom within the unit cell and f_i is the atomic scattering factor of the atom.

Structure factor of Carbon (Graphite)

Graphite can exist with two possible crystal structures; hexagonal and rhombohedral. The most common structure is hexagonal and this was the form considered. The carbon atoms within the unit cell occupy positions at (0,0,0), $(\frac{1}{3},\frac{2}{3},0)$, $(0,0\frac{1}{2})$ and $(\frac{2}{3},\frac{1}{3},\frac{1}{2})$ as shown in Figure 1.1. Diffraction takes place from the following planes: (002), (100), (102), (004), (110).

Substituting in Equation (C) enables the structure factor of each set of planes to be found. The calculations involved are shown in Appendix 1.

The structure factor for each set of planes giving rise to maxime are:-

$$F_{002}^2 = 16f_{00}^2$$

$$F_{100}^2 = f_{100}^2$$

$$F_{101}^2 = 3f_{100}^2$$

$$F_{102}^2 = f_{102}^2$$

$$F_{004}^2 = 16f_{004}^2$$

$$F_{110}^2 = 16f_{110}^2$$

Structure factors of Aluminium

Aluminium has a face centred cubic structure with atoms within the unit cell occupying at (0,0,0), $(0,\frac{1}{2},\frac{1}{2})$, $(\frac{1}{2},0,\frac{1}{2})$ and $(\frac{1}{2},\frac{1}{2},0)$.

The structure factor for any set of planes giving rise to reflections is given by:

$$F_{hkl}^2 = 16f_{hkl}^2$$

(where hkl are all odd or all even). Details of the calculations involved are shown in Appendix 1.

Calculation of "R"

The value of "R" can be readily calculated once the structure has been determined. These values have been calculated for aluminium and carbon in Appendix 1 and the results tabulated in Table 4.13.

Table 4.13 "R" Values for Aluminium and Carbon

Material	C	C	C	C	C	C	Al	Al	Al	Al	Al	Al
Planes	002	100	101	102	104	110	111	200	220	311	222	400
R	17.09	0.586	2.086	0.571	1.090	0.836	34.0	15.8	9.20	9.70	1.74	1.39

4.16(v) Analysis of Wear debris produced from running on an Aluminium disk

The specimens of wear debris were irradiated for exposure times varying from 30 minutes to 8 hours. At the longer exposure times the very weak lines were visible but the stronger lines had densities of blackening greater than 3. This was outside the linear range of the "exposure vs. density of blackening curve" of the Photographic film. For quantitative analysis the specimens were exposed for as long as possible without the density of blackening of any line exceeding a value of 2, where the density of blackening D was defined by the simple relationship,

$$D = \frac{I_o}{I}$$

I_o and I being the intensities of a parallel beam of light before and after passing through the film.

Identification of Components

A microdensitometer trace of the density of blackening against 2θ for a typical powder pattern from wear debris produced upon aluminium is shown in Figure 4.40. The powder photograph showed that the major constituents of the wear debris produced at all loads and currents were aluminium and carbon with traces of Al_2O_3. Although the powder pattern revealed only traces of Al_2O_3 the wear debris may have contained considerably more than was suggested by X-ray analysis since aluminium is known to forn an amorphous layer upon the metal (40).This amorphous oxide would not give rise to a diffraction pattern. The wear debris produced when running at a load of 1kg.f.also contained traces of aluminium carbide.

Quantitative Analysis of Wear Debris.

The intensity of the diffracted X-ray beam was obtained from the microdensitometer trace. The "noise" of the trace, caused by grains of emulsion on the film and fluctuations of the densitometer, was smoothed out and the background level drawn in. The integrated intensities of the maxima from the metal were measured by the product, "peak height"x "width of the peak at half its height" - Quinn(38). This method could not be used on the broad carbon lines, and the integrated intensity was found by measuring the area beneath the peak by dividing the area into a number of triangles.

The value of I/R for each of the diffracted maxima was calculated and plotted against θ. The graph obtained represented the variation in the

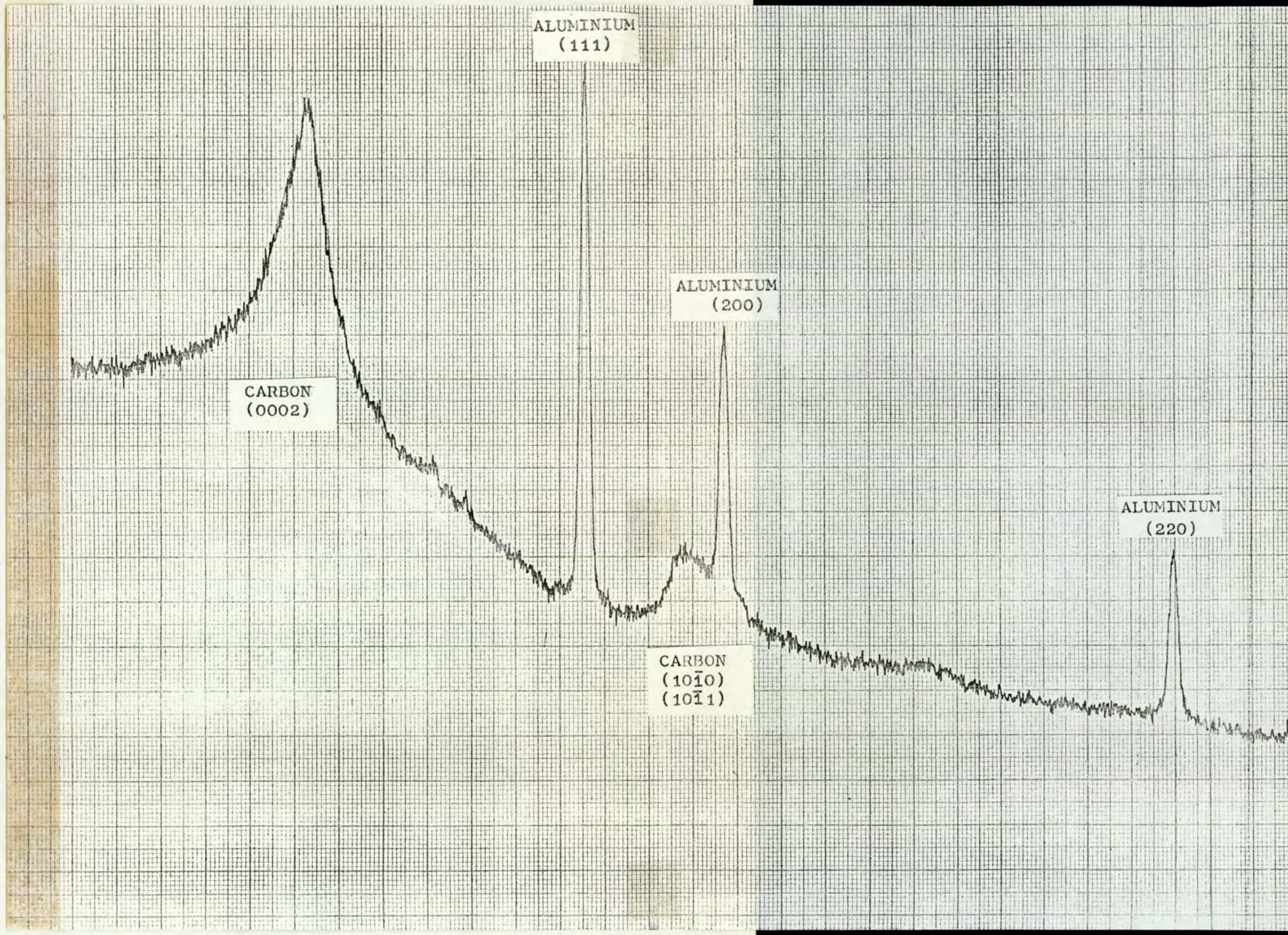

Figure 4.40 Typical Microdensitometer Trace of Density of Blackening of X-ray Film Versus 2 θ (from wear debris formed at a load of 1060gf. on aluminium.).

absorption factor $A(\theta)$ with θ

At an angle θ ; $$\frac{I_A/R_A}{I_B/R_B} = \frac{V_A}{V_B}$$

and $$\log\left(\frac{V_A}{V_B}\right) = \log\left(\frac{I_A}{R_A}\right) - \log\left(\frac{I_B}{R_B}\right)$$

thus if the logs of the ratios (I/R) are plotted against θ the difference in ordinates of the graphs gives the log of (V_A/V_B). Figure 4.41 is such a plot for the diffraction maxima shown in the microdensitometer trace Fig 4.40 the difference in ordinates of the two lines corresponded to a ratio of V_C/V_{AC} of 16. This gave the composition of the wear debris produced running at 1060grm.f.load with no current as 6% Aluminium and 94% carbon, ignoring any trace substances.

Fig 4.42 shows a plot of I/R against θ for the wear debris produced at a load of 1060gms.f and a current of 10 amps. This shows that the amount of aluminium in the wear debris has increased, the composition being 50% aluminium and 50% carbon. The graph of I/R against θ for the wear debris produced at a load of 60gms.f. with no current and a current of 2 amps passing is shown in Fig4.43 with no current passing the amount of aluminium in the wear debris was 2.5% at a current of 2.0 amps the amount had increased to 10%.

Although segregation within the capillary tube due to the method of filling did not occur there was a variation in composition from point to point within the tube, giving a wide range to the composition of each sample.

At loads between 60gms f. and 1060gms.f. without current flowing the amount of aluminium in the debris was within the range 2 - 6% and no effect of load upon the proportion was detected. The effect of current on the composition appeared to be nil, unless arcing occurred beneath the

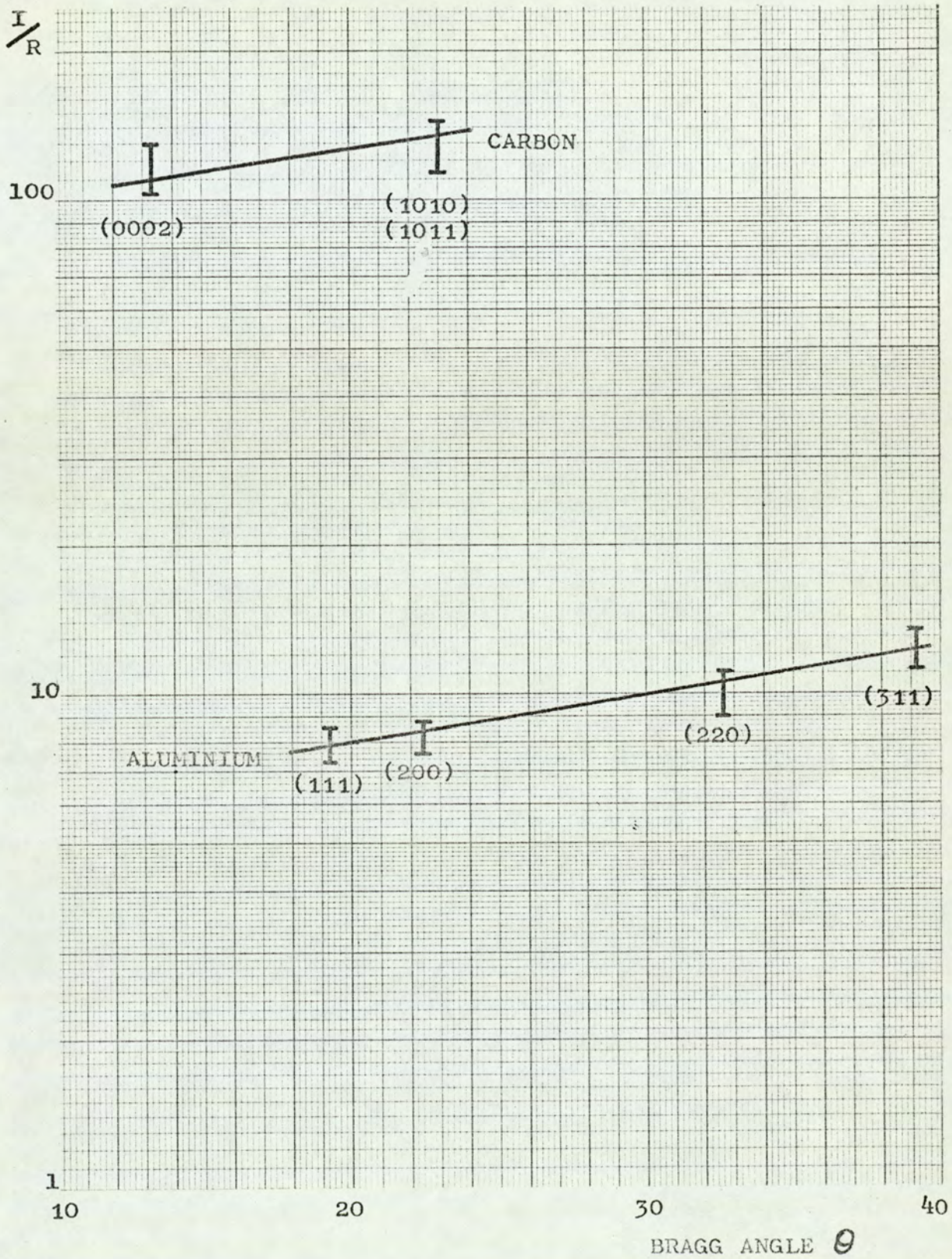

Figure 4.41 Graph of $I/_R$ against Bragg Angle for Wear Debris Produced Sliding on Aluminium at a Load of 1060gf. without Current.

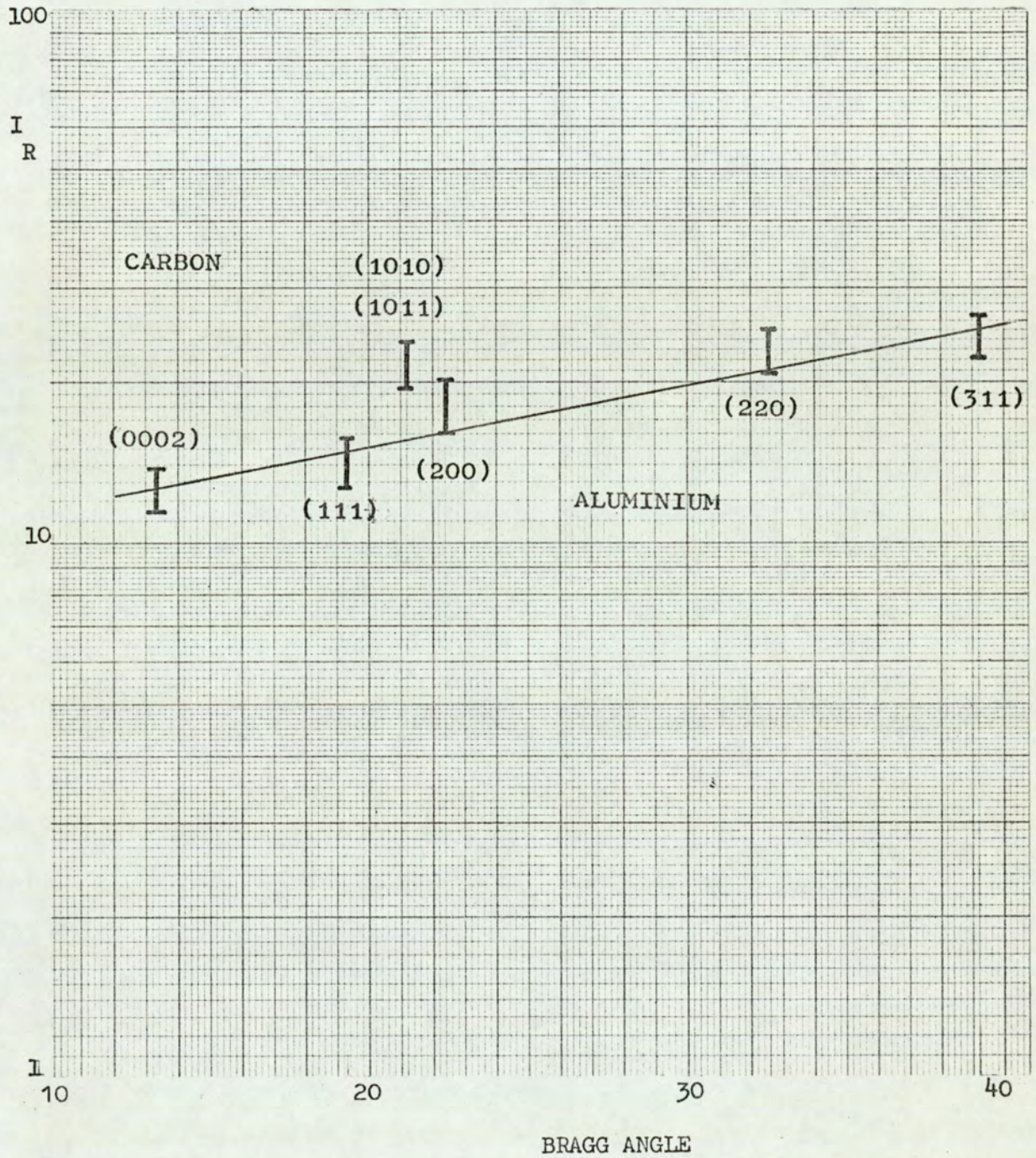

Figure 4.42 Graph of $I/_R$ against Bragg Angle for Wear Debris Produced Sliding on Aluminium at a Load of 1060gf. and a Current of 10.0 amps.

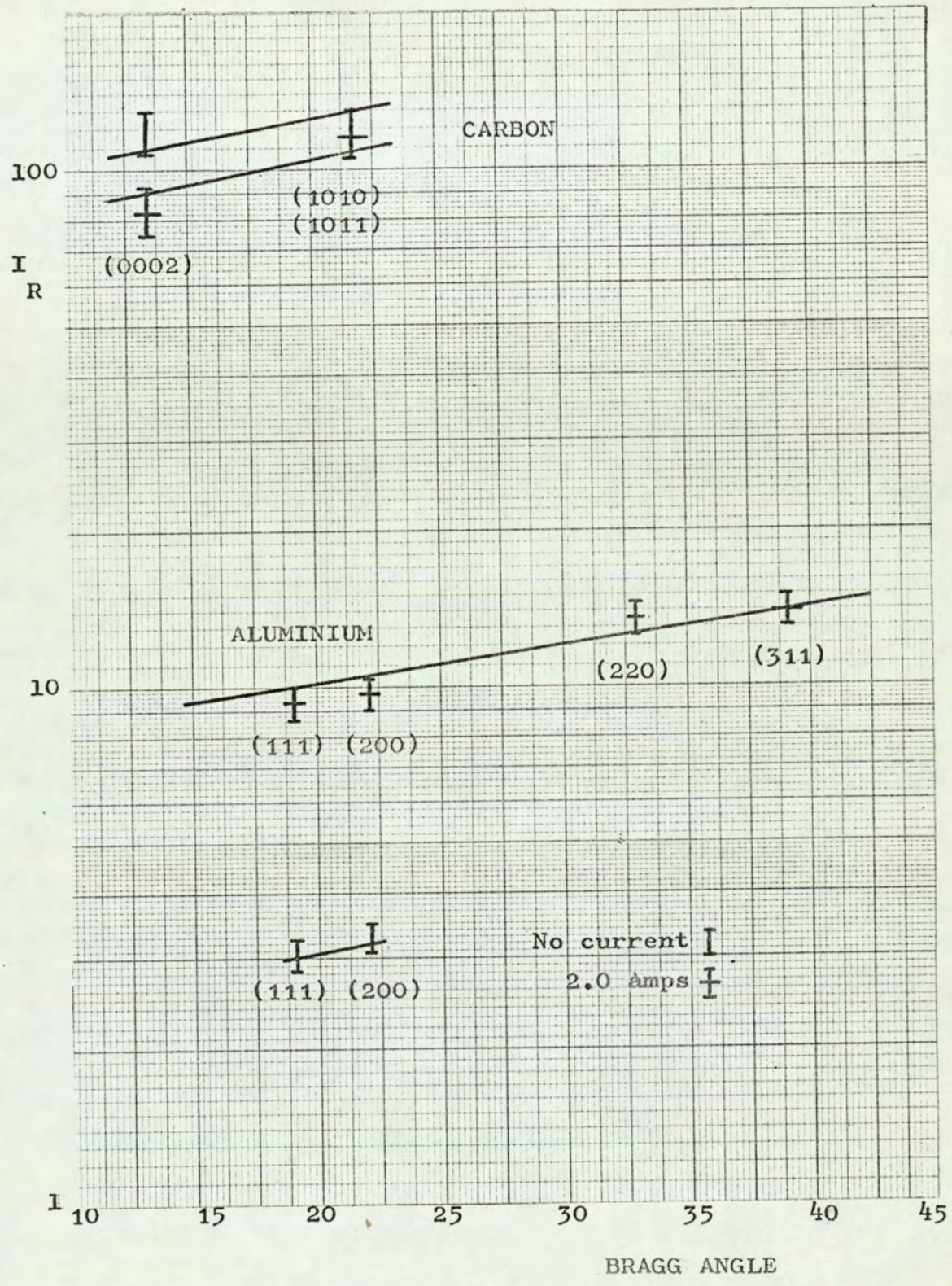

Figure 4.43 Graph of $I/_R$ against Bragg Angle for Wear Debris Produced Sliding on Aluminium at a Load of 60gf. and Currents of 0 amps and 2.0 amps.

brush. At a load of 60gm.f. and a current of 2.0amps light arcing took place beneath the brushes and the amount of aluminium increased to 8-10%. At 460 gms.f. a slight decrease in the amount of aluminium was observed, from 2.6% with no current to 1.4% at lamp and 1.0% at 2.0amps. At 5amps severe arcing occurred and the amount of aluminium rose to 70%. No significant change in the composition of the wear debris outside the range 2 - 6% aluminium was observed with a load of 1060gms f. until a current of 10amps was passed through the brushes, causing arcing and an increase in the aluminium content to 50%.

Chapter 5 Results on Other Disk Materials

5.1 Introduction

Experiments were performed upon electrographite brushes sliding upon disks made from the following materials : copper, gold, hardened EN26 steel, annealed EN26 steel and electrographite (EG14). These disk materials were chosen to give a range of mechanical,physical and electrical properties. EN26 steel was used because this was a bearing steel which had been investigated in tribological investigations concerning the dry wear of steels and because it was easily heat treatable to give a range of hardnesses. The batch of EN26 steel used had the following percentage composition: C(0.43), Mn(0.69), Si(0.25), S(2.010), P(0.007), Ni(2.80), Cr(0.80) and Mo(0.64). The annealed EN26 disks had a hardness of 270VPN and the hardened and tempered disks a hardness of between 550-580VPN.

Investigations into the sliding of electrographite on copper have been reported by many authors, these are described in Chapter 1. However, although the experiments described here have repeated some of the results previously reported, these experiments were necessary to provide evidence that the results obtained on all materials were consistent with the results of other authors, and also to provide direct comparisons between copper and these other materials.

The results obtained from running upon aluminium, described in the previous chapter were used as a guide to decide upon the necessary experiments,and only a small number of runs, carried out under selected running conditions were performed on each disk material. Since the

experiments carried out were substantially the same for each material the results will be discussed in terms of the experiments carried out and parameters measured, rather than discuss each material separately.

5.2. The Wear Rate of Electrographite

Experiments were performed to determine how the wear rate of electrographite varied with load on the various disk materials. Except when running on gold the brushes were run in at a load of either 60gms.f. or 160 gms.f. until equilibrium values of wear rate, contact resistance and frictional force were obtained, the latter two parameters being described in subsequent sections. The brush load was increased in stages upt to 1060 gms.f. the equilibrium values of wear rate, frictional force and contact resistance being measured at each load.

The variations in the wear rate of the electrographite brush with applied load is shown in Figure 5.1. The errors in measurement were estimated from variations in the wear rate taking place over a long period.

The wear rate of electrographite sliding upon copper of hardness 80 VPN. increased in proportion to the applied load over the whole range of loads investigated. No discontinuous increase in wear rate took place, although such an increase has been reported by White (31) and by Lancaster using conical brushes (26).

When running on 24 carat gold, hardness 60 V.P.N. , the wear rates of the brushes were much lower than had been measured when running on other metals. Long runs were necessary to make accurate measurements,

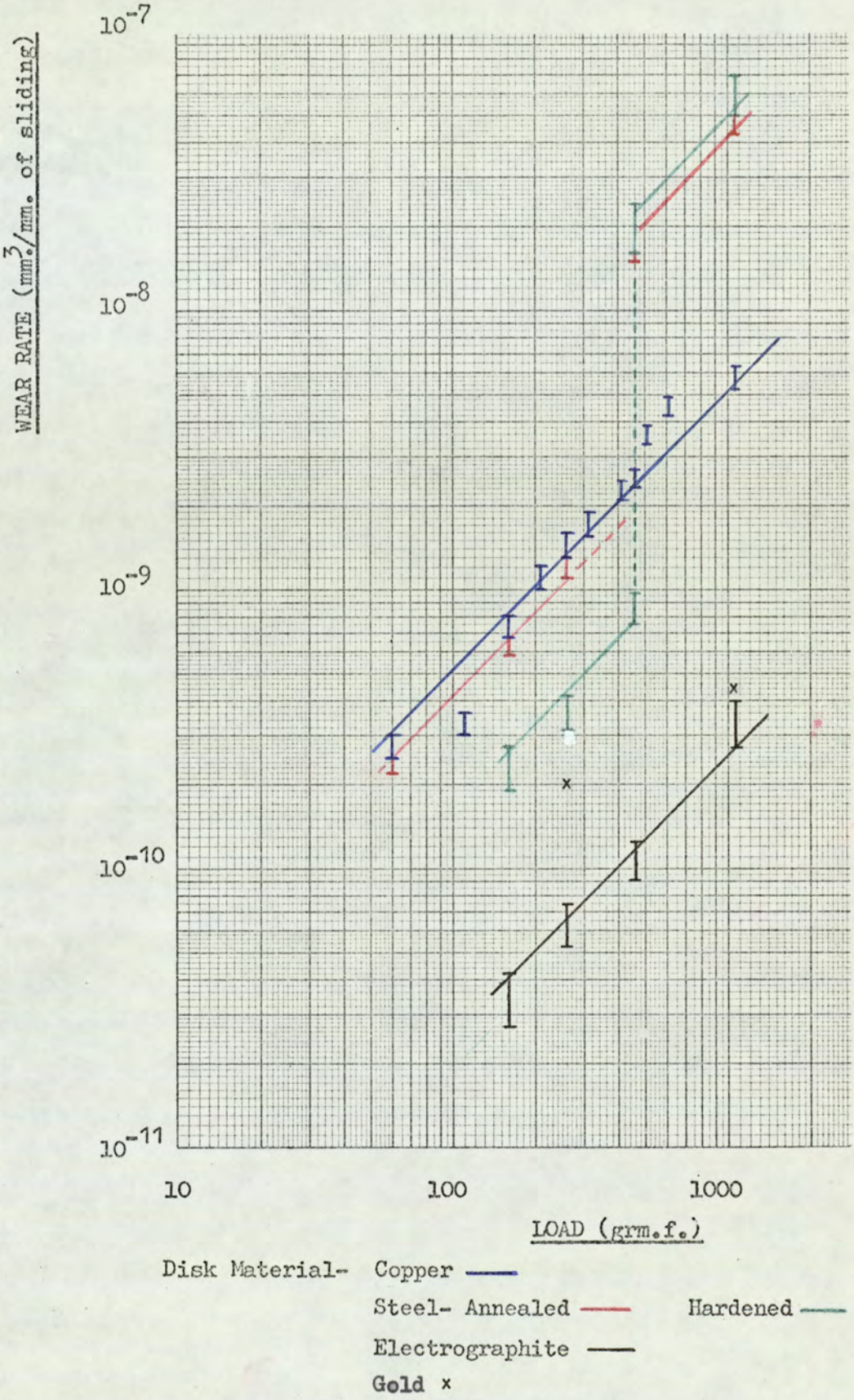

Figure 5.1 Variation in the Wear Rate of an Electrographite Brush with Load when Sliding upon Various Disk Materials.

hence only two accurate determinations of wear rate were obtained, one at 260gf. and one at 1060 gms.f. At intermediate loads the wear rate was monitored for about one day to ensure that no large variations in wear rate occurred. No discontinuity in the wear rate was apparent and it would appear that wear rate increased in proportion to load. One very noticeable feature when running on gold was the absence of any graphite transferred to the disk surface.

A marked transition from mild wear to severe wear took place at a load of 460gms.f. when running electrographite on hardened EN26 steel. Initially the wear rate at this load was low and the contact resistance measured at 1mA current, was relatively high, about 100ohms. After running in the mild wear regime for two days the contact resistance fell to 0.4ohms and the wear rate increased. At load above 460gms.f. the wear rate was high. The wear behaviour of electrographite sliding upon annealed EN26 steel was very similar but was dependent upon the past history of the disk surface. The wear rate of the brushes when running under a load of 260gms.f. was in the mild wear regime, 10.4×10^{-10} mm^3 per mm sliding distance and the contact resistance was high. However, after carrying out the contact resistance measurements the wear rate increased to the severe wear regime and the contact resistance remained low. After the brushes had been lifted clear of the disk for some time the contact resistance increased and the wear rate fell back to the mild wear regime. Similarly when a freshly prepared disk, having been machined only a few hours prior to running was run under a load of 160gms.f. the wear rate was high, about 10^{-8} mm^3/mm of sliding and the contact resistance was low, less than 1ohm. However, after leaving the disk running for two days without the brushes in

contact the wear rate fell to the mild wear regime and the contact resistance increased.

When the brushes were running on steel in the mild wear regime very little graphite was transferred to the disk surface except for narrow bands parallel to the running direction. In the severe wear regime the amount of transferred graphite on both the annealed and hardened disks increased until at a load of 1060gms.f. the whole wear track was covered by a layer of graphite.

The wear rates of brushes sliding on an electrographite disk were low and very similar to the wear rates on gold at the same load. The wear rate of the brushes was proportional to the applied load over the whole range of loads investigated. However, after running for several days at a load of 1060gm.f. the wear rate quite suddenly increased to $10^{-7} mm^3/mm$ of sliding and the frictional force fell from 200gms.f. to 80gms.f. The sudden increase in wear rate was associated with the surfaces of both the brush and disk worn surfaces becoming glazed and the appearance of a high pitched whistle, of frequency 7 - 10 KHz, originating from the brush disk interface.

5.3. The Contact Resistance of Electrographite

The contact resistance characteristic of carbon brushes sliding on copper has been investigated and reported upon by a number of authors including Bickerstaff(21), Davies(20), Holm (19), Shobert(29) and Stebbens (24) and the resistance has been found to depend almost entirely upon oxide films at the brush interface. Some materials other than copper have also been investigated but to a much lesser extent. Thompson

and Turner (41) have investigated the resistance of a highly graphitic brush sliding on copper, aluminium, zinc, mild steel and gold, although the brush was run under a relatively high load, 750gms.f. and carried a high current, 10amp. The contact resistance of brushes sliding on gold has been observed by other authors but mainly to provide information for comparison with results from other metals since gold does not form an oxide layer under normal conditions.

For comparison some results obtained by Bickerstaff are shown in Figure 1.5 . Bickerstaff confined his reported investigations to the positive brush to avoid any effects due to copper picking at the negative brush interface. His results show that after an initical ohmic region the contact resistance began to fall when the contact drop exceeded 0.1 Volts. At high voltage drops the interface again behaved in an ohmic manner. The decrease in contact resistance is generally regarded as being due to electrical breakdown of the oxide film when the applied field exceeds the breakdown strength of the oxide.

During the course of this project it was necessary to repeat some of the experiments described by other authors to obtain results which gave valid comparisons between the different materials since itis highly probable that contact resistance measurements will depend upon the mechanical running conditions, despite efforts to reduce any effects arising from the design of the wear test machine.

5.3(i) Contact Resistance Running Upon Copper

The variation in contact resistance with contact drop across the

interface for brushes running at loads of 60gms.f., 210gms.f., 260gms.f. and 310gms.f. is shown in Figures 5.2 and 5.3. The investigations described here were confined to low values of electric current and contact drop to avoid any possible damage to the two worn surfaces. The results showed that the shape of the characteristic was very much the same as that obtained when running on aluminium at low loads (Figures 4.4 and 4.5)and are also in some agreement with the results of Bickerstaff. However, unlike the aluminium characteristics, the results obtained on copper show a strong dependence upon the brush polarity. Although there was little difference between the values of the low current ohmic resistance of the two brush polarities, the reduction in contact resistance took place at a lower contact voltage beneath the positive brush than the negative brush, about 0.1 volts compared with about 1.0volts.

Table 5.1 shows values of contact resistance obtained at loads up to 1060gm.f. The value of the low current ohmic contact resistance decreased as the applied load increased. At loads of 610gms.f. and 1060gms.f. the contact resistance was low and difficult to measure at low currents and it may be possible that electrical breakdown had already occurred at the electric currents used to measure contact resistance. These values of contact resistance are however high compared with other author's results obtained at high currents at all loads on copper(19) (21) and on other materials and this indicated that even at these high loads copper oxide was having a very significant effect upon contact resistance.

5.3(ii) Contact Resistance Measurements on Gold

The resistance between a carbon brush and a metal surface has been

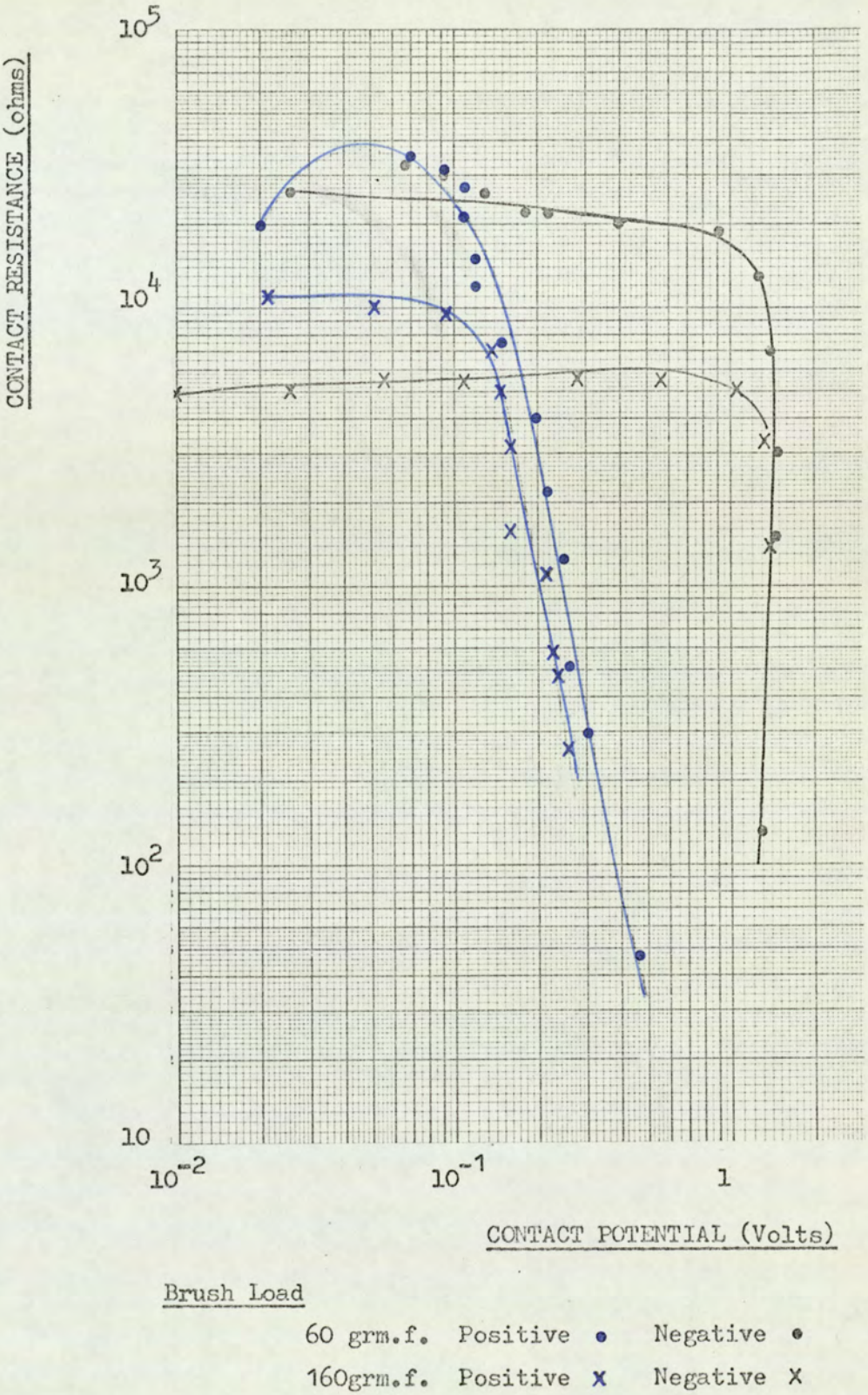

Figure 5.2 Variation in Contact Resistance of Electrographite with Contact Potential when Sliding upon Copper.

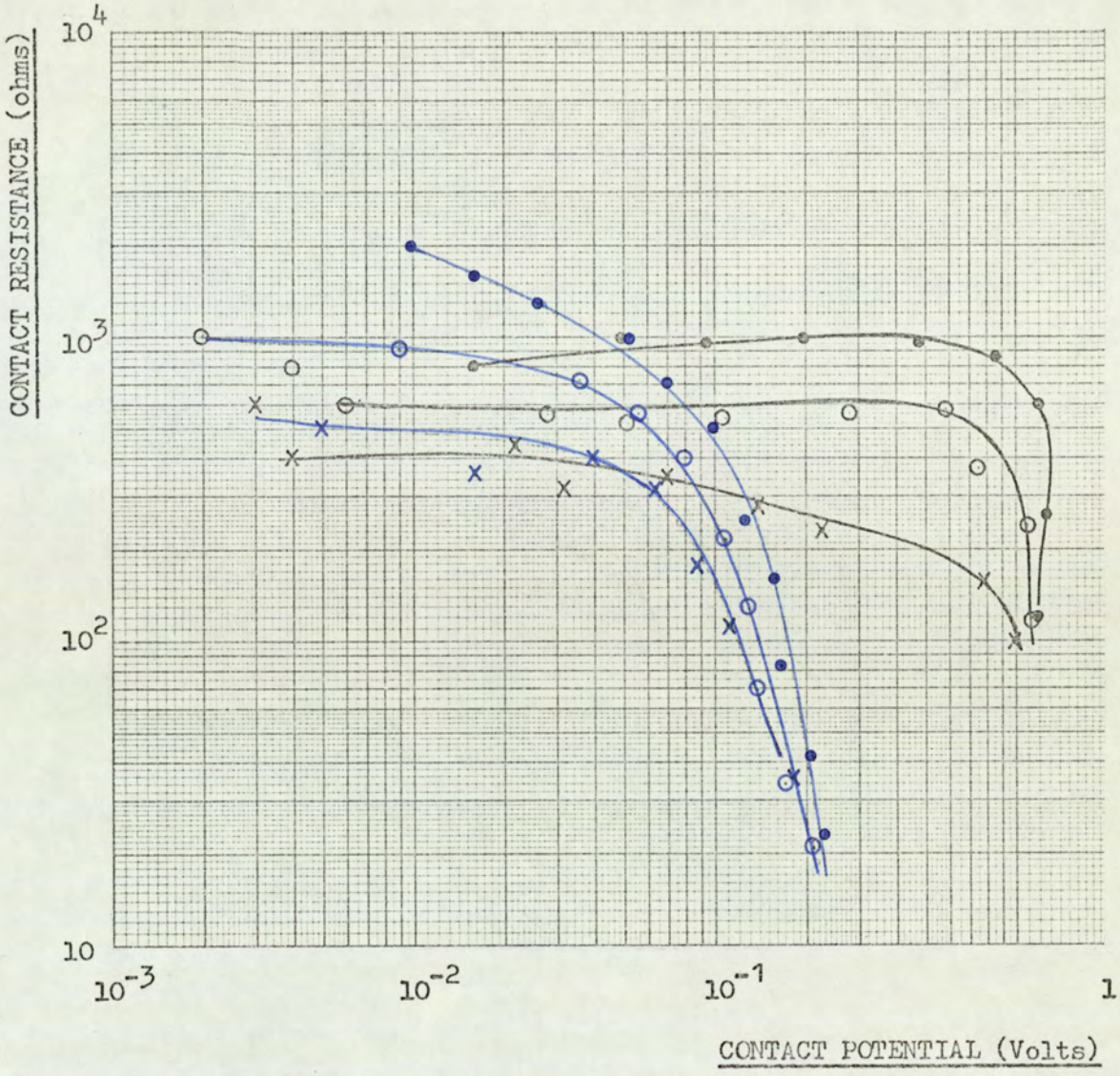

Figure 5.3 Variation in Contact Resistance of Electrographite with Contact Potential when Sliding upon Copper.

Table 5.1. Contact Resistance of an Electrographite Brush sliding on Copper

Load	Current	Positive Brush		Negative Brush	
		Voltage Drop	Contact Resistance (OHMS)	Voltage Drop	Contact Resistance (OHMS)
60 gf.	1 μA	20mV	20K	26mV	26 K
	2	70	35K	66	33 K
	3	92	30K	94	31 K
	4	110	27K	110	27 K
	5	110	22K	130	26 K
	8	120	15K	180	22 K
	10	120	12K	220	22 K
	20	150	7.5K	400	20 K
	50	200	4.0K	920mV	18.4 K
	100	220	2.2K	1.28V	13 K
	200	250	1.25K	1.4	7 K
	500 μA	260	520	1.5	3 K
	1mA	300	300	1.5	1.5K
	10mA	470	47	1.3	1.30
160 gf.	1 μA	8mV	8.0K	5mV	5. 0K
	2	22	11K	10	5. 0K
	5	52	10K	26	5.2K
	10	94	9.4K	56	5.6K
	20	140	7.0K	110	5.5K
	30	150	5.0K	154	5.1K
	50	160	3.2K	280	5.6K
	100	160	1.6K	560mV	5.6K
	200	220	1.1K	1.06V	5.03K
	400	230	575	1.34	3.35K
	500 μA	240	480	1.45	2.9K
	1mA	260	260	1.4 V	1.4K

Table 5.1 Continued

Load	Current	Positive Brush		Negative Brush	
		Voltage Drop	Contact Resistance (OHMS)	Voltage Drop	Contact Resistance (OHMS)
210 gf.	2μA	8.0mV	4.0K	-	-
	5	10	2.0K	2mV	400
	10	16	1.6K	8	800
	20	26	1.3K	16	800
	50	52	1.0K	50	1K
	100μA	70	700	95	950
	200μA	100	500	200	1K
	500μA	126	250	480	960
	1mA	160	160	860mV	860
	2	165	82	1.20V	600
	5	210	42	1.28V	260
	10	230	23	1.20V	120
260 gf.	2μA	2mV	1.0K	2mV	1.0K
	5	4	800	4	800
	10	9	900	6	600
	50	36	720	28	560
	100	56	560	52	520
	200	80	400	108	540
	500μA	108	216	280	560
	1mA	130	130	580	580
	2	140	70	740	370
	5	170	34	1.2V	240
	10mA	210	21	1.14V	114

Table 5.1. Continued

Load	Current	Positive Brush		Negative Brush	
		Voltage Drop	Contact Resistance (OHMS)	Voltage Drop	Contact Resistance (OHMS)
310 g f.	2μA	2 V	1.0K	2.0mV	1.0K
	5	3.0	600	3.0	600
	10	5.0	500	4.0	400
	50	18	360	22	440
	100	40	400	32	320
	200	64	320	70	350
	500μA	88	176	140	280
	1mA	112	112	230	230
	5	180	36	780	156
	10	200	20	1.0V	100
360 g f.	10μA	1.0mV	100	2.0mV	200
	50	12	240	6.0	120
	100	24	240	10	100
	200	46	230	-	-
	500μA	80	160	48	96
	1mA	108	108	100	100
	5mA	160	32	330	66
	10	180	18	700	70
	50	230	5.0	800	16
410 g f.	100μA	2-3	20-30	2-3	20-30
	500μA	12	24	12	24
	1 mA	24	24	25	25
	5mA	62	12	120	24
	10mA	90	9	200	20
460 g f.	200μA	14	70	3	15
	500μA	32	64	37	14
	1mA	36	56	14	14
	5mA	110	22	80	16
	10mA	140	14	150	15

Table 5.1. Continued

Load	Current	Positive Brush		Negative Brush	
		Voltage Drop	Contact Resistance (OHMS)	Voltage Drop	Contact Resistance (OHMS)
510 g f.	50μA	1.0mV	50	1.0	50
	100	1.0mV	10	1.0	10
	200	1.0mV	5.0	1.0	5.0
	500μA	2.0	4.0	2.0	4.0
	1mA	3.0	3.0	3.0	3.0
	5	9.0	1.8	10	2.0
	10	15	1.5	15	1.5
	50	51	1.0	120	2.4
	100	86	0.9	150	1.5
560 g f.	500μA	1.0	2.0	1.0	2.0
	1mA	2.0	2.0	1.0	1.0
	5mA	6.0	1.2	6.0	1.2
	10	10	1.0	6.0	0.6
	50mA	40	0.8	30	0.6
	100	60	0.6	70	0.7
	500	180	0.4	300	0.6
	1A	250	0.2	450	0.45
610 g f.	1mA	1.5	1.5	1.5	1.5
	100	60	0.6	80	0.8
	500	170	0.34	190	0.38
	1A	150	0.15	200	0.20
1060 g f	1mA	1.0	1.0	1.0	1.0
	100	70	0.7	80	0.8
	500	160	0.30	160	0.32
	1A	140	0.14	180	0.18

shown by many authors to be largely determined by an oxides at the brush-metal interface. Since gold does not form a coherent oxide at normal temperatures the contact resistance of electrographite brushes sliding on gold must have been due entirely to the constriction resistance of the contacts. A chemisorbed monolayer of oxygen forms on gold in air but the electric current would have passed through this layer by tunnelling without suffering any interference - Holm (22).

The experiments on gold were carried out to give information about how the real area of contact between the brush and the disk varied with running time. Prior to the experiments the brushes were lightly abraded with fine emery paper attached to the disk surface to ensure that the two running surfaces were parallel and that contact was possible over the whole apparent area of the brush face. After abrasion the brushes were thoroughly washed in petroleum ether.

The static contact resistance was measured using a current of 1mA, first with the load increasing in stages from 60gms.f. to 1060gms.f., then with the load decreasing,the measurements were repeated using an electric current of 1.0amps. The measurements were carried out with the disk stationary before any running had taken place, with the brush contacting the same region of the disk track each time. The variation in contact resistance with load is shown in Figure 5.4. The curve was the same for the load increasing or decreasing using electric currents of 1mA or 10amps, and no difference between the positive and negative brushes was detected. As would be expected the contact resistance decreased with increasing load, due to the increase in the real area of contact.

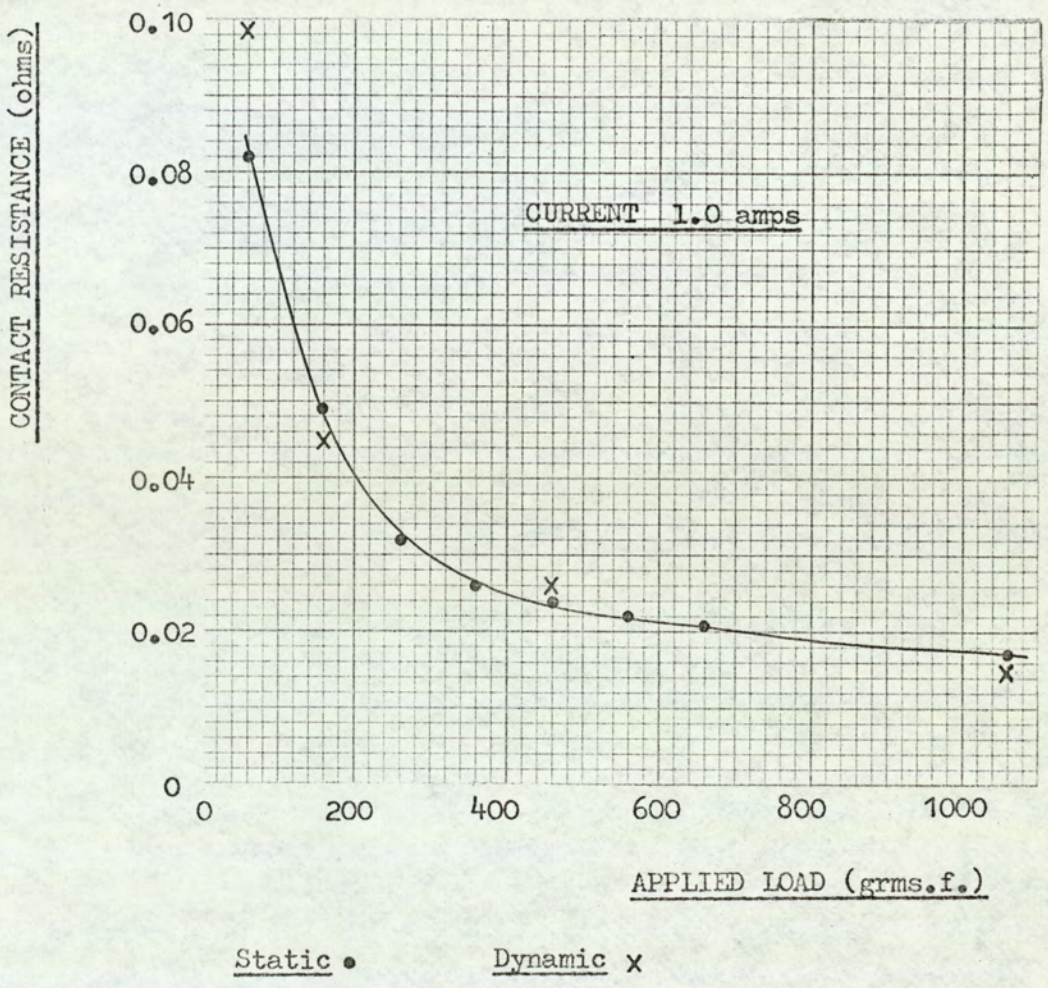

Figure 5.4 Contact Resistance of an Electrographite Brush on Gold Under Static and Sliding Conditions.

The contact resistance was also measured at various times during running, with the disk rotating. The results of these measurements are also shown in Figure 5.4 and it can be seen that these points lie very close to the static contact resistance curve. The results were very significant since they indicated that, during the experiment, the real area of contact did not increase during running, contrary to the suggestions of Bickerstaff (21) and E.Holm(18). In a later section it will be shown that frictional force increased during running at 60gm.f. load even though no decrease in contact resistance occurred.

5.3(iii) Contact Resistance on EN26 disks

The contact resistance behaviour of electrographite brushes sliding on both annealed and hardened steel disks was, as was the wear behaviour, very similar to that of electrographite sliding upon aluminium.

At low loads, below the load at which the transition from mild wear to severe wear occurred, the contact resistance was high and behaved in the same manner as on other metals (except gold). A decrease in the contact resistance resulted when the voltage drop across the interface exceeded a critical value. Table 5.2 shows the variation in contact resistance with current and voltage drop for brushes running in the mild wear regime under loads of 60gms.f. and 260gms.f. on hardened EN26 steel. Similar results for brushes running under the same conditions on an annealed EN26 disk are shown in Table 5.3. As previously described, when running on hardened steel at a load of 460gms.f. in the mild wear regime the contact resistance, measured at 1.0mA current, was about 100ohms, whilst in the severe wear regime the contact resistance was

Table 5.2. Contact Resistance of Electrographite sliding upon a Hardened EN26 steel disk

Positive brush only

60g f.Load			260g f. Load		
Current	Voltage	Contact Resistance (ohms)	Current	Voltage	Contact Resistance (ohms)
10μA	180mV	18K	10μA	5mV	500
50	620	12.4K	50	18	360
100	900	9.0K	100	39	390
200μA	1.20V	6.0K	500μA	190	380
1mA	1.30	1.3K	1mA	350	350
5	1.34	270	5	960	192
10	1.40	140	10	1.22V	122
20	1.42	71	20	1.22	61
30	1.44	48	30	1.24	41
50	1.44	29	40	1.20	30
100	1.45	14.5	50	1.22	24
500	1.44	2.9	80	1.30	16
1.0 A	1.62	1.6	100	1.30	13
2.5 A	1.62	0.65	200	1.36	6.8
5.0	1.62	0.32	300	1.40	4.6
10A	1.75	0.17	500	1.44	2.9
			800	1.46	1.8
			1.0A	1.50	1.5
			2.0	1.55	0.77
			10	1.8	0.18

Table 5.3 Contact resistance of electrographite Sliding upon an annealed EN26 Steel disk

Positive Brush only

Load 60gf.			260 g f. Load		
Current	Voltage Drop	Contact Resistance (ohms)	Current	Voltage Drop	Contact Resistance (ohms)
10μA	10mV	1.0K	10μA	4.0mV	400
100μA	35	350	100μA	25	250
200	75	375	200	40	200
400	150	375	400	80	200
600μA	220	360	600μA	120	200
1mA	330	330	1mA	170	170
2	450	225	2	260	130
5	860	172	5	750	150
10	900	90	10	900	90
20	960	48	20	960	48
30	960	32	30	940	31
40	920	23	40	940mV	23
60	1.00V	16.6	60	1.01	17
100	1.06V	10.6	100	1.08	10.8
500mA	1.18	2.4	500	1.28	2.6
1.0A	1.20	1.2	1.0A	1.32	1.3
2.0A	1.32	0.65	2.0A	1.40	0.7
5.0A	1.36	0.27	5.0A	1.50	0.3
10.0A	1.20	0.12	10.0A	1.20	0.12

0.4 ohms measured at 1mA and decreased to 0.18 ohms at 10ams. At loads in the severe wear regime on both materials, 460gms.f and 1060gms.f., the contact resistance measured at 1mA current was low, about 0.3 - 0.4 ohms and decreased slightly with current to a value of 0.14 - 0.18 at 10 amps current. A comparison between the contact resistances, of brushes running on copper and steel, at loads of 460gms.f. and 1060gms.f. revealed that the contact resistance on steel was much lower than on copper. Since the copper had a much higher conductivity and was much softer, one would expect the opposite to be true. The greater resistance when running upon copper must have been due to oxide layers at the contacts.

5.3.(iv) The Contact Resistance of an Electrographite Brush Sliding upon an Electrographite Disk

The contact resistance of an electrographite brush sliding upon electrographite was, as would be expected in the absence of oxide, very low. The contact resistance was measured at one load only 60gms.f. and the results are shown in Table 5.4. The resistance was measured with the electric current passing through the interface in both directions and no polarity effect occurred. A slight decrease in contact resistance was detected at high brush currents.

Table 5.4. Contact Resistance of Electrographite Sliding upon Electrographite

Current through brushes increased after each reading.

Brush Load 60gf.

Current	Voltage Drop	Contact Resistance (ohms)
50μA	0.015mV	0.3
100	0.03	0.3
200μA	0.07	0.28
1mA	0.29	0.29
5	1.45mV	0.29
20	5.7	0.29
50	14.9	0.30
100	31	0.31
500	145	0.29
1.0A	280	0.28
2.0	0.53 reducing to 0.50	0.26 → 0.25
4.0	0.88 " " 0.65	0.22 → 0.16
5.0	0.80 " " 0.73	0.16 → 0.15

5.4. The Frictional Force of Electrographite

5.4(i) Electrographite Sliding upon Copper

The frictional force of carbon brushes sliding upon copper has been fully investigated by a number of authors, as outlined in Chapter 1. Carbon brushes sliding upon materials other than copper have also been investigated but to a much lesser extent, the most common alternative materials being steel, carbon and gold (17), (18), (42). Unfortunately these experiments have been carried out under a wide variety of running conditions using many different types of carbon material, and because of this diversity in the operating conditions the results obtained cannot be related to the results described here. However, the experiments of Bale (43), Davies (20), Holm (19), Lancaster and Stanley (17), Quinn (10) and White (31) were carried out on electrographite brushes under conditions similar to those described here. The limited number of results obtained from running upon copper confirmed that the frictional force was behaving in a manner very similar to that described by these authors.

Those authors who have measured the frictional coefficient of electrographite upon copper at high currents are in agreement with each other that the frictional coefficient under these conditions is within the range 0.14-0.17. At low currents there is a much wider variation in the measured values of frictional coefficient, from 0.2 to 0.35. This wide range of values could possibly arise from the diversity of the operating conditions, the changing parameters having a greater effect upon friction at low currents.

The no current equilibrium value of frictional coefficient obtained in these experiments at 60gf. load was 0.3. This value was in agreement

with that quoted by Quinn (10) and was within the range reported by Bale, who carried out an investigation into the effect of the hardness of the copper upon friction.

The behaviour of the coefficient of friction with electric current was the same as upon aluminium at the same load, although the irregular behaviour of the friction limited the extent of the investigation. The frictional force remained constant until a current of 50 MA was passed through the brushes when a decrease in friction occurred. The friction decreased further with increasing current until at a current of 10 amps the coefficient of friction had decreased to 0.16.

The effect of applied load upon the friction coefficient has been investigated in detail by Quinn (10) who showed that a decrease in friction occurred with increasing load. The results obtained here also showed some decrease in frictional coefficient with load, although the erratic behaviour of the friction prevented direct confirmation of Quinn's results. The variation in friction with load is shown in Table 5.5.

Load gf.	Frictional Force gf.	Coefficient of Friction
60	18	0.3
110	23-27	0.21-0.25
160	28-30	0.18-0.19
460	80-95	0.18-0.21
560	110-114	0.19-0.20
1060	156-216	0.15-0.20

Table 5.5 Variation in coefficient of friction of electrographite sliding upon copper with applied load

At the higher loads, 560gf. and 1060gf., electric current had no effect upon friction until high currents, 5 amps were passed through the brushes when a decrease in friction took place. This high current friction was erratic but the frictional coefficient was within the range 0.14-0.17 found by other authors.

5.4(ii) Electrographite Sliding upon EN26 Steel

The hardness of the EN26 steel had little effect upon frictional force, provided measurements were made in the same wear regime. Table 5.6 shows the variation in coefficient of friction with electric current for both the annealed and hardened disks at a load of 60gf. At an electric current of about 40 mA the friction began to decrease and further increases in electric current produced greater reductions in friction. At a higher load in the mild wear regime the frictional force behaved in a similar manner. Table 5.7 shows the variation in friction with electric current at a load of 260 gf. When running under the higher load no decrease in friction was detected until a current of 100 mA was passed through the brush. These results showed that in the mild wear regime the frictional force was independent of the hardness of the metal but was strongly dependent upon the applied load and electric current.

Above the transition load, in the severe wear regime, the coefficient of friction was lower than in the mild wear regime, 0.14 at a load of 1060 gf. No decrease in frictional force occurred until an electric current of 5.0 amps was passed, when a reduction in friction of 12% took place. Upon increasing the current to 10 amps a further reduction in friction of 10% occurred.

Hardened EN26 Steel			Annealed EN26 Steel		
Load 60 gf.			Load 60 gf.		
Current	Frictional Force gf.	Frictional Coefficient	Current	Frictional Force gf.	Frictional Coefficient
0	18.5	0.31	0	18.5	0.31
10 μ A	18.5	0.31			
50	18.5	0.31			
200	18.5	0.31	200 μ A	18.0	0.30
1 mA	18.5	0.31	1 mA	18.0	0.30
5	18.5	0.31	5	18.0	0.30
10	18.0	0.30	10	18.0	0.30
30	18.0	0.30	30	17.5	0.29
			40	17.0	0.28
50	17.0	0.28			
100	17.0	0.28	100	16.5	0.275
500 mA	16.0	0.27	500 mA	16.0	0.27
1 A	14.0	0.24	1 A	15.8	0.27
2.5 A	13.5	0.23	2.0 A	14.5	0.245
5.0 A	11.0-13.0	0.18-0.22	5.0 A	11.0	0.18
10.0 A	9.5	0.16			

Table 5.6 Variation in friction with electric current on annealed and hardened EN26 steel disks at a load of 60 gf.

Hardened EN26 Steel			Annealed EN26 Steel		
Load 260 fg.			Load 260 gf.		
Current	Frictional Force gf.	Frictional Coefficient	Current	Frictional Force gf.	Frictional Coefficient
0	66.0	0.252	0	64.0	0.246
10 μA	66.0	0.252	10 μA	64.0	0.246
100	66.0	0.252	100	64.0	0.246
500 A	66.0	0.252	600 A	64.0	0.246
1 mA	66.0	0.252	1 mA	64.0	0.246
5	66.0	0.252	5	64.0	0.246
10	66.0	0.252	10	64.0	0.246
50	66.0	0.252	40	62.0	0.24
80	66.0	0.252	60	62.0	0.24
100 mA	64.0	0.246	100 mA	61.0	0.234
200	62.0	0.24			
500	62.0	0.24	500	59.0	0.227
1 A	58.0	0.22	1 A	57.0	0.22
2 A	56.0	0.216	2 A	52.0	0.20
5 A	52.0	0.20	5 A	47.0	0.18
10 A	42.0	0.16	10 A	41.0	0.16

Table 5.7 Variation in friction with electric current on annealed and hardened EN26 steel disks at a load of 260 gf. operating in the mild wear regime.

5.4(iii) Electrographite Sliding upon Gold

Measurement of the frictional force during running showed that friction increased with time of running at a load of 60 gf., during the same period no change in contact resistance occurred. This experiment was stopped before equilibrium was fully established, the equilibrium value of frictional force may therefore be higher than the value quoted.

Table 5.8 shows the variation in friction with time of running, electric current and load.

Load	Time of Running (Hours)	Frictional Force gf.	Coefficient of Friction	Electric Current
60 gf.	12	14	0.24	0
	48	15	0.25	0
	108	15	0.25	0
	180	18	0.30	0
	↓	18	0.30	500 mA
		18	0.30	1.0 A
	↓	15	0.25	5.0 A
	181	14	0.24	10 A
160 gf.	24	46	0.29	0
460 gf.	24	120	0.26	0
		124	0.27	0
1060 gf.	70	290	0.27	0
		320	0.30	0

Table 5.8 Variation in friction for electrographite sliding upon gold.

From Table 5.8 it can be seen that although the frictional force decreased with electric current, no decrease in friction with applied load occurred.

5.4(iv) Electrographite Sliding upon Electrographite

When sliding an electrographite brush upon an electrographite disk no increase in frictional force with time of running occurred. The friction rapidly reached an equilibrium value which appeared to be independent of the applied load. Under a load of 60 gf. the coefficient of friction had a value of 0.15-0.17 and remained within this range until an electric current of 5 amps was passed through the brushes, when the coefficient of friction fell to 0.10. At a load of 160 gf. the frictional coefficient was about 0.17.

Under a load of 1060 gf. the frictional coefficient rapidly attained an equilibrium value of 0.19-0.20 and remained at this value for several days running. However, the frictional coefficient suddenly dropped to 0.08, this fall being associated with a marked increase in brush wear rate and glazing of the running surfaces.

5.5 Physical Analysis of Worn Surfaces.

Physical analysis of the surfaces formed during sliding upon materials described in this chapter was carried out using electron probe microanalysis and scanning electron microscopy but was confined to a comparison of these surfaces with those formed upon aluminium.

With the exception of when running upon electrographite the nature of the surfaces formed depended upon which wear regime the brush was operating in rather than the disk material.

Below the transition load when running upon annealed EN26 steel the topographies of both the brush and disk surfaces were the same as the mild wear topographies formed when running upon aluminium. The surface of the disk contained smooth, isolated islands of transferred graphite and the brush surface became overlaid by a smooth, continuous graphite film similar in appearance to that shown in Figure 4.27. No detailed investigation into the nature or thickness of the brush film formed from running upon steel could be carried out.

Above the transition load the surfaces behaved in the same manner as described in Chapter 4for aluminium, the amount of laid down graphite upon the steel surface increasing to 100%coverage. Due to the small number of specimens examined it was impossible to select characteristic steel surfaces or determine the effect of load or elecric current upon the disk topography. The brush topography formed above the transition load was extremly smooth and highly polished with little cracking or flaking of the surface. Once again however the small number of specimens available prevented a detailed examination.

A topographical study of the surfaces formed upon the hardened EN26 steel could not be succesfully carried out due to difficulty in cutting specimens from the disk without destroying those surface features of interest. A replica technique was attemted but because areas of

graphite were removed from the surface with the replicating plastic a false topography was obtained. Investigations into the hardened steel surfaces were confined therefore to optical examinations. From this limited investigation it would appear however that the hardened steel disk topography in both the mild and severe wear regimes differed little from the surfaces formed upon the annealed steel and aluminium in the same regimes. Examination of brush surface showed once again the presence of an overlaid graphite film with fatigue type cracking at loads below the transition load. Above the transition load the brush surface had the characteristic severe wear topography of a highly polished surface with little evidence of fatigue type cracking..

Elecron probe microanalysis of the worn brush surfaces revealed the presence of transferred iron from the annealed and hardened disks but no detailed investigation into the effect of load or electric current upon the amount of transferred iron was performed.

When sliding upon the copper disks both the disk and brush surfaces retained the fatige type topography characteristic of mild wear up to the highest load used, 1060gf. Figure 5.5 shows the surface of the copper wear track formed at a load of 460gf. Lateral and transverse fatigue type cracking is clearly visible together with tilted fingers of graphite, described by Fullam and Savage (6). These tilted graphite flakes were found only in certain areas on the copper disk and were not generally characteristic of mild wear running on all materials. Scanning electron microscopy of the brush surface formed against copper showed that the brush topography at all loads was characteristic of that formed under mild wear conditions, a coherent surface film of graphite with widespread cracking and flaking. Electron probe microanalysis of the brush surface showed small particles of transferred copper.

Optical examination of the wear track formed upon the gold disk

10 μ

(a)

5 μ

(b)

Figure 5.5 Surface Topography of Copper Disk Formed During Mild Wear Running at a Load of 460gf.

revealed the complete absence of any transferred graphite film, although some loose graphite wear debris was present upon the surface. The brush surface however attained the typical mild wear topography described for aluminium, a coherent surface film with fatigue cracking.

When sliding upon an electrographite disk the nature of the surfaces formed was entirely different from those formed when sliding against metals. No graphite films were formed upon either the wear track on the disk or the brush surface. Both running surfaces became smooth and highly polished but retained their porous structure. The surfaces after running had the same appearance as the metallurgically polished surface shown in Figure 4.26 (a).

When sliding under a load of 1060gf. the brush surface took on a highly glazed appearance which was associated with a marked increase in wear rate and a fall in friction. No change in the surface topography could be detected to account for these phenomena.

5.6 X-Ray Analysis of Wear Debris.

The principles involved in the analysis of the wear debris have been outlined in section 4.16 for aluminium and these principles apply equally to analysis of the debris produced upon other materials.

5.6(i) Wear Debris Produced upon Copper.

Structure Factors of Copper and Cuprous Oxide (Cu_2O)

Copper has a face centred cubic structure with atoms at (0,0,0), $(0,\frac{1}{2},\frac{1}{2})$, $(\frac{1}{2},0,\frac{1}{2})$, $(\frac{1}{2},\frac{1}{2},0)$.

The structure factor for any set of planes giving rise to reflections is given by;

$$F_{hk}^2 = 16\, f_{hk}^2$$ where hk are allodd or all even.

Cuprous oxide has a cubic structure containing 4 copper atoms and 2 oxygen atoms per unit cell. Copper atoms occupy positions at $(\frac{1}{4},\frac{1}{4},\frac{1}{4})$, $(\frac{3}{4},\frac{3}{4},0)$, $(\frac{3}{4},\frac{1}{4},\frac{3}{4})$, $(\frac{1}{4},\frac{3}{4},\frac{3}{4})$ and oxygen atoms occupy sites at (0,0,0) and $(\frac{1}{2},\frac{1}{2},\frac{1}{2})$.

The structure factor of the (111) and (220) planes are;

$$F_{111}^2 = 16 f_{cu}^2 \quad \text{and} \quad F_{220}^2 = \left[4f_{cu} + 2f_o\right]^2$$

where f_{cu} and f_o are the scattering factors of the copper and oxygen ions respectivelly.

Calculation of "R".

Once the structure factor has been found the value of "R" can be calculated. These calculations are shown in Appendix I and the results tabulated in Table 5.9.

Material	Cu	Cu	Cu	Cu	Cu	Cu	Cu_2O	Cu_2O
Planes	111	200	220	311	222	400	111	220
"R"	397	142	76.3	84	31	16	200	54

Table 5.9 Values of "R" for Copper and Cuprous Oxide.

Microdensitometer traces were obtained from the X-ray powder photographs of the wear debris produced running on copper. From the microdensitometer trace the integrated intensity (I) of the diffraction maxima from those planes giving rise to a reflection was measured. The values of $I/_R$ for the diffraction maxima were calculated and plotted against the Bragg angle θ . for each constituent of the wear debris.

Figures 5.6, 5.7 and 5.8 show the graphs of $I/_R$ against θ obtained from the wear debris formed at loads of 510gf., 560gf., and 1060gf. respectively. Shown in Table 5.10 are the proportions of Carbon, Copper and Cu_2O in the wear debris produced at these loads and the percentage composition of the wear debris.

Componant material	LOAD					
	510gf.		560gf.		1060gf.	
	Proportion	%	Proportion	%	Proportion	%
C	21	93	15	90	24	94
Cu	1	4.4	1	6.0	1	3.9
Cu_2O	0.6	2.6	0.6	4.0	0.6	2.1

Table 5.10 Composition of Wear Debris Produced from Sliding upon Copper.

From Table 5.10 it can be seen that the relative proportions of Cu and Cu_2O remain constant with load. The % composition of the wear did not vary with load over the range investigated.

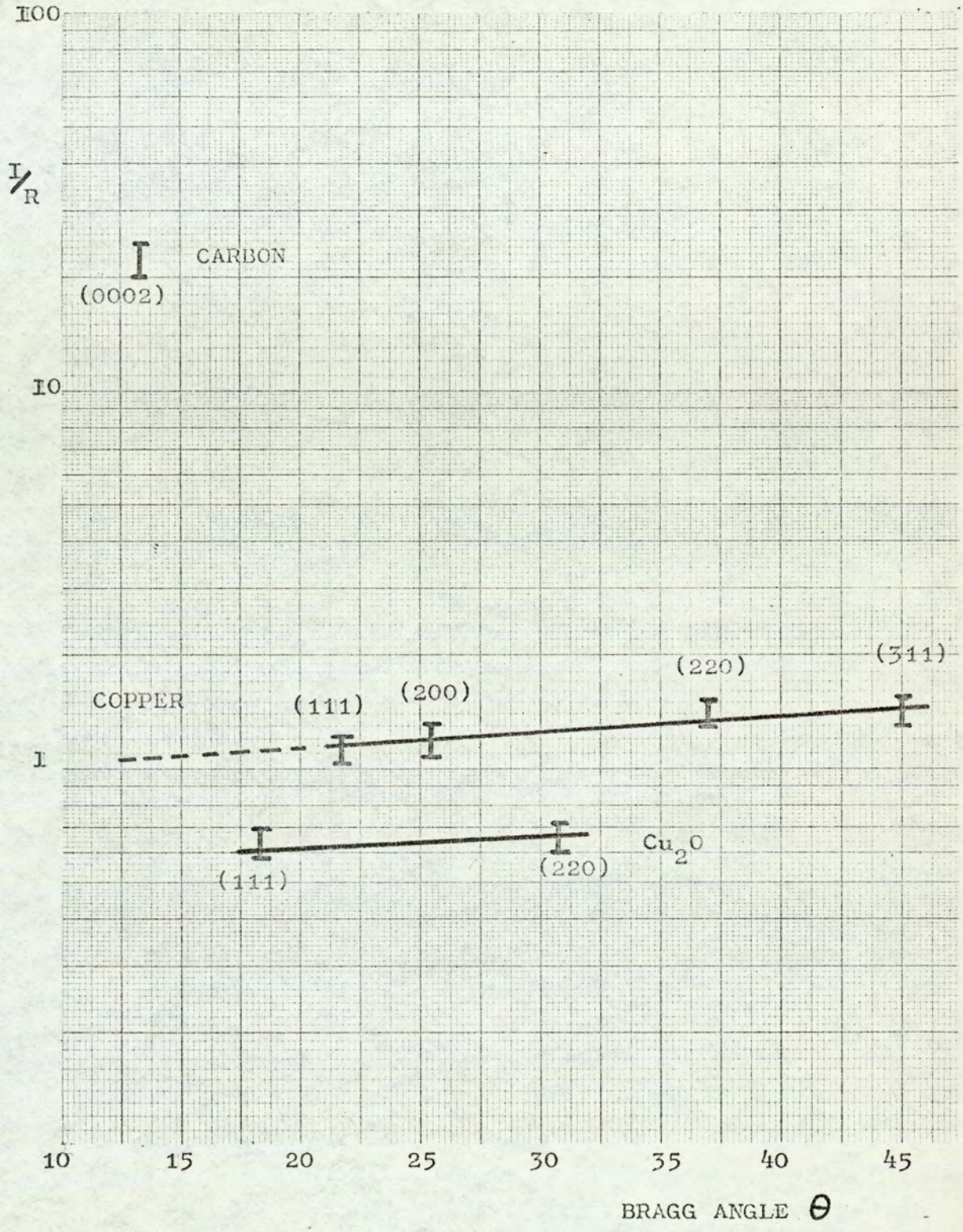

Figure 5.6 Graph of $I/_R$ against Bragg Angle for Wear Debris Produced from Sliding on Copper at a Load of 510gf.

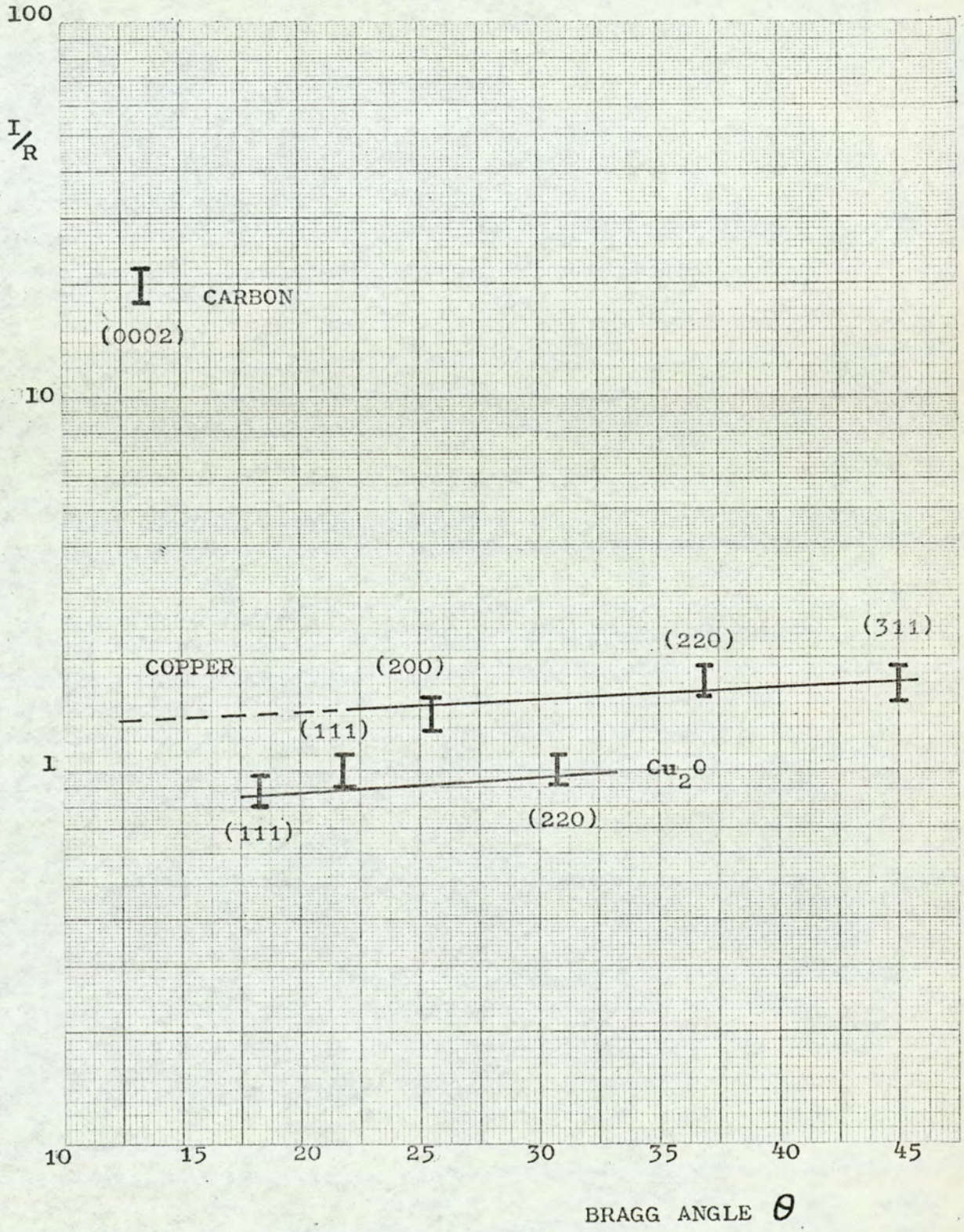

Figure 5.7 Graph of $I/_R$ against Bragg Angle for Wear Debris Produced from Sliding on Copper at a Load of 560gf.

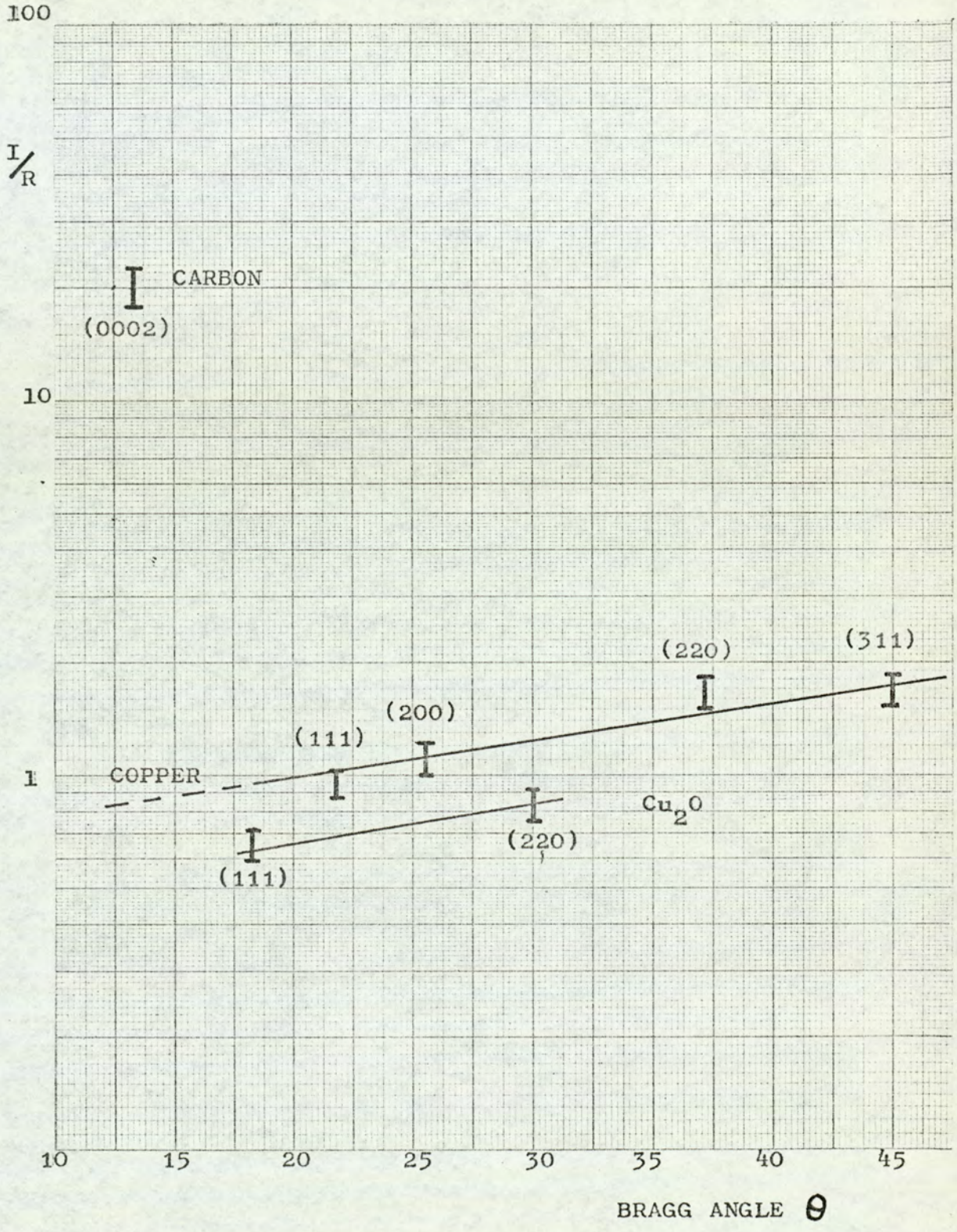

Figure 5.8 Graph of $I/_R$ against Bragg Angle for Wear Debris Produced from Sliding on Copper at a Load of 1060gf.

5.6 (ii) Wear Debris Produced on other Materials.

Insufficient wear debris was collected from running on Gold for a succesful X-ray analysis to be carried out.

When sliding upon EN26 steel disks sufficient wear debris was collected at the higher loads for an X-ray photograph to be obtained. However due to the extremly weak diffraction lines from the minor constituents no quantitative analysis could be performed. Although the lines from iron and its oxides could be detected by the naked eye they could not be distinguished from the background by the microdensitometer. The major componant of the wear debris was carbon with traces of iron and iron oxide constituting less than 1% of the debris.

Chapter 6 Discussion of Results

6.1 The Wear Rate Transitions and Oxide Film Breakdown

The results discussed here apply mainly to electrographite sliding without electric current, except for brief periods when the contact resistance or frictional force were being investigated. The effect of current upon wear will however be briefly discussed.

The results, obtained from running upon aluminium, described in Chapter 4, showed that at low loads the wear rate was low and acceptable to brush users. The wear could be considered to be in the "mild wear regime" and the results were comparable with those of electrographite sliding upon copper. Figure 4.1 shows the variation in wear rate of the electrographite with applied load. At a load of 260 g.f. the wear rate underwent a transition from a mild wear regime to severe wear. Unfortunately this transition load is within the normal operating range of loads for electrographite ($2\frac{1}{2}$-10 p.s.i.) and hence would make the use of aluminium unsuitable because of this high wear rate and unpredicable behaviour.

Proportional analysis of the wear debris using X-ray diffraction proved difficult at loads in the mild wear regime due to the small amounts of debris available and hence no definite relationship between the wear of the aluminium and the applied load could be established. At a very low load, 60 g.f., the wear of the aluminium was comparable with that of copper under similar conditions, but since the proportion of aluminium in the debris remained approximately constant with load it would appear that the wear rate

of the aluminium undergoes a similar transition to the electrographite. For high brush loads the wear of the pure aluminium was unacceptably high.

At the wear rate transition load a marked change in contact resistance behaviour also took place. An investigation into the effect of electric current on the contact resistance showed that at loads below the transition load the contact resistance behaved in the same manner as has already been established upon copper (19) (21), this is shown in Figures 4.2, 4.3 and 4.6. After an initial ohmic region the contact resistance began to fall when a critical potential difference, about 1.1 volts, was exceeded. Beyond this range any increase in electric current produced a further decrease in contact resistance.

When the load was increased above the transition load a substantial reduction in contact resistance occurred. The contact resistance was low even at small currents and very little reduction in contact resistance was produced by increasing the current. If the oxide film theory used to explain the contact resistance behaviour of copper (19) is extended to include aluminium, and the similarities in behaviour show that this is justified, then the contact resistance at the interface was controlled primarily by the metal oxide film, rather than the constriction resistance of the junctions.

It would thus appear that, at a critical load, mechanical disruption of the aluminium oxide on the disk surface takes place producing a transition to the severe wear regime..

One of the major obstacles in determining the effect of applied load upon the interface arises from the difficulty in calculating the real area of contact at the interface, and the magnitude of the stresses set up in

the contacting materials. Lancaster (32) has shown that the stresses set up in the contact surfaces when an electrographite brush slides on copper are elastic. This was established from observations of the slopes of surface irregularities. The calculations used however relied upon the Young's modulus of the carbon material. The normally quoted values are obtained using either tensile specimens or small compression specimens and it is very unlikely that these quoted values will be the same as the Young's modulus of the contact asperities or surface films. The same difficulty applies to the measurement of hardness of carbon brush material. The most reliable estimates are made using a microhardness tester, but this must inevitably crush the brush material into the pores and give a false reading.

The nature of the contact at the interface must also be influenced by the graphite film which has been found to form on both the brush and metal surfaces. The effect of these films upon the load distribution is unknown and it was highly unlikely that the elastic modulii of the graphite films were the same as those of the bulk carbon. Thus it can be seen that it was extremely difficult to accurately assess the stresses acting at the interface for any load and even more difficult to determine how these stresses varied with load, since scanning electron microscopy has shown that the thickness of the surface films varied with load.

The difficulty in calculating the stresses at the interface resulted in an experimental method being used. The contact potential waveform, displayed on an oscilloscope, was used to show whether plastic or elastic deformation of the metal was taking place. The experiments described in section 4.8 have shown that the contact potential waveform between the electrographite brush and metal disk was determined primarily by the contact

configuration on the metal surface, in agreement with the results of Holm (19) and Stebbens (24). A steady, or slowly changing, waveform indicated that the contact configuration was making repeated contact with the brush and therefore had been elastically deformed.

When an electrographite brush was run on aluminium at a load below the transition load the contact potential waveform was steady and repeatable and changed very little over a 24 hour period, indicating that, at these low loads, the metallic asperities were making repeated contact. When the brush load was increased above the transition load the oscilloscope trace became very unstable and no repeatable waveform could be obtained, indicating that the metallic asperities no longer made repeated contact. The rapidly changing contact configuration could have arisen for two reasons, either the metallic asperities were being deformed plastically by contact with the brush, or, an aluminium wear fragment was being produced at each encounter resulting in a continuously changing topography.

If the latter case had been the cause of the unstable waveform an increase in the wear rate of the aluminium would be expected and X-ray diffraction suggests that this may indeed have occurred. However, a closer investigation shows that the increase in wear rate detected by X-ray diffraction is very much lower than would be expected.

At loads below the transition load the waveform was very steady and the probability of producing a wear particle at an encounter was very small. Some idea of the order of magnitude of this probability can be found by considering the K-factor of the wear process, first introduced by Archard (44).

The wear rate of a sliding member ω is given by:

ω = KA where A is the <u>real</u> area of contact and K is the probability of a wear fragment being formed at an asperity encounter . The area of contact can be calculated from

$$A = \frac{W}{P_m}$$

where W is the applied load and P_m is the hardness of the contact material. In the case of electrographite sliding upon aluminium this assumption will not be valid for the reasons given previously, however this will give an order of magnitude for the K-factor.

Therefore, we have $\omega = \frac{K W}{P_m}$

For the <u>pure</u> aluminium used the hardness P_m is approximately 2×10^4 g.f. mm^{-2}.

At 260 g.f. load in the mild wear regime the wear rate of the aluminium is approximately 10^{-10} mm^3/mm sliding. Hence substituting in

$\omega = \frac{K W}{P_m}$ gives $10^{-10} \frac{mm^3}{mm} = K.260 \text{ g.f.} \frac{1}{2 \times 10^4 \text{ g.f.}} mm^3$

$$\frac{10^{-10} \times 2 \times 10^4}{260} = K$$

<u>Hence $K \sim 10^{-8}$</u>

This is a low K factor consistent with the very low wear rates involved in this sliding situation. An approximate calcualtion of the K factor from the length of time elapsing before the waveform has changed completely gives a value for K of approximately 10^{-7}.

After the transition load has been exceeded the unstable trace showed that the contact configuration was rapidly changing. Had this change been produced by the formation of a wear fragment at every encounter the K factor would have to have increased to a value of $1\text{-}10^{-1}$ with an increase, in wear rate of about 10^{6} times. No such increase in the wear of the aluminium was found, the measured increase being of the order of 10 times. It was thus highly unlikely that the rapidly changing waveform was due to the formation of a wear fragment at every encounter. It is proposed that the rapidly changing waveform at loads above the transition load was caused by the asperity configuration changing due to plastic deformation of the soft aluminium without the formation of an aluminium wear fragment at every encounter.

Thus to summarise the wear rate characteristics of electrographite sliding upon aluminium at various loads we have : -

Below transition load

The brush was operating in a mild wear regime with wear rates of about $10^{-9}\text{-}10^{-10}$ mm^3/mm sliding, this wear rate being proportional to the applied load. The contact resistance at the interface was relatively high, $10^{2}\text{-}10^{4}$ ohms and decreased with increasing electric current once a critical potential had been exceeded. This contact resistance behaviour suggested the presence of a mechanically undisrupted oxide film at these loads. The contact potential waveform indicated that at these loads the stresses in the aluminium were below the elastic limit of the aluminium and repeated asperity encounters occurred.

Above transition load

At the transition load the wear rate increased to a more severe regime and the wear rate appeared to be increasing at a greater rate than the increase in load. At the transition load the contact resistance

decreased and was afterwards affected very little by electric current, indicating severe disruption of the oxide film at the metallic contacts. At loads above the transition the contact potential waveform was unstable due to plastic deformation of the aluminium contact asperities.

Thus, the transition from the mild to the severe wear of the electrographite sliding upon aluminium, and the mechanical disruption of the oxide film were strongly connected. The mechanical disruption of the oxide probably resulting from the onset of plastic deformation of the aluminium, this ,however, will be discussed later.

Measurement of the wear rate of an electrographite brush sliding upon copper (section 5.1) at various loads revealed that no transition from mild wear to severe wear occurred within the range of loads investigated. The wear rate of the electrographite increased in proportion to the applied load with no discontinuities in the graph. The absence of any transition when running upon copper suggested that the presence of the transition when running on aluminium was due to a change occurring at the metal surface, rather than a load dependent change taking place in the graphite material.

The wear rates of electrographite sliding upon copper shown in Figure 5.1 were of the same magnitude as the wear rates of electrographite sliding upon aluminium in the mild wear regime and remain within this mild wear regime for all loads, with wear rates varying between 2×10^{-10} mm^3/mm sliding and 7×10^{-9} mm^3/mm sliding.

The contact resistance behaviour of electrographite sliding upon copper was also different from the behaviour of electrographite sliding upon aluminium and no sharp change in the contact resistance

characteristics occurred with load. The shape of the contact resistance versus potential difference curve was the same as has been reported by a number of previous authors (21),(42).

After an initial ohmic region, at low potential differences and low currents, the contact resistance began to decrease, when a critical potential difference was exceeded. When the brushes were run under a load of 60g.f. the value of this critical potential was approximately 0.1 volts for the positive brush and 1.0 volts for the negative brush. The value of breakdown voltage for the positive brush was in agreement with the value obtained by Bickerstaff (21) at a similar load, however, his results were restricted to the positive brush due to "copper picking" at the negative brush interface. Apart from the values of breakdown voltage there were no marked differences between the characteristics of the positive and negative brushes. Electron probe microanalysis has shown that wear particles were transferred to both the negative and positive brushes from all the metal surfaces under investigation , but these particles did not appear to have any great effect upon the running characteristics.

In contrast to the results of Bickerstaff (See Figure 1.5) these experiments showed that as the brush load was increased the value of the low voltage ohmic resistance decreased, this is shown in Figures 5.2 and 5.3 and at higher loads in Table 5.1. This result was not unexpected, since an increase in load should result in an increase in the real area of contact and a consequent decrease in contact resistance. The results also showed however that as the brush load was increased the value of the potential at which breakdown occurred was also decreased, possibly due to a reduction in the oxide film thickness. From these results it would thus appear that when the electrographite brushes were run upon

copper the thickness of the copper oxide film decreased with increasing brush load but complete mechanical breakdown did not occur at the loads used.

The contact potential waveform obtained at all loads was steady and repeatable, showing that multiple asperity encounters were occurring even at high loads, up to 1060gf. Under a load of 1060gf. the wear rate of the brush running upon copper, although still operating in the mild wear region, was comparable with the wear rate of electrographite sliding on aluminium at 260g.f. in the severe wear region. In the latter case, however,the wavetrace was unstable and not repeatable. This was further evidence that the nature of the potential waveform was determined by the asperity configuration of the metal rather than that of the electrographite.

The results discussed so far, for aluminium and copper disks, suggest that possibly one of the most important factors in determining the wear behaviour of the electrographite was the hardness of the disk material. The transition from mild wear to severe wear of electrographite sliding upon aluminium (20VPN) corresponded to the onset of plastic deformation of the metal whilst the absence of any such transition on copper (80VPN) was due to the harder copper resisting plastic deformation until loads outside the range of investigation were reached. However, this explanation must be rejected, or at least severely modified, when the results obtained upon other materials, notably steel, are considered.

The results obtained when running upon EN26 steel showed (Figure 5.1) that a transition from mild wear to severe wear occurred at unexpectedly low loads on both the annealed and the hardned disks. The wear rate of the electrographite sliding upon hardened EN26(550-580 VPN) was slightly

less than on copper or aluminium in the mild wear region at the same load. At a load of 460gf however the wear rate of the electrographite increased from a value of 8.5×10^{-10} mm^3/(mm sliding) in the mild wear region to a value of 2×10^{-8} mm^3/(mm sliding), and at loads above 460g.f. the wear continued in this severe wear region the wear rate of electrographite was comparable with the wear rate of electrographite sliding upon aluminium, although still slightly less (6×10^{-8} mm^3/mm sliding compared with 2×10^{-8} mm^3/mm sliding at 1060g.f.load).

When sliding upon hardened steel the wear transition occurred at a definite load, 460gf., and could easily be reproduced. However, the wear transition which took place upon the annealed steel (270VPN) was unpredictable, occurring at loads as low as 160g.f. and the transition was influenced by the past history of the disk.

Irrespective of the transition load or disk history there was, as when running upon aluminium, a strong connection between the brush wear and the contact resistance characteristic. The behaviour of the contact resistance between the electrographite and the steel disk was more erratic than when running on either aluminium or copper. The value of the low voltage ohmic resistance varied with time of running and the breakdown voltage was irregular. The erratic behaviour prevented an accurate determination of the variation in contact resistance with either electric current or brush load. Despite this difficulty, however, it was obvious that when the brush was operating in the mild wear regime, at a load below the transition load, the contact resistance behaved in a manner consistent with there being a mechanically undisrupted oxide film at the interface. The contact resistance characteristics of the positive brush running the mild wear region at loads of 60g.f and 260g.f. on the annealed steel and the hardened steel are shown in Tables 5.2 and 5.3

respectively. These resistance values show that when a critical voltage was applied across the interface a reduction in contact resistance occurred, as on copper and aluminium. When running under loads above the transition load in the severe wear region, the contact resistance was characteristic of "metallic" contact, low and unaffected by electric current indicating that mechanical disruption of the iron oxide had taken place.

X-ray powder diffraction analysis of the wear debris collected during running upon both the hardened and annealed steel at all loads and currents showed that the major constituent of the debris was, as expected, carbon with only minute traces of iron or its oxides present. The diffraction lines from these minority constituents were visible only to the naked eye and their intensities could not be recorded with the microdensitometer, indicating that the amount of iron in the wear debris was considerably less than 1%. Thus the wear of the steel was extremely low, even when the wear of the electrographite was in the severe region. Monitoring of the contact potential waveform revealed, not unexpectedly, that the contact asperities upon the hardened and annealed steel disks were making repeated contact with the brush indicating that the stresses in these contact asperities were below the elastic limit of the steel.

The similarities in the wear rates at loads below the transition load on aluminium and steel and for copper (no transition) suggests that in this region the hardness of the underlying metal had only a minimal effect, although for these three materials the wear rate decreased slightly with increasing hardness. The narrow range of values of transition load, 160g.f - 460g.f. for a wide range of material hardnesses, 20-580VPN, and the transition from mild to severe wear on annealed steels at a lower load than on the much softer aluminium also suggests that the hardness of the metal could not have had a direct influence upon the wear transition.

This is further supported by the fact that although the stresses on the copper and steel disks stayed below the elastic limits of the metals a transition occurred upon the steel but not upon the softer copper.

The results discussed here have shown that there is a very strong connection between mechanical disruption of the metal oxide and the transition from mild wear to severe wear, and this oxide disruption rather than the material hardness would appear to be the prime factor in determining the wear behaviour. Consider now why mechanical disruption of the oxide films on aluminium and steel occur at relatively low brush loads, between 160gf and 460gf, whilst the oxide upon copper remains undisrupted up to a load of 1060gf even though a reduction in oxide film thickness takes place. An examination of the mechanisms of oxide formation and the crystallography of the oxide films reveals a possible explanation of these occurences.

The initial stage in the oxidation of metals is the formation of a physisorbed monolayer of oxygen molecules on the surface of the metal. These molecules are held onto the metal by weak Van der Waals forces (0.05 eV). However, after dissociation of the oxygen molecules the atomic oxygen is chemisorbed onto the surface with much stronger binding forces (1-8eV). Growth of the oxide film takes place by movement of either the metal ions or oxygen ions through the film, the rates of oxidation being dependent upon the temperature and oxygen pressure (45).

Measurement of the thickness of oxide layers on copper sliding against graphite brushes (22)has shown that the thickness varies between 10Å to 60Å. The measurement of contact resistance and applied potential described in Chapter 4 indicate that at a brush load of 60gf the thickness

of the oxide on the aluminium disk was approximately 40Å, assuming that electrical breakdown of the oxide occurs when an electric field of 2×10^8 volts)/metre is exceeded. This value of oxide thickness is consistent with values obtained for the equilibrium film thickness obtained in static oxidation experiments and indicates that light loads have very little effect upon the aluminium oxide film thickness (45).

These results indicate that the oxide layers formed during the sliding experiments were less than 100Å thick and we will therefore only consider the growth and structure of thin oxide films. The lowest energy state of an oxide will be when the oxide exists in its undeformed bulk form. However, when a thin oxide film grows upon the surface of a metal its structure will be influenced by the forces at the interface between the metal and oxide.

Experiments have been carried out by Mehl, McCandless and Rhines (46) in which they studied the formation of thin cuprous oxide films upon single crystals of copper. They found that the cube axes of the oxide lattice and the cube axes of the parent metal lattice were parallel. The oxide film was formed simply by an expansion of the lattice of the atomic copper in the metal to the copper ion lattice in the oxide without a change in orientation. The lattice parameters of the metallic copper and the copper ions in the oxide being 3.61Å and 4.26Å respectively. Similar work carried out by Bardolle and Bernard (47) and by Mehl et al (46) has shown that a similar orientation relationship exists for the oxidation of iron. The oxide grows on the parent metal with a crystallographic orientation such that oxidation can occur simply by an expansion of the metal lattice to that of the oxide.

These findings show that the metallic ions try to maintain the crystal structure of the metal within the oxide. This original structure can however only be continued into the oxide if its unit cell is

distorted, since the lattice parameters of most oxides differ from those of the parent metal lattice. Mehl, et al (46) have found that thin oxide films grown upon copper do in fact suffer such distortions.

A mathematical model proposed by Frank and Van der Merwe (48) to explain the formation of dislocation has also been suggested by Cabrarra and Mott (49) to explain the growth of thin oxide films. This theory shows that if the mismatch between the lattice of the metal and the lattice of the metallic ions within the oxide is below a certain value then the oxide will grow with the lattice spacing of the underlying metal. The amount of permissible mismatch varies from metal to metal but is normally between 9 - 15%. The oxide film produced under these conditions is deformed and will not be in its lowest energy state, although it will be in the thermodynamic equilibrium.

The theory of Frank and Van der Merwe is restricted to the formation of thin films since as the oxide thickness increases the strain within the oxide also increases until at a critical thickness the pseudomorphic film recrystallises to the structure and parameters of the bulk oxide. The thickness at which recrystallisation occurs depends upon the initial stresses in the oxide at the interface. At the point where recrystallisation of the oxide occurs flaws must develop to account for the mismatch with a consequent weakening of the oxide at this point.

It has thus been shown, both theoretically and experimentally, that thin oxide layers formed upon the surfaces of metals can grow with a deformed, highly strained lattice. However, the oxides growing upon real surfaces, these formed by engineering methods, will also contain cracks, dislocations and pores within their structures.

Kubachewski and Hopkins (50) suggest that the ratio of the unit

cell in the oxide to the volume of the unit cell in the metal may give an estimate of the stresses set up within the oxide. The stresses set up as a result of the difference in unit cell volumes will increase as the film thickness increases and may eventually overcome the attractive forces at the interface, rather than relieve the stresses by recrystallisation. Whether or not this happens will depend upon the relative strengths of the forces at the interface and within the oxide and the magnitude of the lateral stresses within the oxide.

Evans (51) has used wedge shaped oxide films to show that the stresses set up in NiO increase as the oxide film thickness increases, and confirmation that the stresses set up in the oxide film do depend upon the ratio of volume of oxide lattice to metal lattice has been obtained by Dankov and Churaev(52). They measured the bending of thin mica strips coated one side only by a thin metal layer, as the metal oxidised. In the case of iron and nickel, both of which have volume ratios greater than unity, the strips bent with the oxide film on the convex side. In the case of magnesium, which has a volume ratio less than unity (0.81), the oxide film was on the concave side of the strip.

The strength with which the oxide film adheres to the parent metal will obviously depend upon the amount of mismatch between the lattices since a highly strained film will attempt to relieve the stresses by detaching itself from the metal. According to Evans (51) however, the effect that the compression of the oxide has upon the breakup of the film will also depend upon the forces between particles within the oxide. When these cohesive forces within the oxide are high and the adhesive forces between the oxide and metal are low the strain at the interface is relieved by mechanical failure at the interface, causing the oxide to blister way from the metal underneath. If the cohesive forces are low

but the adhesion high, strain relief will occur by cracking of the oxide without detachment from the underlying metal. When the volume ratio of the lattices is only slightly above or below, unity, the lateral stresses in the oxide will be small and will have little effect upon the metal to oxide binding.

The first oxide layer to form upon a copper surface is cuprous oxide. However, as the film thickens, cupric oxide may also be formed.

The nature of oxide formed upon steel is more complex and it was difficult to determine which oxides were most prominent upon the dish surfaces since x-ray diffraction revealed lines from both FeO and Fe_2O_3. However, the volume ratio of the copper oxide to copper lattices is considerably less than the ratios for either of the iron oxides, therefore, one would expect the lateral stresses at the iron-iron oxide interface to be more disruptive than the lateral stresses at the copper-cuprous oxide interface. This has been confirmed by Baukloh and Thiel (53) who found that during oxidation experiments blistering of iron oxide away from the parent metal occurred, but no blistering of the oxide occurred on copper when oxidised under the same conditions.

It would thus appear that the internal lateral stresses formed by the mismatch of the metal-metal oxide lattices are greater for iron than for copper and that iron oxide can be more easily detached from the metal than can copper oxide. Thus internal stresses will assist any external stresses, as produced during sliding, in shearing the oxide away from the underlying metal. Failure will occur with a lower external shearing force upon iron than upon copper, hence mechanical failure of the oxide

upon the steel disks will take place at a relatively low brush load compared with the load required upon copper.

The internal stresses set up within the pseudomorphic oxide film increase with increasing film thickness until a point is reached when the oxide can no longer support these stresses, and recrystallisation of the thin film to the structure of the bulk oxide occurs at this thickness. When recrystallisation takes place flaws and dislocations must be formed within the oxide to compensate for the change in structure and these will weaken the film considerably. In a sliding contact the thickness of the oxide will depend upon the depth at which recrystallisation takes place. During sliding contact the internal stresses will be reinforced by external stress arising from the applied load and frictional force. The internal stress increases with increasing film thickness and the stress which the oxide can withstand before recrystallisation occurs will be reduced, resulting in lower film thicknesses, as these external forces are increased. Thus the thickness of the oxide film on the metal should decrease with increasing applied load.

Measurement of the contact resistance and applied potential has shown that such a reduction in oxide film thickness apparently occurred with applied load when brushes were run upon copper disks. However, when running upon steel disks this effect was not noticeable, due in part to the irregular behaviour of the contact resistance. It is also possible that mechanical rupture of the oxide away from the metal occurs at a load loo low to affect the recrystallisation depth due to the cohesion within the oxide being greater than its adhesion.

The initial oxide film growing upon aluminium has an amorphous structure (40) and consists of clusters of Al_2O_3 molecules (54). After a high initial oxidation rate the film virtually stops growing when it has reached a limiting thickness of about 45Å (55). Cabrarra and Mott have suggested that aluminium oxide grows in this amorphous state because the initial mismatch between the lattices is too great to support the growth of a pseudomorphic film. Thus the oxide grows with an energy state less than that of the pseudomorphic structure but higher than for the bulk undeformed oxide. Aluminium oxide is a very strong, hard material and examples of its use are as abrasive materials and filament holders for electron microscopes, thus the cohesive forces within the oxide must be very high and the oxide is not easily deformed. Any stresses set up at the aluminium-aluminium oxide interface will therefore be relived by the oxide separating from the metal, rather than cracking of the oxide. If at the wear rate transition load the elastic limit of the aluminium is reached, as is indicated by the results, then severe deformation of the aluminium at the interface must occur. This deformation of the aluminium stresses the interface between the aluminium and oxide and these stresses are relieved by the oxide film detaching itself completely from the metal at this point.

When sliding electrographite brushes upon aluminium a transition from mild wear to a more severe wear occurs when the brittle aluminium oxide was mechanically disrupted due to the stresses in the aluminium exceeding its elastic limit. No such transition took place when electrographite was run upon copper since the elastic limit of the metal was not exceeded and the oxide film remained undisrupted. As the brush load was increased the thickness of the oxide film decreased because recrystallisation of the pseudomorphic oxide occurred nearer to the copper-cuprous oxide interface.

However, due to the small mismatch between the metal and oxide lattices the stresses produced during sliding did not completely remove the oxide from the copper at the loads considered.

The elastic limit of the EN26 steel was not reached during running but the results showed that mechanical disruption of the oxide and a wear transition still occurred. The larger lattice mismatch between the iron and its oxide results in high stress at the interface. Disruption of the oxide occurs when the externally applied forces result in the stresses at iron-iron oxide boundary becoming too great for the adhesive forces to resist. The hardness of the metal appears to have some effect upon the value of the transition load. Whilst it is unlikely that the hardness of the steel will affect either the cohesive forces within the oxide or the forces of adhesion between the steel and oxide, it is possible that the hardness of the steel may have an effect upon any stresses produced at the interface due to movement or creep of the metal. This could explain the low breakdown load when running upon a newly-prepared annealed steel disk. Stresses must be set in the steel surface during machining and these would be relieved slowly with time due to creep of the steel. This movement would, however, impose an additional strain at the oxide boundary and reduce the transition load. When the disk was left for some time after machining all these additional stresses due to machining would have been relieved by thermally activated movement.

We can thus see that the apparently irregular behaviour of the wear rate transition loads can be explained in terms of the mechanisms involved in the formation and breakdown of the oxides of metals involved. We now have to consider why mechanical disruption of the oxide films result in a marked increase in the wear rate of the electrographite.

6.2 Possible Wear Mechanisms

A number of authors (19), (42) and carbon brush technologists have suggested that aluminium would be totally unsuitable as a sliding contact due to the formation of hard, abrasive aluminium oxide or carbide particles. The results discussed here suggested that under the slip ring conditions investigated, abrasion did not play an important role in the wear mechanism. Even in the severe wear regime very little aluminium oxide or carbide was present and it was not until catastrophic wear of the brush occurred, produced by sparking at the interface, that any significant amounts of these compounds were detected. It is proposed that fatigue and adhesive wear mechanisms were far more important than abrasive wear under the majority of conditions investigated, even when running upon aluminium.

Adhesion between two sliding surfaces arises from the forces of attraction which exist between the atoms of the two materials at the sliding contact interface. When the two surfaces are sliding together these adhesive forces can transfer material from one surface to the other. When shear takes place (as it must if motion is to be maintained) it can occur either at the newly formed adhesive junction, in which case no wear fragment will be formed; or within one of the contacting materials, normally the weaker, in which case a wear fragment will be produced. The newly formed wear particle can either remain attached to the other sliding surface in which case back transfer is possible, or it can be lost completely from the system. Thus it can be seen that adhesive wear will be a complex two-way process. The two surfaces will be in a state of dynamic equilibrium where wear fragments from both surfaces may be transferred, back transferred and eventually lost from the system.

As well as this adhesive wear there will also be a fatigue wear

mechanism taking place where cyclic stressing of the two interfaces may result in a wear particle detaching itself without necessarily transference. Which of these two wear mechanisms predominates will depend upon the magnitude of the adhesive forces at the interface and the strength of the underlying material. The forces of adhesion are produced by Van der Waal type forces at the interface, or by valency bonding.

When the electrographite was sliding under mild wear conditions contact was being made between the surface of the bursh and a mechanically undisrupted oxide film covering the surface of the metal disk. This picture is obviously over simplified, since some penetration of the oxide must have occurred. However, we shall consider that for the most part brush contact was made through the oxide film which prevented adhesion between the metal and electrographite. This would seem a reasonable assumption, since the contact resistance behaviour when running under mild wear conditions suggested the presence of such a film.

After the system had been completely run in both the brush and disk appeared very highly polished when viewed with the naked eye, or with an optical microscope. Scanning electron microscopy of the aluminium, copper and steel surfaces, produced by mild wear, revealed that the running tracks on the metals contained isolated islands or narrow bands of transferred electrographite. Although these very smooth areas of graphite covered a relatively small fraction of the possible contact area they were close enough together to form the main load bearing areas during contact. Scanning electron microscopy also revealed that the brush surface did not simply become polished, but was completely covered by an extremely smooth, compacted graphite film. This film had an appearance quite different from the bulk brush material and covered the whole brush surface, even the porous regions. The separate identity of this film

is shown clearly in the micrographs shown in Figures 4.27, 4.28 and 4.36. Sliding therefore occurred between the very smooth film laid on the brush and either the smooth areas of transferred graphite on the disk or the smooth oxide covered polished metal. Under the conditions abrasive wear of the surfaces was negligible and the main wear mechanisms were by fatigue or adhesion. However, several factors pointed towards fatigue, rather than adhesion being the principal mechanism during mild wear.

The shear forcesbetween the two sliding surfaces arose from either graphite to graphite adhesion, when the brush was in contact with the transferred graphite; or from graphite to metal oxide adhesion. The valency bond between carbon atoms is extremely strong under normal circumstances and the bonds from unpaired atoms at the crystallite edges would contribute to adhesion. However, the lubricating properties of graphite have been attributed to saturation of any excess bonds by adsorbed oxygen or water molecules (4),(5). The adhesion of graphite crystallites arose therefore from weak Van der Waals forces between basal planes or between the adsorbed molecules at the crystallite edges. Similarly, when the brush was in contact with the metal oxide the adhesive forces were derived from weak Van der Waal interactions. Atmospheric gases are rapidly chemisorbed onto the surface of oxides (56) and this adsorbed molecular layer would have reduced even further adhesion between the oxide and graphite.

When an adhesive contact has been made shear will normally occur along the weakest path available. The compressive shear strengths of the metal oxides concerned were considerably greater than the shear strengths of the parent metals (57),(58) and fracture zones were unlikely to occur within the oxide unless the recrystallisation thickness had been reached. The weakest possible fracture surface on the disk surface was

the interface between the metal and metal oxide, but shear along this junction did not occur until the transition loads upon aluminium and steel were reached. The appearance of the surface suggested that once the film had been formed upon the brush the cohesive forces holding it together were high (using the same criterion applied by Evans to oxidation), and it was unlikely that the bonds holding the film together, or to the bulk brush materials, were weaker than the adhesive forces between the sliding interface.

Thus it would appear that shear occurred mainly at the newly formed adhesive junction, without the formation of a wear fragment. However, a certain number of fracture surfaces must be produced within both the metal and electrographite. The presence of transferred graphite on the disk surfaces shows that adhesion resulted in some shear within the brush material. Electron probe microanalysis of the brush running surface and X-ray diffraction of the wear debris showed that in the mild wear regime wear of the disk metals was also occurring, even when sliding upon hardened EN26 steel. The presence of transferred metal on the brush film suggested that some isolated shear within the metals also occurred.

Whilst adhesive wear must inevitably take place it would appear to play a relatively minor role in the mild wear process, the predominant mechanism being that of fatigue wear. At the contact asperities the two surfaces were subjected to both compressive and tensile stressed and this cyclic stressing eventually resulted in failure within the surfaces at stress levels much lower than could normally be withstood in purely tensile compressive loading. Evidence suggesting that a fatigue type failure occurs for graphite at stresses within the elastic limit has been reported by Lancaster (32).

The scanning electron micrographs from the brush surfaces show that

fatigue was a very important mode of failure when brushes were operating in the mild wear regime. Cracking, blistering and flaking of the surface film suggested that once the film had been formed cyclic stresses were transmitted by the surface film into the bulk material underneath. At first sight it would appear doubtful whether these stresses could be supported by the film without failure, since the graphite film must have been formed from degraded bulk brush material, produced in the first instance possibly by abrasive wear, and would be expected to contain many flaws and cracks which would act as ideal points for the initiation of fatigue cracks. However, reflection electron microscopy has shown that the surface of the brush consisted of highly oriented crystallites. The basal planes of the crystallites were parallel to each other and inclined at angles from 22° to 7° to the running plane. Thus when compaction of the film occurred the crystallites orientation was such that a high density of packing was achieved, the relationship between the frictional coefficient (μ) and the basal plane inclination (δ) was such that the resultant force on the crystallites within the film was normal to the basal planes, and the stress could be transmitted by elastic deformation into the bulk material beneath.

Clark and Lancaster(33) have shown that failure of rubbed carbons occurs in a cyclic manner, the length of the cycle depending upon the stress at the contact. Initially the contacting surfaces became polished, followed by blistering and break up of this polished layer and an increase in the rate of wear. The cycle then repeated. The phenomena described by Clark and Lancaster involved the breakdown of the whole contact area. There was no evidence, from either wear rate measurement or physical analysis of the surfaces to suggest that such a cyclic process was taking place over the whole brush face . The scanning electron micrographs shown

in Chapter 4 revealed however that a similar fatigue mechanism may have been taking place continuously over small areas of the brush face. The continual presence of the compacted film on the brush face requires a fatigue mechanism whereby wear of the underlying brush material can occur without complete disruption of the brush surface.

The scanning electron micrographs suggest that in the mild wear regime the following wear mechanism was occurring. Cyclic stressing of the interface resulted in fatigue failure of small areas of the bulk brush material below the surface film, due to the stresses being transmitted elastically through the film into the supporting brush material. This failure enabled the film to crack, blister and eventually break away from the surface. Upon the surface of a single brush were areas which may have been in various stages of such a fatigue process. Cyclic stressing of the brush material resulted in lateral and longitudinal cracking of the surface film, Figures 4.27(b) and 4.27(c) show the onset of such cracks upon a brush run upon aluminium. Similar surface details have been found on the surfaces brushes run upon steel, gold and copper in the mild wear regimes. Propagation of the cracks through the surface resulted in complete detachment of the film from the underlying material, shown in Figure 4.28, and eventual breakdown and degradation of the failed area (Figure 4.27(d). Once failure had occurred this region ceased to be a major load bearing area and cyclic stressing was transferred to another small area of the brush face.

The newly formed cavity, deeper than the surrounding film thickness, then became the source for collection of degraded electrographite either from the disk surface or other areas of the brush face, and the surface film began to reform. Fatigue failure of the surrounding film was occurring continually until this region once again became a major load

bearing area.

Since adhesion between the two surfaces played a minor role in the mild wear process the difference in the metal surfaces had little effect upon wear rate. The forces of adhesion between graphite sliding upon aluminium oxide, copper oxide and iron oxide, covered by adsorbed layer, will be comparable with each other. The magnitude of the cyclic stress will depend only upon the applied brush load. Thus we would expect wear rate to be strongly dependent upon applied load, since an increase in stress reduces the number of cycles to failure. The results showed that in the mild wear regime the wear rate was proportional to the applied load but depended very little upon the disk material.

Thus it would appear that wear of the electrographite in the mild wear regime was a combination of adhesive wear and fatigue wear; the adhesive wear playing a minor role. Wear of the disk material was very small and the presence of metallic particles upon the brush surface suggested an adhesive wear mechanism. Under these circumstances the ratios of the wear rates of the metals should be inversely dependent upon the ratios of their surface energies (59). The surface energies of aluminium, copper and iron and estimated by Rabinowicz (60) to be 900, 1100 and 1700 erg/cm^2 respectively. Whilst no information could be obtained on the surface energies of the hardened or annealed EN26 disks it is reasonable to assume that they are as large, if not considerably greater than, for pure iron. The x-ray powder analysis of the wear debris does show some correlation with the expected behaviour. The percentages of aluminium and copper in the wear debris by within the range 2-6% for both materials, whilst the amount of steel present was estimated at less than 1%, maybe as low as 0.1% . Unfortunately an accurate estimation of the amounts of metal in the debris was not possible and the values of surface energy

must be in some doubt also. However, these results show an interesting trend and are worth further investigation in more detail.

It has been shown that when a critical load was applied to the brush, mechanical disruption of the oxides upon the aluminium and steel occurred, producing a marked increase in the brush wear rate. The removal of the protective oxide barrier from the contact asperities enabled adhesion between the electrographite and metal to occur. The effect of this increased adhesion can be clearly detected by optical and scanning electron microscopy of the worn surfaces. At loads above the transition load the worn surfaces of the aluminium and EN26 steel disks were almost completely covered by a film of transferred graphite. The increased adhesion when sliding upon the exposed metal can be explained in terms of tribological compatibility and increased chemical reactivity.

If the compatibility criteria of Rabinowicz (59) is extended to include carbons and graphites, and there would appear to be no reason why this cannot be done, then a satisfactory explanation is possible for the increased wear rate when sliding upon steel. When two compatible metals are slid together the adhesion is high and the wear rate is also high. When two incompatible metals are slid together the adhesion and wear are low. The compatibility of metals is judged by the degree of mutual solubility that the metals exhibit. On this assumption similar metals sliding together make poor tribological pairs. When a large number of metal pairs are considered (60) this compatibility criteria has been shown to have some degree of reliability in predicting tribological performance. However, it cannot be rigidly applied to every case since many anomalous results have been obtained.

When carbon is sliding upon unprotected iron or steel we would expect high adhesive wear since the two materials are very compatible. The body centred cubic structure of iron readily accepts carbon atoms into the interstital sites, producing high mutual solubility. The high degree of compatibility produces large adhesive forces at the interface. Sheer does not now readily occur at the newly formed junction but takes place within either the carbon or steel surfaces, with the production of an adhesive wear fragment. Due to its high surface energy the probability of sheer occurring within the steel was small. However, the presence of minute traces of steel in the wear debris and upon the brush surface showed that this probability had a finite value.

However, when the carbon-aluminium sliding system is considered it is more difficult to explain the increased adhesion in terms of compatibility. The face centred cubic aluminium structure does not readily accept carbon into the interstitial sites and the mutual solubility is small. There will, however, be an increase in chemical reactivity when contact is made with the unprotected aluminium instead of the chemically inert aluminium oxide. Mutual solubility and chemical reactivity between the materials must play an important role in the high adhesive wear since some investigators into the use of aluminium alloys as commutator materials have experienced "welding" of the graphite brush to the commuator under static conditions (61). The increased adhesion may, however, arise from a mechanical origin, rather than from physical or chemical interactions. Above the transition load the aluminium surface was undergoing plastic deformation and it is possible that under these conditions more intimate contact was being made between the aluminium and graphite, producing greater adhesive bonding. Ploughing and mechanical interlocking of the two materials

was also possible under plastic deformation conditions.

Physical analysis of the worn surfaces produced during sliding provided further evidence of a change from fatigue wear to adhesive wear at the transition load. Reflection electron diffraction of the disk and brush surfaces revealed that the transferred graphite on the disk and the graphite at the running face of the brush exhibited a high degree of preferred orientation. A summary of these results is shown in Table 4.12 and it may been seen that the angle of inclination of the crystallite basal planes was 7°-8°, for surfaces formed under loads above and below the transition load. This similarity of tilt angles in the mild wear and severe wear regions eliminates change in crystallite orientation as a possible cause of the wear transition.

The most obvious difference between the surfaces produced in the two wear regimes was the marked increase in the amount of graphite transferred to the aluminium and steel surfaces when the transition load was exceeded. This macroscopic change was a clear indication of the increased adhesion between the disk surface and the electrographite. Scanning electron microscopy however revealed further difference, on a microscopic scale, between the mild and severe wear surfaces.

Provided that catastrophic wear of the brushes did not occur the surfaces formed upon the aluminium and steel were very similar. Scanning electron micrographs of typical areas of the wear tracks produced upon aluminium in the mild wear regime (60g.f. load, no current) are shown in Figures 4.24 (a),(b) and (c). A comparison of these micrographs with those from surfaces formed under severe wear conditions, Figures 4.25(a), (b),(c),(d),(e) and (f) reveals slight but significant changes in the

nature of the transferred graphite. Below the transition load the wear tracks upon the aluminium and steel disks consisted of isolated islands and narrow bands of smooth transferred graphite. These areas of transferred graphite showed typical fatigue characteristics of cracking and blistering in certain regions. The nature of the disk topography suggested that the graphite was undergoing a process of transference, consolidation and orientation collowed by cyclic stressing which resulted in eventual failure of the graphite and the formation of a wear particle. At loads above the transition load the topography of the transferred graphite varied widely from area to area upon the same wear track and also from load to load. The wide variation made it impossible to select any one surface as being typical of severe wear. The topography of the graphite ranged from being extremely uneven with a flaking, layered structure, to very smooth with tiny areas of the film apparently ripped from the surface. The topography of the graphite laid down under a load of 1060 g.f. was extremely smooth with some areas overlaid by islands of much rougher transferred graphite. Although it was not possible to obtain one surface typical of severe wear, suggesting rapidly changing topographies, it was significant that there was an absence of fatigue characteristics upon the surfaces formed in the severe wear regime, suggesting that another wear mechanism was dominant.

The difference between the disk surfaces formed in the two wear regimes is shown more clearly by a comparison of surfaces formed upon copper under mild wear conditions at a load of 460 g.f.(Figures 5.5(b) and 5.5(b)) with those formed under the same load upon aluminium and steel in the severe wear regime. The effect of cyclic stressing of the transferred graphite on the copper is revealed in the form of longitudinal and lateral cracking of the surface prior to complete fracture. This type of cracking is a common feature upon the surface of metals undergoing mild fatigue wear (62).

Much more convincing evidence of a change from fatigue wear of the brush to adhesive wear was obtained from a microscopic examination of the brush surface. When sliding under mild wear conditions upon metals the running face of the brush became overlaid by a smooth film of degraded brush material which reflection electron diffraction has shown to be highly oriented. Scanning electron microscopy suggested that this film was able to support the applied load and that fatigue breakdown of the film as a result of cyclic stressing played the major role in the brush wear mechanism.

The surfaces formed during severe wear sliding exhibited neither the formation of a surface film nor fatigue cracking of the surface. A detailed examination of the subsurface structure showed that the bulk brush material, consisting of carbon grains about 2 μ diameter, continued right up to the sliding interface. Some degradation of the carbon at the interface must have occurred however to give the brush surface its polished appearance. Reflection electron diffraction revealed that orientation of the graphite crystallites occurred even in the severe wear regime, and assuming a penetration depth of 2 μ for the electrons (63) this corresponds to diffraction from a surface layer about 100Å thick, which is below the resolution of the microscope. Some orientation of the wear derbis packed into the brush faces could also have occurred. Thus a very thin film may have been formed upon the surface but it is doubtful whether such a thin film could effectively have acted as a separate load bearing structure independent of the brush substrate.

No fatigue cracking of the severe wear surface occurred, the most

common irregularity being shallow holes in the smooth brush surface, such as shown in Figures 4.29 and 4.32. The absence of any fatigue type cracks and the presence of such holes suggest a wear mechanism involving the removal of graphite material without the necessity of prior fatigue failure. Such a process could be that of adhesive wear. The smoothness of the brush surface suggeststhat wear above the transition load was by a more continuous process than in the mild wear regime, involving the removal and re-distribution of small particles from the brush surface as well as the production of the large wear fragments.

Two more systems now need brief disucssion, the sliding of an electrographite brush upon a gold disk and the sliding of an electrographite brush upon an electrographite disk. The experiments upon these materials were performed to clarify points arising during sliding upon other metals, mainly concerned with friction. As a result their contribution to the investigation into wear was extremely limited.

Gold was chosen as one contact material because the absence of oxide upon the surface ensured that contact was always between the electrographite and the unprotected metal, conditions which led to severe adhesive wear upon aluminium and steel. However, in spite of this lack of oxide the wear rate of the electrographite was very low; $2.0 \times 10^{-10} mm^3/(mm\ sliding)$ at 260gf load and $4.4 \times 10^{-10} mm^3/(mm\ sliding)$ at 1060gf load, thus the electrographite was undoubtedly undergoing a mild form of wear. These wear rates were lower than upon other metals in the mild wear regime at the same load, which was rather surprising since the hardness and surface finish of the gold were comparable to those of the copper disks, therefore the fatigue

stresses and wear rates should have been of the same magnitude. The surface of the worn brush was typical of one formed under mild wear conditions, a smooth compacted graphite film with fatigue type cracking and failure. One noticeable feature of this sliding system was, however, the complete absence of any adhered graphite film transferred to the gold surface. This was an extremely important absence since it indicated that there was little or no adhesion between the electrographite and unprotected gold. This was not a surprising result since gold is chemically very unreactive and the solubility of the two materials is low. No reaction, physical or chemical occurred even when gold and electrographite were kept in contact for some considerably time at the melting point of gold. Even though gold is chemically inert this incompatability does not extend to all sliding systems. For instance, adhesion between gold and copper readily occurs, with a transference of gold (64) and since these two materials are very soluble the compatability criteria is supported in this instance.

The low adhesion between the gold and graphite resulted in the adhesive component of the wear process being much lower than on other metals, the wear of the brushes being due almost entirely to the fatigue wear component. The difference between the wear rates on gold and the wear rates on less inert metals at the same load illustrates to some extent the relative importance of adhesive wear in the two wear regimes.

The wear rate of an electrographite brush when sliding upon an electrographite disk was also extremely low. In this case, however, the topography of the two sliding surfaces did not show the typical fatigue wear characteristics. No surface film was formed upon either

the disk wear track or the brush running face. Both surfaces became highly polished but retained their porous structures, the surfaces having an appearance very similar to metallurgically polished specimens. The appearance of these surfaces suggested that they could be in the initial stages of the fatigue type failure cycle proposed by Clark and Lancaster (33) for rubbed electrographites. The loads used by Clark and Lancaster were much greater than applied to the brush here, 2.4 kg.f/mm^2 compared with 0.04 kg.f/mm^2. With the greatly reduced load it was possible that the length of the initial failure cycle had been considerably extended and that no surface degradation had occurred to produce the surface film.

These short experiments were originally instigated to investigate the proposal by Lancaster (26) that the adhesion between graphite sliding upon graphite was greater than the adhesion between graphite and metal surfaces.

However, since degraded films were not formed upon the surfaces any direct comparison is bound to be somewhat unrealistic and the results incomparable rather unrealistic, however, both the wear rate and friction of the apparently undegraded electrographite were much smaller than upon metal surfaces.

An extension of the Rabinowitcz compatability criteria (59) to include graphite sliding upon graphite would require the adhesion between the similar materials to be high. The high carbon-carbon bond would satisfy this requirement if saturation of unpaired bonds did not occur, however, the interfacial layer of the adsorbed molecules reduced the adhesive forces between the two surfaces to very small values. The lack of adhesion between the two surfaces was further indicated by

the absence of any material transferred from one surface to another. It would thus appear that wear of electrographite sliding upon a similar material occurs by the fatigue mechanism proposed by Clark and Lancaster (33).

The effect of electric current upon the wear rate of electrographite sliding upon metals, other than aluminium, has been investigated by a number of authors and no further detailed investigation was carried out. Electric current has been found to have a very varied effect upon the wear rate of the carbon brush and polarity effects have been observed by a number of authors (36), (20), (65), and several hypotheses have been proposed to explain these polarity effects. In general however the effect of electric current has been found to be strongly dependent upon the two contacting materials used, the wear machine and the conditions of operation (19), (26), (31), (42).

Electric current had little effect upon the brush wear rate when running on aluminium unless sparking occurred beneath the brush, resulting in catastrophic failure of the brush. When sliding in the mild wear regime at a load of 60 g.f. the wear rate of the negative brush increased by a factor of two when a current of 1.0 amps was passed through the brush. The wear rates when passing current were not, however, measured for long periods of running, and in view of some of the large fluctuations in wear rates, little significance can be attached to this result. No effect of electric current on wear rate was detected at any other load until catastrophic wear conditions were attained.

The onset of catastrophic failure produced an increase in brush wear of a factor of 10^2 to 10^3 times and the rate of wear of the aluminium, obtained from X-ray analysis of the wear debris, also increased dramatically.

Associated with catastrophic failure of the brushes on aluminium were, an increased temperature of running of the brush, indicating a large increase in interfacial temperature; very large fluctuations in frictional force (increasing by as much as factors of five for very short periods); and the presence of aluminium oxide and aluminium carbide in the wear debris.

Scanning electron microscopy of the brush and disk surfaces produced during catastrophic failure showed topographies which indicated that a wear mechanism other than fatigue or adhesion was of major importance. The surface of the brush was completely different from brush surfaces formed in either the mild wear or severe wear regimes. No compacted surface film was formed in the brush, which retained its open, porous structure, and very little polishing of the contacting regions occurred. The brush had a heavily scored, etched, or eroded, appearance, shown in Figure 4.33(c). The surface produced on the aluminium was also very different from in the two other regimes. The amount of transferred graphite adhering to the aluminium was small and the aluminium surface had a very rough, dull grey appearance. Scanning electron microscopy showed little evidence of the formation of any transferred graphite film, most of the adhered graphite being in the form of separate particles. The surface of the aluminium was very heavily deformed and Figures 4.33(a) and (b) show features consistent with very high temperatures and softening, or possibly

melting of the aluminium surface. Further evidence to support softening of the aluminium was the formation, in some instances, of tiny slivers of aluminium (similar to lathe turnings) by the leading edge of the brush.

It would appear that wear takes place under catastrophic conditions by several mechanisms, initiated by the high temperatures produced at the interface. Electrical erosion of the brush occurred and it is probable that temperatures high enough to oxidise the carbon material were also reached (17). The presence of heavy scoring on both the brush and disk suggests that wear of both surfaces by an abrasive mechanism was also occurring, caused by large particles of aluminium oxide and aluminium carbide trapped between the two surfaces. Although the mechanisms of erosion and oxidation, and abrasion predominate it was possible that increased adhesive wear also occurred. Higher adhesive forces would arise from increased reactivity between the two surfaces and possibly from increased areas of contact caused by softening of the aluminium.

The large fluctuations in frictional force during catastrophic wear were probably caused by large particles of aluminium oxide or aluminium carbide embedded in the brush surface producing very high ploughing frictional forces.

6.3 The Frictional Force of Electrographite.

The results quoted in Chapters 4 and 5 revealed two main frictional characteristics requiring discussion. These were the reduction in frictional force with increasing electric current upon metals and the increase in friction with running time.

Figures 4.11 and 4.12 show how the coefficient of friction varied with electric current on aluminium at a load of 60gf. When a relatively small current was passed through the brush a significant decrease in friction occurred and increasing the current produced further decreases in friction. Similar behaviour was found at other loads on aluminium, and on other metals when sliding in the mild wear regime. In general, the higher the load the greater the elecric current required to initiate the decrease in friction. When operating in the severe wear regime it was necessary to pass currents of the order of 1-5 amps to produce a fall in friction as opposed to currents of 30 to 100mA. in the mild wear regime.

Several theories have been proposed to explain this decrease in friction with electric current, the most notable being those of Holm (18), and Lancaster and Stanley (17). The proposal by Holm was that the frictional force was controlled by the specific force of friction between contacting graphite platelets. Holm proposed that this specific force of friction was temperature dependent and decreased as the temperature increased. However, the theory of Holm cannot be used to explain the results described here, as shown below.

Since the specific force of friction was, according to Holm, dependent only upon the temperature of the contact, the process must be reversible. A decrease in temperature should therefore produce an increase in friction. Hence a reduction in current should result in an increase in frictional force back to its original value almost instantaneously. This

did not occur. Figure 4.10 shows that the decrease in friction began to take place as soon as the current was increased, the recovery back to its original high value, however, took a considerably longer time. If a reversible temperature change was responsible for the decrease in friction it would be expected that the recovery of the friction would be dependent upon the rate of cooling of the graphite crystallites. This was not the case, the recovery of the friction was determined by the distance of sliding after the current was reduced, thus indicating that a permanent change in one or both surfaces was responsible for the frictional behaviour. Recovery necessitated sliding or surface wear to regain the original topography.

Consideration of the temperatures produced during sliding also pointed to a rejection of Holm's hypothesis. The variation in temperature at a point 0.5mm. below the running face when sliding on aluminium at a load of 60gf. is shown in Table 4.9. Although these temperatures do not represent the junction temperatures they give information about the behaviour of the interface since any rise in temperature of the junctions must be reflected in the bulk brush temperature. Table 4.9 shows that no increase in the brush temperature occurred when a current of 50mA. was passed through the brush even though a decrease in frictional force had taken place. The results indicated that the interface temperature and hence the measured temperature were dependent upon both the electric current and frictional force, rather than the temperature controlling the frictional coefficient. In some instances both the friction and temperature increased with time of running during the initial stages of sliding. This was contrary to Holm's hypothesis and no mechanism can be imagined which could have caused an increase in temperature with running time other than increased power dissipation due to higher friction. It was also possible that decreased power dissipation due to a reduction in frictional

force with current counteracted the Joule heating effect of the current and tended to maintain a constant temperature. The small increases in temperature associated with the passage of current certainly did not approach the increases in temperature required by the Holm theory to produce the substantial reduction in the specific force of friction necessary to cause the fall in friction.

Any mechanism proposed to explain the decrease in friction with electric current must be a non-reversible process requiring wear of the brush to return to the original state. Such a mechanism has been proposed by Lancaster and Stanley (17) based on oxidation of the brush material. They suggested that preferential oxidation of the brush binder occurred when a critical current was passed through the brush, resulting in a break-up of large contact areas into a number of smaller contacts with a smaller real area of contact and a reduction in friction. They also suggested that oxidation could only take place if a critical contact temperature was exceeded, this temperature for electrographite was in the range 900-1350 ^{o}C. It was very unlikely that temperatures as high as this were produced by the small currents causing a reduction in friction in the mild wear regime. There was, however, a possibility that temperatures in the lower end of this range were reached during arcing, or at the high currents necessary to produce the fall in friction in the severe wear regime, or on an electrographite disk.

Another argument for rejecting the Lancaster and Stanley hypothesis arose from consideration of the brush topography. The mechanism they proposed requires a brush contact surface composed of two types of carbon material, the non-graphitic binder and a graphitised phase. An examination of the brush running face has shown however that the surface was overlaid by a degraded carbon film, even when an elecric current was passing through the interface. If preferential oxidation of the brush

material had occurred due to the passage of current the degraded surface film could not have formed as a two-phase material but would have consisted only of the graphitised carbon, and the oxidation process would have ceased. Further reduction in friction with current could not have occurred until a two phase surface had reformed. The results showed,however, that the decrease in friction began immediatly the current was increased.

The results described in Chapters 4 and 5 suggest that changes taking place in the brush surface were responsible for the frictional characteristics, rather than changes in the metal surface. Contact potential waveform monitoring of the electrographite - aluminium interface showed that the shape of the waveform did not change when the current was increased even though the frictional force had decreased. Since the shape of the waveform was determined by the contact configuration of the metal surface, no change in the metal topography could have been occurring. A comparison of the results obtained on different metals also indicates that changes of the brush surface were responsible for the friction behaviour. Section 4.9 describes the frictional force characteristics on soft aluminium (hardness 20 VPN.) and a comparison of these results with those described in Chapter 5 for other materials of greater hardness shows that there was very little difference in the frictional behaviour over a wide range of hardnesses. The similarity in the results is very clear when a comparison is made of the friction on annealed and hardened EN26 steel disks shown in Tabes 5.6 and 5.7. The frictional force and its variation with currentwere identical on both the annealed (270 VPN.) and the hardened (550-580 VPN.) steels. It is very unlikely that the effect of electric current would have been the same on all these materials with such a wide range of surface characteristics and hardnesses. It would thus appear that the frictional behaviour was independent of the contact

metal, provided wear was taking place in the same wear regime. Whatever mechanism was responsible for the frictional characteristics it must have involved changes in the surface of the electrographite brush.

Investigations into the friction and wear of thin films of solid lubricants and soft metals on harder substrates have been carried out by a number of authors (66), (67) and (68). In general it has been found that the frictional force of the solid film varied with film thickness, the friction increasing with increasing film thickness. The low friction of such coatings has been explained by considering the simple relationship

$$f = s/p \qquad \text{- Bowden \& Tabor (66)}$$

where: f - is the coefficient of friction

p - is the flow pressure of the contacting material

s - is the shear strengh of the material at the interface.

For a thin film on a hard substrate "s" is determined by the shear srength of the soft film and "p" by the hardness of the substrate, leading to a low coefficient of friction. The increase in friction with increasing film thickness is caused by the stress bearing hard material being replaced by the softer film. Hence the flow pressure of the material adjacent to the interface (p) decreases, producing an increase in the coefficient of friction.

Rabinowicz (69) has developed a more complex model to explain variations in friction with film thickness and has been able to show some correlation between the predictions of this model and results obtained in practice.

Whitehouse, Nandan and Whitehurst (70) have carried out experiments on solid lubricant films, including graphite, over the thickness range 5×10^{-3}mm. to 20×10^{-3}mm. For molybdenum disulphide and calcium fluoride

microscopy, the examination showing that the thickness of the graphite film decreased with increasing electric current. The technique used to examine the film and measure its thickness was difficult and only a very small number of measurements could be made on each specimen. The results are therefore open to criticism on statistical grounds and also on the basis that it was difficult to judge the exact position of the interface between the film and bulk material in some instances. Even from this small number of specimens, however, it was apparent that a change in the nature of the film occurred with increasing current.

The specimens formed either without current,or with a small current of 1mA., exhibited typical mild wear surface characteristics. An apparently self-supporting graphite film covered the brush face and contained evidence of fatigue failure (Figures 4.28, 4.36 and 4.37). The thickness of this surface film was estimatad to be about 1μ m. However, when the current was increased to 500mA., there was a change in the specimen topography. Although the brush was still covered by a compacted graphite film, the instances of fatigue failure were greatly reduced and the brush film topography appeared to depend upon the underlying brush sructure more than at the lower currents. The thickness of the surface film had decreased from the no current value to a value of about 0.3-0.5μ m., and this decreasein thickness probably reduced the load bearing capacity of the film.

The surface formed at a load of 2.0 amps showed none of the topographical features associated with the films formed at lower currents. No surface film could be detected using scanning electron microscopy and the bulk brush material appeared to continue right up to the polished running face. Reflection electron diffraction revealed,however,that a very thin oriented surface layer was formed. This surfac layer could not, however, have been self-supporting and the load was carried almost

they found an increase in friction with film thickness, in agreement with other workers, although the theory of Rabinowicz could not fully explain the behaviour. The results obtained for the graphite film were much more complex and did not agree with the model. The authors did not attempt to explain this anomaly.

If the thin film of graphite formed upon the brush surface is considered to act as a thin film lubricant the variation in frictional force can be explained in terms of the formation of this film from the brush and the variation in film thickness. This hypothesis is based on the assumption that the film formed upon the brush is softer than the bulk brush material. Although this could not be confirmed, it is a reasonable assumption, since the brush film had been formed from degraded and compacted bulk material. The frictional results will be discussed in terms of this hypothesis in a qualitative manner only. No quantitative attempt will be made to correlate the observed frictional behaviour or the properties of the graphite film with the theory of Rabinowicz, since no information was available about the flow pressures of either the film or the bulk brush material or about the real area of contact.

Scanning electron microscopy of the brush surfaces formed on aluminium at a load of 60gf. revealed an explaination other than those of Holm or Lancaster and Stanley for the decrease in frictional coefficient with electric current, based upon the lubrication properties of thin films. When sliding at this load, the coefficient of friction was independent of electric current until a critical current of 30mA. was passed, when a decrease occurred. The frictional coefficient was reduced further as the current was increased, approaching the low value measured during the initial stages of sliding. A small number of brush surfaces formed at this load and various electric currents were studied by scanning electron

entirely by the bulk brush material.

The dependence of the frictional coefficient upon the thickness of the brush surface film can be explained qualitatively in terms of the theories of Bowden and Tabor (66) and Rabinowicz (69). Once the surface film had been fully developed during the initial stages of running it was sufficiently thick to support the load by a distribution of stress within the film, the underlying bulk material acting only as a supporting substrate for the film. The coefficient of friction was thus determined by the shear strength of the crystallites at the interface and the flow pressure of the surface film, so that the friction was high. The reduction in thickness of the film due to the passage of electric current lowered the load-bearing capacity of the film and the stresses at the surface were distributed between the film and bulk material. Hence, the coefficient of friction was determined by the shear strength of the film and the flow pressures of both the film and bulk material, causing a reduction in friction. At the higher currents the self supporting graphite film was no longer formed and the load was carried only by the bulk material. The frictional coefficient was therefore determined by the flow pressure of the bulk material and the shear strength of the extremly thin oriented surface layer, resulting in a low coefficient.

The second frictional characteristic requiring explaination is the increase in friction with time of running. When sliding an electrographite brush on aluminium at a load of 60gf., the frictional force between the brush and disk increased with time of running from an initial value of 5gf. to an equilibrium value in the range 22-25gf. (section 4.9). This increase in friction with time of running, or sliding distance, occurred for all loads and materials (with the exeption of electrographite). In some instances, however, the run was stopped before full equilibrium was

established.

E. Holm (18) has attributed this initial increase in friction to an increase in the real area of contact between the brush and metal as they wore to make more intimate contact. Although this could possibly account for the increase in friction during the very initial stages of sliding it is doubtful whether this could explain the prolonged increase encountered in some instances, since the brush had bedded in completly and worn considerably during this period. The potential waveforms also show that little change in the contact configuration of the metal surface occurred over long periods in the mild wear regime. The results obtained from running on gold confirmed that the increase in frictional force during running could not be due entirely to a change in contact area. The lack of oxide on the gold surface ensured that the contact resistance between the brush and disk was produced only by the constriction resistance of the contacting asperities. Any increase in real area of contact due to more intimate running would therefore be indicated by a decrease in contact resistance. The results shown in Figure 5.4 revealed that no decrease in contact resistance with time of running occurred on gold, although the contact resistance decreased with applied load as expected, due to an increase in area of contact. During the period in which the dynamic contact resistance was being monitored, the frictional force was also recorded and Table 5.8 shows that at a load of 60gf. the friction increased considerably during this period. Thus it can be seen that, in this instance, the increase in frictional force was not due to an increase in real area of contact.

The increase in frictional force with time of running can also be explained in terms of thin film lubrication, by the formation of the surface film on the brush during the initial stages of sliding. Contact

was first made between the hard bulk brush material and the metal surface, the cofficient of friction was therefore determined by the shear strength of the graphite crystallites, and the hardness of the bulk material, hence the friction was low. As the film thickness increased, due to running, a greater proportion of the load was supported by the film rather than the bulk material. The flow pressure of the contact was then dependent upon the hardness of the film, and since this was lower than that of the bulk material, the coefficient of friction increased. Once the film had attained an equilibrium thickness the increase in friction ceased. Such an increase in friction was obtained only when a brush contact film was formed, and removal of the film (by abrasion,when running on gold) resulted in the friction returning to its original low value. When sliding on an electrographite disk, no film was formed on either the brush or disk and no increase in friction with sliding distance was detected.

CHAPTER 7 CONCLUSIONS

The aims of this research, given in detail in Chapter 1 may be sumarized as follows:-

(i) General Wear Mechanisms - The formulation of a general theory to explain the wear of electrographite against any contact material.

(ii) The Use of Aluminium As The Contact Material - To investigate the suitability of aluminium as a substitute for copper as a slip ring, or commutator metal, with special emphasis on the failure of that system.

and (iii) The Friction of Electrographite - To obtain more information about the friction behaviour of electrographite and investigate the decrease in coefficient of friction with electric current.

Let us now see how far the above objectives have been achieved in this research.

General Wear Mechanisms

Three separate wear regimes were established, referred to as mild wear, severe wear, and catastrophic wear.

(a) Mild Wear involves wear rates of the brushes of the order of 10^{-9} - 10^{-10} mm^3/(mm of sliding) or less, and is acceptable to brush users for continuous running electrical machines.

(b) Severe Wear of the brushes occurred on some metals and involved wear rates in the range 10^{-7} - 10^{-8} mm^3/(mm of sliding). Provided no serious damage to the metal surfaces occurred (unlikely upon steel surfaces) this regime may be acceptable to brush users for intermittent running on fractional H.P. motors.

(c) Catastrophic Wear of the brushes was encountered when sliding upon aluminium and produced wear rates of 10^{-6} mm^3/(mm of sliding) and above, and resulted in serious damage to the metal surface. Catastrophic

wear was caused by electric current producing arcing at the interface and would be totally unacceptable to the majority of brush users.

Several wear mechanisms were involved in the sliding of the brushes. These were fatigue, adhesion, abrasion and oxidation. Pure fatigue wear produced the lowest wear rates, on gold and electrographite disks, whilst abrasion and oxidation produced the high catastrophic wear rates. Under most sliding conditions wear has been attributed to fatigue and adhesion, but which one of these mechanisms predominated was determined by the sliding conditions and disk material.

When sliding upon aluminium and EN26 steel disks a transition from mild wear to severe wear occurred if a critical load was exceeded. Associated with the transition was a change in contact resistance characteristics which indicated that mechanical disruption of the oxide film had taken place.

Wear in the mild wear regime was attributed primarily to fatigue failure of the graphite films produced upon the disk and brush surfaces. When sliding upon an electrographite disk no surface films were formed and wear was probably occuring by fatigue failure of the bulk material. During mild wear running, little adhesive wear occurred, the oxide films on the aluminium, copper and steel surfaces preventing adhesive contact. Sevére wear was produced by adhesion between the two contact materials, once the protective oxide film had been mechanically disrupted. Severe wear was not encountered if the oxide film was present or if the adhesive forces between the contacting materials were low, as in the case of gold and electrographite disks. The mechanisms involved in the catastrophic wear encountered upon the aluminium disks were chiefly those of erosion and oxidation of the brush surface produced by electrical sparking and

abrasion of the surfaces by particles of aluminium oxide and aluminium carbide Damage to the aluminium surface resulted from softening of the aluminium and from abrasive wear.

With the amount of information available a general wear theory involving any contact metal is difficult to propose, except to give the following broad guidlines. When fatigue wear of the surfaces predominates the wear rates of the brush will be in the mild wear regime, but when adhesion is the major wear mechanism a transition to the severe wear regime will occur. However, which of these mechanisms predominates will be strongly dependent upon the contact metal. Each metal surface must be considered individually to determine whether or not oxide film disruptions and severe wear will occur under the operating conditions imposed.

Mechanical disruption of the oxide from the metal, and hence the possibility of adhesive wear, will take place when shear forces at the oxide - metal interface overcome the binding forces between the oxide and metal. When the lattice mismatch was large, as in the case of iron and its oxide, the internal stresses at the interface were large, and low externally applied stresses, produced by the sliding of the brush, were able to overcome the binding forces. Thus the transition occurred at a low load. In the case of a copper surface the oxide - metal lattice mismatch was small and much higher external shear forces were required to disrupt the oxide. The transition load on copper was outside the range of loads investigated. Breakdown of the oxide film upon the aluminium was produced, not by shearing of the oxide away from

the metal due to externally applied stresses, but by increases in the stresses at the oxide - metal interface caused by plastic deformation of the soft aluminium. Plastic flow of the other metals investigated did not occur.

Before the wear hypothesis can be used to predict the wear behaviour of a metal-electrographite combination information must be obtained about the oxide-metal mismatch and the stresses produced, as well as the shear stresses produced at the sliding interface, to determine whether mechanical disruption of the oxide will occur at the load applied. More information must be obtained about the tribological compatability of the two surfaces to predict whether or not adhesive wear will result from the oxide breakdown.

The Suitability Of Aluminium As A Sliding Contact

Pure aluminium was not found to be a suitable substitute for copper as a slip-ring or commutator material due to plastic deformation at a relatively low load (within the normal operating range of the brushes) producing severe wear of the brush material. The onset of severe wear may also lead to unstable conditions at the interface, thus causing arcing at the interface and catastrophic wear.

Hardening of the aluminium by alloying can raise the elastic limit of the metal, and the value of the load at which the mild wear-severe wear transition occurs may be increased to outside the normal brush loading range. Preliminary investigations using an aluminium-copper alloy (71) have shown that at a load above the transition on pure aluminium the electrographite showed mild wear characteristics, indicating an increase in transition load. Such alloys may be suitable for slip

rings and commutators provided arcing and catastrophic failure can also be prevented by choice of suitable brush materials or commutator conditions.

The contact resistance behaviour of the interface during mild wear sliding was of the same form on aluminium, copper and steel. After an initial high resistance ohmic region the contact resistance decreased when a critical potential difference was applied across the interface. These results are consistent with a mechanically undisrupted oxide film upon the metal surface, the decrease in contact resistance being due to electrical breakdown of the film (19). When passing electric current through brushes running on these metals in the mild wear regimes it would appear that complete electrical breakdown of the oxide did not occur. A very thin oxide film was possibly still present on the contact and presented adhesive contact. The electric current passed through this film by tunnelling without interference. Where neither electrical nor mechanical breakdown had occurred, the thickness of the oxide, and hence the contact resistance, was determined by the recrystallisation depth of the oxide, which in turn depended upon the external stress applied. Thus the higher the load, the thinner the oxide film.

The Friction of Electrographite

The frictional force characteristics of electrographite study on all the metals investigated behaved in a manner which has been previously reported by a number of authors, including Lancaster and Stanley (17), Holm (18) and Davies (20). The friction increased with time of running to an equilibrium value, and if an electric current exceeding a critical

value was passed through the brush a decrease in friction occurred. The values of electric current producing the fall in friction in the mild wear regime were however, much lower than previously reported.

APPENDIX I

Calculation of intensities of diffracted lines

For a set of planes ($hk\ell$) the structure factor $F_{hk\ell}$ is given by:

$$F^2_{hk\ell} = \left\{\sum_{i=1}^{n} f_i \cos 2\pi(hx_i + ky_i + \ell z_i)\right\}^2 + \left\{\sum_{i=1}^{n} f_i \sin 2\pi(hx_i + ky_i + \ell z_i)\right\}^2$$

(i) Structure factor of graphite

The combination of sets of planes and atoms is shown in Table 1.

TABLE 1

Atom	i	x_i	y_i	Z_i
C	1	0	0	0
C	2	$\frac{1}{3}$	$\frac{2}{3}$	0
C	3	0	0	$\frac{1}{2}$
C	4	$\frac{2}{3}$	$\frac{1}{3}$	$\frac{1}{2}$
DIFFRACTING PLANES		0	0	2
		1	0	0
		1	0	1
		1	0	2
		0	0	4
		1	1	0
		h	k	ℓ

(002) Planes

$$F^2_{002} = f^2_{002}\left\{\cos 2\pi(0.0 + 0.0 + 0.2) + \cos 2\pi(0.\tfrac{1}{3} + 0.\tfrac{2}{3} + 2.0)\right.$$

$$\left.+\cos 2\pi(0.0 + 0.0 + 2.\tfrac{1}{2}) + \cos 2\pi(0.\tfrac{2}{3} + 0.\tfrac{1}{3} + 2.\tfrac{1}{2})\right\}^2$$

$$+f^2_{002}\left\{\sin 2\pi(0) + \sin 2\pi(0) + \sin 2\pi + \sin 2\pi\right\}^2$$

$$= f^2_{002}(1+1+1+1)^2$$

$$\underline{F^2_{002} = 16\, f^2_{002}}$$

The atomic scattering factor (f) can only be placed outside the summation if all the atoms within the unit cell are identical.

(100) Planes

$$F^2_{100} = f^2_{100}\left\{\cos 2\pi.0 + \cos 2\pi.\tfrac{1}{3} + \cos 2\pi.0 + \cos 2\pi.\tfrac{2}{3}\right\}^2$$

$$+ f^2_{100}\left\{\sin 0 + \sin\frac{2\pi}{3} + \sin 0 + \sin\frac{4\pi}{3}\right\}^2$$

$$= f^2_{100}\,(1-\tfrac{1}{2}+1-\tfrac{1}{2})^2 + f^2_{100}\,(0.866-0.866)^2$$

$$\underline{F^2_{100} = f^2_{100}}$$

(101) Planes

$$F^2_{101} = F^2_{101}\left\{ \cos 2\pi.0 + \cos 2\pi.\tfrac{1}{2} + \cos 2\pi\left(\tfrac{2}{3} + \tfrac{1}{2}\right)\right\}^2$$

$$+ \quad f^2_{101}\left\{ \sin 0 + \sin \frac{2\pi}{3} + \sin\pi + \sin \frac{7\pi}{3} \right\}^2$$

$$= \quad f^2_{101}\left\{ 1 - \tfrac{1}{2} - 1 + \tfrac{1}{2} \right\}^2 + f^2_{101} \quad \left(0 + \sqrt{\tfrac{3}{2}} + 0 + \sqrt{\tfrac{3}{2}}\right)^2$$

$$\therefore \quad \underline{F^2_{101} = 3f^2_{101}}$$

(102) Planes

$$F^2_{102} = f^2_{102}\left\{ \cos 2\pi.0 + \cos 2\pi.\tfrac{1}{3} + \cos 2\pi.1 + \cos 2\pi\left(\tfrac{2}{3} + 1\right) \right\}^2$$

$$+ \quad f^2_{102}\left\{ \sin 0 + \sin \frac{2}{3}\pi + \sin 2\pi + \sin \frac{10\pi}{3} \right\}^2$$

$$= \quad f^2_{102}\left(1 - \tfrac{1}{2} + 1 - \tfrac{1}{2}\right)^2 + f^2_{102} \quad \left(0 + \sqrt{\tfrac{3}{2}} + 0 - \sqrt{\tfrac{3}{2}}\right)^2$$

$$\therefore \quad \underline{F^2_{102} = f^2_{102}}$$

(004) Planes

$$F^2_{004} = f^2_{004} \quad \cos 0 + \cos 0 + \cos 2\pi.2 + \cos 2\pi.2 \quad ^2$$

$$+ \quad f^2_{004} \quad \sin 0 + \sin 0 + \sin 4\pi + \sin 4\pi \quad ^2$$

$$\therefore \quad \underline{F^2_{004} = 16\, f^2_{004}}$$

(110 Planes)

$$F^2_{110} = F^2_{110} \cos 0 + \cos 2\pi 1 + \cos 2\pi 0 + \cos 2\pi .1 \quad ^2$$

$$+ f^2_{110} \sin 0 + \sin 2\pi + \sin 0 + \sin 2\pi ^2$$

$$\therefore \quad F^2_{110} = 16 f^2_{110}$$

(ii) Structure factors of Aluminium and Copper

Both these materials have the face centred cubic structure shown. The positions of the atoms being, (0.0,0), $(0,\frac{1}{2},\frac{1}{2})$.

$(\frac{1}{2},0.\frac{1}{2})$ and $(\frac{1}{2},\frac{1}{2},0)$.

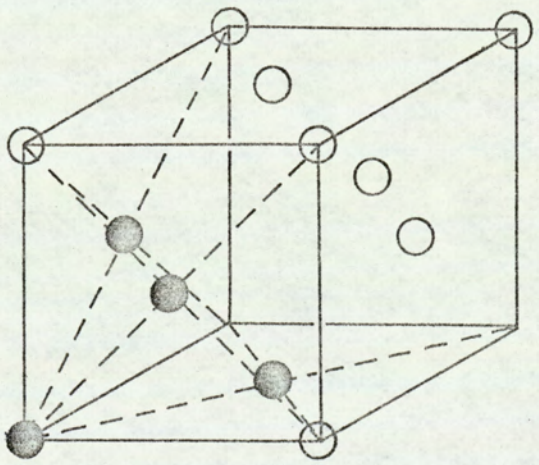

● Atoms within unit cell.

Reflections occur from the following sets of planes : (111), (200), (220),(311),(222),(400),(331),(420),(422).

The combinations of planes and atoms is shown in Table 2

i	x_i	y_i	z_i
1	0	0	0
2	$\frac{1}{2}$	$\frac{1}{2}$	0
3	0	$\frac{1}{2}$	$\frac{1}{2}$
4	$\frac{1}{2}$	0	$\frac{1}{2}$
DIFFRACTING PLANES	1	1	1
	2	0	0
	2	2	0
	3	1	1
	2	2	2
	4	0	0
	3	3	1
	4	2	0
	4	2	2
	h	k	1

Table 2

(111) Planes

$$F_{111}^2 = f_{111}^2\left\{\cos 2\pi.0+\cos 2\pi(\tfrac{1}{2}+\tfrac{1}{2}+0)+\cos 2\pi(0+\tfrac{1}{2}+\tfrac{1}{2})+\cos 2\pi(\tfrac{1}{2}+0+\tfrac{1}{2})\right\}^2$$

$$+ f_{111}^2\left\{\sin 0+\sin 2\pi+\sin 2\pi+\sin 2\pi\right\}^2$$

$$\therefore \quad \underline{F_{111}^2 = 16f_{111}^2}$$

(200) Planes

$$F_{200}^2 = f_{200}^2 \left\{ \cos 0 + \cos 4\pi + \cos 4\pi + \cos 4\pi \right\}^2$$

$$\therefore \quad \underline{F_{200}^2 = 16 f_{200}^2}$$

For each set of planes giving rise to a diffraction maxima the structure factor is given by

$$\underline{F_{hkl}^2 = 16 f_{hkl}^2}$$

Structure factor of Cu_2O. The positions of the Copper and Oxygen atoms within the unit cell are shown in Table 3.

Atom	i	x_i	y_i	z_i
Cu	1	1/4	1/4	1/4
Cu	2	3/4	3/4	1/4
Cu	3	3/4	$\frac{1}{4}$	3/4
Cu	4	$\frac{1}{4}$	3/4	3/4
O	5	0	0	0
O	6	$\frac{1}{2}$	$\frac{1}{2}$	$\frac{1}{2}$
Diffracting Planes		1	1	1
		2	2	0
		h	k	l

Table 3

$$F^2_{hkl} = \left\{ \sum_{i=1}^{n} f_i \cos 2\pi(hx_i+ky_i+lz_i) \right\}^2 + \left\{ \sum_{i}^{n} f_i \sin 2\pi(hx_i+ky_i+lz_i) \right\}^2$$

111 planes

$$F^2_{111} = \Big(f_{cu}\cos 2\pi\cdot\tfrac{3}{4} + f_{cu}\cos 2\pi\tfrac{7}{4} + f_{cu}\cos 2\pi\cdot\tfrac{7}{4} + f_{cu}\cos 2\pi\cdot\tfrac{7}{4} + f_o\cos 2\pi\cdot 0 + f_o\cos 2\pi\cdot\tfrac{3}{2}\Big)^2$$

$$+\Big(f_{cu}\sin\tfrac{6\pi}{4} + f_{cu}\sin 2\pi\cdot\tfrac{7}{4} + f_{cu}\sin 2\pi\cdot\tfrac{7}{4} + f_{cu}\cos 2\pi\tfrac{7}{4} + f_o\sin 0 + f_o\sin 3\pi\Big)^2$$

$$F^2_{111} = \Big(f_{cu}\cos\tfrac{6\pi}{4} + 3 f_{cu}\cos 2\pi\tfrac{7}{4} + f_o\cos 0 + f_o\cos 3\pi \Big)^2$$

$$+\Big(f_{cu}\sin\tfrac{6\pi}{4} + 3f_{cu}\sin\tfrac{7\pi}{2} + f_o\sin 0 + f_o\sin 3\pi \Big)^2$$

$$=\Big(f_{cu}\,0 + 3 f_{cu}\,0 + f_o\cdot 1 + f_o(-1) \Big)^2$$

$$+\Big(f_{cu}(-1) + 3 f_{cu}(-1) + f_o\,0 + f_o\,0 \Big)$$

$$F_{111} = \Big(4 f_{cu} \Big)^2$$

(220) planes

$$F^2_{220} = \Big\{ f_{cu}\cos 2\pi\cdot 1 + f_{cu}\cos 2\pi\cdot 3 + f_{cu}\cos 2\pi\cdot 2 + f_{cu}\cos 2\pi\cdot 2 + f_o\cos 0 + f_o\cos 2\pi\cdot 2 \Big)^2$$

$$+\left\{ f_{cu}\sin 2\pi + f_{cu}\sin 6\pi + f_{cu}\sin 4\pi + f_{cu}\sin 4\pi + f_{o}\sin 0 + f_{o}\sin 4\pi \right\}^2$$

$$=\left\{ f_{cu}\ 1. + f_{cu}.1 + f_{cu}.1 + f_{cu} + f_{o} + f_{o} \right\}^2$$

$$+\left\{ f_{cu}\ 0. + f_{cu}.0 + f_{cu}.0. + f_{cu}.0 + \right.$$

$$F_{220}^2 = \left\{ 4f_{cu} + 2f_{o} \right\}^2$$

(iii) Caculation of Intensities

Having determined the structure factor , the other quantities contained in the equation for the intensity of the diffracted beam are easily calculated or found from standard tables, and the expected intensity of each diffracted beam can be computed.

(iv) The Lorentz Polarization factor

$$Lp = \frac{1+\cos^2 2\theta}{\sin^2\theta\cos\theta}$$

(for a cylindrical specimen in a capillary tube)

The appropriate values of this factor can easily be calculated or looked up in tables knowing the angle of diffraction 2θ.

(Tables contained in Lipson & Wooster, Macmillan 1961)

(v) Atomic Scattering factor (f)

Values of atomic scattering factors at various angles of $\sin\theta/\lambda$ are

given in crystallographic tables (e.g. International tables for X-ray Crystallography) . The variations in f with $\sin\theta/\lambda$ for Aluminium, copper and Carbon are shown in Figure I.1. From this graph the value of "f" corresponding to each diffraction maxima was found.

(vi) Debye-Waller Temperature factor

The atomic scattering factor at a temperature T°K is given by

$$f_T = fe^{-2B \sin^2 \theta/\lambda^2}$$

When B is the Debye parameter, made up of two components, Bo which is derived from the zero point energy of the atom and B_T derived from thermal vibrations of the atom.

Values of Bo and B_T at 293°K are given for C, Al and Cu in Table 4

Atom	Bo	B_T	B=Bo+Br
Al	0.28 0.25	0.64 0.47	0.92 0.72
Cu	0.15 0.13	0.44 0.34	0.59 0.47
C	0.13	0.38	0.51

Table 4

(International Tables for X-Ray Crystallography Vol 111).

Thus, having found B the value of $e^{-B\sin\theta/\lambda}$ can be determined for each maxima.

Table 5 shows the calculated values of R for each of the observed diffracted maxima from Carbon, Copper, Aluminium and Cu_2O.

The $(10\bar{1}0)$, $(10\bar{1}1)$ lines of carbon are very close together and the peaks cannot be resolved. Since the integrated intensity of the lines are being measured the expected intensity from these two peaks can, to a close approximation be taken as the sum of the R values for the two lines.

Material	Planes hkl	M	θ	2θ	dÅ	$2d$Å	$\sin\theta/\lambda$	$V R^3$	$\frac{1+\cos^2 2\theta}{\sin^2\theta\cos\theta}$	$e^{-B\sin\theta/\lambda}$	F^2_{hkl}	f_{hkl}	R
C	002	2	13.3	26.6	3.35	6.7	0.1493		34.94	0.989	$16f^2$	4.40	17.09
C	100	6	21.22	42.44	2.13	4.26	.2347		12.68	0.974	f^2	3.17	0.586
C	101	12	22.21	44.42	2.04	4.08	.2451	35.2	11.43	0.969	$3f^2$	3.00	2.086
C	102	12	25.36	50.72	1.80	3.6	.2778		8.420	0.962	f^2	2.75	0.5708
C	004	2	27.4	54.8	1.70	3.4	.2941		7.086	0.959	$16f^2$	2.55	1.090
C	110	6	38.73	77.46	1.23	2.46	.4065		3.43	0.919	$16f^2$	1.93	0.836
	111	8	19.3	38.5	2.338	4.676	.2139		15.62	0.965		9.0	34.0
Al	200	6	22.4	44.78	2.024	4.048	.2470		11.20	0.951		8.5	15.8
Al	220	12	32.6	65.19	1.431	2.862	.3494		4.809	0.907		7.3	9.20
Al	311	24	39.2	78.3	1.221	2.442	.4095	66.4	3.361	0.874	$16f^2$	6.6	9.70
Al	222	8	41.3	82.52	1.169	2.338	.4277		3.106	0.863		6.4	1.74
Al	400	6	44.4	88.86	1.012	2.024	.4938		2.860	0.825		5.7	1.39
Al	331	24	56.1	112.18	.9289	1.858	.5382		2.974	0.792		5.2	4.40
Al	420	24	58.4	116.7	.9055	1.811	.5522		3.166	0.785		5.1	4.40
Al	422	24	68.8	137.7	.8266	1.653	.6042		4.916	0.750		4.6	5.10

Table 5 Calculation of "R" Values for Carbon and Aluminium.

Material	Planes hkl	M	θ	2θ	dÅ	2dÅ	Sin θ / λ	V_A^3	$\frac{1+\cos^2 2\theta}{\sin^2\theta\cos\theta}$	$e^{-B\sin\theta/\lambda^2}$	F^2_{hke}	F_{hke}	R
Cu	111	8	21.67	43.34	2.088	4.176	0.239		12.03	0.972		22.0	396.6
Cu	200	6	25.24	50.48	1.808	3.616	.277		8.573	0.962		20.4	142.0
Cu	220	12	37.10	74.20	1.278	2.556	.391		3.701	0.927		16.7	76.32
Cu	311	24	45.01	90.02	1.090	2.180	.458	47.24	2.828	0.900	$16f^2$	14.6	84.02
Cu	222	8	47.62	95.24	1.044	2.088	.479		2.742	0.891		14.1	31.25
Cu	400	6	58.53	117.06	0.9038	1.8076	.554		3.175	0.860		12.4	16.19
Cu	331	24	68.37	136.74	0.8293	1.6586	.603		4.812	0.835		11.4	75.02
Cu	420	24	72.50	145.00	0.8083	1.6166	.618		6.109	0.825		11.2	89.76
Cu_2O	111	8	18.22	36.45	2.465	4.930	.202	77.86	17.78	0.980	$16f^2_{cu}$	23.6	201
	220											4.6	54

Intensity of (220) reflection of Cu_2O determine by comparison with A.S.T.M. index card

Table 5 (cont.) Calculation of "R" Values for Copper and Cuprous Oxide.

Figure I.1 Atomic Scattering Factors of Aluminium, carbon and Copper.

REFERENCES

1. Bragg, W.L., "Introduction to Crystal Analysis". G.Bell & Sons Ltd., London.
2. Jenkins, R.O., Phil.Mag. 17, 457 (1943)
3. Van Brunt, C. Gen.Elect.Review p.16 (July 1944)
4. Savage, R.H. J.Appl.Physics 19, No 1.p.1 (1948)
5. Van Brunt, C and Savage, R.H. Gen.Elect.Review p.16 (July 1944)
6. Fullam, E.F. and Savage, R.H. J.Appl.Physics 19 pp.654-661, (1948)
7. Campbell, W.E. and Kozac, R. Trans.A.S.M.E., 70, 491 (1948)
8. Deacon, R.F. and Goodman , J.F. Proc.Royal Soc. A p243 (1958)
9. Porgess, P.V.K. and Wilman, H . Proc.Phys.Soc 73, 514 (1960)
10 Quinn, T.F.J. Brit.J.Appl.Physics. 14, p.107 (1963)
11 Quinn, T.F.J. Brit.J.Appl.Physics. 15, p573 (1964)
12 Midgley, J.W and Teer, D.G. Nautre 189 (1961)
13 Arnell, J.W., Midgley, S.W and Teer, D.G. Proc.Inst.Mech.Engrs. 179 Pt3J. p.115 (1964-65)
14 Langley, R.I., Midgley, J.W., Strang, A and Teer, D.G. Proc.1st.Lub. & Wear Convention 1963, Paper 17 (Inst.Mech.Engrs.London)
15 Bolman, W and Spreadborough, J Nature, 186, p.29 (1960)
16 Hayes, M.E., 1947, "Current Collecting Brushes in Electrical Machines" (London: Pitman)
17 Lancaster, J.K. and Stanley, I.W Brit.J.Appl.Phys. 15 p.29 (1964)
18 Holm, E. J.Appl.Phys. 33 No.1, p.156
19 Holm, R., "Electric Contact Handbook", Third Ed. Springer-Verlag, Berlin, (1958)

20	Davies, W.	Inst.of Elect.Engrs., Monograph 271U December (1957)
21	Bickerstaff, A.E.,	Proc. Third Conf.Industrial Carbon and Graphite. Soc.Chem.Industry, London (1970)
22	Holm, R.,	J.Appl.Physics 39 No.7. p.3294
23	Holm, E.,	4th Inter.Res.Symp.on Electric Contact Phen., Swansea, Wales. 7-15-18 (1968)
24	Stebbens, A.E.	I.E.E.Conf.Pub. No 11 p.74 (1964)
25	Bickerstaff, A.E.	Proc.Fifteenth Holm Seminar on Electric Contact Phenomena, p. 41 Chicago-Illinois Inst.Tech)
26	Lancaster, J.K.,	Britt.S.Appl.Phys. 13 p.468 (1962)
27	Spry, W.T., and Scherer, P.M.	Wear, 4, p137 (1962)
28	Holm, R.,	Wiss.Veroff.Siemens-Werk, 17 p.43 (1938)
29	Shobert, E.I.	Proc.5th International Conference on Electric Contact Phenomena.V.D.E - Berlin p.244 Munich 1970)
30	Bickerstaff, A.E.,	Proc.5th International Conference on Electric Contact Phenomena V.D.E. - Berlin p.254 (Munich 1970)
31	White, J.R.	Wear, 13 p.145 (1969)
32	Lancaster, J.K.	Nature 196 p368 (1962)
33	Clark, W.T. and Lancaster, J.K.	Wear, 6, 467 (1963)
34	Bickerstaff, A.E.	Proc.4th Int.Res.Symp.on Electrical Contact Phenomena, 1968 p.72 (Swansea: Inst. Phys. and Inst. of Elect.Engrs)
35	Bickerstaff, A.E.	"Private Communication" 1972
36	Thompson,S.E and Turner, M.J.B.	Nature 126 p.329 (1962)
37	Averbach, B.L. and Cohen, M.	Metals Technologu T.P.2342
38	Quinn, T.F.J.	Advance in X-ray analysis, 10, 311 Plenum Press, New York
39	Klug, H.P. and Alexander, L.E.	"X-ray Diffraction Procedures" Wiley, New York (1954)

40	Broukere, L.	J.Inst.Met. 71, p.131 (1945)
41	Thompson, J.E. and Turner, M.J.B.	Wear 6 p.30 (1963)
42	Shobert, E.I.	"Carbon Brushes" Chemical Publishing Co., New York, 1965
43	Bale, E.S.,	Internal Report, Morganite Carbon Co Ltd London
44	Archard, J.F.	J.Appl.Phys. 32. 1420 (1961)
45	Hauffe,K.	"Oxidation of Metals". Plenum Press, New York, 1965.
46	Mehl, R.F., McCandless, E.L. and Rhines, F.N.	Nature, Lond., 134 1009 (1934)
47	Bardolle, J., and Bernard, J.C.R.,	Acad. Sci. Paris, 232 (1951) 231
48	Frank, F.C., and van der Merwe, J.H.	Proc.Roy Soc 198 A p.205 (1949)
49	Cabrera, N., and Mott, N.F.	Rep.Progr.Phys. 12 p.163 (1948-49)
50	Kubashewski, O., and Hopkins, B.E.	"Oxidation of Metals and Alloys" Butterworths, London 1953
51	Evans, U.R.,	Inst. Metals Symp. on Internal Stresses in Metals and Alloys p.291 (1947)
52	Dankov, P.D., and Churaev, P.V.	C.R.Acad. Sci. V.R.S.S. 73 p.1221
53	Baukloh, W., and Thiel, G	Korros, Metallsch, 16 p121 (1940)
55	Hass,G.,	Z.anorg Chem. 96 p.254 (1947)
56	Hayward, D.O., and Traprell, B.M.W.	"Chemisorption" 2nd Edition Butterworths (1964)
57	Bridgmann, P.W.	Phys.Rev., 48 No 10, p.825 (1935)
58	Bridgmann, P.W.	Proc.Am.Acad.,Arts.Sci. 71 p.387 (1937)
59	Rabinowicz, E.,	"Friction and Wear of Materials" John Wiley and Sons, New York (1965)
60	Rabinowicz, E.,	Trans.A.S.L.E. 14 p.198 (1971)

61	Dunbar, R.E.	Private Communication (1971)
62	Quinn, T.F.J.	Proc.I.Mech.E. 182, Pt3N (1967-68)
63	Quinn, T.F.J.	Ph.D.Thesis, London University (1964)
64	Buckley, D.H.	"Friction, wear, and Lubrication in Vacuum" N.A.S.A.Publication (1971)
65	Fisher, J. Campbell, K.J. and Quinn T.F.J.	Paper presented at 1st.Conference on Solid Lubrication, Denver Col (1971) Published: Trans.ASLE, 15, No.3 (1972)
66	Bowden, F.P. and Tabor, D.	Bull 145, comm of Australia Counc.Sci. Ind.Res. p.39
67	Tsuya, Y., and Takagi, R.	Wear 7, p.131 (1964)
68	Crump, R.E.,	A.S.L.E. Preprint 56LC- 8 (1956)
69	Rabinowicz, E.	A.S.L.E. Trans. 10, p.1 (1967)
70	Whitehouse, G.D., Nandan, D., and Whitehurst, C.A.	A.S.L.E. Trans. 13, p.159 (1970)
71	Fisher,J., Quinn, T.F.J. and Sullivan, J.L.	Proc.3rd Conf. on Ind.Carbon & Graphite, Soc.Chem.Ind. (1970)

ACKNOWLEDGMENTS

This research was carried out at the University of Aston in Birmingham during the tenure of a Science Research Council CAPS Studentship. I should like to record my thanks to the co-operating body Morganite Carbon Co., Ltd., London, for financial and technical assistance.

I should like to thank my supervisor, Dr. T.F.J. Quinn for help and encouragement during the course of the research programme. Thanks are also due to Mr. A.E. Bickerstaff for many helpful discussions.

I should like to acknowledge the contribution from members of the academic and technical staff of the departments of Physics and Metallurgy. In particular I should like to record my appreciation of Mr. F. Lane and the staff of the Physics workshop for assistance with the building of the wear test machine and preparation of disks and specimens.

Finally I should like to thank Mrs. D.G. Hill for the patience she has shown in typing this thesis.

APPLICATION OF SCANNING ELECTRON MICROSCOPY TO THE STUDY OF GRAPHITE/METAL INTERFACES

By J. FISHER, T. F. J. QUINN and J. L. SULLIVAN

(*Department of Physics, The University of Aston in Birmingham, Gosta Green, Birmingham, 4*)

Electrographite brushes have been run against copper, duralumin, and stainless-steel discs at a mean speed of about 9,000 mm/sec, under a load of 0·4 kgf, and with a current density increasing in stages from 0 up to 0·15A/mm², the positive and negative brushes being run on separate tracks. Equilibrium conditions were established at each value of current density, as revealed by measurements of brush wear, brush friction, and contact resistance between the brushes and the tracks on the disc. Selected typical portions of the four brush and track surfaces were examined at magnifications varying from about 100 × up to about 30,000 ×, using the powerful technique of scanning electron microscopy.

The electrical and mechanical behaviour of these graphite/metal systems is briefly discussed. The wear rates of the negative electrographite brushes are larger than those of the positive brushes for all systems. A correlation between the electrical contact resistance and the coefficient of friction is shown to exist.

The topographies of the various surfaces, as revealed by the scanning electron microscope, are discussed. Some evidence is given for a fatigue wear mechanism through 'blistering' and cracking of surface films on both the brush and disc surfaces of these graphite/metal systems.

Introduction

Most of the previous research into the friction and wear of carbon brushes has been concerned with the sliding of graphite on copper, since most electrical machines are generally operated with copper commutators or slip rings. However, some machines are now using steel as the contact material. For example, high-carbon steel is used in the slip rings of high-speed alternating current generators, and stainless steel is often used on high-speed machines which have to run at high ambient temperatures. Very little is known about the friction and wear behaviour of graphite on metals other than copper. For this reason, the Tribology Laboratory in this Department has embarked on a systematic investigation of the fundamental and practical aspects of using alternative contact materials, such as duralumin and stainless steel. A small amount of graphite-on-copper work is also being carried out for the purposes of comparison.

This paper is a report on some of the early results of this project, with special emphasis on the results of the scanning electron microscopy used to study the topographies of the various contact surfaces. This technique has very special relevance to graphite/metal interfaces, since such interfaces will not normally suffer a plastic replication process (prior to examination by conventional transmission electron microscopy) without disintegration and shearing at levels other than the actual contacting interface. Previously, reflection electron microscopy has been used for directly studying the topography of worn graphite contact films, for example in the electrographite-on-copper work of Quinn.[1] This technique has the disadvantages of providing a perspective view of the surface, and a relatively poor resolution (about 300Å). On the other hand, the scanning electron microscope provides near-normal viewing of the specimen surface, a high resolution, and a very wide range of magnifications. Very little has yet been published on the application of scanning electron microscopy to graphite sliding on metals. White[2] has used this technique to provide some evidence for a fatigue mechanism of wear applicable to electrographite sliding against copper. It is shown that the results of the present investigation are also consistent with a fatigue mechanism operating in the wear of electrographite on other contact materials, as well as on copper.

Experimental

The brushes were made from electrographite (EG14) (kindly supplied by Morganite Carbon Limited). The discs were machined with a tungsten carbide tool to provide an initial surface finish of about 6×10^{-6} mm centreline average (*CLA*). The *CLA* measurements taken tangentially to the direction of machining were very slightly different from the measurements taken radially. The discs were run horizontally to facilitate the measurements of friction and wear. A mechanical method was used for measuring the frictional force on each brush, and an electrical capacitance method was used for measuring the changes in brush height with increase in wear.

Each brush was run with zero current until steady frictional force values were obtained at a load of 0·4 kgf and at linear speeds of 8600 and 10,200 mm/sec. These were attained after about 2–3 days continuous running. The current through the brushes was then increased in stages up to 5A. This final current was far above the recommended current density of 0·08A/mm². In fact, it corresponded to a current density of about 0·15A/mm² At each stage, equilibrium values of friction, wear, and contact voltage were obtained before passing on to the next higher stage.

Sections of selected portions (about 6 × 6 mm) of the running track were cut from each disc. These, together with the running surfaces of the brushes, were mounted for viewing in the scanning electron microscope.

Results and Discussion

This section deals mainly with the results of the examination of the brush and track surfaces by scanning electron microscopy. Obviously, these scanning electron micrographs can relate only to the final high current density equilibrium surfaces. Further work is already under way, in the authors' laboratory, in which the

equilibrium surfaces at each current density are being systematically examined. This should determine whether or not the features about to be described are, in fact, only high current density features. Before describing these features, however, an account of the general electrical and mechanical behaviour of the electrographite/metal system will be given.

Electrical and mechanical behaviour of the systems

There was a marked tendency for the negative brushes running on duralumin and stainless steel to wear significantly more than the positive brushes. This is in agreement with the results of Davies,[3] who found that the negative brush wore more than the positive brush when slid against copper. The graph of wear rate *versus* current is shown in Fig. 1.

The coefficients of friction, on the other hand, seem to be independent of current direction for both duralumin and stainless-steel contact materials. Fig. 2 shows the relationship between coefficient of friction and current for both materials. The low current behaviour of the friction coefficient of duralumin may be significant (see below). Both materials showed that the friction coefficient tends towards an equilibrium value at high current densities. This behaviour is in agreement with the results reported by Lancaster & Stanley,[4] who used copper and mild-steel discs.

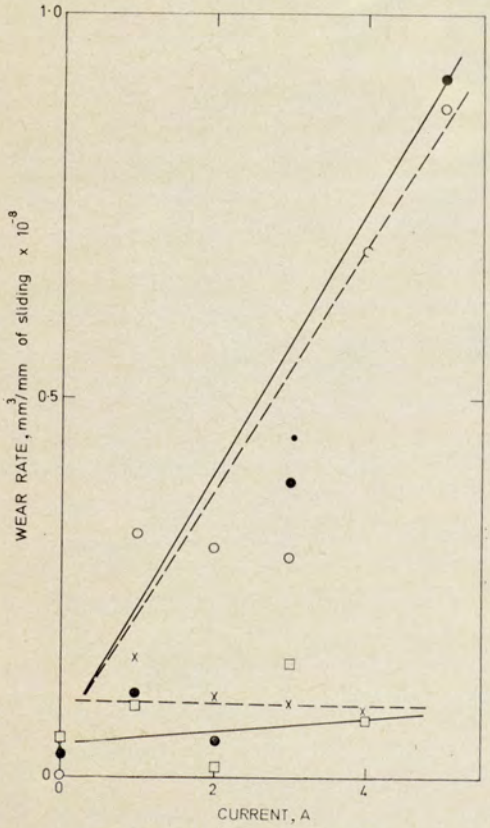

Fig. 1. *Wear rate* versus *current for electrographite brushes sliding on duralumin* (———) *and stainless steel* (— — —)
Speed: ~ 9000 mm/sec; load: 0·4 kgf
Stainless steel: ×, positive brush; ○, negative brush
Duralumin: □, positive brush; ● negative brush

The contact resistance behaviour of the electrographite on stainless steel also followed the same trend as that reported by Lancaster and Stanley[4] for their electrographite on copper and mild-steel systems, namely, a decrease in contact resistance with increasing current towards equilibrium values at high currents. The behaviour of the duralumin system was markedly different, showing a maximum contact resistance between about 2 and 3A. Fig. 3 shows the contact resistance *versus* current for both the duralumin and stainless-steel systems.

There is a possible correlation between the coefficient of friction and the contact resistance, as indicated by the similarity of the curves in Figs 2 and 3. By plotting friction coefficient *versus* contact resistance, a straight line relationship was obtained (see Fig. 4) for the stainless-steel points. The duralumin points relating to low current experiments are clearly anomalous, whilst the high current points all lie close to the lines drawn through the stainless-steel points. This graph is most important, since it shows a simple relationship between the contact resistance (an electrical measurement) and the coefficient of friction (a mechanical measurement), both

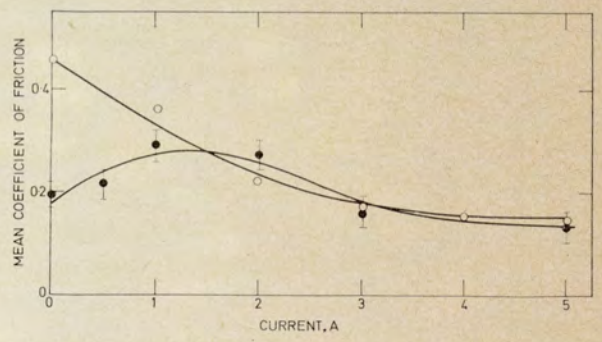

Fig. 2. *Friction coefficient* versus *current for electrographite brushes sliding on duralumin* (●) *and stainless steel* (○)
Speed: ~ 9000 mm/sec; load: 0·4 kgf

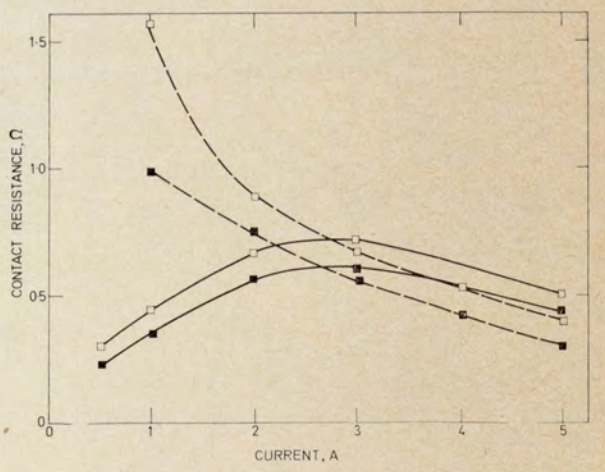

Fig. 3. *Contact resistance* versus *current for electrographite brushes sliding on duralumin* (———) *and stainless steel* (— — —)
Speed: ~ 9000 mm/sec; load: 0·4 kgf
□ Positive brush; ■ negative brush

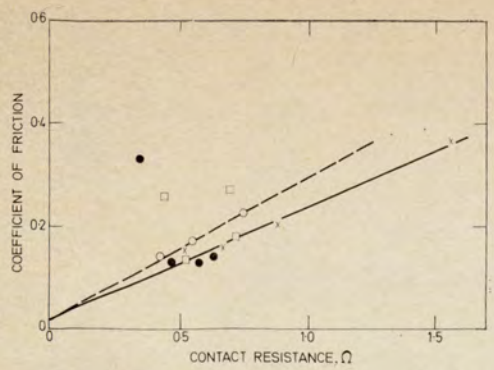

Fig. 4. *Coefficient of friction* versus *contact resistance for electrographite brushes sliding on duralumin* (———) *and stainless steel* (— — —)

Speed: ~ 9000 mm/sec; load: 0·4 kgf
Stainless steel: ×, positive brush; ○, negative brush
Duralumin: □, positive brush; ●, negative brush

of which must be intimately related to the nature of the interface between the electrographite brush and the contact films formed on the disc. This result shows how relevant the scanning electron microscopy of the contact surfaces must be to any real understanding of the behaviour of graphite/metal interactions during sliding.

Topographies of the systems

At least 100 scanning electron micrographs were taken of the equilibrium surfaces of the brushes and the tracks. Only a small selection are presented here.

This selection has been made on the basis of showing as many relevant features as possible, using the minimum number of photographs. It will be recalled that one of the aims of the project was to compare the relative efficiences of duralumin and stainless steel as contact materials against that of copper. For this reason, one or two significant features of the contact film formed on copper are shown in Fig. 5.

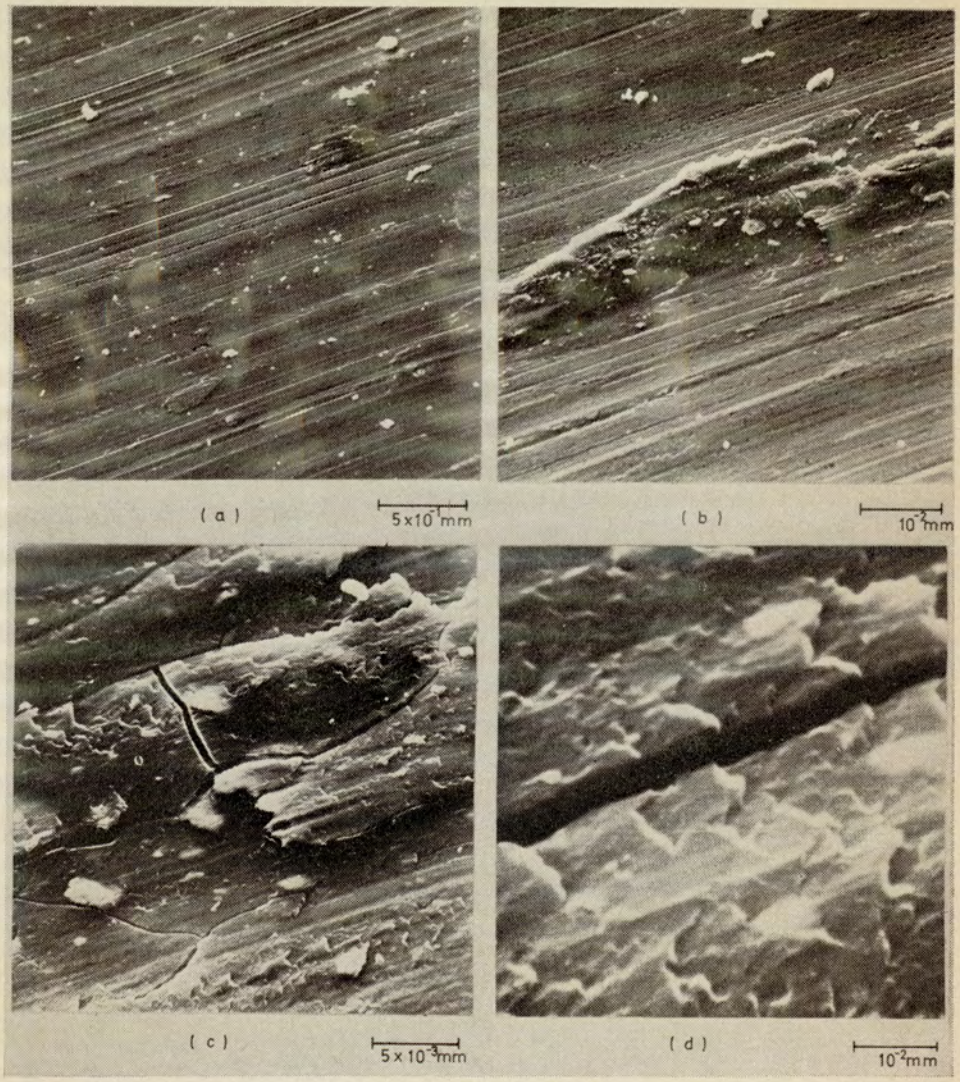

Fig. 5. *Scanning electron micrographs of contact film on positive track formed on copper disc*

(a) General view of surface; (b) enlarged view of flake; (c) enlarged view of part of (b); (d) enlarged view of part of (c)

This is a good example of the value of having a wide range of magnifications available. Fig. 5(a) shows the smooth continous nature of the contact surface, which almost certainly consists mainly of electrographite and the occasional large flake standing apparently proud of the surface. Fig. 5(b) shows an enlarged version of one of these flakes. This flake is contiguous with the contact film at its lower edge. It is also severely cracked. An enlarged view of this cracked flake is shown in Fig. 5(c). Similar crack systems have been found to occur in the surfaces of steels when slid against each other under unlubricated conditions.[5,6] Fig. 5(d) is an enlarged portion of a region near to one of the cracks in Fig. 5(c), from which can be seen a definite overlapping flake effect. The trailing edges of the flakes are standing proud of the surface. Such tilted flakes are in accord with the electron diffraction evidence obtained from similar electrographite on copper surfaces.[1] The overlapping flakes were not so well defined in the reflection electron micrographs obtained by Quinn,[1] and, in fact, he found no evidence of the cracks at all. This is to be expected, since the contrast of cracks is much lower for reflection electron microscopy than for scanning electron microscopy, or transmission electron microscopy of replicas, of cracked surfaces.

It may be noted that White[2] has also reported the presence of cracks in the surfaces of electrographite brushes which had been sliding on copper discs. He concluded that these cracks were evidence for the fatigue wear mechanism proposed by Clark & Lancaster.[7] He also found evidence that the cracks and flakes probably result from the collapse of 'blisters' on the surface.

Although no such 'blisters' have been found in the surfaces of the electrographite/copper system covered by the present investigation, extensive areas of 'blisters' have been found in the surfaces of the electrographite/duralumin and the electrographite/stainless-steel systems. Fig. 6 shows some typical blistered areas in the equilib-

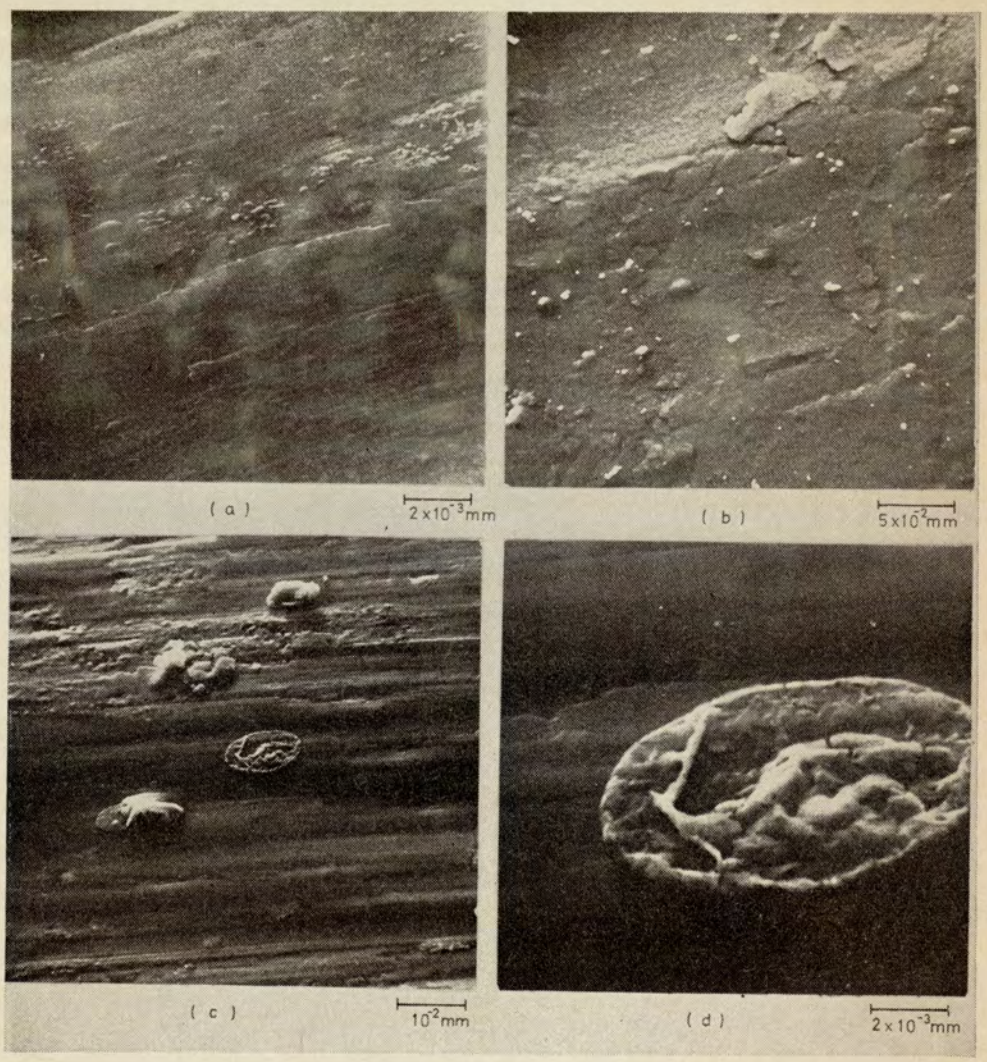

Fig. 6. *Typical blistered areas of surfaces*

(a) Surface of track formed on duralumin disc by positive electrographite brush;
(b) surface of negative electrographite brush which has been running on duralumin;
(c) surface of track formed on stainless steel by negative electrographite brush;
(d) enlarged view of the collapsed blister in (c)

rium surfaces of both systems. Fig. 6(c) shows one blister which has collapsed (in the centre of the micrograph) and one blister which seems about to collapse (in the lower left of the micrograph). Fig. 6(d) is an enlarged view of the collapsed blister of Fig. 6(c).

Various other interesting scanning electron micrographs have been obtained from the surfaces of these specimens. Their relevance to possible wear mechanisms is not too clear. In general, they tend to show that there is very little difference between a positive and negative brush surface, or a track formed under a positive or negative brush, for the three systems investigated. The difference in wear rates between the negative and positive brushes does not lead to any apparent differences in the final equilibrium surface topographies. The micrographs do, however, show a tendency for the brush surfaces to be rougher than the tracks formed on the discs, a tendency already reported (for zero current only) by Quinn[1] in his reflection electron microscope investigation of electrographite sliding on copper.

Conclusions

The preliminary results reported in the previous section indicate that the mechanism of wear by fatigue of the surface films may hold for systems other than electrographite on copper. The strong correlation between contact resistance and friction coefficient emphasises that any investigations of the electrical and mechanical behaviour of graphite/metal interfaces must be concerned with the real area of contact between the brush and its accompanying track on the metal. The use of scanning electron microscopy in the present investigation shows that the technique can be of invaluable assistance in investigating what actually goes on at the real area of contact.

Obviously, much more work is required, especially work directed towards an understanding of the effect of any preferred orientation of the electrographite crystallites upon both the electrical resistance and the mechanical resistance (friction). Although not reported in this paper, preliminary electron diffraction studies of the brush tracks on the duralumin disc have revealed that a strong preferred orientation does exist in both the brush and track surfaces. There must be a strong connexion between friction, electrical contact resistance, wear, and the 'strength' of any preferred orientation present in the surfaces.

This preliminary investigation has already shown that the process of wear of electrographite/metal systems may not be different from those occurring in metal/metal systems. One is continuously being forced to acknowthat graphite (especially an artificially made graphite such as electrographite) may not be so very different from a metal insofar as its mechanical behaviour in a sliding situation is concerned.

Acknowledgments

The authors are indebted to Dr. D. Arrowsmith and Mr. J. Fuggle, of the Metallurgy Department of The University of Aston in Birmingham, for their kind co-operation with regard to the use of the scanning electron microscope.

They would also like to thank the members of the Workshop of the Physics Department of The University of Aston for their help in designing and making the brush and disc wear machine.

Finally, the authors wish to thank Prof. S. E. Hunt, Head of the Department of Physics at The University of Aston in Birmingham, for his encouragement at all stages of the research.

References

1. Quinn, T. F. J., *Br. J. appl. Phys.*, 1963, **14**, 107
2. White, J. R., *Wear*, 1969, **13**, 145
3. Davies, W., *Instn elect. Engrs Monogr. No. 271 U*, 1957 (London: Institution of Electrical Engineers)
4. Lancaster, J. K., & Stanley, I. W., *Br. J. appl. Phys.*, 1964, **15**, 29
5. Quinn, T. F. J., *Proc. Instn mech. Engrs*, 1967–68, **182**, (Pt 3N), 203
6. Quinn, T. F. J., & Woolley, J. L., *Lubrication Engng*, 1970, **26**, 312
7. Clark, W. T., & Lancaster, J. K., *Wear*, 1963, **6**, 467

DISCUSSION

P. K. C. Wiggs (Morganite Carbon Ltd, London, S.W.11):—The direct relationship quoted between contact resistance and friction is observed only on high-speed electrographite brushes; on other types the contact resistance falls with increasing current but friction does not. When running conditions of EG14 graphite on copper are changed, the friction and resistance change also. Under those conditions in which friction force is unusually high, resistance is low, so that superimposed on the direct relationship observed with change of current, is a reciprocal relationship when other conditions change. This seems to indicate that there is some relationship between mechanical and electrical contact areas.

The lower wear rates quoted, at the bottom of the graph (Fig. 1) are comparable with those found on practical electric motors, when sparking is not significant. The high rates at the top of the graph are some 30 times greater.

Author's reply:—We realise that the relationship between contact resistance and friction coefficient has not been universally established, especially under practical running conditions. Nevertheless, in later experiments which we have been carrying out with EG14 graphite running on aluminium, we have again been able to demonstrate the validity of a direct relationship between contact resistance and friction coefficient. These later experiments (to be reported in detail elsewhere) show that this relationship holds for a wide range of brush pressures, including pressures normally used under

practical conditions. We agree with you that there must be some relationship between mechanical and electrical contact areas.

A. E. Bickerstaff (Morganite Carbon Ltd, London, S.W.11):—Could you explain how the observation of cracks and blisters in the carbon film, transferred on to the metal counterface, constitutes evidence supporting a fatigue method of wear for the brush?

Author's reply:—We have found evidence of blisters and cracks on both brush and track surfaces. In this initial paper, we were merely following White[2] in suggesting that these features could support a fatigue wear mechanism. In subsequent papers, we will examine this suggestion in much more detail, after we have examined many more graphite/metal sliding systems.

Reprinted From ASLE TRANSACTIONS
Volume 15, Number 3, July 1972

VOLUME 15, 192–200
ASLE TRANSACTIONS

The Effect of Current on the Lubrication of Sliding Electrical Contacts

J. FISHER, K. J. CAMPBELL, and T. F. J. QUINN
The University of Aston in Birmingham, Birmingham, 4, England

This paper describes experiments designed to examine the effects of current on the lubricant properties of electrographite brushes running against slip rings of pure aluminium and stainless steel. The range of current densities carried from 0 to 0.2 A.mm^{-2}. It is shown that the effects of increasing current are generally beneficial in so far as friction and contact resistance are concerned. However, the wear of the brushes running on aluminium was unacceptably high.

The results of these experiments are discussed in terms of the surface topographical changes (revealed by scanning electron microscopy) caused by the passage of current through the contact between the brushes and the slip rings. A mechanism of surface film breakdown with increasing current is postulated as a possible cause of the heavy wear of the brushes running on aluminium.

INTRODUCTION

Most of the previous research into the lubrication of carbon brushes has been concerned with the sliding of graphite on *copper,* since most electrical machines are operated with copper commutators and slip rings. However, some machines use other metals as the contact material. For instance, high carbon steel is used in the slip rings of high-speed alternating current generators, and stainless steel is used in high-speed electrical machines which have to be run at high ambient temperatures.

The increased use of aluminium as a substitute for copper as an electrical conductor *under stationary conditions* has prompted some machine manufacturers to attempt using aluminium as a commutator material. Unfortunately, the wear rate of both the aluminium and the brushes tends to be very high. This has prevented the substitution from becoming a viable economic proposition.

This paper is a report of some of the results of an investigation into the causes of failure of the aluminium-electrographite sliding system when current is passed. For comparison, a few experiments were also carried out on the well-behaved stainless steel-electrographite system.

The changes in frictional force and contact resistance with changes in current are fairly well known for the copper-electrographite system (*1, 2, 3*). Most investigators agree that the changes in contact resistance are due to a breakdown of the copper oxide film in the *real* area of contact (*4*). Several hypotheses have been proposed which relate the frictional force to the current, but none have been generally accepted (*5*). As far as the authors are aware, however, there has been no work *published* on the behavior of the aluminium-electrographite system. In the present paper, the results obtained on the aluminium-electrographite system and the stainless steel-electrographite system are discussed in terms of the tendency for the contact films of the former system to disintegrate with the increase in current. This discussion, of course, includes the effect of current upon surface topographies, as revealed by a systematic investigation with the scanning electron microscope.

EXPERIMENTAL DETAILS

The experiments were carried out on two machines of the same basic "pin and disk" geometry. The disks rotated in a horizontal plane, and the brushes were held vertically against the disks in slots cut in the brush holders. Loads were applied to the brushes by means of weights on a weight-pan sliding in the brush holders.

Two brushes were run on different radii tracks on each disk. When current was passed through the system, one brush acted as the positive brush, carrying conventional current *from the brush to the disk,* while the other brush acted as the negative brush.

Presented at ASLE International Conference on Solid Lubrication, held in Denver, Colorado, August 24–27, 1971

The wear of the brushes, which were of a constant cross section of 5 mm × 5 mm, was found by measuring their change in length. On the prototype machine, this change was measured either by a micrometer head fixed to the base of the machine, or by measuring the change in capacitance between two horizontal plates, one fixed to the top of the brush and the other one fixed to the base of the machine. On the other test rig, which is shown in Fig. 1, the wear was found in a similar fashion, i.e., by measuring the distance between a capacitance plate attached to the top of the brush, and the capacitance probe of a commercially available distance-measuring bridge. The output from this instrument was monitored by a potentiometric chart recorder, thereby giving a continuous recording of the wear rate.

The frictional forces between the brushes and the disks were measured in basically the same way on both machines. On the prototype machine, the brush holders were free to swing in a horizontal plane on light bearings. During running, the brushes were held steady on the disk by mechanical stops. The frictional force was found by measuring the force required to swing the holders away from the stops. The brush holders on the latter machine were fixed to the supporting pillar by a crossed-spring arrangement. This enabled the brush holders to move only in a plane parallel to the disk surface. The brush holders were constrained by strain gauge transducers. These held the brush holders rigidly in position, and also measured the frictional force. The outputs from the strain gauge bridges were fed into a chart recorder, and a continuous trace of friction obtained.

Fig. 1—Photograph of wear test rig showing disk, brushes and measurement transducers.

The contact resistance of the brush-metal interface was found by measuring the potential difference between the brush and disk, using a valve voltmeter or potentiometric chart recorder. Contact of the measuring circuit to the metal disk was made through a pair of silver-graphite brushes running on a copper ring attached to the rotating shaft of the machine.

The aluminium disks were made from soft, pure aluminium sheets. They were machined to a surface finish of 125×10^{-6} mm (5μ in) Center Line Average (CLA). The stainless steel disks had a surface finish of 12×10^{-6} mm (0.5μ in) (CLA). Although stainless steel is much harder than aluminium, it is similar to aluminium in the way it forms a strong oxide layer.

The brush material used in the experiments was a high-speed electrographite material. The brushes were all cut from the same block of material, with the running faces parallel to the same direction within the block.

Four series of experiments were carried out on brushes running on aluminium, and one on brushes running on stainless steel. The sliding speed was 9,000 $mm.s^{-1}$.

In the first three series of experiments, various brushes were run against aluminium disks under three different loads, 1.6N, 4.7N and 10N. At each of these loads the brushes were run first with no current passing, then with currents ranging from 0.5A to 5.0A. At each load and current, the brushes were run until steady values of frictional force and contact resistance were obtained. When this stage was reached, the run was discontinued. Further experiments were then carried out under different conditions of load and current, using a new disk and new brushes.

The fourth series of experiments carried out on aluminium used the same disk and brushes throughout the run. A light load, 0.6N, was used, and the current was varied from 10^{-5}A to 2.0A. Values of contact resistance, friction force, and wear rate were measured. This experiment was stopped at a current of 2.0A, since arcing occurred beneath the negative brush at this current.

For the purpose of comparison, a short experiment was also carried out with brushes running on a stainless steel disk. The same brushes and disk were used throughout the run with a load of 4.7N. Frictional force, contact resistance, and wear rate were measured at currents up to 5.0A.

Selected portions of all worn brush and disk surfaces were examined by scanning electron microscopy. A small amount of electron probe microanalysis was also carried out on one of the aluminium surfaces. Selection was made on the basis of which topography was "typical" and which was "interesting," with more emphasis being placed on the "typical" worn surface topographies.

EXPERIMENTAL RESULTS

Frictional Force and Current

The effect of the current through each brush upon the measured average equilibrium value of the coefficient of friction is shown in Fig. 2 for four different loads on the

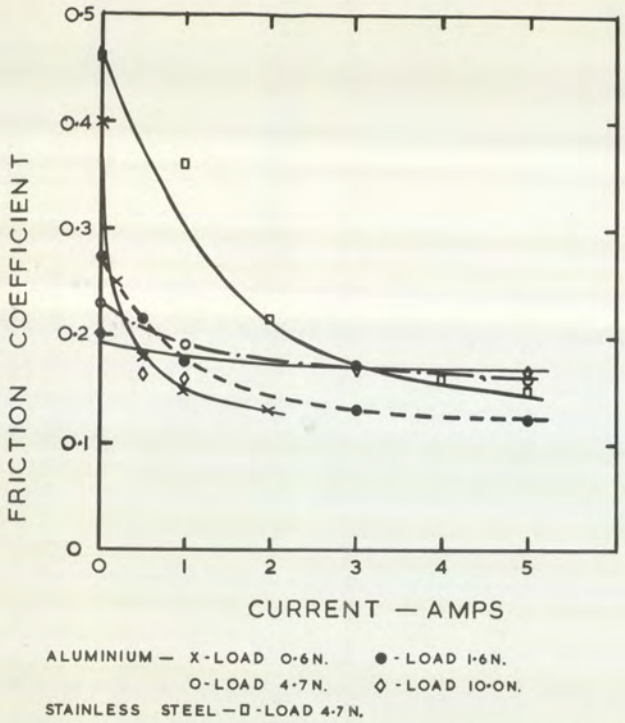

Fig. 2—Variation in coefficient of friction with current for electrographite sliding on aluminium and stainless steel.

electrographite-aluminium system, and one load on the electrographite-stainless steel system. This shows that the friction coefficients all decrease with increasing current. A significant aspect of this decrease is that there seems to be a tendency for all the experiments to provide a friction coefficient of about 0.15 at currents greater than about 2A. This could indicate that the electrical factors over-ride all others, when considering the lubrication of sliding contacts through which high density currents are passing. One cannot neglect the other factors completely, however, as shown by the small increase in the friction coefficient with increasing load for the electrographite-aluminium system *at 5A current*.

It is interesting to see what is the form of the "friction coefficient versus current" curve at very low currents, i.e., at currents less than about 100mA. Figure 3 shows the

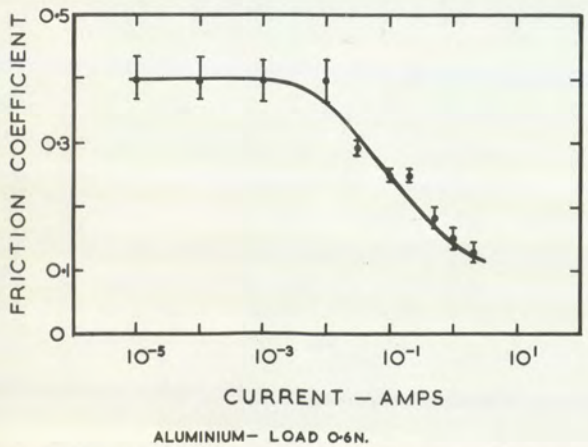

Fig. 3—Variation in coefficient of friction with current, at low currents, for brushes sliding on aluminium under a light load.

low current part of the 0.6N load experiments on the aluminium disk, from which one sees that the zero current value of about 0.4 for the friction coefficient was, in fact, maintained with increasing current from zero up to about 30mA. Above this value of current, the friction dropped through a range of decreasing values at each increment of current. This decrease was always achieved within a very short time of changing the current, e.g., within about 5 minutes. Upon *reducing the current,* the friction began to *increase* immediately. However, it did not reach an equilibrium value for several *days* afterwards, in strong contrast to the several *minutes* required to reach equilibrium after an *increase* in current.

The zero current results are of interest, since they are relevant to the *normal* conditions under which a solid lubricant is used. Figure 4 shows the reduction in friction coefficient with load for the brushes running on aluminium disks. A similar reduction of coefficient of friction with load has also been reported for the unlubricated sliding of steels (*6*). This is an apparent violation of the law of friction which states that the coefficient of friction should be *independent* of the load. It indicates just how little is still known about the fundamental interactions between sliding surfaces.

Contact Resistance and Current

The variation of the contact resistance between the brushes and the aluminium disk is shown in Fig. 5 for a constant load of 0.6N. It can be seen that there is an extremely high contact resistance ($\sim 10^4$ ohms) for currents less than about 100μA, indicating the presence of an insulating oxide film on the aluminium surface. Increasing the current above this value leads to a considerable reduction in contact resistance, e.g., about 1 ohm at 1A current. The difference between the positive and negative brush contacts was only appreciable at the very low currents. A striking feature of Fig. 5 is the effect of reducing cur-

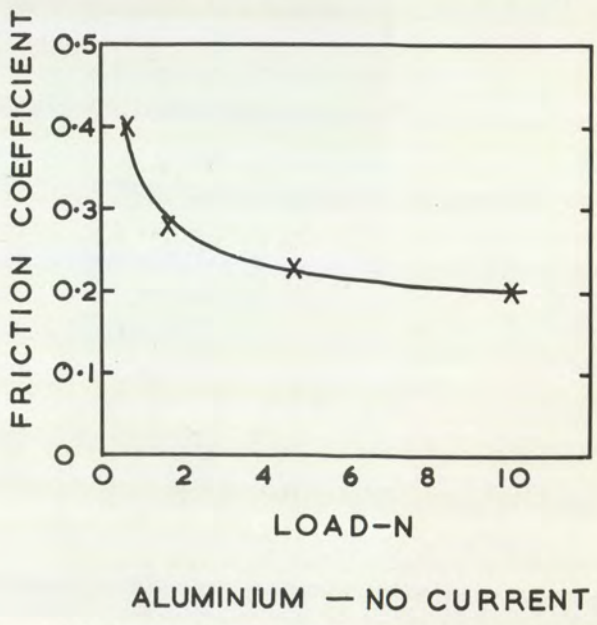

Fig. 4—Variation in coefficient of friction with load for brushes sliding on aluminium without current.

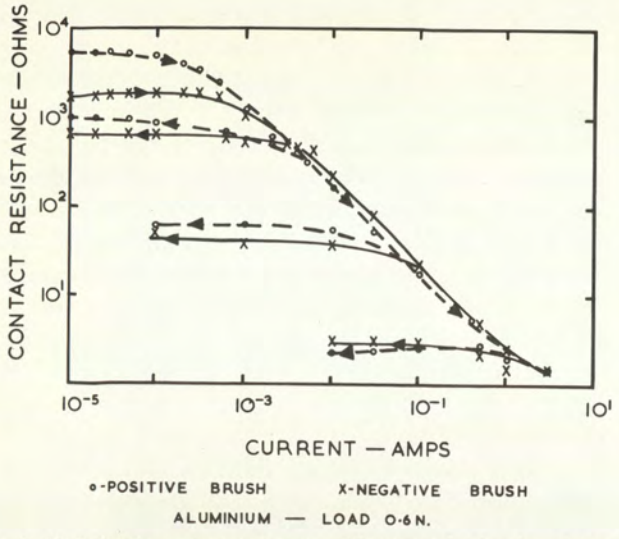

Fig. 5—Variation in contact resistance with current for brushes sliding on aluminium under a light load.

rent after increasing from zero up to about 5mA. Here, one can see that the contact resistance does *not* return to its previous high value but, instead, tends towards an equilibrium value an order of magnitude smaller. A similar effect was found at about 100mA. However, for reduction after reading 1A, there was very little change in contact resistance. This indicates a possible *breakdown* in the aluminium oxide film with increasing current, and will be discussed later on.

A similar form of behavior is indicated by plotting the potential applied across the brush-metal interface against the contact resistance (see Fig. 6). The arrows on this graph (and on Fig. 5) indicate whether the current is being increased or decreased. Figure 6 shows that the contact resistance was initially high, and remained high, until the potential across the interface exceeded about 1.1 volts. Above this, the contact resistance decreased rapidly, and very little increase in potential was required to pass large currents. This experiment was stopped at 2A, because arcing occurred beneath the negative brush. This arcing appeared to have no effect upon the contact resistance.

Figure 7 shows the variation in contact resistance with currents in the range 0.5 to 5A for loads of 1.6N, 4.7N and 10N. It will be noted that there is a tendency for the contact resistance to approach the same value (about 0.5 ohms) at the highest currents, in much the same way as Fig. 2 showed that the friction coefficient also tended toward a constant value at high currents.

Figure 8, the variation of contact resistance between the brushes and the *stainless steel* disk with changing current, shows a similar form as that shown in Fig. 7, namely a tendency towards a value of 0.5 ohms at high currents.

Friction Coefficient and Contact Resistance

Comparison of Fig. 3, 5, and 8, shows that *both* the contact resistance and the coefficient of friction varied in the same way as the current is increased. This similarity in behavior is shown by plotting values of contact resistance against coefficient of friction for increasing current

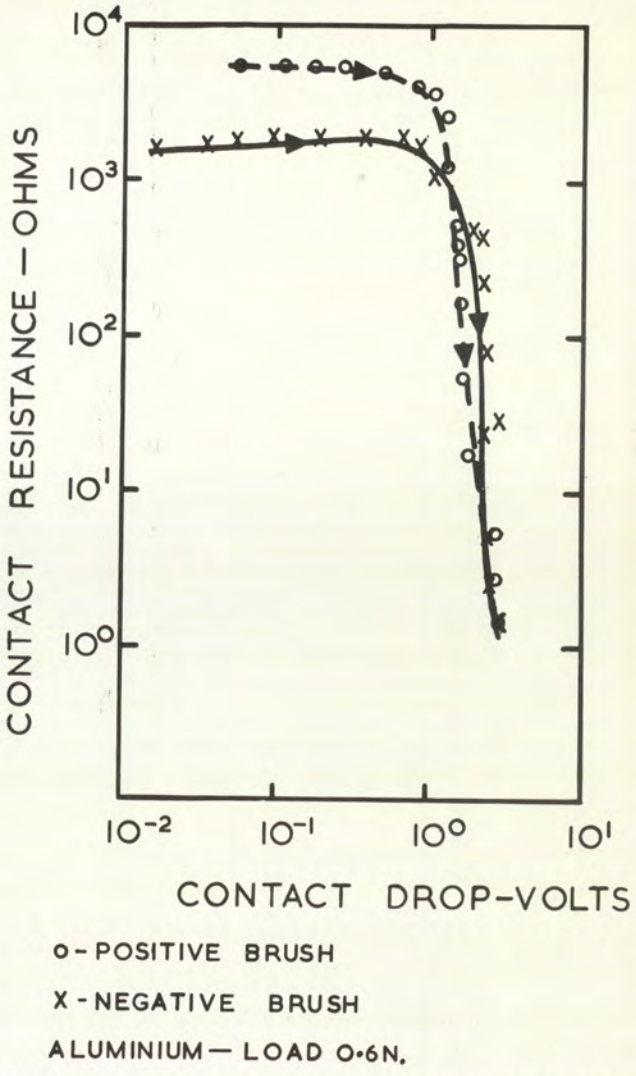

Fig. 6—Variation in contact resistance with applied voltage for brushes sliding on aluminium under a light load.

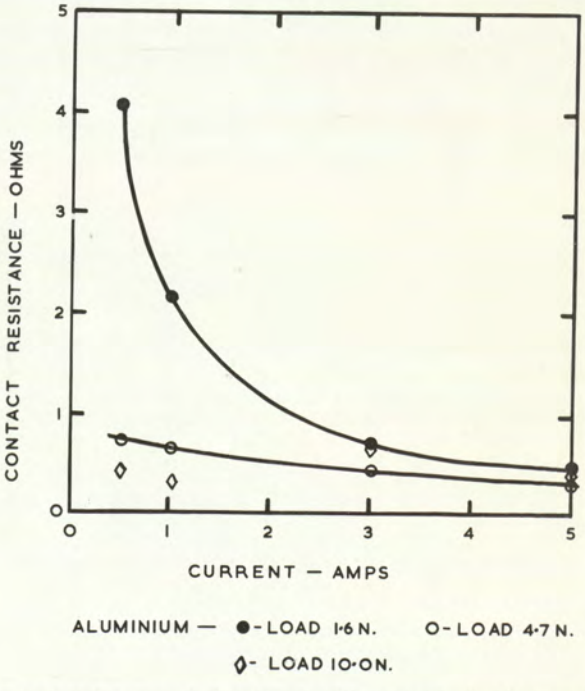

Fig. 7—Variation in contact resistance with current for brushes running on aluminium.

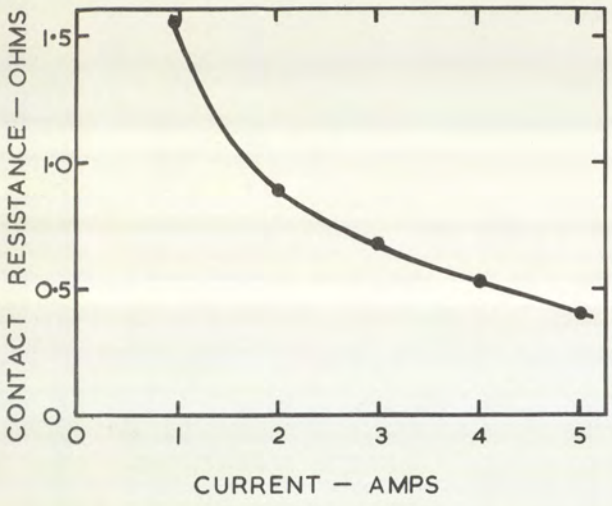

Fig. 8—Contact resistance against current for brushes sliding on stainless steel.

(Fig. 9). It can be seen that there is a *linear* relationship between the contact resistance and the coefficient of friction. This relationship clearly indicates a strong connection between these two *independent parameters*—possibly a common dependence upon the real area of contact? This will be discussed later.

The Wear Rates

The wear rate of the brushes was the most difficult parameter to measure, mainly because of the very small wear which took place. Also, at any given load and current, the wear rates of the brushes running on aluminium varied over quite a large range of values. Owing to these factors, only general trends could be found from the wear data.

At a load of 0.6N and with zero current passing through the brushes to the aluminium disk, the average wear rate of the brushes was 3.0×10^{-10} mm^3/mm sliding. No increase in wear rate of the positive brush could be detected up to a current of 2.0A. The average value of the wear rate of the negative brush increased with current. At a current of 2.0A, sparking occurred under the negative brush, thereby causing a very large increase in wear rate.

With a load of 1.6N, the wear rate appeared to follow a similar pattern as with the 0.6N load, although the wear rates at the heavier load were unexpectedly lower. Once again, the wear rate of the negative brush was greater than that of the positive brush.

The wear rates of the brushes at loads of 4.7N and 10N were very erratic, and no steady value could be obtained. Owing to the very wide range of wear rates, no *significant* change in wear rate with load or current could be detected. Once again, the very high wear rates at the high currents were probably due to arcing beneath the brushes.

By comparison with the wear rates of the brushes running on aluminium, the wear rates of the brushes running on the stainless steel were low and well behaved. Figure 10 shows the wear rates for brushes loaded at 4.7N against a stainless steel disk. No increase in the wear rate of the positive brush could be detected, but a steady increase in

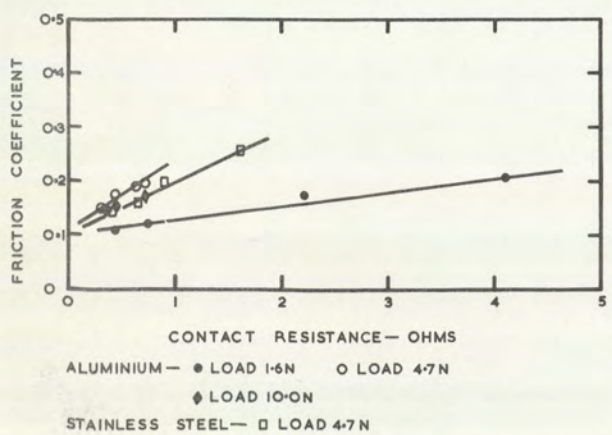

Fig. 9—Coefficient of friction against contact resistance for brushes sliding on aluminium and stainless steel.

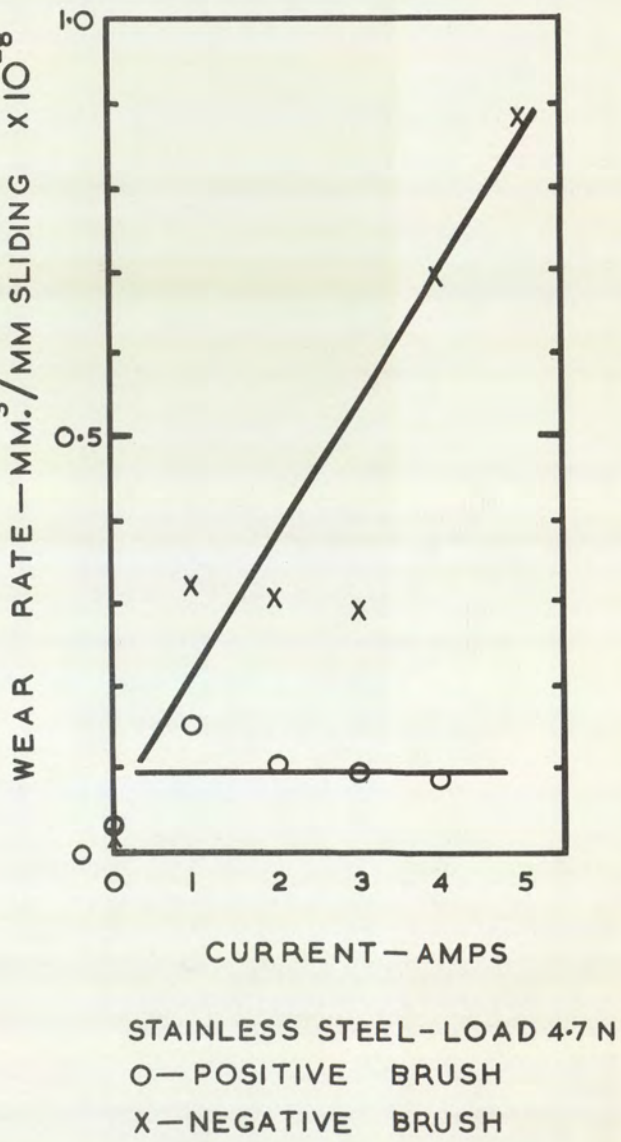

Fig. 10—Variation in wear rate of brushes sliding on stainless steel with current.

the wear rate of the negative brush took place as the current was increased. It should be noted that the wear rates obtained from running on stainless steel are an order of magnitude *less* than those obtained on aluminium and are comparable with those of brushes running on copper.

Why should the wear rate of brushes running against aluminium be so much more than that of brushes against stainless steel or copper? The abrasive nature of aluminium oxide could be contributing to the increased wear. One possible way of investigating the relative wear behavior is to study the relative surface topographies using a technique with a very wide range of magnifications and a comparatively high resolution, namely, scanning electron microscopy. The following section deals with just such a study.

Relative Surface Topographies

A very large number of micrographs were taken during the experiments. A selection of micrographs has been chosen which show the general changes which took place in the generated surfaces as the conditions of sliding were changed.

The surfaces of the aluminium disks. At a load of 1.6N and with no current flowing through the brushes, the surface generated on the aluminium appeared smooth and uniform. Scanning electron microscopy revealed that the aluminium surface was covered by a smooth, layered, graphite film as shown in Fig. 11(a).

The passage of current through the brushes tended to break up the graphite film into smooth islands or ridges standing above surrounding rough regions. Figures 11(b) and 11(c) show typical areas of the positive track after the passage of a current of 1.0A. The film laid down upon the surface has a much more ragged appearance than with no current passing.

After a current of 5.0A has been passed through the brushes, the film has been almost completely broken up into smooth islands as shown in Fig. 11(d).

The effect of *increasing the load* was also to break up the graphite film. Figures 12(a) and 12(b) show the surfaces generated by loads of 4.7N and 10N respectively, with no current passing.

The effect of current at these higher loads was to break up the graphite film and roughen the aluminium surfaces. The extent of the break-up of the film with a load of 4.7N after a current of 1.0A can be seen in Fig. 12(c). Figure 12(d) shows the surface at the same load, but after a current of 5.0A. At this high current, very little smooth graphite film remains on the surface except in isolated islands. The rough areas surrounding these islands appear to consist of loose debris, and areas where the underlying aluminium has bubbled through the graphite, as shown in Fig. 13(a).

At the highest load, 10N, the passage of current had the same effect as at the lower loads. The highest attainable current before catastrophic wear of the brushes took place was 3.0A. Figure 13(b) shows that, under these conditions, the surface was of the same appearance as in Fig. 12(d).

At a current of 5.0A, catastrophic wear of the brushes occurred, and severe damage was caused to the aluminium surface. No smooth areas of film could be found. The surface consisted mainly of areas where either the graphite film or underlying metal had been deformed into the wave-like appearance of Fig. 13(c).

The surfaces of the brushes run against aluminium. The surface of the brushes after running was all of the

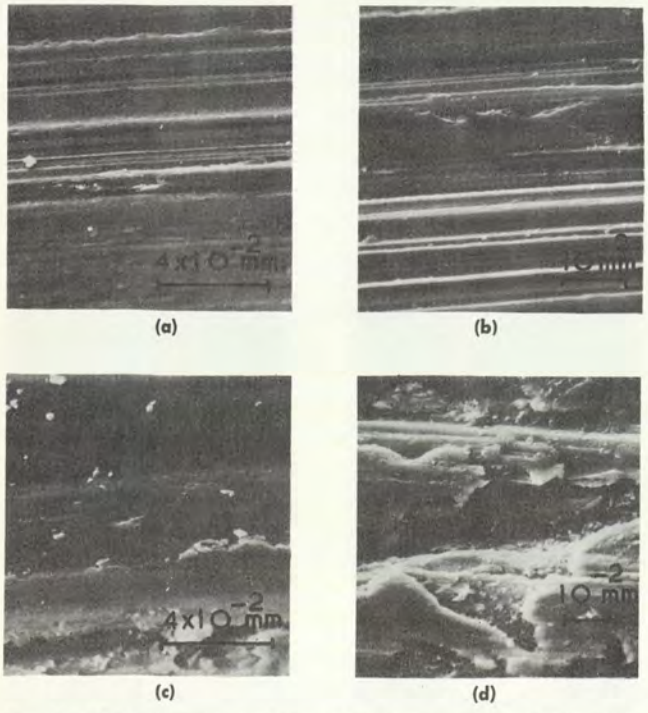

(a) (b) (c) (d)

Fig. 11—Effect of passage of current upon topography of aluminium surfaces.

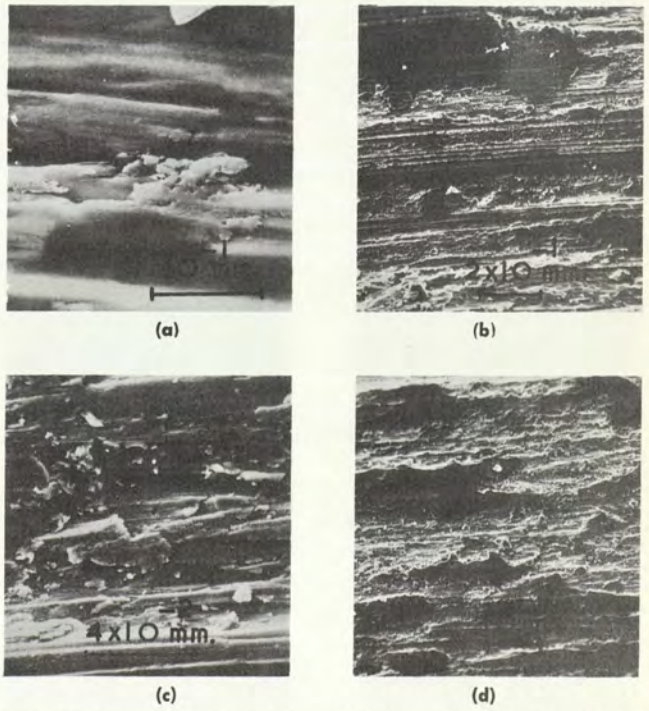

(a) (b) (c) (d)

Fig. 12—Effect of load and current upon the topography of the aluminium.

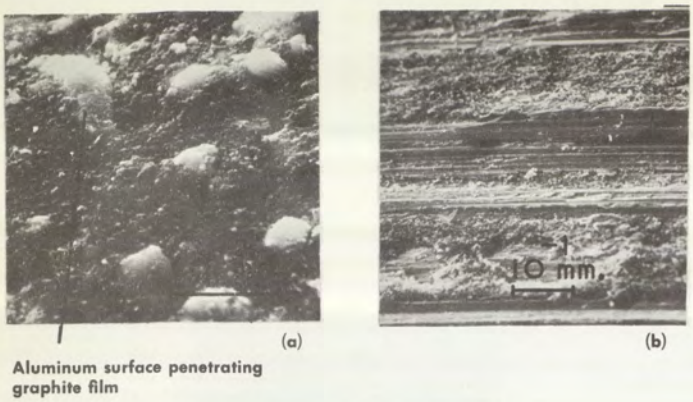

Fig. 13—Effect of load and current upon the topography of the aluminium.

same appearance. A thin graphite film was formed on the running surface, and provided that catastrophic wear of the brushes did not take place, changes in load and current had no significant effect upon the nature of the surface.

Figure 14(a) shows the surface of a brush run under a light load, 1.6N, with no current passing, and Fig. 14(b) shows the surface of the positive brush under a heavy load, 10N, and a current of 3.0A. There was very little difference in the surfaces of the brushes under these two different conditions. Under all running conditions, it was usual to find a large number of bright particles on, or embedded in, the brush surface. These can be seen clearly in Fig. 15(a), which relates to a brush which has been run at a load of 4.7N with no current. Electron probe microanalysis reveals that these particles are aluminium transferred from the disk surface to the brush. Figure 15(b) shows a backscattered electron micrograph of the surface of the same brush as in Fig. 15(a). Figure 15(c) shows a photograph of the distribution of X-rays emitted from aluminium over the same area.

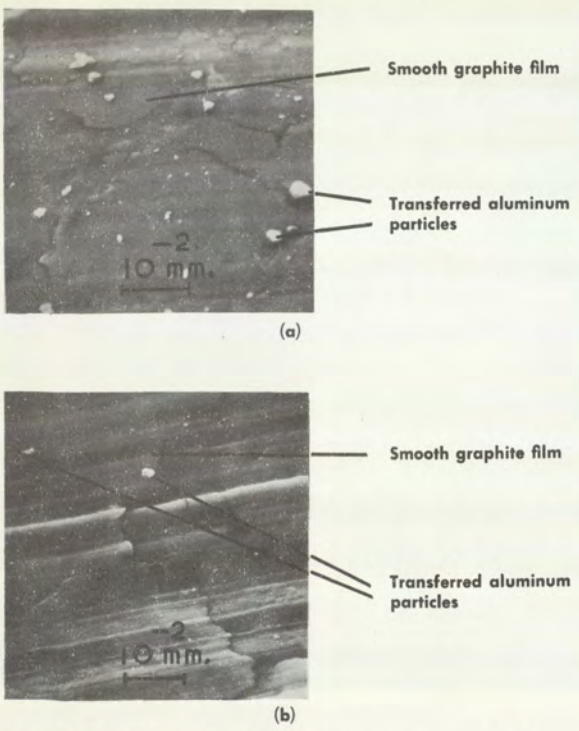

Fig. 14—Typical brush surfaces after running on aluminium

The surfaces generated by running on stainless steel. A typical area of the film formed on stainless steel at a load of 4.7N and current of 5.0A is shown in Fig. 16(a). A complete film of graphite covered the surface and very little underlying metal could be seen. The raised islands were very smooth, and a common feature of the film was cracking and blistering of the smooth regions, as in Fig. 16(b).

As in the case of brushes running on aluminium, the surfaces of the brushes running on stainless steel were composed of a laid-down graphite film. The only *significant* difference between the brushes running on the different metals was the absence of metallic debris on the surface of the brushes run on stainless steel.

DISCUSSION

It is very clear from the foregoing that the solid lubricant properties of electrographite brushes are considerably

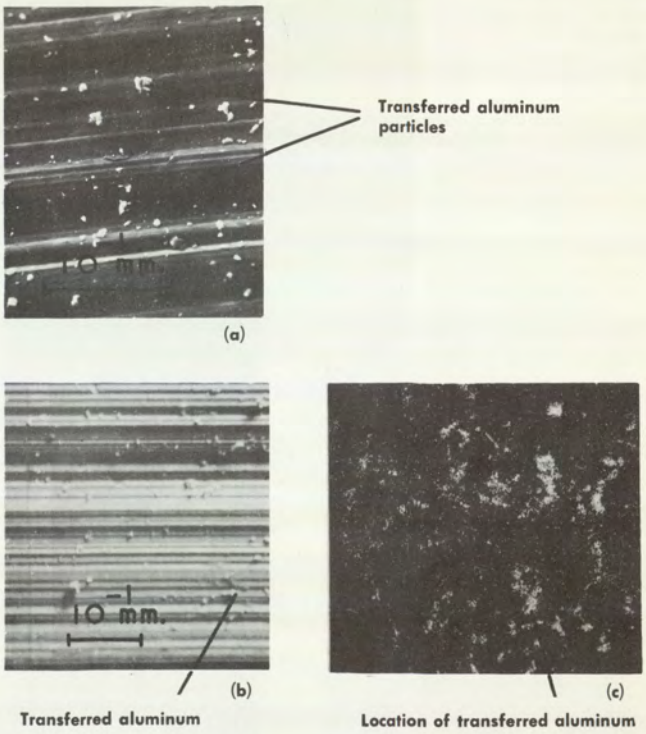

Fig. 15—Surface of brush after running on aluminum and the distribution of aluminium on the surface as revealed by electron probe microanalysis.

(a)

(b)

Fig. 16—Typical surfaces formed upon stainless steel

modified by the passage of current through the contact region between the brush and the slip ring. In fact, for the two contact materials used in these experiments, the effect of current seems to be beneficial as far as the coefficient of friction is concerned. The similar effect of current upon the contact resistance is also beneficial from the point of view of the ability of the system to collect current. Unfortunately, the position is not so good when one considers the high wear rates of the brushes at high currents, especially when running against aluminium. This is, of course, the main reason why aluminium has tended to be rejected as an alternative contact material to copper in electrical machines.

The key to the friction and wear behavior of electrographite brushes when used under electrically conducting conditions probably lies in: (1) the breakdown of the oxide film present on the contact material at low currents, and (2) the abrasive nature of both the oxide particles and the electrographite wear particles. Undoubtedly, aluminium oxide particles are much more abrasive than the cuprous and ferric oxide particles expected to be present when copper and steel materials are used in slip rings. Hence the high relative wear rate for the electrographite-aluminium system. The conditions under which metal oxide films break down are clearly the most important factors governing the use of that metal as a contact material. This is where the study of the contact resistance is most relevant.

The variation in contact resistance with current between the electrographite brushes and the aluminium and the stainless steel disks, follows the same pattern as the behavior of similar brushes running on copper. Bickerstaff (*1*) has shown that a low-voltage ohmic region exists on copper, provided that the voltage across the interface does not exceed 0.1v.

The method of conduction of electricity from the brush to a copper disk is well understood (*5*). The ohmic region at low voltages is attributed to the electric current passing through a thin oxide layer (*7*) which is broken down when the field strength across the interface exceeds the breakdown strength of the oxide. After this initial breakdown, an increase in current causes enlargement of the electrical contact region by fritting (*4*) and the resistance of the contact is further reduced. The similarity between the contact resistance—current curves for copper, aluminium, and stainless steel indicates that the same mechanism of oxide film breakdown operates in each instance. The low value of the contact resistance which persists when the current is *reduced after breakdown,* suggests that the aluminium oxide film does not immediately reform. This could be due to the action of the sliding brush. The approach of contact resistance to a constant low value at high currents is probably due to the complete disruption of the oxide film. This would cause the electrical contact area to approach a constant value, perhaps a value close to the area of mechanical contact.

The similarity in the behavior of contact resistance and coefficient of friction and the linear relationship between them at medium currents suggest that breakdown of the oxide film may also be responsible for the reduction in friction as the current is increased. The rapid approach to equilibrium upon increasing the current could be due to the immediate breakdown of oxide. The slow reoxidation which takes place upon reduction of the current would then cause the slow rate of increase in friction.

Comparison of the micrographs obtained by scanning electron microscopy of the surfaces found upon aluminium and stainless steel suggests that the wear mechanisms are *not* the same.

A characteristic of the surface formed upon the stainless steel was the relatively smooth film formed by several layers of graphite. Break-up of this film appeared to be preceded by cracking and blistering, suggesting that a fatigue mechanism was responsible.

The film formed on aluminium, however, was very irregular. Melting and deformation of the underlying aluminium was apparent. These features indicate that that failure of the graphite film on aluminium may be due to softening or deformation of the substrate resulting in movement and break-up of the film. This idea is supported by the detection of large amounts of aluminium transferred to the brush surface.

The large difference in topographies found under different conditions did not appear to have much effect upon either the friction or contact resistance, but could be related to the wear rate. In the case of stainless steel, a smooth, complete graphite film was laid down. Due to the

support of the underlying metal, the deformation taking place at the interface between the brush and laid-down film was probably elastic, thereby causing the wear of the brush to occur by a fatigue mechanism. In the case of brushes running on aluminium, plastic deformation of the underlying metal would result in the film being unsupported. The deformations at the surface are no longer elastic, and rapid break-up of the film on both the aluminium disk and the brush would take place. An increase in current, or load, would result in increased plastic flow of the aluminium, which may be responsible for the increase in wear rate.

ACKNOWLEDGMENTS

The authors are indebted to Morganite Carbon Company, London, for their support of the work described in this paper. Special thanks are due to A. R. Ford and A. E. Bickerstaff for their advice and encouragement. One of the authors (J. Fisher) is receiving support from the Science Research Council.

REFERENCES

(1) Bickerstaff, A. E., "Contact Resistance of Carbon Brushes," *Proc. 3rd Conference on Industrial Carbons and Graphite*, Soc. of Chem. Industry, London, 1970.
(2) Davies, W., "The Sliding Contact of Graphite and Copper," The Institute of Electrical Engineers, Monograph 271V, 1957.
(3) Lancaster, J. K. and Stanley, I. W., "The Effect of Current on the Friction of Carbon Brush Materials," *Brit. J. Appl. Phys.* **15**, 29–41 (1964).
(4) Holm, R., "Electric Contacts Handbook," Springer-Verlag, Berlin, 3rd ed., 1958.
(5) Shobert, E. I., "Proc. 5th International Conference on Electric Contact Phenomena," V.D.E.-Berlin, Munich, 1970.
(6) Quinn, T. F. J. and Woolley, J. L., "The Unlubricated Wear of 3% Cr–½% Mo Steel," *Lub. Eng.* **26**, 312–321 (1970).
(7) Holm, E., "Proc. 4th International Research Symposium on Electric Contact Phenomena," Inst. of Phys. & Inst. of Elect. Engrs., Swansea, 1968.